JUL 2 7 1982

DISTRIBUTION:
Document Control (50-397)
LB #2 Reading File
RAuluck
EHylton
TNovak

bcc: NRC PDR
Local PDR
NSIC
PRC

Docket No. 50-397

MEMORANDUM FOR: J. Knight, Assistant Director for Components & Structures Engineering, DE

W. Johnston, Assistant Director for Materials & Qualifications Engineering, DE

D. Muller, Assistant Director for Environmental Technology, DE

T. Speis, Assistant Director for Plant Systems, DSI

W. Houston, Assistant Director for Radiation Protection, DSI

L. Rubenstein, Assistant Director for Core & Containment Systems, DSI

J. Kramer, Deputy Director Division of Human Factors Safety

B. Grimes, Director Division of Emergency Preparedness, OIE

FROM: A. Schwencer, Chief Licensing Branch No. 2, DL

SUBJECT: REVIEW/CONCURRENCE OF WNP-2 SSER

Attached is a draft of the WNP-2 SSER for your comment and concurrence. All comments/concurrence must be received by the project manager by C.O.B. Thursday, July 29, 1982.

Please course of your review of the SSER, please ensure that appropriate sections include statements as to how the review conforms to the SRP (NUREG-0800).

Please contact the Project Manager, Raj Auluck, x29778, Room 333 if you desire additional information.

/S/

A. Schwencer, Chief
Licensing Branch No. 2
Division of Licensing

8208040594 820727
PDR ADOCK 05000397
E PDR

Attachment: As stated

cc: See next page

OFFICE	LB#2:DL	LB#2:DL				
SURNAME	RAuluck:kab	ASchwencer				
DATE	7/27/82	7/ /82				

7 Instrumentation and Control
7.3 Engineered Safety Features Systems
7.3.2 Specific Findings
7.4 Systems Required for Safe Shutdown
7.4.2 Specific Findings

TABLE OF CONTENTS

TABLE OF CONTENTS (continued)

1 INTRODUCTION AND GENERAL DESCRIPTION

1.1 Introduction

The Nuclear Regulatory Commission's Safety Evaluation Report (SER) (NUREG-0892) in the matter of the Washington Public Power Supply System's (WPPSS) application to operate the Washington Public Power Supply System Nuclear Project Number 2 (WNP-2) was issued in March 1982. At that time, the staff identified items that were not yet resolved with the applicant. These items were categorized as:

(1) Outstanding items which needed resolution prior to the issuance of an operating license.

(2) Items for which the staff had completed its review and had determined positions for which there appeared to be no significant disagreement between the applicant and the staff. Further information was needed, however, to confirm these positions.

(3) Items for which the staff had taken positions and would require implementation and/or documentation after the issuance of the operating license. These would be conditions to the operating license.

The SER issued in March 1982 did not include the WNP-2 geology and seismology review. This SER supplement provides the NRC staff's evaluation of the geology and seismology sections of the applicant's Final Safety Analysis Report (FSAR). This supplement also contains NRC staff evaluation of the open items that have been resolved and addresses changes to the SER that resulted from receipt of additional information from the applicant.

Copies of this SER supplement are available for inspection at the NRC Public Document Room, 1717 H Street, NW, Washington, D.C., and at the Richland City

Library, Swift and Northgate Streets, Richland, Washington. Single copies may be purchased from the sources indicated on the inside front cover.

The NRC Project Manager assigned to the operating license application for WNP-2 is Dr. Rajender Auluck. Dr. Auluck may be contacted by calling (301) 492-9778 or writing:

Dr. Rajender Auluck, P.E.
Division of Licensing
U.S. Nuclear Regulatory Commission
Washington, D.C. 20555

1.7 Summary of Outstanding Items

In Section 1.7 of the SER, the staff identified outstanding issues that were not resolved at the time of issuance of the SER. In this supplement the staff discusses the resolution of a number of these items previously identified as open. The items identified in Section 1.7 of the SER are listed below with the status of each item. If the item is discussed in this supplement, the specific section is identified. The resolution of the remaining outstanding issues will be discussed in future supplements to the SER.

Item	Status	Section
(1) Geology and seismology	Resolved	2.5
(2) Internally generated missiles	Awaiting further information	--
(3) Tornado missile protection for diesel generator (DG) exhaust	Under review	--
(4) Turbine missiles	Under review	--
(5) Component supports	Resolved	3.9.3.3
(6) Equipment qualification	Awaiting further information	--
(7) Condensation oscillation and chugging load specifications	Resolved	6.2

Item	Status	Section
(8) Pressure interlocks on emergency core cooling injection valves	Awaiting further information	--
(9) Modification of automatic depressurization system logc	Awaiting further information	--
(10) Standby service water system instrumentation and control (I&C) design	Awaiting further information	--
(11) Engineered safety feature reset control	Resolved	7.3.2.7
(12) Remote shutdown system I&C design	Resolved	7.4.2.3
(13) Control system failures	Awaiting further information	--
(14) Adequacy of station electric distribution system	Awaiting further information	--
(15) Quality group classification for the DG auxiliary systems	Awaiting further information	--
(16) Diesel engine cooling heater preheat	Resolved	9.5.5 (SER)
(17) Diesel engine lube oil system's ability preclude dry starting	Resolved (Tech Spec)	9.5.7
(18) Blockage of the DG combustion air intake and exhaust system	Awaiting further information	--
(19) Shift supervisor training program	Resolved	13.2.2.5
(20) Administrative procedures: limitation on working hours	Resolved	13.5.1.4
(21) Criteria for testing hot pipe containment penetrations	Awaiting further information	--
(22) Emergency planning program	Awaiting further information	--
(23) Control room design review	Awaiting further information	--
(24) Anticipated transients without scram (ATWS)	Awaiting further information	--
(25) General Design Criterion (GDC) 51	Resolved	6.2.7

Item	Status	Section
(26) TMI II.E.4.2 (operability of purge valves only)	Awaiting further information	--
(27) TMI II.K.3.2.8, qualification of accumulators on ADS valves	Resolved	6.3.6
(28) Pipe break in the BWR scram system	Awaiting further information	--
(29) Steam bypass from a stuck open wetwell-to-drywell vacuum breaker	Awaiting further information	--

1.8 Confirmatory Issues

In SER Section 1.8, the staff identified 22 confirmatory issues that were not resolved at the time of issuance of the SER. To that list, the staff has added the following concern:

X

1.9 License Conditions

In SER Section 1.9 the staff identified 12 license conditions. During its subsequent review, the staff changed this list of license conditions as follows:

Item	Status	Section
(13) Remote shutdown system	Addition	7.4.2.3

2 SITE CHARACTERISTICS

2.5 Geology and Seismology

The WNP-2 site is on the Hanford Reservation within the Pasco Basin, a physiographic and tectonic subdivision of the Columbia River Basalt Plateau Tectonic Province, which the applicant calls the Columbia Plateau Tectonic Province. The Hanford Reservation is also the site of the Department of Energy's Basalt Waste Isolation Project, for which a comprehensive program of geological, geophysical, and hydrologic studies of the basin was initiated in 1977. These studies will continue at least for 5 years after the issuance of this SSER, during which time new geological and geophysical information and interpretations will be released periodically by DOE. This SSER, therefore, represents the staff's best judgment based on present knowledge of the region. Updated SSERs will be issued whenever any significant new information becomes available. The staff has requested that the applicant maintain a continuing interaction with DOE and provide new information and interpretations to the staff.

As a result of regional and site investigations performed by the applicant since the issuance of CP-SERs for WNP-2 in 1972 and for WNP-1 and -4 in 1975, and the efforts of DOE since 1977, the knowledge of the area has been greatly enhanced. The increasing amount of new information has changed some of the ideas about the area and, therefore, this OL-SSER may contain information and interpretations that differ from those described in the CP-SERs for the aforementioned sites. It should be noted, however, that none of the changes alter the staff's CP-SER conclusions concerning the safety of the site. Moreover, the new information has increased the staff's confidence that the site will not be subjected to any hazards that would pose a problem to the health and safety of the public.

For this SSER the staff has reviewed all available relevant geologic and seismologic information obtained since the issuance of the CP-SER and CP-SSER in 1972, as well as the CP-SER and CP-SSER for the WNP-1 and -4 sites in 1975 (which reviewed and updated the information because it is on virtually the same site), in accordance with the newly revised SRP (NUREG-0800, July 1981).

In the CP-SER for WNP-2 and for WNP-1 and -4, the staff and its advisor, the U.S. Geological Survey (USGS), concluded:

(1) Geologic and seismologic investigations and information provided by the applicant, and required by Appendix A to 10 CFR 100, provided an adequate basis for determining that no capable faults exist at the plant site or within 8 km (5 mi).

(2) Ground motion values of 0.25 and 0.125g used as the zero period limit of appropriate response spectra for the safe shutdown earthquake (SSE) and operating basis earthquake (OBE) are adequately conservative. This conclusion was based upon the following considerations, as stated in the CP-SER of WNP-1 and -4:

no new page

A. The maximum random earthquake in the Columbia Basin Tectonic Province can be as great as intensity VII and can result in that intensity at the site;

B. The Rattlesnake-Wallula Lineament represents the most significant seismically active structure. We view it as having the potential of generating earthquakes of intensity VIII at a distance of little more than 10 miles from the site.

no new page

After careful review of (1) the new information as provided and evaluated by the applicant, (2) the letter reports from USGS and Dr. D. B. Slemmons, attached to this SSER as Appendices G and H, the staff concludes that there is no basis for altering its conclusions stated in the CP-SER concerning the safety of the site of WNP-2.

Some differences from interpretations and information in the CP-SERs (based on recent information) include the following:

(1) Capable faults have been found in the site vicinity and region (described in Section 2.5.1.1.2).

(2) The Rattlesnake-Wallula alignment is regarded as a continuous, capable, faulted structure at or near the surface for a distance of approximately 120 km (discussed in Section 2.5.1.1.2).

(3) The free field ground motion from swarm earthquakes in the immediate vicinity of the site was found to exceed the SSE in the high frequency range (above 10 Hz). (The derivation of this ground motion is discussed in Section 2.5.2.4.2 of this SSER, and the significance of exceeding the SSE is discussed in SSER Section 3.7).

For this review, the staff has evaluated the FSAR and subsequent documents and information including excavation mapping, the trenching and drilling program, and new determinations on faults in the site vicinity. The staff has concluded that the applicant has (1) performed site and regional geologic and geophysical investigations, (2) reviewed all available pertinent literature, and (3) provided the staff with all information necessary to evaluate, assess, and support the applicant's conclusions concerning the safety of WNP-2 site from the geologic and seismologic standpoint. In addition, the applicant has met the requirements of

- GDC 2 with respect to protection against natural phenomena such as faulting.

- 10 CFR 100 (Reactor Site Criteria) with respect to the identification of physical characteristics such as geology (faulting) and seismology (near-site events) used in determining the suitability of the site.

- 10 CFR 100, Appendix A (Seismic and Geologic Siting Criteria for Nuclear Power Plants) with respect to obtaining the geologic and seismic information necessary to determine (1) site suitability and (2) the appropriate design of the plant. In complying with this regulation, the applicant also meets the staff's guidance in Regulatory Guide 1.132, "Site Investigations for Foundations of Nuclear Power Plants," applicable to the development of geologic and seismologic information relevant to the stratigraphy, lithology, geologic history, and structural geology of the site, and Regulatory Guide 4.7, "General Site Suitability for Nuclear Power Stations."

° The applicant did not use the Regulatory Guide 1.60 response spectrum at the CP stage. As discussed in OL-SER Section 3.7, the applicant's response spectrum has been found to be equivalent to Regulatory Guide 1.60.

The following sections present the staff's review of the geologic and seismologic information and bases for the staff's conclusions.

2.5.1 Geology

Because of the rapid progress in the acquisition of geologic information of the area, the staff reviewed the present state of knowledge of the stratigraphy and tectonics to provide a background for the conclusions reached in its evaluation of the geologic safety of the site.

Some of the conclusions reached for which the following section provides the background and justification are

(1) The main deformation of the region culminated between 10 and 5 million years before the present (MYBP).

(2) The region is still undergoing north-south compressive strain but at very low rates.

(3) There is evidence that some of the sedimentary deposits that are post-Ringold Formation (10-³ MYBP) and pre-Missoula flood deposits are more than 700,000 years old.

(4) The clastic dikes within the Missoula flood deposits were probably injected by high hydraulic pressures into the contemporaneously deposited sediments, making them Pleistocene in age.

(5) A variety of age-dating techniques have increased confidence in dating faults and capping materials.

(6) Some surface faults on Gable Mountain, the Central Fault, South Fault, and North-Dipping Reverse Fault, 14 km from the site, are considered capable, but of relatively low seismic potential.

(7) The Southeast Anticline Fault is capped by unfaulted Ringold and is, therefore, not capable within the meaning of Appendix A to 10 CFR 100.

(8) Subsurface faults within 8 km of the site identified by the staff and the USGS on seismic reflection profiles most likely do not project to the surface as suggested by 140 drill holes and trenching done during the early stages of construction.

(9) Umtanum Ridge may be part of an imbricate thrust zone of primary faulting but is most likely not capable.

(10) The dominant structure of seismic significance to the site, the Rattlesnake-Wallula Alignment (RAW) of the Cle Elum-Wallula Zone of Deformation (CLEW), is a continuous, 120-km-long, most likely right-lateral strike-slip fault, capable at its southern half and assumed capable in the northern half.

(11) The Cold Creek Lineament is not a tectonic structure.

2.5.1.1 Regional Geology

The Columbia River Basalt Plateau Province is surrounded on three sides by older terrains: to the north, the Okanogan Highland which includes rocks from the Precambrian Era (600+ MYBP), through the Mesozoic Era (240-63 MYBP), and was deformed in the late Cretaceous (138-63 MYBP) to early Tertiary time (63-2 MYBP); to the east, the Precambrian rocks of the Northern Rocky Mountains Province and the Mesozoic Idaho Batholith north and south respectively; to the south, the Blue Mountains, exposing Paleozoic (570-240 MYBP) and early Mesozoic rocks, deformed in late Cretaceous to late Cenozoic time (63 MYBP [illegible]), and capped by relatively undeformed Columbia River flood basalts. On the west, the Cascade Mountains expose only Cenozoic-age rocks of volcanic and sedimentary origin.

The Columbia River Basalt Plateau consists of a thick sequence of Miocene-age (24-5-MYBP) flood basalts and sedimentary interbeds overlying Precambrian to early Tertiary rocks, and is, in turn, overlain by sediments of Pliocene (5-2-MYBP), Pleistocene (2M-10,000-YBP), and Holocene (10,000-YBP-present) ages. Deformation of the region due to north-south compression preceded and accompanied the outpouring of the Tertiary flood basalts, which were extruded between 16.5-6 MYBP, and produced faults, folds with associated faults, and subsiding basins.

The Pasco Basin, one of the basins formed during the early deformation, is underlain by 3000 m of Miocene-Pliocene-age basalts and sedimentary or volcaniclastic interbeds that exhibit varying degrees of deformation. Overlying the bedrock is 220-360 m of Pliocene-age fluvio-lacustrine sediments, Pleistocene-age fluvio-glacial and aeolian deposits, and Holocene surficial units.

2.5.1.1.1 Stratigraphy and Methods of Age Dating

2.5.1.1.1.1 Basalt Formations

The bedrock of the area is the Yakima Basalt Subgroup of the Columbia River Basalt Group. It consists of three basalt formations; from oldest to youngest, they are the Grande Ronde, Wanapum, and Saddle Mountains Basalt. All of these formations have two or more members, each of which comprises several basalt flows. The Grande Ronde Basalt, extruded 16.5-14.5 MYBP, is the most extensive. It underlies almost all of the Columbia River Plateau and Pasco Basin, is the thickest of the basalt formations, and makes up 85% of the Yakima Basalt Subgroup. The Wanapum Basalt, the second most voluminous, was extruded between 14.5-13.6 MYBP. Its various members are the most extensively exposed of all basalt units in the anticlinal ridges of the Yakima fold belt. The Saddle Mountains Basalt, the youngest of the basalt formations, was extruded 13.5-6 MYBP and makes up only 5% of the Yakima subgroup.

The two younger basalt formations contain significant discontinuities between flows in the form of clastic interbeds generally referred to as the Ellensburg Formation.

2.5.1.1.1.2 Sedimentary Units

The Ringold Formation of Late Miocene to Pliocene age, which overlies the basalt in the Pasco Basin, is interpreted from fossil and paleomagnetic data to be 10-3 MY old and because of consistent thinning on anticlinal bedrock highs, to have been folded with the underlying basalts. A gradual decrease in deformation upward in the section is noted in borings in the basin. This mainly fluvially derived deposit is divided into four textural units: a basal gravel which rests conformably on the basalts in the Pasco Basin; a lower sand-silt-clay unit above; a middle, well-indurated, conglomerate cemented with calcium carbonate and silica; and an upper sand-silt-clay unit. The thickness of the Ringold Formation in the Pasco Basin varies in three ways: (1) from the center of the basin outward towards the edges it thins from a maximum of 360 m to 0; (2) within the basin it varies with the subsurface basalt topography as the area was deforming during deposition; and (3) in places the Ringold was channeled, dissected or completely eroded, causing younger sediments to rest directly on the basalts.

It had been assumed by the applicant (Woodward-Clyde, 1981a) that there was no sedimentary record from the end of Ringold deposition 3 MYBP until the late glacial-melt floods towards the end of the Pleistocene. Flood gravels dated at about 200,000 YBP by caliche rinds on basalt clasts are present on the west and east of the Pasco Basin and were thought to be the oldest post-Ringold sediments. However, recently the staff was provided with two reports on paleomagnetic studies of post-Ringold, pre-Missoula gravels in the Pasco Basin (1) under the Skagit/Hanford site, and at various surface locations on the periphery of the basin and (2) at the Southeast Anticline Fault (Sierra Geophysics, 1982a and b). The studies indicate the presence of reversed magnetization of some of the gravels, suggesting an age of greater than 730,000 years, which is the time of change from the Matuyama Reversed Polarity epoch to the Brunhes Normal Polarity. These studies are discussed further in Section 2.5.1.1.1.3.

Aeolian deposits resting directly on basalt to the east of the Pasco Basin, and not found in the same locations as the Ringold, were originally thought to be the time equivalent of the Ringold. However, bone fragments in one loess exposure was identified as Pleistocene in age. Because of the presence of very thick petrocalcic soils developed in the loess, it is assigned to an earlier age than the dominant Palouse loess, which is correlated with the time of Wisconsinan glaciation (75,000 - 10,000 YBP) of the midcontinent.

The Palouse Formation is more widespread than the pre-Palouse loess and is distinguished by three separate soil horizons developed within the formation. These have not been dated but are interpreted--because they underly the catastrophic flood gravels of the late Pleistocene--to be of early Wisconsinan age (75,000-35,000 YBP). A younger, lighter colored loess overlies the eroded surface of the Palouse loess in most places.

The youngest Pleistocene flood deposits are the Missoula flood gravels, known as the Pasco Gravel, and the slackwater fine-grained Touchet beds. These fine sand and silt beds are recognized by their distinctive rhythmic succession similar to the Bouma turbidite sequence and by the presence of clastic dikes thought to have been injected into the Touchet beds under high hydraulic pressure during the Missoula floods. The age of the gravels has been determined by the presence of a layer of Mount St. Helens set "S" ash, which was dated at 13,000 YBP.

The last Pleistocene deposits were loess and alluvium and are also dated at 12,000 YBP by volcanic ash that underlies the loess. The ash overlies eroded Touchet beds. Holocene deposits consist of loess and alluvium, the latter confined to present river courses. While resembling Touchet beds from which most of the sediment was derived, the Holocene alluvium may be distinguished by a lack of rhythmic structure, restriction to present stream valleys, and the absence of clastic dikes.

2.5.1.1.1.3 Age Dating of Stratigraphic Units

The applicant has undertaken many absolute and relative age-dating methods for the site area and region because the gaps in the geologic record have led to an absence of cross-cutting evidence in some instances that could bracket the time of critical events, such as a fault. All of the methods provide increased insight into the knowledge of the age of stratigraphic units in this area. Some of the techniques, however, have limitations in their use in the Pasco Basin.

Therefore, in areas where clear cross-cutting relationships are not known, the staff relies on varied sources of information to form its judgments of the timing of events critical to its determination of the safety of the site. Some of these sources and techniques are briefly reviewed below.

Two paleomagnetic studies (Sierra Geophysics, 1982a and b), one for the Southeast Anticline investigation and one at the Skagit/Hanford site, have provided evidence that sedimentary units of 730,000 YBP are present in and around the Pasco Basin. This fills the large gap in the stratigraphic record between 10-^{3}-MY-old Ringold and 200,000-yr-old Pleistocene sediments. Because of the possible lensoid character of the sediments dated, extrapolation from one locale to another may require more detailed stratigraphic correlation of the units in the area before the information can be used on a regional basis. However, the presence of undeformed units of 730,000 YBP increases the staff's confidence in the safety of the site and the surrounding region.

The Ringold Formation is dated at 10-^{3} MY on the basis of fossil and paleomagnetic information and is deposited as stream sediments in the low-lying Pasco Basin. Although it is not present on the various anticlinal ridges outside the basin, it is present throughout the basin and proved valuable in determining the noncapability of the Southeast Anticline Fault (Golder, 1982).

The pre-Wisconsinan flood deposits of 200,000-yr age are limited in extent and restricted to two localities at the southwest edge of the Pasco Basin. But they overlie the Ringold Formation within the basin and therefore may be useful in proving noncapability of faults at depth that may be found close to the site.

The late Pleistocene or Missoula flood deposits have volcanic ash marker beds that limit the age to between 13,000 and 19,000 YBP. This can give insight into ages of faults even if they are too young to meet the 35,000-year criteria of noncapability in Appendix A to 10 CFR 100. The presence of the clastic dikes is useful in determining relative ages of deformation, if the hydraulic injection hypothesis during catastrophic flooding is accepted as the mechanism of their emplacement. The applicant has provided convincing arguments and evidence to support this mechanism (Woodward-Clyde 1981a), including:

(1) The dikes are restricted to the Pasco gravels and Touchet rhythmic beds and underlying strata. None have intruded younger sediments.

(2) The dikes appear to have intruded from above downward into the strata, with only a few intruding upward.

(3) All dikes occur below the maximum level of the Missoula flood waters.

(4) Dikes are found frequently truncated by younger flood deposits.

The staff concludes from this line of reasoning that the dikes formed during the late Pleistocene meltwater floods.

Another tool in the rock record that has been used in an effort to constrain time of faulting in the area is isotopic dating of caliche rinds on basalt gravel and calcrete soils which record the weathering process. Uranium-thorium isotopic dating techniques have been applied to the rind and/or soil of unfaulted units capping faults, such as the Finley Quarry Faults, giving probable ages of between 75,000 and 200,000 YBP (Woodward-Clyde, 1981c).

Where faults in the area are uncapped because of erosion or nondeposition, their ages are determined based upon the weight of geologic evidence, including the degree to which different units have been folded or offset within the sequence, the relationships of the folding and faulting processes to each other, and other information that may shed light on the relative time of an event. These are described in the relevant sections.

2.5.1.1.2 Regional Structure and Tectonics

Much new information is now available about the structural history and tectonics of the Columbia River Basalt Plateau and surrounding region because of the investigations at the Hanford Reservation. This information includes subsurface data from drilling, geophysical studies, and reflection and refraction seismology. Some details of the structure, tectonics, and ages of deformation are not yet available and are, therefore, subject to interpretation.

The information now available indicates that the tectonic character of the area has not changed through time and that the area is still undergoing north-south compression, at very low strain rates. This which may be localized mainly along the eastern boundary of CLEW, known as the Rattlesnake-Wallula Alignment (RAW), and the ridges at the northeast and southwest edges of the Yakima fold belt. Some of the evidence for ongoing tectonic activity includes (1) the capability of faults associated with east-west trending folds to the southwest (Toppenish Ridge) and the northeast (Gable Mountain), (2) the microearthquake swarms associated with Saddle Mountain at the north end of the Pasco Basin, and (3) offset of late Pleistocene and possibly Holocene sediments along RAW (Shannon and Wilson, 1979). For further discussion of microearthquake swarms and the seismic potential of Toppenish Ridge and Gable Mountain, see Section 2.5.2 and Appendix H of this SSER.

2.5.1.1.2.1 Yakima Fold Belt

The Pasco Basin is surrounded on three sides by the anticlinal ridges of the Yakima fold belt, which appear to have been developed at least in part during deformation that was contemporaneous with basalt extrusion. Investigations in the Pasco Basin and vicinity suggest that the peak of deformation was in the late Miocene, between 10 and 5 MYBP, with evidence of waning deformation through the deposition of the Ringold Formation and continuing to the present. Several folds in the belt have thrust faults associated with them. The faults were originally interpreted by the applicant to be the results of the relative low ductility of the basalt that resulted in brittle behavior during folding, causing faults to develop. The applicant has reevaluated this position and now regards at least some of the faults to be primary, i.e., not the effects of folding (WNP-2 FSAR).

Umtanum Ridge, with several reverse faults associated with the overturned fold, is now thought by the applicant's consultants to be part of an imbricate thrust zone partially detached from the basement. The zone includes Frenchman Hills and Saddle Mountains. This is a departure from the original interpretation of primary folding, with faulting being secondary to the folding process. Drilling into the basal fault has shown no displacement of Quaternary deposits. The applicant has further indicated that 6-MY-old basalts were not involved in the thrusting and/or folding of this structure. The staff concludes that the fault is most likely not capable and therefore does not affect the design basis of the plant.

2.5.1.1.2.2 Gable Mountain Faults

Gable Mountain, part of the eastern extension of Umtanum Ridge that rises above the sediments in the Pasco Basin, contains five faults. A detailed investigation of the folds and faults of Umtanum Ridge-Gable Butte-Gable Mountain performed by NESCO (Northwest Energy Services Co.) for the Skagit/Hanford PSAR, and referenced by the applicant in the WNP-2 FSAR, was undertaken to improve the data base and to resolve differences of opinion concerning the relationships of these structures. The study included photogeologic analysis, mapping, trenching, drilling, and geophysical investigations.

At the CP stage of investigation, two surface faults were known on Gable Mountain: the Central and West Faults. The recent investigation for Skagit led to the discovery of three more faults: the North-Dipping Reverse Fault; the South Fault, which was originally mapped as an extension of the Central Fault, and the DB-10 Fault. Trenching led to the recognition of displacement of Missoula-age gravels (19,000-13,000 YBP) along the Central Fault.

Gable Mountain is a west-northwest-trending anticline deformed by second generation folds that cross the main fold axis obliquely. The capability of faults associated with this structure is of concern because Gable Mountain, which comes within 14.6 km (9 mi) of the site, is the closest surface structure. Discussion and details of the new and reevaluated faults follow.

Central Fault: The closest known capable fault to the site, the Central Fault, is 18 km (11.5 mi) to the northwest. A steeply dipping reverse fault, this structure crosses the Gable Mountain fold trend between the east and west anticlines at a high angle, strikes east-northeastward, and dips to the southeast. Drill cores indicate a maximum cumulative stratigraphic displacement of 60 m (200 ft). The offset of 19,000-13,000-yr-old glacial flood deposits observed in the trenches occurs only at the base of the sediments and appears to be no more than 6 cm (0.2 ft) of reverse movement. The staff has seen the trenches and concurs with the applicant's assessment of the amount of the latest displacement. The rate of displacement is estimated to be 7.62 cm (3 in.)/13,000 yrs or 6×10^{-4} cm/yr.

The observed length of the fault is 335 m (1100 ft), but the total length estimated by the applicant is 3 km (2 mi). This estimate is based in part on the evidence in the trenches, where the amount of offset decreases to zero to the north. The south end of the fault is not constrained by definitive techniques, but drill core evidence suggests that the fault dies out southward. Because the fault cannot be traced beyond the fold, it is assumed to be associated with the folding process.

Thus the maximum length of the fault is assumed to be the width of the Gable Mountain fold that it crosses. The staff accepts this assessment of the fault length as reasonable on the basis of the geologic information available, including the observed dying out of surface displacement in the trenches.

The applicant interprets the Central Fault as originating as a tear fault in the brittle basalt during folding, which implies a minor secondary tectonic structure of shallow depth and, therefore, of relatively little seismic significance. The applicant also hypothesizes an alternative and nontectonic origin for the latest displacement, involving hydraulic uplift caused by extremely high fluid pressures during the catastrophic late glacial floods.

That the region was once subjected to high fluid pressure is recognized in the presence of clastic dikes in the Missoula flood deposits, and, therefore, nontectonic offset on the fault is conceivable. However, the fact that the region is still undergoing tectonic strain in the form of north-south compression--as indicated by the presence of microearthquake swarms in part of the area, historic and recent macroearthquakes, and young faults on Toppenish Ridge and near Wallula Gap--argues for the tectonic capability of the Central Fault. The staff therefore considers it prudent and in the interest of conservatism to assume the displacement to be of tectonic origin.

Discussion of the maximum magnitude earthquake likely to occur on the Central Fault will be found in Section 2.5.2 and in Appendix H of this SSER.

North-Dipping Reverse Fault: A previously undetected buried fault striking east-west with a regionally anomalous dip to the north was encountered during the drilling program. The fault is actually a zone of numerous imbricate thrusts that displaces the limb of the West Anticline. Reverse dip-slip displacement is interpreted from drilling data to be 135 m (445 ft). Although the fault can be traced for 610 m (2000 ft) along the south flank of the West Anticline of the Gable Mountain structure, it is interpreted to be the length of the West Anticline, 6.6 km (4 mi), because of the assumption that the fault was generated by folding of brittle basalt layers.

There is no direct information on the age of latest movement. However, the structural relationship of the North-Dipping Reverse Fault to a probable capable fault such that--in the judgment of the staff--movement on one (the South Fault discussed below) is likely to cause movement on the other, indicates to the staff that the fault should also be considered capable, in accordance with Appendix A to 10 CFR 100.

South Fault: On the south limb of the Gable Mountain West Anticline is the curvilinear east-west trace of the South Fault, about 45 m (1500 ft) south of the southern termination of the Central Fault and 350 m (1150 ft) north of the projected surface trace of the essentially parallel North-Dipping Reverse Fault.

Originally mapped as a continuation of the Central Fault, the South-Dipping South Fault is now viewed by the applicant as separate and unconnected with that fault. This view is based on information obtained from trenching, drill cores, and down-hole geophysical logs done for the Skagit/Hanford application.

Based on drill hole data, the South Fault is apparently confined to the hanging wall of the North-Dipping Reverse Fault, terminating downward at the basal shear zone of the north-dipping reverse imbricate thrusts, about 61 m (200 ft) below the surface. Cumulative dip-slip displacement on the fault is about 15 m (50 ft).

The observed length from trench and drill core data is 518 m (1700 ft), but the maximum length is interpreted to be the length of the West Anticline, 6.6 km (4 mi), partly because of its association with the North-Dipping Reverse Fault. The South Fault's confinement to the hanging wall of the North-Dipping Fault, and its opposite dip, has led to the interpretation that it is a minor anthithetic fault related to the folding of the West Anticline of Gable Mountain.

Slickensides on clastic dikes injected along the fault plane indicate a young age for the faulting, as the dikes are thought to have derived from glaciofluvial sediments correlated with Missoula flood deposits 19,000 - 13,000 YBP.

Based on this observation, the staff concludes that the South Fault is capable according to the guidelines of Appendix A to 10 CFR 100. Discussions of the seismic significance of this and other Gable Mountain faults are in Section 2.5.2 and Appendix H of this SSER.

West Fault: Another small surface fault, the West Fault, was previously mapped as a reverse fault. Trenching for the Skagit/Hanford investigation of Gable Mountain has provided information that shows the fault to cross the West Anticline striking N34°E with normal, down-to-the-west, cumulative displacement of 7.6 m (25 ft). The fault is inferred to be 0.8 km (0.5 mi) in length, occurring mainly across the hinge area of the west fold where the maximum displacement is observed. These relations suggest to the applicant that the faulting is the result of differential strain along the fold hinge. Although no minimum age for the fault could be determined because of the absence of cover materials younger than the basalts, the small size of the fault, especially compared to the Gable Mountain faults determined to be capable, is considered by the applicant to render the fault of no seismic significance. The staff concurs with this assessment for the reason stated. Further discussion of this is in Section 2.5.2 of this SSER.

DB-10 Fault: A buried fault about 1.6 km (1 mi) south of the east end of Gable Mountain was identified by drilling and investigated by geophysical techniques. It appears to be a 0.8 km (0.5 mi) north-south striking fault across the hinge area of the East Anticline, with a maximum stratigraphic displacement of 50 m (165 ft). Although minimum age data are lacking, the applicant considers this fault to be of no seismic significance because of its small size, (as with the West Fault). The staff concurs with this assessment. Further discussion of this is in Section 2.5.2.

All of the foregoing faults on Gable Mountain were investigated by NESCO for Skagit, and described by the applicant from a report on Gable Mountain by Golder Associates (Golder, 1981a); they are characterized by the applicant as secondary and genetically related to the folding process. Although this observation has not been clearly demonstrated, the dying out of the fault north and south on the fold limbs, the gradual increase of stratigraphic throw to a maximum at the fold hinge, and the anomalous orientations of the faults with respect to the regional strain (north-south compression) do support the secondary nature of the faulting on Gable Mountain. The staff, therefore, accepts this interpretation.

The seismic significance of the Gable Mountain faults, however, is of concern because at 16 km (10 mi) from the plant, they are the closest known capable faults to the site. Estimates of the maximum magnitude earthquake that may be expected to occur on any of these faults are discussed in Section 2.5.2 and in Appendix H of this SSER. They are considered conservative because the staff has determined them to be capable despite such factors as: (1) the possible nontectonic origin of the latest movement on the Central Fault and (2) the possible secondary origin of the faults with folding the primary response to regional strain. the staff considers that these factors have some merit.

A related, en echelon structure, the Southeast Anticline, is bounded on the eastern limb by a fault that was encountered in a drill core recently. The applicant undertook an investigation to determine the geometry, age, and structural relationships of the fault (Golder, 1982). The investigation included an extensive drilling program to determine the dip direction and angle, which strata were involved in the faulting, and the amount of offset. A full report of this investigation has provided evidence that the fault is capped by unfaulted lower Ringold. This limits the age of faulting to more than 10 MYBP, the estimated age of the oldest Ringold. The applicant concludes, therefore, that the fault is not capable according to the definition in Appendix A to 10 CFR 100.

The staff, on a visit to the site area, viewed the cores of the Southeast Anticline Fault and observed the brecciated zones of the basalt in the cores. Cores of Ringold determined by the applicant to overlie the upward projection of the fault were coherent and showed no sign of deformation. Accordingly, the staff concurs with this assessment and finds the Southeast Anticline Fault not capable.

2.5.1.1.2.3 Cle Elum-Wallula (CLEW) Zone of Deformation

The Cle Elum-Wallula (CLEW) Zone of Deformation is a broad zone trending northwest-southeast in which the Yakima fold belt appears to have been folded and subsequently deformed. Folds outside the belt to the northeast and southwest trend roughly east-west, while within the belt the sinuous axial traces trend northwest-southeast.

On the west, the deformed folds are bounded by the Cleman-Snipes Lineament from at least the west side of Cleman Mountain at the north end, southeastward through the west side of Snipes Mountain, to Horse Heaven Hills, which truncate the lineament. This linear feature parallels the eastern boundary.

The eastern boundary, the Rattlesnake-Wallula alignment (RAW), which is 19.5 km (11.9 mi) from the site, has several features suggesting ongoing deformation. They are the Wallula Gap Fault and its southern extension, which has indications of a youthful age and therefore probable capability (described later in this section and in the report from the staff consultant, D. B. Slemmons, attached as Appendix H of this SSER).

Three fundamental considerations concerning CLEW with respect to the WNP-2 site are: (1) the capability of faults within and at the eastern boundary, the RAW, (2) the length of RAW for purposes of maximum magnitude estimates, which involves determination of whether RAW consists of short fault segments or one long through-going fault, and (3) the nature of the fault (strike-slip, reverse slip, or reverse-oblique).

The staff concludes, based on evidence presented in the following sections and in Appendix H, that

(1) RAW is demonstrably capable south of Wallula Gap and is assumed to be capable from Wallula Gap northwest to the bend in Rattlesnake Mountain.

(2) RAW is approximately 120 km (72 mi) long and is assumed to be continuous at or near the surface.

(3) RAW is most likely a right lateral strike-slip fault with some component of reverse-oblique motion.

(4) The Cold Creek Lineament is not a tectonic structure, and, therefore, not a part of the CLEW/RAW Zone of Deformation.

Several faults and fault-like features occur within and at the boundaries of the zone. Most faults parallel the folds but a few younger faults and linear features within CLEW cut across the trend of the folds such as the Moxee Valley and Wenas Valley linear structures. The most significant features are discussed below.

Moxee Valley and Wenas Valley Faults: In a remote-sensing study of the region done for the WNP-1 and -4 PSAR, two series of possibly related linear structures were identified using Landsat imagery and aerial photography (Glass, 1977, Appendix 2R-K). In the report, parts of both linear zones were described as possibly offsetting Holocene alluvium.

Because Moxee Valley and Wenas Valley are 65 km (40 mi) and 95 km (57 mi) from the site at their closest approach and therefore not considered of any seismic significance, these structures were not reported in the WNP-2 FSAR. However, the staff considered that the capability of faults within CLEW would be indicative of continuing present-day deformation and would bear on the probable capability of other faults within and at the boundaries of the zone. Therefore the applicant was asked to examine these two linear features.

As described in the WNP-1 and -4 PSAR, the Moxee Valley Fault consisted of two branches. A single fault trend~~ing~~s north-northwest, beginning on Rattlesnake Hill and crossing Moxee Valley, Yakima Ridge, and Cold Creek Valley and terminates on Umtanum Ridge. In places right lateral displacement of basalt can be seen, but no offset of young alluvium was observed. In Moxee Valley, it was reported that a more westerly trending branch of the fault parallelled the valley and appeared as a zone of short parallel shears or linear features. These were described in the report as displacing young alluvium.

Further northwest, almost on strike with the "western branch" of the Moxee Valley Fault, a linear feature in Wenas Valley--described as a possible normal, oblique, fresh-looking fault--was observed.

A reconnaissance investigation by the applicant of these two valleys led to the determination that (1) the Wenas Valley "Fault" was more likely a gravity-induced slip along a weak sedimentary interbed between steeply dipping basalt units on the south flank of Umtanum Ridge; (2) the "young alluvium" supposedly displaced by the "western branch" of the Moxee Valley Fault was, in fact, a bedrock surface with no evidence of fault displacement; and (3) the eastern or main branch of the Moxee Valley Fault did not displace any young deposits anywhere along the trace of the fault as far as it was followed.

On a visit to the area, the staff concurred with the applicant's view that the Wenas Valley features are more likely to have been the result of gravity rather than tectonics, partly because a normal fault in a synclinal valley that formed from compression was inconsistent with the regional stress regime. The normal fault would require north-south extension in a zone known to be undergoing north-south compression.

The staff also examined the bedrock surface on what was called the western branch of the Moxee Valley Fault. This was originally described as young alluvium, which led to the postulation of a young fault. The staff agreed with the applicant's observation that there was no evidence of faulting on the subtle escarpments that caused the linear features. Although the applicant postulated differential erosion along joints parallel with Moxee Valley as the probable origin of the linear features, few joint sets were observed to warrant such features. The staff concurs, however, with the assessment that the features are probably not of tectonic origin, because the bedrock along the subtle escarpments showed no evidence of faulting or other signs of deformation.

The Cold Creek Lineament, a linear feature that appears remarkably straight and continuous on Landsat imagery and lower altitude aerial photography, is subparallel to the RAW alignment. It can be traced from Wallula Gap, trending slightly more northerly than the RAW trend, through Kennewick, Richland, Horn Rapids Ditch, and Cold Creek, up to and across the eastern end of Umtanum Ridge. Because the lineament is 85 km (53 mi) long and at its closest approach comes within 12.5 km (8 mi) of the plant site, the applicant undertook a detailed investigation--including field analysis and examination of cores from other studies that cross the lineament, and aeromagnetic, gravity, and seismic reflection and refraction data. The staff, on a visit to the area, observed the field and core evidence that strongly supported a nontectonic origin for the lineament. Some of the evidence and lines of reasoning that support the nontectonic origin are:

(1) The Kennewick segment of the lineament consists of a linear terrace of gravels that locally has vegetation of contrasting colors on and at the base of the terrace. Where exposed, the gravels show no evidence of offset or tectonic disturbance.

(2) At Pasco, the straight course of the Columbia River close to the Cold Creek Lineament segment between Kennewick and Richland, is developed on gravels. Cores of the basalt bedrock 30.5 m (100 ft) below the river bed, taken recently in connection with construction of a bridge across the Columbia River, show no sign of shearing or other evidences of deformation. Also

cores taken at regular intervals across the river show no change in elevation of specific basalt and sedimentary interbed units.

(3) The Horn Rapids segment of the lineament has basalt exposures that show no sign of shearing or other evidence of deformation. The thin edge of the Ice Harbor Basalt crosses the lineament here and shows no sign of lateral offset.

(4) Basalt cores from the Horn Rapids vicinity that cross the lineament taken in 1971 (Blume, 1971) show no sign of deformation or change in elevation of any units.

(5) Aeromagnetic data (Weston, 1978 and 1980) across the lineament show no characteristic signature or magnetic expression of the lineament along its entire extent.

(6) Seismic reflection data from Rockwell (1981) at the northern end shows no evidence of a subsurface planar structure across the lineament.

Based on this evidence the applicant concludes, and the staff concurs, that the Cold Creek Lineament is not a tectonic structure and most likely developed from surface fluvial and sedimentation processes.

Rattlesnake-Wallula (RAW) Alignment: The eastern boundary of CLEW, which is 19.5 km (11.9 mi) from the plant site, separates CLEW and the Pasco Basin. This boundary varies in character from the north end where Umtanum and Yakima Ridge Anticlines, just south of the east-west course of the Columbia River, plunge abruptly below the basin sediments. South of that Rattlesnake Hill turns from an almost east-west trend to a north-northwest-south-southeast trend. At its southern termination, where the Yakima River valley crosses from the fold belt to the Pasco Basin, a series of small, doubly plunging anticlines form the boundary, continuing with the southeasterly trend of Rattlesnake Hill, to Wallula Gap. At the Gap, the alignment becomes the Wallula Gap Fault, and the anticlines gradually change to a monocline south of the gap. This alignment can be traced from the bend in Rattlesnake Hill to the Hite Fault east of Milton-Freewater, making the total length of RAW 120 km (72 mi).

The applicant has mapped several small faults in the anticlines along the RAW trend. In each case the fault parallels the fold and, therefore, the CLEW boundary. In two places the faults have been investigated in detail. In Finley Quarry, at the north end of the Butte, and at Yellepit, just north of Wallula Gap, trenching and radiometric dating of caliche rinds and volcanic ash beds have been used to investigate the capability of these faults.

The fault zone at Finley Quarry consists of three reverse faults with total cumulative apparent displacement estimates of less than 61 m (200 ft). At least two of the faults are capped by gravels with calcareous rinds that have been dated by uranium/thorium methods and determined to be at least 75,000 years old and may be as old as 200,000 to 250,000 years old. The staff has examined these exposures and evaluated the applicant's arguments. While they have considerable merit, the staff concludes that for a fault zone of such complexity and length and for the estimated amount of offset, it is prudent to consider that this zone has had multiple movement. In this context, the 500,000-yr limit for noncapability established in 10CFR Appendix A should be utilized. These faults therefore are part of the evidence for the capability of RAW.

Two fault strands--one, N64W, trending southeast from Finley Quarry, and the other from Yellepit and Horse Heaven Hills at N80W--cross Wallula Gap east-southeastward and merge into the Wallula Gap Fault. This linear fault can be traced to the NNE-trending Hite Fault, east of Milton-Freewater.

Several more southeasterly trending splays, mapped as normal faults (Shannon and Wilson, 1979), characterize the Wallula Fault Zone. These include Vansycle Canyon, Warm Springs Canyon, and Little Dry Creek Canyon. Along the Wallula Gap Fault and the splays--interpreted as reidel shears (subsidiary shears resulting from secondary strains along a strike-slip fault) off a main right lateral fault--are several indications of late Pleistocene and/or Holocene displacement. The applicant has listed several localities with evidence of youthful, late Quaternary faulting offsetting undated colluvium, Palouse Formation, Touchet Formation, and younger loess. The westernmost locality is the Finley Quarry Fault already mentioned. Youthful faulting is also recognized in Vansycle Canyon, Warm Spring Canyon, the Barrett Fault (which cuts Touchet beds and offsets clastic dikes) the Milton-Freewater Fault, the Buroker Fault east of Walla Walla (where the base of the Palouse Formation is offset 0.5 m), a youthful appearing fault south of Umapine, and Little Dry Creek Fault (where basalt and Palouse beds are displaced about 0.5 m).

Although most of the evidence for recent faulting is on reidel shear splays of the main Wallula Gap Fault, their presence within the fault zone and apparent relationship to it leads to the assumption that the Wallula Gap segment of RAW is capable.

Length of RAW: In the applicant's view, RAW consists of three distinct domains in the site vicinity: (1) Domain I at the north end is composed mainly of folds north of Rattlesnake Hill; (2) Domain II consists of discontinuous aligned folds and faults, and (3) Domain III is a continuous reverse-oblique fault with little folding along the trend, south of Wallula Gap.

This interpretation of the CLEW boundary is important to the applicant's argument for the segmentation of RAW (Domain II of the CLEW boundary) because it bears on the maximum magnitude earthquake possible, assuming capability of this part of RAW, which is closest to the plant site. If RAW consists of short fault segments it constrains the size of the earthquake that is possible. The applicant indicates there is no evidence that the faults mapped on the anticlinal ridges from Rattlesnake Hill southward continue between the ridges, and that the longest fault segment is the mapped fault near the north end of Rattlesnake Hill, which is 7 km (4.2 mi) long. This hill is 19.5 km (11.9 mi) from the plant site.

However magnetic and gravity data along several traverses between the Butte and Game Farm Hill (K-hill) by Rockwell (Cochran, 1981) were interpreted by the investigator to show a fault that the investigator regarded as an extension of the Finley Quarry Fault. In addition, the investigator postulated a second fault splaying from the Finley Quarry Fault.

The applicant rejected Cochran's interpretation on the basis that (1) the sharp negative magnetic anomalies directly on strike with the mapped fault in Finley

Quarry did not match the magnetic signature of the mapped fault, (2) the negative gravity anomalies coincident with the magnetic anomalies were not asymmetrical and therefore do not indicate a fault, and (3) there is geologic field evidence of a buried channel in the basalt at the approximate location of the negative anomalies. The applicant's preferred interpretation of Cochran's data is that of a buried channel in the basalt.

One of the applicant's main arguments is that the two magnetic profiles across the mapped fault on the Butte were considerably different from each other as well as from the other profiles and, therefore, it is not possible to characterize an identifying signature for the fault.

While the staff does not dispute these points, several other factors not considered by the applicant must be given weight in evaluating Cochran's data and interpretation. These include the following:

(1) In response to an early question (360.005), the applicant's geophysics consultants modeled several aeromagnetic traverses across RAW as a fault on several of the brachyanticlines; the magnetic signature was almost identical to Cochran's profiles.

(2) The applicant's consultants modelled a series of profiles from aeromagnetic data along several other flight lines--both across and between the brachyanticlines--that show identical signatures and are aligned so remarkably that the interpretation of a linear, throughgoing fault is difficult to avoid.

Based on the foregoing, the staff concludes that for the purpose of evaluating the seismic design, RAW is a throughgoing capable fault 120 km (74.6 mi) long.

Several tectonic models have been proposed to account for the geometry and anomalies of CLEW, including right lateral strike-slip faulting at depth deforming the partially detached basalt cover (Laubscher, 1981; Davis, 1981), detachment folding of the basalt over a deep-seated rigid buttesss (Price, 1982), or detached flexures over fault ramps (Bruhn, 1982). All these authors agree, however, that the structures are the response to regional strain resulting from north-south compression.

Of the several tectonic models that have been proposed, right lateral strike-slip, (very likely with some reverse-slip component), probably best explains most of the observed features along this zone of deformation. The evidence for strike-slip motion on RAW includes:

(1) A linear structure with an orientation compatible with right lateral strike-slip motion due to north-south compression, which has been ascertained by the east-west orientation of folds outside CLEW, and fault plane solutions from local earthquakes.

(2) The incompatibility of a northwest-southeast thrust fault orientation with north-south compression; even if movement on RAW is reverse-oblique, the origin of a northwest-southeast fault cannot have been thrust or reverse with north-south compression.

(3) Horizontal slickensides along many faults along RAW.

(4) An en echelon arrangement in correct orientation of subsidiary faults (Vansycle Canyon, Warms Springs Canyon) mapped as normal faults (down to the northeast on northwest-southeast orientation) and as reidel shears (secondary shears) related to a northwest-southeast strike-slip fault.

(5) A linear and continuous fault from Rattlesnake Hill to Milton-Freewater is characteristic of strike-slip faulting.

The staff concludes, therefore, that RAW is a throughgoing capable, right lateral strike-slip fault with some reverse and/or reverse-oblique motion, and is about 120 km (74.6 mi) long from Rattlesnake Hill to the Hite Fault. (See ~~Slemmons,~~ Appendix H of this SSER, for supporting arguments.)

2.5.1.2 Site Geology

WNP-2 is in the Pasco Basin, a subdivision of the Columbia River Basalt Plateau Tectonic Province. The basin is surrounded on three sides by structures of the Yakima fold belt and RAW, and on the east by the Channeled Scablands, a relatively low relief area, with no visible bedrock structures, that was dissected by glacial and glacial meltwater scouring.

The surface of the basin is covered with wind-blown deposits and dunes. The WNP-2 site is south of a dune-covered area of low undulating topography, 5.4 km (3.2 mi) west of the north-south course of the Columbia River.

The stratigraphy and substructure of the site and vicinity were determined by 140 boreholes drilled by the applicant and others, excavation mapping, and geophysical investigations. Below the site, the bedrock consists of basalt of the Columbia River Basalt Group with intercalated Ellensburg Formation sediment, up to about 152 m (50o ft) below the surface. This is overlain by 137 m (450+ ft) of the lower and middle members of the Ringold Formation consisting of silt, clays, and gravels. Overlying this and below the aeolian deposits are up to 30.5 m (100 ft) of glaciofluvial deposits, mainly Pasco Gravels of Missoula flood origin.

The configuration of the basalt surface as shown by top of basalt structure contours developed from borehole, seismic refraction, gravity, and magnetic data is of broad, low undulations or irregular discontinuous folds. The site is located above a depression just east of the east limb of the Cold Creek syncline, one of the major structures in the basalt. The Ringold becomes thin and thickens, depending in part on the basalt surface topography.

The applicant reports that examination of aerial photography and ground inspection uncovered no evidence of surface faulting. However, in a report to DOE by Rockwell (RHO-BWI-ST-14), subsurface structures designated normal faults or dikes in the Pasco Basin, some within 8 km (5 mi) of the plant, have been identified. The determination was based on aeromagne ic data modelled mathematically by a technique known as Werner Deconvolution. In response to an informal question from the staff concerning this information, the applicant pointed to an explanation within the ST-14 report that states:

↓

It should be emphasized that a fault-like solution does not necessarily mean that an actual fault is present. Rather, the fault-like solution indicates that a horizontal magnetic source terminates at a particular location. In the Cold Creek syncline, horizontal termination of magnetic sources (lava flows) can be caused by flow pinchout, possible abrupt changes in the magnetic properties of a flow, steep anticlinal/synclinal flanks, as well as fault displacement.

The applicant has stated that some of the Werner solutions, checked with seismic refraction and reflection data, do not have corresponding structural features at depth, and others are gently dipping limbs of folds. The applicant suggests that the structure interpreted from Werner solutions to be at the surface at the plant site is, in fact, the plant itself causing the anomaly. Inasmuch as excavation mapping at the plant site showed evidence of faulting, the staff accepts this evaluation.

However, the staff reviewer of the Skagit/Hanford application and the staff's advisor, USGS, recently identified numerous anomalies in seismic reflection and refraction data in the site area, some within 8 km (5 mi) of the plant, that may be interpreted as faults in the basalt. The resolution of the data is not fine enough to determine which if any suprabasalt strata are offset, so that capability of these possible faults cannot be assessed on these data alone. However, on the basis of the early construction drilling program in the WNP-2 site area, borehole data from other studies out to more than 16 km (10 mi) of the site, a continuity study of the Ringhold Formation exposed in the Cliffs of the Columbia River, and excavation mapping, no capable faults or faults in the suprabasalt strata have been identified within 8 km (5 mi) of the site.

The Skagit/Hanford applicant is presently engaged in an integrated review of subsurface data. The WNP-2 applicant has committed to maintain communication with the Skagit/Hanford applicant to keep abreast of developments in that review. Barring newly developed information to the contrary, the staff anticipates a satisfactory resolution of the seismic profiles that will not adversely affect its assessment of the safety of the site. At present, therefore, the staff concludes there are no capable faults at or within 8 km of the plant site.

2.5.1.3 Volcanic Hazards

2.5.1.3.1 Ash Fall

Because the WNP-2 site is situated less than 150 mi (250 km) from the present or recent active volcanoes of the Cascade Mountains, a review of potential ash-fall is necessary in evaluating the safety of the site. Several thin seams of volcanic ash (2.5-5 cm (1-2 in.)) intercalated with sedimentary interbeds in the Pasco Basin vicinity have been reported in the FSAR and in other studies of the region. Some of these are from Mount St. Helens (222 km (138 mi) from the site) dating back to 13,000 YBP; Glacier Peak (230 km (143 mi) from the site); and Mount Mazama (about 402 km (250 mi) from the site). The most recent major eruption of Mount St. Helens--that of May 18, 1980--left a very thin dusting over the area. Occasionally lenses of ash up to 1.5 m (5 ft) thick and tens ?? of feet or less in area have been observed. The applicant argues that small lenses of this type cannot have been free airfall material, which leaves a layer of uniform thickness over a relatively wide area, and must therefore be reworked ash redeposited by streams in lenses. The staff agrees with this interpretation.

In estimating a design ashfall, the applicant considered the distance versus thickness curves used for the Pebble Springs site developed by the USGS, adapting them for potential ashfall from Mount Adams, 165 km (107 mi) from the site (the closest volcano to the site), and Mount Rainier, 193 km (125 mi) from the site. However, the USGS considers it prudent to use potential ashfall from Mount St. Helens, 222 km from the site, because it has a history of more continuous recent activity than Mount Rainier, and from Mount Adams, because it is the closest volcano to the site. (See Appendix G to this SSER.)

The design thickness chosen--7.4 cm (3 in.) of compacted ash--is conservative because it lies above the newly developed Mount St. Helens thickness-vs-distance curves of the USGS, based on the most recent measurements of Mount St. Helens ashfall.

The applicant, in the FSAR, used figures accepted in the Pebble Springs SER for the percentage of compaction that would result in the design ash thickness. At that time, 20%-40% was considered a reasonable estimate. Recent experience with Mount St. Helens 1980 ashfall suggests that compaction may be as high as 75% (see Appendix G). Based on the difference between the earlier and later, more conservative, compaction estimates of 50-60%, the amount of loose, uncompacted ash that will compact to the design thickness is 14.8-18.5 cm (5.8-7.4 in.), as opposed to 9.1-10.6 cm (3.6-4.2 in).

The ashfall rate based upon these new figures for uncompacted ash over an hypothesized 20-hour ashfall would be 0.74-0.92 cm/hr (0.3-0.36 in./hr).

The applicant estimates the median grain size of ash as 0.075 mm. Information on particle size from the Mount St. Helens ashfall of May 18, 1980 (Sarna-Wojcicki et al., 1981) indicates that the amount of ash of 0.075 mm estimated (50% of total) by the applicant is conservative.

? The applicant has committed to confer with the Trojan nuclear plant management to develop a warning system similar to ~~Trojan's~~ and tied to the USGS warning system. Specific design considerations to handle ashfall are discussed in Sections 2.4, 8.3, and 9.1 of this report.

2.5.1.3.2 Potential Lava Flow

? Although the Columbia Plateau and Pasco Basin consist of ~~several thousand feet~~ hundreds of meters of lava flows, the last lava flow to occur in the region was 6×10^6 YBP. The tectonic setting and relations that gave rise to the volcanism are no longer present, and, based on present understanding of tectonic processes, are not likely to return within the lifetime of a nuclear power plant. The applicant, in assessing the potential for a fissure flow at the site, references a probabilistic assessment conducted for DOE for the nuclear waste repository site at Hanford. The results of that study suggest that the annual percent probability for lava flows is extremely low, on the order of 8×10^{-6}. The staff considers this a reasonable assessment based on the aforementioned tectonic considerations and therefore concludes that lava flows will not be a hazard to the site.

2.5.2 Seismology

2.5.2.1 Background and Summary

The staff's OL review has been based on seismological information in the FSAR and its amendments. The review has concentrated on the following topics:

(1) Additional information on magnitude estimates of historical earthquakes within 320 km (200 mi) of the site.

(2) Seismicity in the site region (within 25 km, 15.6 mi) that the CP review.

(3) Determination of the maximum earthquake on faults or structures that have been found to be capable.

(4) Determination of the vibratory ground motion at the site as a result of (a) swarm earthquakes in the immediate vicinity of the site, (b) maximum earthquake on faults and structures that have been found to be capable, and (c) the largest historical earthquake within the Columbia River Basalt Plateau Tectonic Province that has not been associated with a tectonic structure.

(5) A comparison of the ground motions estimated above with the SSE approved for the CP.

In addition, the staff has reviewed current information regarding the December 14, 1872 earthquake and its potential impact on the licensing of the WNP-2 site.

These topics resulted from a review of the information that has been made available since the CP review, either in the literature or during subsequent analysis of the seismic conditions at the WNP site. This new information is described below.

2.5.2.2 Tectonic Province

The staff has used the tectonic province approach in assessing the appropriate design basis for earthquakes because none of the historic earthquakes of the region can be definitively associated with any known structure. Appendix A of 10 CFR 100 defines tectonic province as "a region of the North American continent characterized by a relative consistency of the geologic structural features contained therein."

The applicant has determined, and the staff concurs, that the WNP-2 site lies within a region termed by the applicant the "Columbia Plateau Tectonic Province." The Columbia Plateau is comprised of a series of Miocene-Pliocene basalt flows with sedimentary interbeds overlain by unconsolidated, occasionally cemented, Pliocene-Quaternary sediments. Because of the onlapping of the Columbia River basalts onto the adjacent provinces and the uncertainties regarding the distances that the surrounding geologic provinces continue beneath the basalts, the issue of the tectonic province boundary for ground motion estimates is discussed in more detail in Section 2.5.2.3.5. This section discusses the closest approach of an earthquake similar to the December 14, 1872 event which has been located in the Northern Cascades-Okanogan Tectonic Province north of the Columbia Plateau.

2.5.2.3 Historic Seismicity and Maximum Earthquake Potential on Faults and Structures Which Have Been Found To Be Capable

In the 1972 CP review, the staff and USGS used a Modified Mercalli Intensity (MMI) of VIII to characterize the maximum earthquake that could affect the WNP-2 site. This earthquake was assumed to occur along the northwest trending Rattlesnake-Wallula Lineament 19.5 km (12 mi) from the site. No attenuation of seismic energy was assumed to occur. That is, it was assumed that Modified Mercalli Intensity VIII could directly affect the site. During the OL review, the staff concluded that magnitude is a better indicator of earthquake source strength than intensity.

Intensity is a measure of observed damage and felt effects. It depends upon the size of the earthquake, its depth, the distance from the earthquake source, the nature of the geologic materials between the source and the point of observation, and the geologic conditions at the point of observation itself. Although an attempt is made in the intensity scale to account for differences in structural design, it is only done in a very general way.

Magnitude is a measure of earthquake source size using instrumental recordings of ground motion at different distances. Different magnitude scales measure different components of motion in different frequency ranges and care must be exercised in choosing the appropriate scale for the intended purpose. Local magnitude (M_L), the original magnitude scale, was developed from recordings of small earthquakes ($M_L < 5.0$) at distances between 20 and 600 km (12.5 and 375 mi) in southern California. It is determined utilizing the largest ground motion recorded on the Wood-Anderson seismograph. As a result, it is particularly sensitive to short period (about 0.8 seconds) horizontal motion. It is not applicable at distances greater than 600 km (375 mi) and must be used with great care outside of California. Surface wave magnitude (M_s) was developed subsequently to complement M_L for earthquakes of greater size and at different locations. It is determined from longer period (20 seconds) motion. Richter magnitude (M), as it is commonly used (but very often not precisely used), is equal to M_L for magnitudes less than about 6 and M_s for larger earthquakes (Nuttli, 1979). From the results of Nuttli (1979), Kanamori (1979), and Heaton et at. (1982), M_L is about equal to M_s for magnitudes near 6.0. According to Kanaomori (1979), at magnitudes greater than 6, the average M_L begins to deviate and becomes less than the average M_s for the same earthquake.

For the purposes of the WNP-2 review, the staff has utilized M_L where appropriate and possible. M_L gives an estimate of the ground motion at periods less than 1 second, which are the periods of interest for nuclear power plants. However, in deriving estimates for the maximum earthquake to be assumed on structures that have been found to be capable, the staff has had to use M_s and moment magnitude. As Kanamori (1978) states: "The amplitude of a seismic wave represents the energy released from a volume of crustal rock whose representative dimension is comparable to the wave length." Seismic waves used in the determination of M_L may only reach wave lengths of 6 km (3.7 mi). They cannot adequately reflect the energy release of earthquakes associated with ruptures tens of kilometers long. Seismic waves used in the determination of M_s have wave lengths of about 60 km (37.5 mi). Thus, in estimating earthquake size from fault studies, the most directly relatable magnitude scale based upon rupture lengths less than hundreds of kilometers would be M_s.

Empirical data relating magnitude (M_s) to fault parameters, such as Wyss (1979) and Slemmons (1982), are limited by the lack of fault parameter observations for magnitudes less than about $M_s = 6.0$. Thus, their fault parameter relationships are not easily applied to faults of limited dimensions. In these instances the staff has utilized the moment magnitude M relationship derived by Hanks and Kanamori (1979). Moment is defined to be the material rigidity (μ) times the fault area (A) times the average dislocation (d). If estimates can be made for the fault area and displacement, the moment magnitude of Hanks and Kanamori (1979) provides a convenient quantification of earthquake size. It is important to note that moment magnitude (M) is determined from the seismic moment and is related to actual faulting dimensions (moment can be determined from a variety of data, as discussed by Purcaru and Berckhemer, 1982).

2.5.2.3.1 Largest Historical Earthquake Within Columbia Plateau Tectonic Province

The largest historical earthquake within the Columbia Plateau was the July 16, 1936 Milton-Freewater earthquake. The Modified Mercalli Intensity of this event was MMI = VII (Coffman and Von Hake, 1972). The magnitude was estimated to be M_s = 5.75 (Gutenberg and Richter, 1965) and originally M_L = 6.1 (Woodward-Clyde, 1980a; WNP-2 FSAR, Amendment 18). As discussed in subsequent sections of this SSER, the applicant's consultant has recently submitted a report outlining how the M_L was determined and why it may be an overestimate of the source strength of the 1936 earthquake. The original instrumental epicenter was listed as 46.2°N and 118.2°W, while a recent instrumental data relocation places the event at 46.21°N and 118.23°W (Woodward-Clyde 1980a).

There has been much discussion concerning the association of this earthquake with either the Hite Fault system, which trends north-northeast, or the Rattlesnake-Wallula Lineament, which trends northwest. As discussed in the CP-SER for the WNP-1 and -4 (May 1975), "it appears likely that the intensity VII 1936 Milton Freewater event was associated with this structure" (Rattlesnake-Wallula Lineament). However, in past licensing actions, the staff has assumed an intensity MMI = VII (the same intensity as the 1936 earthquake) to be the maximum random earthquake in the Columbia Plateau. As noted, arguments exist for both association and nonassociation of the 1936 earthquake with structure.

The spatial and temporal location of aftershocks, along with the fault plane solution, tends to support a north-northeast trending fault plane, consistent with the Hite Fault system. An earthquake that occurred on April 8, 1979 has a fault plane solution that could be compatible with the Hite Fault system; its location, when connected to the 1936 epicenter, results in a line which is roughly parallel to the Hite Fault. The above evidence would suggest a northeast trending fault as the source of the 1936 earthquake.

The epicentral location of the 1936 earthquake is not well constrained. The location is 20 to 30 km (12.5 to 18.7 mi) west of the surface trace of the Hite Fault, with 90% confidence limits on location of about 11 km (6.9 mi) in the north-south direction and 16 km (10 mi) in the east-west direction. As discussed in Section 2.5.2.3 and as shown on Figures 2.5.5-20 and 2.5.5-21 of the WNP-2 FSAR, "No well defined correlation exists between the earthquake activity in the 320 km (200 mi) radius region surrounding the site, and individual mapped geologic structures, such as faults, grabens, or anticlines." This includes the Rattlesnake-Wallula Lineament. After reviewing the earthquake history of the Columbia Plateau, the staff, in general, agrees with the above conclusion. The Cleman-Snipes Lineament (south and west of the Rattlesnake-Wallula Alignment) may have historical (prior to 1969) seismicity associated with it (see FSAR Figure 2.5-52). However, in reviewing the detailed microearthquake monitoring during the past 11 years, one finds no obvious seismic lineation patterns that could be associated with any surface geologic structures including the Cleman-Snipes Lineament (whose closest approach is about 50 km (31.3 mi), southwest of the WNP-2 site).

Regarding the 1936 earthquake, the staff advisor, USGS, concludes that the fact that no known fault exists near the earthquake location "suggests the possibility that unknown faults may be buried near the site beneath the Columbia Plateau basalts and that an earthquake of 1936 type might occur on such a fault" (Appendix G). In addition, the USGS states: "association of the 1936 earthquake with a specific structure such as the Hite Fault or the Wallula Alignment is sufficiently uncertain that the possibility must be considered that a 1936 type earthquake could occur in the vicinity of the site."

Based upon the above discussion, it is the staff's position that the 1936 earthquake has not been definitively associated with a known geologic structure or fault because of the lack of constraint on the epicentral location and the lack of correlation between seismicity and geologic structure within the Columbia Plateau. As a result of this position, the staff requested that a site-specific response spectrum be developed assuming that an event similar to the 1936 earthquake occurred close to the WNP-2 site.

In recent OL reviews (Sequoyah SER, March 1979; Fermi SER, June 1981; Midland SER, May 1982) the staff has utilized the magnitude of historic earthquakes for defining the size of the target event for the site-specific spectrum. As discussed in FSAR Section 2.5.2.1.1.1, the 1936 earthquake had estimated magnitudes of $M_S = 5.75$ and $M_L = 6.1$. The applicant has developed a site-specific spectrum utilizing the M_L of 6.1 (discussed in SER Section 2.5.2.4.1). However, in recent discussions between the staff and applicant, questions have developed regarding the M_L magnitude. These questions were prompted by the following:

(1) In the 1980 Woodward-Clyde Report, the magnitude determined was 6.1 at distances ranging from about 300 to 2500 km (198 to 1563 mi). The maximum amplitudes were measured at periods ranging from 2.1 to 14 seconds. This was seen to be inconsistent with M_L determinations (see SER Section 2.5.2.3).

(2) The M_L formula was developed assuming Southern California attenuation. Attenuation of seismic waves is regionally dependent (see for example Singh, 1981), such that, assuming Southern California attenuation for regions of the Pacific Northwest causes the M_L to be overestimated.

(3) As part of a 1981 Woodward-Clyde report, the moment of the 1936 earthquake was determined. Using the empirical formula of Thatcher and Hanks (1979), this moment (3.6×10^{24} dyne-cm) would be more equivilant to an M_L of 5.7 to 5.8. In addition, the results of Nuttli (1979), Kanamori (1979), and Heaton et al. (1982) demonstrate that M_L should be about the same as M_s for magnitudes near 6.0 (M_s = 5.7 to 5.8 for the 1936 earthquake).

The applicant's consultant has provided the staff with a study on the magnitude of the 1936 earthquake (Woodward-Clyde February 1982c). This report states that the magnitude of 6.1 should not be used as an M_L, and that the 6.1 is an overestimate of the M_L for the 1936 earthquake. The magnitude of 6.1 conforms with the original notation of Richter (M). Although M and M_L are calculated in a similar fashion (using the maximum Wood-Anderson trace amplitudes), different distance ranges were used. M_L is normally restricted to distances less than about 5 degrees, while the distance used by WCC for the magnitude calculation was 5 to 15 degrees for the 1936 earthquake. In addition, the propagation paths from the 1936 hypocenter to the seismic stations used include paths, or portions of paths, outside of California that may not conform to Richter's (1936) original plot of log amplitude versus distance (attenuation rate) (Richter, 1958).

The magnitude of the 1936 earthquake was calculated from 17 seismic stations, 11 of which are located in northern and southern California. To study the above discussed effects, recent earthquakes in northern and southern California with known M_L's were analyzed at the Newport, Washington, Wood-Anderson station (which is about 250 km (156 mi) north of the 1936 epicenter). Magnitudes determined at Newport could be compared to known M_L's (from California seismographs) and, by reciprocity, the travel path effects should be the same as with the 1936 event. Thus, differences between M and M_L from recent earthquakes should be about the same as the difference between M and M_L from the 1936 earthquake. Results demonstrate that M appears to be consistently higher than M_L along the path between California and eastern Washington ($M - M_L$ is about 0.35 to 0.50). M of 6.1 minus about 0.35 to 0.50 (M_L = 5.6 - 5.75) is about the same values as the M_s of 5.7 to 5.8 (Gutenberg and Richter, 1949; 2nd edition, 1954), consistent with the results of Nuttli (1979), Kanamori (1979), and Heaton et al. (1982) that M_L would be about equal to M_s for magnitudes near 6.0. The USGS states that "we consider the M_s = 5 3/4 as a more reliable measure of the magnitude of the 1936 earthquake than the M_L magnitude." Based upon the above information, the staff concludes that an M_s = 5.7 - 5.8 is an appropriate representation for the magnitude of the 1936 earthquake. The site-specific spectrum was developed using an M_L = 6.1 as the magnitude. The site-specific spectrum is discussed in detail in SSER section 2.5.2.4.2, including an estimate of the effect of the M_L = 6.1 being an overestimate of the target magnitude.

2.5.2.3.2 Maximum Swarm Earthquake Near the WNP-2 Site

One seismicity pattern that has evolved with microearthquake monitoring within the Columbia Plateau involves the occurrence of earthquake swarms. In general, the swarms are defined by a clustering of events in both space and time. Swarms are typically localized to an area of a few kilometers wide, within the upper 3.0 km (1.9 mi) of the crust. Both in 1969 and 1975 swarm sequences occurred near Wooded Island, about 5 to 10 km (3.1 to 6.2 mi) southeast of the site. Because these events have occurred in close proximity to the site, the staff requested that the applicant evaluate the maximum earthquake potential of this activity and potential ground motion at the WNP-2 site.

The largest magnitude swarm earthquakes have been tabulated by the applicant (FSAR Appendix 2.5J, Amendment 18). For Wooded Island, the largest event was $M_c = 2.91$ in 1969 and $M_c = 2.83$ in 1975. M_c is a duration magnitude (based upon earthquake coda length) that was developed by the University of Washington. The relationship of M_L to M_c is discussed below. The largest swarm event in the Columbia Plateau since 1969 was the $M_c = 4.38$ Royal Slope earthquake, approximately 50 km (31.3 mi) north of the WNP-2 site. Focal mechanism solutions of different swarms have demonstrated that many different fault planes are active in each sequence. Because of the location in the upper few kilometers of the crust, the swarms are thought to occur within the basalt flows, with tectonic fractures or cooling joints thought to represent possible fault planes. A major uncertainty involves the dimensions of potential fracture surfaces to be involved in any one swarm event. The applicant has also studied the association of the past earthquake swarms with areas of groundwater level changes due to irrigation. As shown in Figure 2.5J-36 of the FSAR, the majority of swarm events have occurred in areas of irrigation or areas bordering irrigation, suggesting a causative relationship (triggering mechanism) between swarm seismicity and groundwater level changes.

The applicant's position, as stated in Appendix 2.5J of FSAR Amendment 18, is that the maximum magnitude of $M_c = 3.0$ is appropriate for swarm activity in close proximity to the site. This conclusion is based on

(1) The limited dimension of tectonic fractures. The applicant has estimated that the maximum dimensions of the tectonic fractures are approximately 150 m (490 ft).

(2) The larger swarm earthquakes (above $M_c = 3.0$) that have occurred between Saddle Mountains and Frenchman Hills, 30 to 50 km (18.7 to 31.2 mi) north of the site, in a region of major deformation. Because major deformation is apparently not present at Wooded Island, the applicant concludes that an event larger than $M_c = 3.0$ would not occur because large enough fault surfaces are not known to be present at Wooded Island.

(3) The suggestion that the Columbia River basalts are a low-strain environment and, thus, are not likely to be the source of significant earthquakes (see FSAR Section 2.5J.7.1).

The staff has also evaluated the potential for swarm earthquakes near the WNP-2 site. As a result of this evaluation, the staff requested that the applicant determine the ground motion and response spectrum assuming that an $M_L = 4.0$ earthquake ($M_c = 4.0$-4.4) occurred at a hypocentral distance of 3.0 to 5.0 km from the WNP-2 site. Reasons for reaching this conclusion are that uncertainties exist regarding the swarm earthquake potential near the WNP-2 site.

These uncertainties include the lack of detailed information regarding the size of potential tectonic fractures in the upper 3.0 km (1.9 mi) of the crust in the Wooded Island region and the relatively short instrumental recording period over which observations of maximum magnitude swarms earthquakes have been made.

Although the largest event at Wooded Island has been $M_c = 3.0$, the staff has requested the applicant to assume an $M_c = 4.0$ to 4.4 is possible. An $M_c = 4.4$ is the largest swarm event within 50 km (31.2 mi) of the site during the past 11 years. Malone (1979) has studied the relationship between M_c (coda-length magnitude) and M_L (local magnitude). He has found that M_c is approximately 0.3 units larger than M_L. The staff has used these results and assumed that an $M_c = 4.0$ to 4.4 would be about an $M_L = 4.0$. In determining the closest hypocentral distance to be assumed, the staff has used the following pieces of information.

(1) Past swarm events at Wooded Island have come within 5.0 to 10.0 km (3.1 to 6.2 mi) (epicentral distance) of the site. Typically these events occur at depths of 0 to 3.0 km (0 to 1.9 mi) although for ground motion comparisons the staff has conservatively assumed that the hypocentral distance will be the same as the epicentral distance.

(2) In assessing the closest distance at which future swarm events might occur, the staff has assumed the association of swarm earthquakes with areas of irrigation is reasonable. Utilizing the information contained in Appendix 2.5J of FSAR Amendment 18, the staff has determined that 3 km (1.9 mi) is the closed hypocentral distance for a swarm earthquake, assuming a swarm sequence occurred east of the WNP-2 site in the closest area of irrigation.

Based upon the above information, the staff requested that the applicant estimate the ground motion assuming an M_L = 4.0 earthquake occurred at a hypocentral distance of 3.0 to 5.0 km (1.9 to 3.1 mi) from the site. The ground motion from this event is discussed in SSER Section 2.5.2.4.2.

The staff cannot rule out other hypotheses aside from irrigation (which the staff has used) that may be contributing to the occurrence of the earthquake swarms, or similarly preclude the possibility of swarm events at hypocentral distances less than 3 km (1.9 mi). However, the staff's judgment is conservative because the staff has used the largest known swarm earthquake anywhere within the large Columbia Plateau Tectonic Province, and assumed it to occur closer to the site than any swarm earthquake that has been recorded during the 11 years of monitoring.

2.5.2.3.3 Magnitude of the Maximum Earthquake on Gable Mountain

As discussed in Section 2.5.1.1.2.2, the Central Fault on Gable Mountain has been found to be capable. In addition the North-Dipping Reverse Fault is also assumed to be capable because of its structural relationship with other probable capable faults.* The Gable Mountain structure approaches to within 15 km (9.4 mi) of the WNP-2 site, with the faults being reverse or reverse-oblique slip in character.

As discussed in Section 2.5.1.3.1, the Central Fault on Gable Mountain has a maximum inferred length of 3.0 km (1.9 mi), with a maximum displacement of 6.0 cm (0.2 ft). The North-Dipping Reverse Fault has a known length of about 1.0 km (0.6 mi) and a maximum inferred length of about 6.0 km (3.8 mi). In addition, the majority of geologic evidence (SSER Section 2.5.1.3.1) indicates that the Gable Mountain faults are secondary to the folding, placing a constraint

*Other possible capable faults are the South Fault, the West Fault, and the DB-10 Fault. These (South, West, DB-10) have not been used in assessing the maximum magnetude for the Gable structure because their dimensions (length or displacement of Holocene material) are smaller than the Central Fault or the North-Dipping Reverse Fault; thus their estimated magnitudes would be lower.

on the down-dip width of the faults of 3.0 km (1.9 mi), the approximate width of the Gable Mountain fold. The above fault parameters have been used by the staff, the staff's consultant Dr. D. B. Slemmons, and the applicant to estimate earthquake magnitude on the Gable Mountain structure.

The applicant's best estimate for earthquake magnitude on Gable Mountain is $M_s = 5.0$; however, the range of estimates is $M_s = 3.9$ to 6.6. This range arises from magnitude relationships utilizing potential rupture area, maximum displacement, rupture length, and earthquake moment.

Slemmons concludes for the Central Fault on Gable Mountain ~~(see page 16 of~~ (Appendix H): "the maximum strain rate is about 0.005 mm/yr and the maximum credible earthquake is low and falls below the cutoff magnitude of $M_s = 5.5$ of the data... The seismic moment magnitude value would be similar to the surface magnitude value."

The staff, in making its assessment of the magnitude for the Gable Mountain structure, has reviewed the data base used to develop empirical realtionships between magnitude (M_s) and rupture length and displacement (such as Slemmons, 1982). The staff has found that essentially few or no data exist for rupture lengths as low as 3.0 to 6.0 km and displacements as low as 6.0 cm for reverse or reverse oblique slip faults. The staff has not given any significant weight to these values to derive a magnitude for the Gable Mountain structure.

Because constraints have been placed on possible fault width, the staff has examined the suitability of using rupture area and moment to derive magnitude estimates for Gable Mountain. Wyss (1979) states that his rupture area versus magnitude data should not be used to estimate magnitudes less than 5.7, because of the lack of data below a magnitude of 5.7. The applicant's consultant, however (Woodward-Clyde, 1982), has compiled fault rupture area data for earthquakes with magnitudes as low as 4.2, thereby extending the usefullness of this technique. Woodwood-Clyde (1982a) has conservatively assumed that $M_s = M_L$ in this analysis. Using rupture areas of 9.0 to 18 km² (range for Central Fault and North-Dipping Reverse Fault), M_s values of 4.9 to 5.1 are obtained. Hanks and Kanomori (1979) developed a relationship between moment and moment magnitude that extends to magnitude 3.0. Using rupture areas of 9.0 to 18 km², a maximum displacement of 6.0 cm, and a rigidity of 3×10^{11} dyne-cm, the moment magnitude (Hanks and Kanamori 1979) obtained is 4.8 to 5.0.

It should be noted that there is some uncertainty in the above values because of a lack of absolute knowledge regarding down-dip width and rigidity. The staff has assessed the sensitivity of the magnitude values. Parcaru and Berckhemer (1982) have recently compiled world-wide data on length-to-width ratios for reverse type faults. They state that the average length is about twice the width, with the majority of the data being in the range of length one to four times the width. Using this information and fault area and moment, with rupture areas up to 36 (length equals width) km^2 (best estimate of 9.0 to 18 km^2, most conservative estimate of 36 km^2), the magnitude would increase by about 0.2 to 0.3 M_s units. Although 3×10^{11} dyne-cm is the standard value used, changing the rigidity by a factor of two would also change the magnitude values by about 0.2 M_s units.

Based upon an appropriate utilization of rupture area and earthquake moment, the staff concludes that the maximum earthquake for licensing purposes on the Gable Mountain faults is $M_s = 5.0$. Uncertaintity in fault area or rigidity could change the M_s value by ± 0.50 units. Although these values are conservative, it should be noted that for the WNP-2 site, the staff has assumed the 1936 earthquake site-specific spectrum (see SSER Section 2.5.2.4.1), at about 15 km. This is similar to the closest approach of Gable Mountain. An M_L of 6.1 (M_L used for site-specific spectrum) is much larger than values obtained using the fault parameters that exist on Gable Mountain to derive magnitude estimates. In addition, there is no observed seismicity on or near the Gable Mountain structure, and the slip rate of 5×10^{-4} cm/year (SSER Section 2.5.1.1.3.1) qualitatively suggests very low rates of deformation or very long return periods for earthquakes on the Gable Mountain structure.

2.5.2.3.4 Magnitude of the Maximum Earthquake on the Rattlesnake-Wallula Alignment

As summarized above, the Rattlesnake-Wallula (RAW) alignment was recognized as the most significant seismically active structure at the CP stage. A geologic description of RAW can be found in Section 2.5.1 of this SSER. In addition, Slemmons discusses (Appendix H) the RAW feature in detail. Discussed below are the magnitude estimates for RAW at a distance of 19.5 km (12.2 mi), the closest distance that RAW approaches the WNP-2 site.

Typically, the most utilized method of estimating earthquake potential has been the use of fault-rupture length (applied to surface ruptures). Application of fault-rupture-length earthquake-magnitude methodology by Slemmons (as described in Appendix H), relies upon subsurface estimates of individual rupture lengths or appropriate percentages of estimated total fault length.

The length of the RAW structure is dependent upon the type of faulting assumed. In response to staff question 360.14, the applicant has presented estimates for the RAW structure assuming either reverse-oblique slip faulting or strike-slip faulting. Slemmons estimated the maximum magnitude for RAW based upon primarily strike-slip faulting (details of why strike-slip faulting is assumed is discussed in SSER Section 2.5.1.3.2), with possible minor amounts of local oblique slip motion.

The applicant has used the relationship of Slemmons (1977) between magnitude and rupture length and Wyss (1979) between magnitude and rupture area (source length multiplied by fault width) to estimate maximum magnitudes. For reverse-oblique slip faulting, the maximum magnitude of RAW structural Domain II (see SSER Section 2.5.1.1.2.3) is 6 to 6.5, based upon rupture lengths of 5.0 to 10 km (3.1 to 6.2 mi) and fault widths of 5.0 to 11 km (3.1 to 6.9 mi). Structural Domain II approaches to within 19.5 km (12.2 mi) of the WNP-2 site. The maximum magnitude of structural Domain III is 6.5 of 7.0, based upon rupture lengths of 10 to 20 km (6.2 to 12.5 mi) and fault widths of 5 to 11 km (3.1 to 6.7 mi). Structural Domain III approaches to within about 42 km (26 mi) of the WNP-2 site. Based on the discussion in SSER Section 2.5.1.1.2.3, the staff does not accept the separation of Structural Domains II and III. For strike-slip faulting, the applicant has combined Domains II and III. Using rupture lengths of 16 to 23 km (10 to 14.4 mi) and fault widths of 7.5 to 12 km (4.7 to 7.5 mi), they conclude that the maximum magnitude for RAW is 6 to 6.5.

The methodology of Wyss (1979) to estimate maximum magnitude has some problems associated with it. Wyss postulated that fault area (source length multiplied by fault width) would provide a more accurate and appropriate estimate than length alone. The staff has noted that to apply this methodology, a fault width must be estimated (or constraints placed on fault width such as what was done for Gable Mountain faults). The applicant had made estimates of fault width based upon a dipping fault surface down to 5.0 and 11 km. Seismicity (non-swarm activity), however, is scattered throughout the entire crust. For the RAW structure, determining down-dip fault width involves uncertainty and in some cases may be done somewhat arbitrarily (geologic constraints on down dip width have not been made). Because this method relies upon indirect estimates of fault width for RAW, the staff has given this approach little consideration.

Slemmons has estimated the magnitude for RAW (Appendix H). The staff concurs with Dr. Selmmons' use of 120 km (75 mi) fault length for the RAW structure (see Section 2.5.1.1.2.3), and his use of fractional fault lengths of 15 to 20 km (9.4 to 12.5 mi). Using the relationships of Slemmons (1982) between total fault length and magnitude and fractional fault length and magnitude, Slemmons concludes that the maximum credible earthquake for the RAW structures is $M_s = 6.5$. The staff concurs with this conclusion.

As a supplement to estimating maximum magnitude from fault rupture length, the use of fault slip rate or degree of fault activity has been estimated for the RAW structure. This methodology has been discussed in detail in a past staff SER (San Onofre Units 2 and 3 SER, NUREG-_____). Slemmons provides some discussion on the slip rate methodology (Appendix H). For RAW, the slip rate has been conservatively estimated to be 0.20 mm/yr (Woodward-Clyde 1982b). Using this value and the relationship of Woodward-Clyde (1979) yields a maximum magnitude of 6.4 for the RAW structure (Appendix H).

?

The final pieces of information on RAW come from observed fault activity and seismicity. As discussed in SSER Section 2.5.1.3, no fault along the RAW trend is known to have ruptured for the past 7000 years. Although the definition for noncapability cannot be satisfied, the lack of very recent (past 7000 years) surface rupture may indicate that rates of deformation are very low. This is supported by the conclusions of Dr. Slemmons (Appendix H), who states that the actual slip rate (degree of deformation) may be much lower than assumed. Low rates of deformation are also supported by the observed lack of seismicity along the RAW structure, suggesting long return periods of larger (M_s 6.0 to 6.5) magnitude earthquakes.

2.5.2.3.5 1872 Earthquake

There has been much discussion surrounding the December 14, 1872 north-central Washington earthquake regarding both its size and location. Past conclusions on these topics have been in staff SERs (for example Supplement 1 to the WNP-1 and -4 CP-SER, 1978) and testimony (McMullen and Kelleher, 1978). In addition, USGS has completed a current review of the information available and concluded that the 1872 earthquake epicenter is located in the vicinity of Lake Chelan, with a probable maximum intensity of MMI = IX, and magnitude of M_s = 7.0. In addition, USGS concludes that the 1872 event was in the Northern Cascades Province, at least 90 km (56 mi) from the Columbia Plateau Tectonic Province.

Because of the sparse population in north-central Washington in 1872, there is a large degree of uncertainty concerning estimates of the strength of the December 14, 1872 event. For example, estimates of the maximum intensity range from MMI = VII (as discussed in Appendix 2RB of the WNP-1 and -4 PSAR, 1978) to MMI = IX (USGS/NOAA, 1977), reflecting both a lack of data and assumptions regarding how one treats this sparse data set. As discussed previously, the staff considers magnitude to be a more reliable indicator of earthquake source strength than intensity. Particular problems are associated with determination of intensities greater than Modified Mercalli VIII. Although USGS has not based its maximum intensity estimate on ground effects (landslides or soil liquefaction), very often these intensities (greater than VIII) are based on ground failure that could be very dependent upon local conditions rather than ground shaking. The staff concludes that the maximum intensity for the 1872 earthquake is MMI = IX based on the recommendation of the USGS (Appendix G).

In response to staff question 361.5, the applicant has summarized the estimates of magnitude for the 1872 earthquake. These estimates are centered around an M_s = 7.0 using the relationship of intensity and magnitude to depth proposed by

Shebalin (1959) and Gutenberg and Richter (1956). The staff and USGS concur that the 1872 earthquake is approximately M_s = 7.0, based on the areas shaken at the various intensity levels. In addition, based on the well-documented extensive aftershock sequence, it seems that this earthquake occurred in the crust. This is consistent with recent earthquake monitoring both in the Northern Cascades region, and the Columbia Plateau (see for example, Appendix 2RE of WNP-1 and -4 PSAR; Woodward-Clyde July 1978). Malone (1979), in a recent article on attenuation patterns in the Pacific Northwest, has attempted to model the intensity pattern of the 1872 earthquake. He states that intensities can be modelled assuming an M = 7.4 event at a depth of 60 km (37.5 mi), although he could not rule out a much shallower depth and thus a lower magnitude, because this technique does not produce unequivocal solutions.

The actual epicentral location of this earthquake is also uncertain. The applicant's position, as contained in the WNP-2 FSAR, states the the epicenter is located within a meizoseismal zone that extends from Lake Chelan to southern British Columbia and is within the Northern Cascades-Okanogan Tectonic Province. The USGS states: "Our review of the data lead us to believe that the epicenter of the 1872 main shock is located in the vicinity of Lake Chelan" (Appendix G).

The Lake Chelan region is near the boundary of the North Cascades Tectonic Province and the Columbia Plateau Tectonic Province. Lake Chelan is approximately 140 to 150 km (987.5 to 94 mi) north-northeast of the WNP-2 site. The Columbia Plateau has many distinct features when compared with the Northern Cascades region. These include

(1) The crust is thinner under the Plateau.
(2) The tectonic style and trends of major tectonic structures are different in each province.
(3) There are differences in rock types and ages (Cenozoic basalts within the Plateau compared to metamorphic and plutonic masses north of the Plateau).

In addition, a major crustal boundary is suggested by a steep gravity gradient 1872 earthquake occurred in the Northern Cascade Tectonic Province, whose closest approach is approximately 140 to 150 km (87.5 to 94 mi) north of the WNP-2 site.

While the Northern Cascades appear to be distinctly different than the Columbia Plateau, there exists some uncertainty (as noted in the FSAR and by USGS) as to the exact location of the Columbia Plateau Tectonic Province boundary. By knowing the size of 1872 event (M_s = 7.0), however, the staff can determine how close such an event would have to be assumed before it would exceed the SSE response spectrum. The staff has utilized three different ground motion attenuation relationships, those of Woodward-Clyde (1981), Joyner and Boore (1981), and Campbell (1981). Using the above relationships, the staff has determined that an M_s = 7.0 earthquake would have to occur within 40 km (25 mi) of the WNP-2 site to even approach that of the SSE. The surface boundary of the Columbia Plateau is about 140 to 150 km (87.5 to 94 mi) from the site, more than three times further than the conservative estimate of the 40 km (25 mi). Based on these considerations, the staff concludes that the 1872 earthquake occurred in the Northern Cascades Tectonic Province and that this earthquake has no impact on the seismic design adequacy of the WNP-2 site.

2.5.2.3.6 Summary of Earthquakes for Consideration of Ground Motion at the WNP-2 Site

The various earthquakes that have been assumed for the WNP-2 OL review are as follows (the ground motion from these events is described in Section 2.5.2.4 of this SER):

(1) The swarm-type earthquake (M_L = 4.0) is assumed to occur at a hypocentral distance of 3 to 5 km (1.9 to 3.2 mi) from the site.

(2) For the Rattlesnake-Wallula alignment, an M_s = 6.5 is assumed to occur at a distance of 19.5 km (12.2 mi) from the site.

(3) The largest earthquake not associated with a structure within the Columbia Plateau Tectonic Province is the 1936 earthquake, assumed to occur in the site vicinity.

(4) For the Gable Mountain faults a M_s of 5.0 is assumed to occur at 15 km (9.3 mi), although some uncertainty is attached to this magnitude determination. This is enveloped by the ground motion assumed for the site-specific spectrum (from (3) above).

2.5.2.4 Vibratory Ground Motion: Safe Shutdown Earthquake

2.5.2.4.1 Site-Specific Spectrum For The 1936 Earthquake

As discussed in SSER Section 2.5.2.3.1, it is the staff's position that the 1936 Milton-Freewater earthquake is the largest earthquake within the Columbia Plateau Tectonic Province that has not been associated with a geologic structure. In response to staff question 361.17, the applicant has submitted a site-specific spectrum for an M_L = 6.1 earthquake occurring within an epicentral distance of 0 to 25 km (0 to 15.6 mi). The use and development of site-specific spectrum technique has been discussed in detail in past staff SERs (Sequoyah SER, March 1979; Fermi SER, June 1981) and testimony (Midland testimony, October 1981) and is, therefore, not discussed extensively here.

R.

The applicant developed the site-specific spectrum by searching the strong motion data base for earthquakes of magnitude near M_L = 6.1 (M_L of 5.7 to 6.4 were used), recorded at distances less than about 25 km (15.6 mi). Strong motion recording stations were then chosen to best match the site conditions at the WNP-2 site. Thirty-five sets of strong motion records were found by the applicant's consultant to fit the above screening conditions.

Three spectra were developed using the complete data set. The first gave equal weight to each recording. The mean magnitude of the data was M_L = 6.1 at a rupture-epicentral distance of 16.1 km (10.1 mi). The 84th percentile of this data set is generally enveloped by the SSE spectrum (0.25g, Regulatory Guide 1.60). There is a region of slight exceedance, less than about 10%, between about 5 and 8 Hz. The data set was also examined by weighing the recordings according to the probability of the M_L = 6.1 earthquake occurring within a certain rupture-hypocentral distance band. For example, the area within the 10-to-15-km (6.2-to-9.4 mi) distance band is 20% of the total area within 25 km (15.6 mi) of the site. The portion of the data set within this distance band is less than 10%; therefore, these recordings are given more weight to bring the portion of the data set equal to the portion of the area within the distance band. The mean magnitude of this data set was again found to be M_L = 6.1, but the average rupture epicentral distance was reduced slightly to 15.3 km (9.6 mi). In this case, the SSE spectrum (0.25g, Regulatory Guide 1.60) envelopes the 84th percentile of the site-specific spectrum except for a very minor (less than 5%) exceedance near 7 Hz. The data set was also weighted using distance subsets and rupture-epicentral distance. The mean magnitude was M_L = 6.1 at an average rupture-epicentral distance of 17.7 km (11.1 mi). The 84th percentile of this data set does not exceed the SSE spectrum. The staff consider the site-specific spectrum weighted by rupture-hypocentral distance as appropriate for the WNP-2 site.

As discussed at the end of this section, the minor exceedances of the SSE spectrum are less than the difference between the M_L = 6.1 assumed for site-specific spectrum and the M_s = 5.7 to 5.8, which is the appropriate magnitude for the 1936 earthquake.

In reviewing the response to question 361.17, the staff identified some areas of concern that have been resolved. These concerns dealt with the site conditions at the WNP-2 site (in particular the shear velocity profile) compared to the strong motion sites used in the site-specific spectrum.

These concerns are

(1) In reviewing the strong motion data set for the 1971 San Fernando earthquake (one of the events used in the analysis), it was found that only some of the softer recording sites were chosen.

(2) The shear velocity profile at the WNP-2 site was found to have sharp increase at a depth of about 33 m (100 ft). At a depth of about 85 m (250 ft), there is an apparent shear velocity inversion (sharp velocity decrease). The strong motion recording stations chosen by the applicant did not match the shear velocity increase or decrease. The strong motion

stations were generally soft to stiff soil sites that would fit the WNP-2 shear velocity profile assuming that the velocity contrast at depths between 100 and 250 ft had no affect on the recordings.

Regarding the San Fernando earthquake (item 1), the staff has found that the recordings used by the applicant in the site-specific spectrum are conservative compared to the strong motion recordings that were not used.

The applicant has utilized the computer program SHAKE to assess potential differences between the WNP-2 site and the sites used in the site-specific spectrum in a relative sense (item 2 above). Four idealized soil profiles were developed that generally match the site conditions of the strong motion data base collected. Using a rock input time history, the ratio of the idealized soil profile response to the WNP-2 response was computed. For frequencies above about 3 Hz, the sites used in the site-specific spectrum showed more amplification than the WNP-2 sites. For frequencies less than 3 Hz, the WNP-2 site showed more amplification than the soil sites used in the site-specific spectrum. This is of no significance because the SSE spectrum exceeds the 84th percentile of the site-specific spectrum, and, as discussed in SER Section 3.7.3, the frequency range of interest/concern in WNP-2 Category I structures and systems is always higher than 5 Hz.

An additional item discussed in SSER Section 2.5.2.3.1 involves the fact that the magnitude of $M_L = 6.1$ is an overestimate of the size of the 1936 earthquake. The M_s of 5.7 to 5.8 for the 1936 earthquake was utilized to assess the conservatism of the site-specific spectrum. The average M_s of the data set used for the site-specific spectrum is 6.1. Using a distance of 17 km (10.6 mi) and the relationships of Campbell (1981), Joyner and Boore (1981), and Woodward Clyde (1981), peak acceleration would be about 20% lower if an M_s of 5.7 to 5.8 were achieved as the average magnitude of the site-specific spectrum. This 20% difference is larger than the minor exceedance of the SSE spectrum by the site-specific spectrum.

Using the above information, the staff has determined that the SSE spectrum (0.25g Regulatory Guide 1.60) is conservative compared to the 84th percentile of the site-specific spectrum from an earthquake similar to the 1936 event.

2.5.2.4.2 Ground Motion from Swarm Earthquakes

In determining the ground motion for an $M_L = 4.0$ at a hypocentral distance of 3.0 to 5.0 km (1.9 to 3.1 mi), the applicant has used strong motion records from the 1975 Oroville and the 1980 Mammoth Lakes earthquake sequences. Although other small magnitude, near-field strong ground motion recordings are available (such as from the 1979 Imperial Valley sequence), these recordings have not been used because (1) the site conditions do not match the WNP-2 site, (2) the earthquakes do not have accurate locations, and (3) the digitized strong motion records are unavailable.

Thirty-nine sets of ground motion records were tabulated in the magnitude range of $M_L = 3.8$ to 4.2, and the hypocentral distance range of H = 4.3 to 26.1 km (2.7 to 16.3 mi). It was found that the number of recordings at specific hypocentral distances of 3.0 and 5.0 km were inadequate to directly estimate the response spectrum (such as what was done with the site-specific spectrum). The applicant has used nonlinear regression techniques to predict peak acceleration as a function of distance for the Oroville and Mammoth data sets. A variety of regressions were completed with the range of the 84th percentile uncorrected peak acceleration being 0.15 to 0.31g at a hypocentral distance of 3.0 km (1.9 mi). It was determined that corrected peak accelerations would be about 6% lower than uncorrected values. The applicant used the most conservative estimate of 0.29g (corrected from the 0.31g uncorrected) to anchor the response spectrum from the swarm earthquakes.

The response spectrum shape was also developed from the Oroville and Mammoth data sets. Frequency dependent spectral acceleration amplification ratios were analyzed using strong motion records in the hypocentral distance range 0 to 10.5 km (0 to 6.6 mi). The response spectrum from the swarm earthquakes that was compared to the SSE was based upon the 84th percentile corrected peak acceleration and median frequency dependent spectral acceleration amplification factors. The response spectrum using the 84th percentile peak acceleration and median amplification factors is more conservative than the median peak acceleration and 84th percentile amplification factors for frequencies above 3 Hz. The staff has concluded that the response spectrum proposed by the applicant for an M_L = 4.0 swarm earthquake at a hypocentral distance of 3.0 km is a conservative representation of the ground motion expected from a swarm event. The swarm earthquake response spectrum exceeds the SSE spectrum for frequencies above about 10 Hz. For 5% damping this exceedance is about a factor of 1.5 for frequencies between 15 and 30 Hz. The significance of this exceedance is discussed in SSER Section 3.7.

2.5.2.4.3 Ground Motion from Capable Structures

2.5.2.4.3.1 RAW

As discussed in SSER Section 2.5.2.3.4, a conservative estimate of earthquake magnitude on the Rattlesnake-Wallula Lineament, at 19.5 km (12.2 mi) from the WNP-2 site, is M_s = 6.5. Both the staff and applicant have compared the ground motion (both peak ground acceleration and response spectrum) from this assumed earthquake to that of the SSE (0.25g peak acceleration with a Regulatory Guide 1.60 response spectrum).

The applicant's analysis is contained in response to staff question 360.14. Peak accelerations were estimated from ground motion attenuation relationships in FSAR Appendix 2.5K (for reverse faults) or those of Idriss et al. (1982). The applicant states that the best estimates for the peak ground accelerations range from 0.05g to 0.17g at the median level and 0.11g to 0.25g at the 84th percentile level.

The staff has also used additional ground motion attenuation relationships to evaluate the response spectrum for an M_s = 6.5 at 19.5 km (12.2 mi). For peak acceleration estimates, the staff has used Campbell (1981), Joyner and Boore (1981), and those of Woodward-Clyde (Appendix 2.5K of the WNP-2 FSAR 1981). The relationship of Woodward-Clyde was developed specifically for reverse fault cases, producing larger values compared to those of Campbell (1981) and Joyner and Boore (1981) (whose relationships include all fault types, although predominantly strike slip) for an M_s = 6.5 at 19.5 km (12.2 mi). As discussed previously, it is the staff's position that the Rattlesnake-Wallula zone of deformation represents primarily strike-slip faulting with some local oblique slip motion. The staff has included the values from the FSAR because they yield conservative values compared to the other two. The average of the peak acceleration values (from the three attenuation relationshps) is 0.16g at the median level (range of 0.14 to 0.19) and 0.25g at the 84th percentile level (range of 0.20 to 0.27).

Peak velocity was also estimated for an M_s = 6.5 at 19.5 km (12.2 mi) using the relationships of Joyner and Boore (1981) and Woodward-Clyde (1980). The average of these two relationshps gives a peak velocity of 17.6 cm/sec at the median level (range of 16.4 to 18.9) and 31.4 at the 84th percentile level (range of 31.3 to 31.4).

It should be noted that in deriving the above estimates using the relationship of Joyner and Boore a reduction factor of 12% was utilized. The relationships of Joyner and Boore were derived by using the largest of the two horizontal values recorded at strong motion stations. The staff typically uses both horizontal ground motion values in deriving response spectrum estimates (such as the site-specific spectrum discussed in SER Section 2.5.2.4.1). Campbell (1981) states that an approximate 12% difference exists when only the largest of the two peak ground motion values is used in Joyner and Boore (1981).

Response spectra were developed using the above peak ground motion values and the spectral amplification factors contained in NUREG/CR-0098 (Newmark and R Hall, 1978). Median spectral amplification factors were used with the 84th percentile peak ground motion values, and 84th percentile spectral amplification factors were used with median peak ground motion values. The two response spectra for an M_s = 6.5 at a distance of 19.5 km (12.2 mi) do not exceed the design spectra, a Regulatory Guide 1.60 response spectrum anchored at a peak acceleration of 0.25g.

2.5.2.4.3.4 Gable Mountain and Toppenish Ridge

As discussed in SSER Section 2.5.2.3.3 the staff has concluded that an M_s = 5.0 is a conservative estimate for the magnitude to be considered in making ground motion estimates for the Gable Mountain faults. M_s = 5.0 is based upon the use of fault rupture area and moment magnitude. The Gable Mountain structure approaches to within about 15 km of the WNP-2 site. As discussed in SSER Section 2.5.2.4.1, the average distance for the 1936 earthquake site-specific spectrum is also about 15 km, although the magnitude assumed for the site-specific spectrum (M_L about 6.1) is much larger than that estimated for Gable Mountain. The site-specific spectrum does not exceed the SSE design spectrum and envelopes the ground motion expected from an M_s = 5.0 on the Gable Mountain structure.

Dr. Slemmons has concluded that Toppenish Ridge, a cable structure, has a potential for a maximum magnitude of M_s = 7.4. The Toppenish Ridge structure approaches to within about 70 km (44 mi) of the WNP-2 site. Using the ground motion peak acceleration relationships of Woodward-Clyde (1981), Campbell (1981), and Joyner and Boore (1981), an M_s = 7.4 and a distance of 70 km (44 mi), the staff has determined that the peak acceleration from the maximum earthquake on Toppenish Ridge would not exceed 0.15g. Thus, the maximum earthquake on Toppenish Ridge has no impact on the seismic design adequacy of the WNP-2 site.

2.5.2.4.5 Seismic Exposure Analysis

The applicant has submitted a seismic exposure analysis that estimates the probability of exceeding the vibratory ground motions of the SSE. This approach is utilized in order to account for uncertainties in applying a geologic structure approach to assess the potential vibratory ground motion in the Columbia Plateau.

In studying earthquake hazards, the staff is concerned about the probability that an earthquake or its associated ground motion will occur at a site during a specified period of time. The exceedance probability is the probability over some period of time that an earthquake will generate a level of ground shaking

Surface faulting, some of it capable, found outside the 8 km (5 mi) radius of the site on Gable Mountain and along RAW, has been described in detail in Sections 2.5.1.1.2 and 2.5.1.1.3.

3.28

3 DESIGN CRITERIA FOR STRUCTURES, SYSTEMS, AND COMPONENTS

3.5 Missile Protection

3.5.1 Missile Selection and Description

3.5.1.3 Turbine Missiles

3.5.1.3.1 Review Basis

During the past several years, the results of turbine inspections at operating nuclear facilities indicate that cracking to various degrees has occurred at the inner radius of turbine disks, particularly those of Westinghouse design. In this period, there has been a failure of a Westinghouse turbine disk at one facility ~~at~~ the Yankee Atomic Electric Company. In addition, recent inspections of General Electric turbines have resulted in the identification of disk bore cracks.

In view of current experience and NRC safety objectives, the staff is emphasizing the turbine missile generation probability (turbine system integrity) in its reviews of the turbine-missile issue and eliminating the need for elaborate and somewhat ambiguous analyses of strike and damage probabilities given an assumed turbine failure rate. Although straightforward in principle, the latter calculations have to be based on detailed facility information and assumptions as to missile shape and size, missile energies, barrier-penetration potential, and, ultimately, the likelihood of damaging a facility safety system. Generally, there are significant differences between submittals from licensees or applicants and the final evaluation by the staff. Nevertheless, the staff concludes, based on its reviews of many facilities, that the probability of a turbine missile striking and damaging a safety system is in a relatively narrow range, depending on turbine orientation. More refined analyses or additional calculations for other facilities are unlikely to change this conclusion. Therefore, expensive and time-consuming strike probability analyses by applicants/licensees and/or the staff are judged to be unwarranted.

~~In conclusion,~~ the new approach being used by the staff improves turbine generator system reliability by reviewing and regulating the probability of missile generation. This approach will reduce considerably the analytical burden placed on licensees, conserve NRC resources, and still maintain the high level of protection of public health and safety.

According to GDC 4, nuclear power plant structures, systems, and components important to safety shall be appropriately protected against dynamic effects, including the effects of missiles. Failures that could occur in large steam turbines of the main turbine generator have the potential for ejecting large high-energy missiles that can damage plant structures, systems, and components. The safety objective of this SER review topic is to ensure that structures, systems, and components important to safety are adequately protected from potential turbine missiles. Of those systems important to safety, this topic is primarily concerned with safety-related systems; i.e., those structures, systems, or components necessary to perform required safety functions and to ensure

(1) the integrity of the reactor coolant pressure boundary
(2) the capability to shut down the reactor and maintain it in a safe shutdown condition
(3) the capability to prevent accidents that could result in potential offsite exposures that are a significant fraction of the guideline exposures of 10 CFR 100, "Reactor Site Criteria."

Typical safety-related systems are listed in RG 1.117, "Tornado Design Classification."

The probability of unacceptable damage as a result of turbine missiles (P_4) is generally expressed as the product of (1) the probability of turbine failure resulting in the ejection of turbine disk (or internal structure) fragments through the turbine casing (P_1); (2) the probability of ejected missiles perforating intervening barriers and striking safety-related structures, systems, or components (P_2); and (3) the probability of struck structures, systems, or components failing to perform their safety function (P_3).

According to current NRC guidelines in SRP Section 2.2.3 (NUREG-0800) and RG 1.115, "Protection Against Low Trajectory Turbine Missiles" (Rev. 1), the probability of unacceptable damage from turbine missiles should be less than 1 chance in 10 million per year for an individual plant ($P_4 < 10^{-7}$ per year).

In the past, analyses for CP and OL reviews assumed the probability of missile generation (P_1) to be approximately 10^{-4} per turbine year, based on the historical failure rate (Bush, 1973 and 1978). The strike probability (P_2) was estimated (NUREG-0800) based on postulated missile sizes, shapes, and energies, and on available plant-specific information such as turbine placement and orientation, number and type of intervening barriers, target geometry, and potential missile trajectories. The damage probability (P_3) was generally assumed to be 1.0. The overall probability of unacceptable damage to safety-related systems (P_4), which is the sum over all targets of the product of these probabilities, was then evaluated for compliance with the NRC safety goal. This logic places the regulatory emphasis on the strike probability; i.e. ~~that is,~~ having established an individual plant safety goal of 10^{-7} per year, or less, for the probability of unacceptable damage to safety-related systems as a result of turbine missiles, this procedure requires that P_2 be less than or equal to 10^{-3}. This approach requires a great deal of effort on the part of applicants/licensees and the staff because of (1) its explicit disregard for the "actual" turbine reliability and (2) the difficulty of calculating P_2 in a relatively unambiguous and systematic manner.

The new approach places the burden for demonstrating turbine reliability on the turbine vendor. This shift of emphasis requires nuclear steam turbine manufacturers to develop and implement volumetric (ultrasonic) examination techniques suitable for inservice inspection of turbine disks and shaft and to prepare reports for NRC review which describe their methods for determining turbine-missile-generation probabilities. These methods are to relate disk design, materials properties, and inservice volumetric inspection interval to the design overspeed missile-generation probability, ~~and to~~ related overspeed protection system characteristics, and to relate stop and control valve design and inservice test interval to the destructive overspeed missile-generation probability. After submitting such reports to the staff for review, the vendor will provide to applicants/licensees tables showing missile-generation probabilities versus time (inservice volumetric disk inspection interval for rated speed or design overspeed failure, and inservice valve testing interval for destructive overspeed failure) for their particular turbine. These tables could then be used to establish inspection schedules which meet NRC safety objectives.

It is the staff's view that the NRC safety objective with regard to turbine missiles is best expressed in terms of two sets of criteria applied to the missile-generation probability. One set of criteria is to be applied to favorably oriented turbines, P_1f (total), and the other is to be applied to unfavorably oriented turbines, P_1^4 (total). These criteria may be summarized as follows:

(1) The general requirement for turbine reliability at reactor startup is that P_1f (total) be less than 10^{-4} per year, and that P_1^4 (total) be less than 10^{-5} per year.

(2) When, during operation, the value of P_1f (total) increases to more than 10^{-4} per year, but less than 10^{-3} per year, or the value of P_1^4 (total) increases to more than 10^{-5} per year, but less than 10^{-4} per year, the turbine is permitted to remain in use until the next scheduled refueling outage. At that time the licensee should take action to reduce the missile-generation probability to meet criterion (1) before returning the turbine to service. Exemptions may be granted for valid technical reasons or severe economic hardship.

(3) When, during operation, the value of P_1f (total) increases to greater than 10^{-3} per year but less than 10^{-2} per year, or the value of P_1^4 (total) increases to more than 10^{-4} per year but less than 10^{-3} per year, the turbine is to be isolated from the steam supply within 60 days. At that time the licensee must take action to reduce the missile-generation probability to meet criterion (1) before returning the turbine to service.

(4) If, at any time during operation, the value of P_1f (total) increases to more than 10^{-2} per year or the value of P_1^4 (total) increases to more than 10^{-3} per year, the turbine is to be isolated from the steam supply within 72 hours. At that time the licensee must take action to reduce the missile generation probability to meet criterion (1) before returning the turbine to service.

Applicants and licensees with ~~the~~ turbines from vendors who have not yet performed analyses of turbine-missile generation or who have performed analyses but have not yet submitted formal reports to the NRC for review are expected to meet the following interim criteria, regardless of turbine orientation:

(1) An inservice inspection program for the steam turbine assembly must be developed and implemented to provide assurance that disk flaws that might lead to brittle failure of a disk at speeds up to design speed will be detected. The inservice inspection program for the turbine assembly is to include the following:

- o The turbine should be disassembled at approximately 3-year intervals, during refueling or mainenance shutdowns coinciding with the inservice inspection schedule as required by ASME Boiler and Pressure Vessel Code, Section XI.

- o There should be complete inspection of all normally inaccessible parts such as couplings, coupling bolts, turbine shafts, low-pressure turbine blades, low-pressure disks, and high-pressure rotors. This inspection should consist of visual, surface, and volumetric examinations, in accordance with the procedures of the turbine manufacturer.

(2) An inservice inspection program for main steam and reheat valves which includes the following is to be implemented:

- o At approximately 3-year intervals, during refueling or maintenance shutdowns coinciding with the inservice inspection schedule required by Section XI of the ASME Code for reactor components, all main steam stop and control valves and reheat stop and intercept valves should be dismantled, and visual and surface examinations conducted of valve seats, disks, and stems. Valve bushings should be inspected and cleaned, and bore diameters should be checked for proper clearance.

- o Main steam stop and control valves and reheat stop and intercept valves should be exercised at least once a week by closing each valve and observing directly the valve motion as it moves smoothly to a fully closed position.

3.5.1.3.2 Evaluation

For WNP-2, the steam and power conversion system generates steam in a direct cycle BWR and converts it to electric power in a turbine generator manufactured by Westinghouse Electric Corporation. The placement and orientation of the turbine generator is unfavorable with respect to the station reactor buildings; that is, there are safety-related targets inside the low trajectory missile strike zone. The turbine is a tandem-compound type (single shaft) with one double-flow high-pressure turbine, three double-flow low-pressure turbines, and a rated rotational speed of 1800 rpm. The major portion of manufacture was performed during 1975.

A turbine failure resulting in the rupture of the turbine casing is approximately equivalent to a main steamline failure outside containment. For a BWR, such a failure releases primary coolant steam and radioactivity to the environment. Hence, regardless of the probability of turbine missiles striking safety-related structures, systems, or components, the criteria of SRP 15.6.4 (NUREG-0800) must be satisfied to meet the criteria of this review area.

Destructive Overspeed Failure Prevention

The turbine generator has a turbine control and overspeed protection system which is designed to control turbine action under all normal or abnormal conditions and to ensure that a turbine trip from full load will not cause the turbine to speed beyond acceptable limits, thus minimizing the probability of generating turbine missiles, in accordance with the requirements of GDC 4. The turbine control and overspeed protection system is, therefore, essential to the overall safe operation of the plant.

Turbine control is accomplished with a digital electrohydraulic control (EHC) system. The EHC system consists of an electronic governor using solid-state control techniques in combination with a high-pressure hydraulic actuating system. The system includes electrical control circuits for steam pressure control, speed control, load control, and steam control valve positioning.

There are four methods of turbine overspeed control protection: the normal speed governor (EHC), the overspeed protection controller (OPC), the mechanical overspeed trip mechanism, and the electrical overspeed trip. The EHC modulates the turbine control valves to maintain desired speed load characteristics within 2 to 3 rpm of desired speed. The primary function of the OPC is to avoid excessive turbine overspeed. At 103% of rated speed, the OPC solenoids open, closing the governor and intercept valves to arrest the overspeed before it reaches the trip setting of 111% of rated speed. After turbine coastdown to synchronous speed, the digital system takes control and maintains the turbine generator at synchronous speed. The mechanical overspeed sensor trips the turbine stop, control, and combined intermediate valves by deenergizing the hydraulic fluid systems when 111% of rated speed is reached. This maintains turbine speed below 120% of rated speed and causes the unit to coast down to turning gear operation. The electrical backup overspeed sensor trips these same valves when 111.2% of rated speed is reached by independently deenergizing the hydraulic fluid system. These overspeed trip systems can be tested while the unit is on line. The staff has reviewed these systems and has concluded that the turbine generator overspeed protection system meets the guidelines of SRP 10.2 and can perform its design safety function.

The overspeed protection controller, the mechanical overspeed trip mechanism and electrical overspeed trip are to be inspected and tested periodically during reactor operation. The manner and frequency of the inspection and testing will take into consideration the manufacturer's recommendations in conjunction with the plant generating requirements. Accordingly, the applicant's inservice inspection and testing program for the main steam control and stop valves and reheat intercept and stop valves includes the following: (1) at least once each 40 months, at least one main steam control valve, one main steam stop valve, one reheat intercept valve, and one reheat stop valve are to be dismantled and inspected; and (2) at least once a week, the main steam control and stop valves and reheat intercept and stop valves are to be exercised by closing each and observing the valve motion. Westinghouse has submitted to the staff a report describing an analysis according to which the probability of generating missiles at destructive overspeed is 1.7×10^{-6} per unit per year (Westinghouse, 1974). The staff is reviewing this report to determine the acceptability of the analysis and the adequacy of the manufacturer's recommended and the applicant's implemented overspeed protection inspection and testing, procedures, and schedules. Until this review is completed, the staff accepts the applicant's program.

Design Overspeed Failure Prevention

Failures of turbine disks at or below the design overspeed (nominally 120% of normal operating speed) are caused by a nonductile material failure at nominal stresses lower than the yield stress of the material. Since 1979, the staff has known of the stress corrosion cracking problems in low-pressure rotor disks of Westinghouse turbines. Westinghouse has developed and implemented procedures for inservice volumetric inspection of the bore and keyway areas of low-pressure turbine disks. Westinghouse has also prepared and submitted reports for staff review which describe Westinghouse methods for determining turbine-missile-generation probabilities as a result of stress corrosion cracking (Westinghouse 1981a and 1981b). Results stemming from the methods and procedures described in these reports are accepted by the staff until review of the reports is completed.

Westinghouse has provided the applicant the probabilities of a low-pressure turbine disk or associated blade ring fragment becoming a missile for the WNP-2 turbine. Missile-generation probabilities were provided for each disk on each low-pressure turbine, as a function of inspection interval (i.e., turbine operating time between inspections for cracks). In the analysis which produced these p_1 values, it is assumed that a crack initiates at the beginning of service life or immediately after an inservice inspection during a refueling outage. For a given disk, the probability of rupture as a result of stress corrosion is the probability that a crack exists in the disk bore whose depth is equal to or greater than a calculated critical crack depth. The critical crack depth is calculated using standard fracture mechanics methodology, and is based on actual material properties for the disk and on normal operating temperatures for the turbine. Data from field inspections are used to estimate (1) the probability of crack initiation in the various disk types, and (2) the crack growth rate, assuming cracks initiate at the beginning of service life or after an inservice inspection. Using appropriate probability distributions for crack growth rate and critical crack depth, a numerical analysis technique is used to calculate the probability of disk rupture. This value is a function of the inspection interval during which a crack may initiate and propagate. Energy absorption techniques are used to evaluate whether a given disk or fragment is contained or escapes the turbine casing upon rupture.

The NRC criteria for unfavorably oriented turbines apply to WNP-2. According to the Westinghouse analysis, the total missile-generation probability, P_1, will be less than 10^{-5} per year at startup. To keep P_1 less than 10^{-5} per year, the turbine would have to be inspected at 2-year intervals. With an inspection interval of 3 years, assuming a refueling outage scheduled about every 18 months, P_1 falls in the range 10^{-6} to 10^{-4} per year in the interval between the first and second refueling outages. Therefore, the staff concludes that the missile-generation probability is sufficiently low, provided all low-pressure turbine disks are volumetrically inspected within 3 years or by the second refueling outage. If no cracks are found on inspection, continued use of a 3-year inspection interval is considered acceptable. If cracks are found on inspection, the inspection schedule will have to be changed according to the depth of the cracks and an accompanying Westinghouse analysis.

3.5.1.3.3 Summary

Until staff review of the submitted Westinghouse reports is completed, the staff concludes that the turbine-missile risk for WNP-2 is acceptable provided both of the following conditions are met:

(1) Volumetric inspection of all low-pressure turbines is conducted in accordance with Westinghouse procedures within 3 years of startup or during the second refueling outage.

(2) The NRC criteria (inspection and testing, schedules and procedures) described above (the "new approach") and discussed in Section 3.5.1.3.2 above are implemented.

3.9 Mechanical Systems and Components

3.9.3 ASME Code Class 1, 2, and 3 Components, Component Supports, and Core Support Structures

3.9.3.3 Component Supports

In the WNP-2 SER, the staff stated that the applicant has committed to provide a response to IE Bulletin 79-02 concerning the base plate flexibility effect. The staff had reviewed the information on base plate flexibility described in the applicant's submittal dated April 14, 1982. The applicant has described the method for calculating the loads in the bolts as a result of plate flexibility for various plate and bolt configurations. The applicant also showed by numerical examples the effect of plate flexibility as compared to rigid plate analysis, and indicated the method for calculating the anchor factor of safety. The staff finds that the applicant's analysis satisfies the base plate flexibility requirements of IE Bulletin 79-02 and is acceptable.

Chapter 3
is in CRESS

6 ENGINEERED SAFETY FEATURES

6.2 Containment Systems

6.2.1 Containment Functional Design

The acceptance criteria used as the bases for the staff evaluation are set forth in the following documents: Section 6.2.1.1.c of the Standard Review Plan (NUREG-0800, dated July 1981); "Mark II Containment Lead Plant Program Load Evaluation and Acceptance Criteria" (NUREG-0487, dated October 1978); "Mark II Containment Program Load Evaluation and Acceptance Criteria" (NUREG-0808, dated August 1981); "Guidelines for Confirmatory In-plant Tests of Safety-Relief Valve Discharges for BWR Plants" (NUREG-0763, dated May 1981); and "Suppression Pool Temperature Limit for BWRs" (NUREG-0783 dated August 1981).

6.2.1.8.5 Steam Condensation Oscillation Load

The applicant has submitted a report titled "Comparison of Condensation Oscillation and Chugging Loads for Assessment of WPPSS Nuclear Project No. 2" to support the contention that the condensation oscillation (CO) load is less critical than the chugging load and does not represent a governing load for structures, piping, and equipment in WNP-2.

The staff has completed its evaluation and concludes that, because of the extra margin of conservatism in the WNP-2 plant-unique chugging load sources and because the WNP-2 specification assumes that three vents in a radial row chug simultaneously, the WNP-2 applicant does not need to assess the WNP-2 plant for the CO load. The rationale for the staff conclusion is presented in Appendix F.1.

6.2.1.8.6 Plant-Unique Chugging Load Specifications

When the SER was written, an NRC staff consultant raised a concern regarding the application of one set of chug start times. This application could result in significant "poke through" of the chugging load specifications at certain frequencies and reduction at other frequencies.

In Letter G02-82-324, dated March 15, 1982, the applicant transmitted results of studies performed to address the staff's concern. During a telephone conversation on March 19, 1982, the staff requested additional information to justify the applicant's contention that the asymmetric chugging load case has no significance in the plant design. The applicant provided this information in Letter No. G02-82-362, dated April 5, 1982.

The staff has completed its review of the applicant's response to the staff's concern and concludes that the applicant has adequately addressed this concern and that modification to the load specification described in detail in Appendix F.1 is not required. Appendix F.2 presents the concern and the staff's evaluation and conclusions.

6.2.1.8.8(4) Steam Condensation Submerged Drag Loads

In the SER, the staff stated it would not reach a conclusion on this load until the staff review of the applicant's justification to omit the CO load specification was complete. Based on this review, the staff now concludes that the submerged structure drag load methodology proposed by the applicant is acceptable.

6.2.3 Containment Isolation Control Rod Driver Insert and Withdrawal Lines

Control rod drive (CRD) insert and withdrawal lines depart from the explicit requirements of the GDC and, as discussed below, are found to be acceptable on other defined bases.

Both the CRD insert and withdrawal lines are provided with normally closed, fail-closed, solenoid-operated directional control valves, which open only during routine movement of their associated control rod. The normally closed, fail-open, air-operated scram inlet and exhaust valves open only when required to effect a rapid reactor shutdown (scram). In addition, manual shutoff valves are provided for positive isolation in the unlikely event of a pipe break within a hydraulic control unit. (These units and the valves described above are located outside containment to satisfy testing, inspection, and maintenance requirements). In addition, each CRD insert line is provided with an automatically actuated ball check valve inside containment. The staff finds that the system design represents a departure from the explicit requirements of the GDC. However, in accordance with GDC 55 (which permits departure from its explicit requirement) the staff finds that the CRD containment isolation provision stated above is acceptable on the basis stated in NUREG-0803, "Safety Evaluation Report Regarding Integrity of BWR Scram Systems."

6.2.7 Fracture Prevention of Containmnt Pressure Boundary

The staff safety evaluation assessed the ferritic materials in the WNP-2 containment system that constitute the containment pressure boundary to determine if the material fracture toughness is in compliance with the requirements of GDC 51, "Fracture Prevention of Containment Pressure Boundary."

GDC 51 requires that under operating, maintenance, testing, and postulated accident conditions: (1) the ferritic materials of the containment pressure boundary behave in a nonbrittle manner and (2) the probability of rapidly propagating fracture is minimized.

The WNP-2 containment system includes a ferritic steel primary containment vessel and head enclosed by a reinforced concrete shield structure. The ferritic materials of the containment pressure boundary that were considered in the staff assessment are those that have been applied in the fabrication of the containment vessel and head, equipment hatch, personnel lock, and penetrations and components of the fluid system including the valves required to isolate the system. These components are the parts of the containment system that are not backed by concrete and must sustain loads during the performance of the containment function under the conditions cited by GDC 51.

The WNP-2 containment pressure boundary is comprised of ASME Code Class 1, Class 2, and Class MC components. In late 1979, the staff reviewed the fracture toughness requirements of the ferritic materials of Class MC, Class 1, and Class 2 components that typically constitute the containment pressure boundary. Based on this review, the staff determined that the fracture toughness requirements in ASME Code editions and addenda typical of those used in the design of the WNP-2 containment may not ensure compliance with GDC 51 for all areas of the containment pressure boundary. The staff initiated a program to review fracture toughness requirements for containment pressure boundary materials to define those fracture toughness criteria that most appropriately address the requirements of GDC 51. Before this study was complete, the staff elected to apply in its licensing reviews of ferritic containment pressure boundary materials the criteria for Class 2 components identified in the Summer 1977 Addenda of Section III of the ASME Code. Because the fracture toughness criteria that have been applied in construction typically differ in Code classification and Code edition and addenda, the staff has chosen the criteria in the Summer 1977 Addenda of Section III of the Code to provide a uniform review, consistent with the safety function of the containment pressure boundary materials. Therefore, the staff reviewed the Class 1, Class 2, and Class MC components of the WNP-2 containment pressure boundary according to the fracture toughness requirements of the Summer 1977 Addenda of Section III for Class 2 components.

Considered in the staff review are components of the containment system that are load bearing and provide a pressure boundary in the performance of the containment function under operating, maintenance, testing, and postulated accident conditions, as addressed in GDC 51. These components are the containment vessel and head equipment hatch, personnel airlock, and penetrations and elements of the main steam and main feedwater systems.

The staff assessment of the fracture toughness of the ferritic materials of these components is based on fracture toughness test data provided by the applicant, their metallurgical characterization, and fracture toughness data presented in NUREG-0577, "Potenial for Low Fracture Toughness and Lamellar Tearing of PWR Steam Generator and Reactor Coolant Pump Supports," and ASME Code Section III, Summer 1977 Addenda, Subsection NC.

The metallurgical characterization of these materials, with respect to their fracture toughness, was developed from a review of how these materials were fabricated and the thermal history they experienced during fabrication. The metallurgical characterization of these materials, when correleated with the data in NUREG-0577 and the Summer 1977 Addenda of the ASME Code Section III, provided the technical basis for the staff evaluation of compliance with the Code requirements.

Based on its review of the available fracture toughness data and material fabrication histories, and the use of correlations between metallurgical characteristics and material fracture toughness, the staff concludes that the ferritic materials in the WNP-2 containment pressure boundary meet the fracture toughness requirements that are specified for Class 2 components by the 1977 Addenda of Section III of the ASME Code. Compliance with these Code requirements provides reasonable assurance that the WNP-2 reactor containment pressure boundary materials will behave in a nonbrittle manner, that the probability of rapidly propagating fracture will be minimized, and that the requirements of GDC 51 are satisfied.

7 INSTRUMENTATION AND CONTROL

7.3 Engineered Safety Features Systems

7.3.2 Specific Findings

7.3.2.7 IE Bulletin 80-06

In the SER (NUREG-0892), the staff stated that a full response to IE Bulletin 80-06, "Engineered Safety Features Reset Control," was required and that corrective actions, if needed, were to be completed prior to fuel load.

The applicant has satisfactorily responded to the staff request (Question 031.136) by Letter G02-82-445, dated May 14, 1982. The applicant has confirmed that the analysis has been completed, has committed to modify equipment prior to fuel load, and has committed to preoperational testing to confirm the adequacy of the analysis.

The control circuits for specific reactor core isolation cooling valves, radwaste system isolation valves, reactor heat removal (RHR) sample line valves, and reactor water sample valves are to be modified in accordance with IE Bulletin 80-06.

7.4 Systems Required for Safe Shutdown

7.4.2 Specific Findings

7.4.2.3 Remote Shutdown System

In the SER, the staff stated that the staff would review a forthcoming study of remote shutdown capability and report the results in a supplement to the SER. The staff was concerned that the remote shutdown capability described in the

FSAR might not meet the quality and redundancy standards needed to conform to the staff's interpretation of GDC 19.

The applicant has satisfactorily addressed this issue in Letters G02-82-447, dated May 14 1982, and G02-82-036, dated June 4, 1982.

An alternate remote shutdown system is to be installed. This remote shutdown and alternate remote shutdown systems (panel, indication, and control) are or will be seismically qualified, powered from Class 1E power supplies, and provided with heating, ventilating, and air conditioning that are seperate from each other and from the control room.

The alternate remote shutdown system will be located in critical electrical switchgear room 1, approximately 300 ft from the remote shutdown system. The alternate remote shutdown system will contain RHR loop A valve and pump controls, safety/relief valve solenoid B controls, suppression pool temperature RHR loop A flow, reactor vessel water level, and reactor vessel pressue indicators.

The remote shutdown system is described in the SER.

The applicant has committed (Letter G02-82-447, May 14, 1982) to install the alternate shutdown system during first refueling outage. This committment is acceptable to the staff and will be made a condition of the license.

9 AUXILIARY SYSTEMS

9.5 Other Auxiliary Systems

9.5.4 - 9.5.8 Emergency Diesel Engine Fuel Oil, Cooling Water, Air Starting, Lubrication, and Combustion Air Intake and Exhaust Systems

The applicant, in a letter dated May 25, 1982, provided the standards to which the engine skid-mounted auxiliary systems (fuel oil, cooling water, air starting, lubrication, and combustion air intake and exhaust) piping and associated components were designed. This engine-mounted piping and the associated components (such as valves, fabricated headers, fabricated special fittings, and the like) are designed, manufactured, and inspected in accordance with the guidelines and requirements of ANSI Standard B31.1, "Code for Pressure Piping"; ANSI N45.2, "Quality Assurance Program Requirements for Nuclear Facilities"; and 10 CFR 50 Appendix B. The engine skid-mounted auxiliary system piping and associated components are intentionally overdesigned (subjected to low working stresses) for the application, thereby resulting in high operational reliability. The applicant also provided a comparison of the design with the requirements of ASME Section III Class 3. The results of the comparison indicate they differ from ASME Section III Class 3 in two areas:

(1) ASME requires liquid-penetrant examination for welds over 4-in. IPS (iron pipe size). The applicant stated that only a few welds in cooling water system piping 4 in. and over were not liquid-penetrant examined; in those few cases welds were only visually examined with system at design pressure and temperature for acceptability of weld. The staff finds this partially acceptable.

(2) ASME requires a hydrostatic test to 125 percent of the design pressure. The applicant stated some piping and components were hydrostatically

tested to 150 percent of design pressure and that the rest of the piping would be leak tested at operating pressure during engine operation. The staff finds this also partially acceptable.

In lieu of performing liquid-penetrant examination of all piping 4 in. and over and the hydrostatic tests on all piping, the staff requires only that all diesel engine auxiliary system piping be hydrostatically tested to a minimum of 125 percent of design pressure. Because of the low working stresses, the hydrostatic tests will provide adequate assurance of piping leak tightness and weld integrity. The NRC Regional Office staff will verify these tests. The design of the engine skid-mounted auxiliary system piping and components to the cited design philosophy and standards is considered equivalent to a system designed to ASME Code Section III Class 3 requirements with regard to system functional operability and inservice reliability.

Based on its review, the staff concludes that the engine-mounted piping and components of emergency diesel engine auxiliary systems (fuel oil, cooling water, air starting, lubrication, and combustion air intake and exhaust systems) meet the requirements of GDC 2, 4, 5, and 17; meet the guidance of the cited Regulatory Guides and Standard Review Plans; can perform their design safety function; and meet the recommendations of NUREG/CR-0660 and industry codes and standards. Therefore, on completion of the hydrostatic tests, they are acceptable.

9.5.7 Emergency Diesel Engine Lubrication System

As stated in the SER, the preheat lubrication system for the high-pressure core spray (HPCS) diesel engine is composed of a continuously operating ac pump and a standby dc pump that prelubricate the turbocharger bearings only. The other wearing parts of the engine do not received any lubrication until after the engine starts and the engine-driven lube oil pumps reach full speed. This is not acceptable. The staff requires a prelubrication of the diesel engines because dry starting of the diesel engines under emergency conditions will result in momentary lack of lubrication at the various moving parts (this can eventually lead to failures and resultant equipment unavailability).

The applicant was informed of this problem at a meeting in Bethesda on December 10, 1981. In the Licensing Review Group (LRG)-II position paper dated March 12, 1982 and confirmed at the December 10, 1981 meeting, the applicant stated that the manufacturer's recommendation (GE EMD-MI-9744), will be implemented to correct the staff concern. However, the manufacturer's recommended "fix" does not totally alleviate the problem of dry starting of the engine, in that only the wearing parts located in the lower half of the engine are lubricated. Thus, the staff finds modification only partially acceptable as a means of minimizing dry engine starts. The applicant has been informed of the problem. Until an adequate manufacturer's modification is approved by the staff, the staff will require the applicant to manually prelubricate the diesel engines in accordance with the manufacturer's recommendations at least once a week and before each manual diesel engine start. The weekly prelubrication will deposit a film of lubricant on the engine wearing surfaces. The staff finds this procedure acceptable as a means of mimimizing dry engine starts and will incorporate this requirement into the Technical Specifications. This requirement has been discussed with the applicant, who confirms compliance.

Based on its review, the staff concludes that the emergency diesel engine preheat lubricating oil sysem meets the requirements of GDC 2, 4, 5, and 17; meets the guidance of the cited Regulatory Guides and SRP 9.5.7; can perform its design safety function; and meets the recommendations of NUREG/CR-0660 and industry codes and standards. It is therefore acceptable.

13 CONDUCT OF OPERATIONS

13.1 Organization Structure of Applicant

13.1.1 Management and Technical Support Organization

13.1.1.1 General

The applicant has made organizational changes that combine the project management for design and construction of WNP Units 1, 2, and 3 under one manager and transfer the responsibility of the Manager, Test and Startup for WNP-2 from the WNP-2 project to the Director of Power Generation. W. C. Bibb has been appointed to the position of Director of Power Generation formerly held by A. Kohler, Jr. The Plant Operations Manager for each plant and the Manager, Test and Startup at WNP-2 will now report to the Director of Power Generation.

Mr. Bibb has approximately 26 years experience in the testing, startup, and operation of nuclear plants. He has been with the applicant for 6 years and has served as Deputy Program Director for Startup and Operations of WNP-2 and as Project Manager for WNP-2. Before joining WPPSS, Mr. Bibb held numerous posts with the Nuclear Energy Division of General Electric Company where he was involved with the startup and operation of several boiling water reactors.

The staff concludes that these changes meet the acceptance criteria of SRP 13.1.1 (NUREG-0800). Figure 13.1 has been revised to reflect the corporate reorganization.

13.2 Training

13.2.2 Training for Nonlicensed Personnal

13.2.2.5 Summary and Conclusions

In addition to general employee training, the Shift Support Supervisors will receive specific systems and procedures training before fuel load. This training

Figure 13.1 Washington Public Power Supply System

WASHINGTON PUBLIC POWER SUPPLY SYSTEM

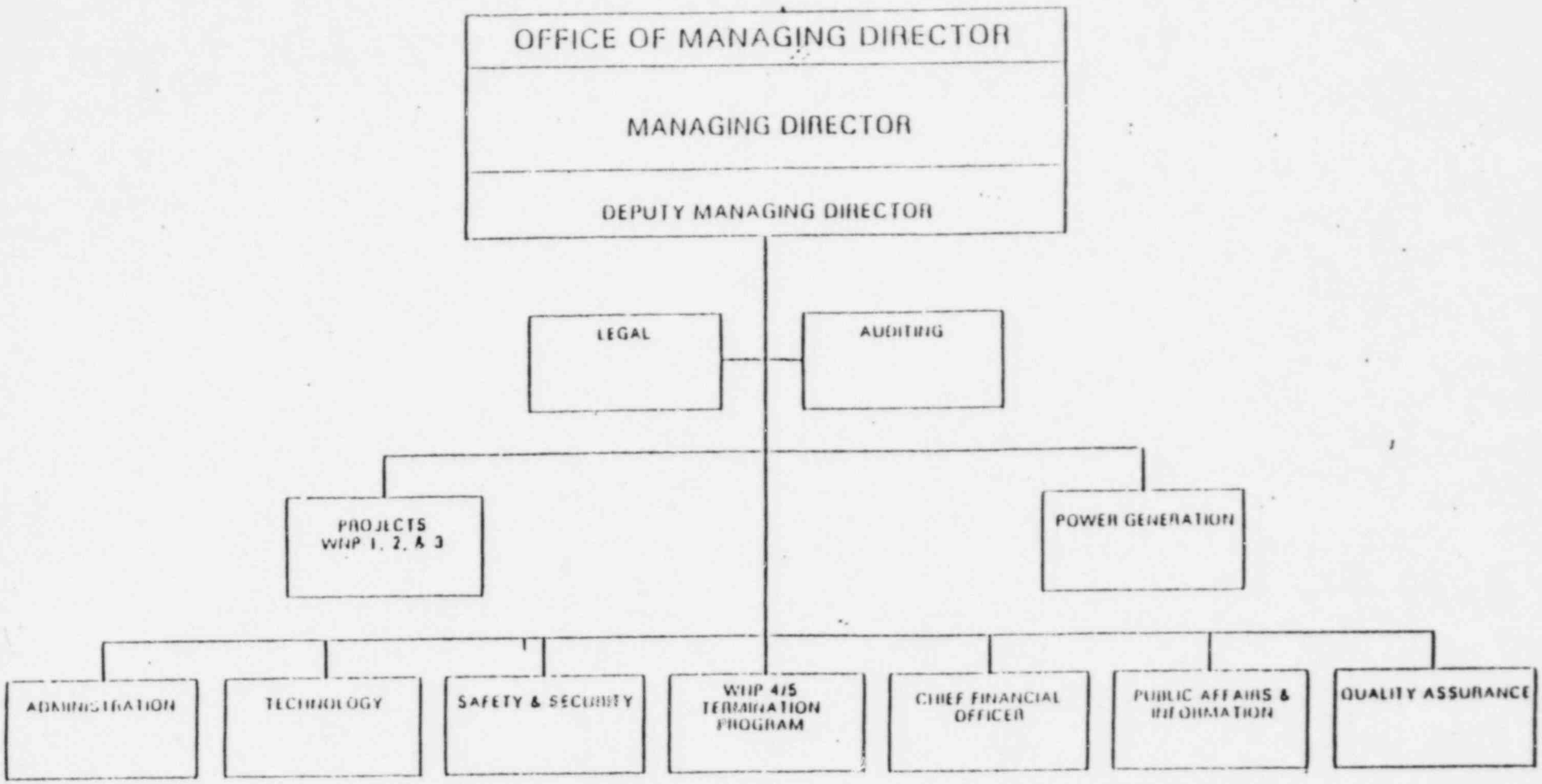

FIGURE 13.1

will enable employees to meet the qualification requirements for the function of fire brigade leader, which is one of the duties of the Shift Support Supervisors.

The staff has reviewed the proposed training program for the Shift Support Supervisors, as related to their role as the fire brigade leader, and finds that it meets the staff position described in BTP MEB-9.5.1 of NUREG-0800.

13.5 Plant Procedures

13.5.1 Adminstrative Procedures

13.5.1.4 Limitations on Working Hours

The applicant has stated that administrative procedures will be established to ensure that, to the extent practicable, personnel are not assigned to shift duties while they are in a fatigued condition that could significantly reduce their mental alertness or their decision-making capability. The controls shall apply to the plant staff members who perform safety-related functions (such as senior reactor operators, reactor operators, health physicists, auxiliary operators, and key maintenance personnel.

Enough plant operating personnel should be employed to maintain adequate shift coverage without routine heavy use of overtime. However, if unforeseen problems require substantial amounts of overtime on a temporary basis, the following guidelines shall be followed:

(1) An individual should not be permitted to work more than 16 hours straight (excluding shift turnover time).

(2) An individual should not be permitted to work more than 16 hours in any 24-hour period, nor more than 24 hours in any 48-hour period, nor more than 72 hours in any 7-day period (all excluding shift turnover time).

(3) A break of at least 8 hours should be allowed between work periods (including shift turnover time).

(4) The use of overtime should be considered on an individual basis and not for the entire staff on a shift.

The staff recognizes that very unusual circumstances may arise requiring deviation from the above guidelines; such deviation shall be authorized by the Plant Manager or the Plant Manager's deputy, or higher levels of management.

The staff has reviewed the applicant's commitment to establish an administrative procedure to limit working hours and finds that it meets the staff position described in Task Action Plan Item I.A.1.3 of NUREG-0737 and in NUREG-0800 and is acceptable.

16 TECHNICAL SPECIFICATIONS

The staff has identified an additional issue that must be included in the Technical Specifications as a conditions of staff acceptance of resolution of these items. It is listed below and is discussed further in the section of this supplement as indicated:

Item	Section
(9) Prelubrication of diesel engines	9.5.7

Chapter 18 is in CRESS

APPENDIX A

CONTINUATION OF CHRONOLOGY

April 8, 1982	Staff issues Safety Evaluation Report.
April 19, 1982	Letter from applicant regarding several recently announced organizational changes.
April 22, 1982	Letter from applicant forwarding revised responses regarding safety concerns associated with pipe breaks in BWR scram systems.
April 26, 1982	Letter to applicant requesting additional information.
April 26, 1982	Letter from applicant transmitting additional geologic information.
May 12, 1982	Letter from applicant submitting information provided staff representatives during a site visit on April 26-27, 1982.
May 14, 1982	Letter from applicant providing information regarding tornado-missile protection for diesel generator exhausts.
May 18, 1982	Meeting with applicant to discuss geology and seismology open items (summary issued June 7, 1982).
May 20, 1982	Letter from applicant transmittng information regarding fast scram hydrodynamic loads on control rod drive systems.
May 20, 1982	Letter from applicant regarding clarification of electrical system information.
May 25, 1982	Letter from applicant regarding SER open items: diesel generator auxiliary qualifications.
May 28, 1982	Letter from applicant providing additional information for seismic analysis performed for small magnitude/short epicentral distance (SM/SD) earthquake.
May 28, 1982	Letter from applicant regarding internally generated missiles (inside containment).
June 1, 1982	Letter to applicant requesting additional information.
June 4, 1982	Letter from applicant transmitting response to concerns regarding staff site visit.

June 4, 1982	Letter from applicant providing additional information regarding the remote shutdown system.
June 4, 1982	Letter from applicant submitting FSAR Amendment 24.
June 7, 1982	Letter to applicant requesting additional information.
June 10, 1982	Letter from applicant transmitting resume of S. C. Bibb, Director of Power Generation.
June 11, 1982	Letter from applicant regarding staff review of Hanford seismic issues.
June 14, 1982	Letter from applicant regarding area vs. magnitude relationship.
June 15, 1982	Letter to applicant regarding analysis of reflection and refraction data shot at Skagit/Hanford site.
June 15, 1982	Letter to applicant regarding review of draft Sierra geophysics report, "Paleomagnetism of Pre-Missoula Gravels from Corehold PM-2 on the Southeast Anticline, Hanford Site, Washington."
June 21, 1982	Letter from applicant regarding GDC 51.
June 22, 1982	Letter from applicant regarding Emergency Preparedness Plan.
June 29, 1982	Letter to applicant regarding letter GO2-82-466, dated May 14, 1982 (WNP-2 Tornado Missile Protection for Diesel Generator Exhausts).

APPENDIX E

NRC STAFF CONTRIBUTORS AND CONSULTANTS

This Supplement No. 1 to the SER is a product of the NRC ataff. The following NRC staff members were principal contributors to this report:

Name	Title	Review Branch
Robert J. Giardina	Reactor Systems Engineer (Mechanical)	Power Systems
Jack E. Rosenthal	Nuclear Engineer	Instrumentation and Control Systems
Farouk Eltawila	Senior Containment Systems Engineer	Containment Systems
Yueh-Li C. Li	Mechanical Engineer	Mechanical Engineering
Leon Reiter	Section Leader	Geosciences
Stephan Brocoum	Section Leader	Geosciences
Jeffrey K. Kimball	Geophysicist/Seismologist	Geosciences
Ina B. Alterman	Geologist	Geosciences
Joseph Halapatz	Materials Engineer	Materials Engineering
Frederick R. Allenspach	Nuclear Engineer (Management Systems)	Licensee Qualification
Rajender Auluck	Project Manager	Licensing Branch No. 2

Consultants who contributed to this report were:

Name	Affiliation
George Bienkowski	Princeton University
John Lehner	Brookhaven National Laboratory
C. Economus	Brookhaven National Laboratory
C. C. Lin	Brookhaven National Laboratory

APPENDIX B

BIBLIOGRAPHY

Algermissen, S. T. and D. M. Perkins, "A Probabilistic Estimate of Maximum Ground Acceleration in the Contiguous United States," USGS Open-File Report 76-416, 1976.

American National Standards Institute, Standard N45.2, "Quality Assurance Program Requirements for Nuclear Facilities."

---, Standard B 31.1, "Code for Power Piping."

American Society of Mechanical Engineers, Boiler and Pressure Vessel Code, Section III, 1977 Summer Addenda.

Applied Technology Council, "Tentative Provision for the Development of Seismic Regulations for Buildings," National Bureau of Standards Special Publication 510, June 1978.

insert fr. next pg.

Bruhn, R., "Preliminary Analysis of Deformation in Part of the Yakima Fold Belt, South-Central Washington," draft report prepared for Washington Public Power Supply System, Richland, WA, 1981.

Bush, S. H., "Probability of Damage to Nuclear Components," Nuclear Safety, 14, 3, May-June 1973.

Campbell, K. W., "Near-Source Attenuation of Peak Horizontal Acceleration," Seismol. Soc. Amer. Bull., v. 71, 1981.

Cochran, M. P., "Geophysical Investigation of a Segment of the Rattlesnake Hills Lineament (abstract)," American Geophysical Union Transactions, v. 63, 1982.

Coffman, J. L. and C. A. Von Hake, "Earthquake History of the United States," NOAA-U.S. Department of Commerce Publication 41-1, 1973.

---, "A Reassessment of Turbine Generator Failure Probability," Nuclear Safety, 19, 6, November-December 1978.

Golder Associates, "Gable Mountain: Structural Investigations and Analyses," ~~R~~eport prepared for Northwest Energy Services Company, 1981a.

---, "Geologic Structure of Umtanum Ridge: Priest Rapids Dam to Sourdough Canyon," ~~R~~eport prepared for Northwest Energy Services Company, 1981b.

---, "The Southeast Anticline Fault: Evaluation of Attitude and Displacement," submitted to Washington Public Power Supply System, Richland, WA, 1982.

Gutenberg, B. and C. F. Richter, "On seismic waves (third paper)," Gerlands Beitrage Zur Geophysik, v. 47. p. 73-131, 1936

---, Seismicity of the Earth, Princeton University Press, 1949; 2nd ed, 1954.

---, Seismicity of the Earth and Associated Phenomena, Hafner Publishing Company, New York, 1965.

Hanks, T. C. and H. Kanamori, "A Moment Magnitude Scale," Jour. Geophys. Res., 84: p 2348, 1979.

Heaton, T. H., F. Tajima, and A. W. Mori, "Estimating Ground Motion Using Recorded Accelerograms," manuscript submitted to Seismol. Soc. Amer. Bull., 1982.

Idriss, I. S., D. Sadigh, and M. S. Power, "Variations of Peak Accelerations and Velocities with Magnitude to Close Distances to the Source," paper prepared for presentation at April 1982 meeting Seismol. Soc. Amer., 1982.

move above John Blume and Associates, "Subsurface geological investigations for the FFTF project in Pasco Basin," Report JABE-WADCO-07, prepared for WADCO, Richland, WA, 1971.

Joyner, W. B. and D. M. Boore, "Peak Horizontal Acceleration and Velocity from Strong - Motion Records Including Records from the 1979 Imperial Valley, California, Earthquake," Seismol. Soc. Amer. Bull., v. 71, 1981.

Kanamori, H., "Qualification of Earthquake," Nature, v. 271, 1978.

---"A Semi-empirical Approach to Prediction of Long Period Motions from Great Earthquake," Seismol. Soc. Amer. Bull., v. 69, 1979.

Malone, S. D., "Annual Technical Report on Earthquake Monitoring of the Hanford Region, Eastern Washington," ~~R~~eport prepared for the U.S. Department of Energy and Washington Public Power Supply System by the Geophysics Program, University of Washington, Seattle, 1979.

Malone, S. D., and S. S. Bor, "Attenuation Patterns in the Pacific Northwest Based on Intensity Data and the Location of the 1872 North Cascades Earthquake," Seismol. Soc. Bull., v. 59, 1979.

Newmark, N. M., and W. J. Hall, "Development of Criteria for Seismic Review of Selected Nuclear Power Plants," NUREG/CR-0098, 1978.
US NRC Report

Nuttli, O., "The Relation of Sustained Maximum Ground Acceleration and Velocity to Earthquake Intensity and Magnitude," Report 16, State-of-the-Art for Assessing Earthquake Hazards in the United States, Miscellaneous Paper S-73-1, U.S. Army Engineer Waterways Experiment Station, Vicksburg, MS, 1979.

Price, E. H., "Structural Geometry, Stain Distribution, and Tectonic Evolution of Umtanum Ridge at Priest Rapids and a Comparison with Other Selected Localities within Yakima Fold Structures, South-Central Washington," Rockwell Hanford Operations, Richland, WA, RHP-BWI-FA-138, 1982.

Puracru, G., and H. Berckhemer, "Quantitative Relations of Seismic Source Parameters and a Classificatoin of Earthquakes: Tectonophysics," Seismol. Soc. Amer. Bull.,v. 84, 1982.

Richter, C. F., "An Instrumental Earthquake Magnitude Scale," Seismol. Soc. Amer. Bull. v. 25, 1935.
91

---, "Elementary Seismology, W. H. Freeman and Co., San Francisco, 1958.

Rockwell Hanford Operations, C. W. Myers and S. M. Price, eds, "Subsurface geology of the Cold Creek syncline," RHO-BWI-ST-14, Richland, WA, 1981.

Schnable, P. B., J. Lysmer, and H. B. Seed, "SHAKE, A Computer Program for Earthquake Response Analysis of Horizontally Layered Sites," EERC Report 72-12, Univ of Calif, Berkeley, 1972.

Shannon and Wilson, Inc., "Geologic Reconnaissance of the Wallula Gap, Washington-Blue Mountains-LaGrande, Oregon Region," Report submitted to Washington Public Power Supply System, Richland. WA, 1979.

Shebalin, N. V., "Determination of Focal Depth from Macroseismic Data with Consideration of the Influence of the Low Velocity Layer, in Problems in Engineering Seismology," No. 2, Akad. Nank. SSR Inst. Fiziki Zemli Trudy 5(172); translation P. J. Barosh, U.S. Dept. Comm., NTIS Rept TT-67-61781, 1959.

Sierra Geophysics, Inc., "Paleomagnetism of Pre-Missoula Gravels, Pasco Basin and Vicinity, Washington," submitted to Golder Associates, 1982a.

---, "Paleomagnetism of Pre-Missoula Gravels from Corehole PM-2 on the Southeast Anticline, Handord Site, Washington," submitted to Golder Associates, 1982b.

Singh S., "Regionalization of Crustal Q on the Continental United States," Ph.D. Dissertation, St. Louis University, 1981.

Skagit/Hanford Nuclear Projects, Preliminary Safety Analysis Report, prepared by Northwest Energy Services Company, Kirkland, WA, 1982.

Slemmons, D. B., "Determination of Design Earthquake Magnitudes for Microzonation," in Proceedings of the Third International Earthquake Microzna tion Conference, 1982.

--- "Fault Assessment, review of State-of-the-Art Methods," Assoc. Eng. Geologists Bull., in press.

Thatcher, W. and T. C. Hanks, "Source Parameters of Southern California Earthquakes, "Jour. Geophys. Res., 78, 1973.

U.S. Geological Survey, National Oceanograpphic and Atmospheric Administration, Ad Hoc Working Group on Intensities of Historic Earthquakes, "Maximum Intensity of the Washington Earthquake of December 14, 1872," USGS, Denver, Co, April 1977.

U.S. Atomic Commission, "Safety Evaluation of the WPPSS Nuclear Project No. 2," 1972.

U.S. Nuclear Regulatory Commission, IE Bulletin 79-02.

move NUREG-

~~---, "Safety Evaluation of the Washington Nuclear Projects 1 and 4," 1978.~~

---, ~~U.S. Nuclear Regulatory Commission~~, NUREG-0011 Safty Evaluation of the Sequoyah Nuclear Plants Units 1 and 2," 1979.

---, NUREG-0023, "Safety Evaluation of the WNP-1 and -4 Nuclear Plant, 1978.

---, NUREG-0487, "Mark II Containment Lead Plant Program Load Evaluation and Acceptance Criteria," October 1978.

---, NUREG-0577, "Potential for Low Fracture Toughness and Lamellar Tearing of PWR Steam Generator and Reactor Coolant Pump Supports," October 1975.

---, NUREG-0712, "Safety Evaluation of the San Onofre Nuclear Plant," December 1980.

---, NUREG-0763, "Guidelines for Confirmatory In-plant Tests of Safety-Relief Valve Discharges for BWR Plants," May 1981.

---, NUREG-0783, "Suppression Pool Temperature Limit for BWRs," August 1981.

Westinghouse, "Procedures for Estimating the Probability of the Generation ~~of~~ and Striking of Missiles from a Nuclear Turbine," March 1974.

---, "Procedures for Estimating the Probability of Steam Turbine Disc Rupture from Stress Corrosion Cracking," WSTG-1-P, May 1981a.

---, "Missile Energy Analysis Methods for Nuclear Steam Turbines," WSTG-2, May 1981b.

---, NUREG-0798, "Safety Evaluation of the Enrico Fermi Nuclear Plant Unit 2," June," June 1981.

---, NUREG-0800, "Standard Review Plan," July 1981.

---, NUREG-0803, "Safety Evaluation Report Regarding the Integrity of BWR Scram Systems," August 1981.

---, NUREG-0808, "Mark II Containment Program Load Evaluation and Acceptance Criteria," August 1981.

---, Supplemental Testimony of R. McMullen and J. Kelleher to WNP-1 and WNP-4, Docket Nos. 50.460 and 50-513, 1978.

---, Testimony of Jeffrey Kimball before the Atomic Safety and Licensing Board, Midland Nuclear Plant Docket Nos. 50-329/330, 1981.

? ---, NUREG-_____. "Safety Evaluation Report Related to the Operation of Midland Plant, Units 1 and 2," 1982.

NUREG/CR-0098 (see Newmark, above).

NUREG/CR-0660, "Enhancement of On-Site Emergency Diesel Generator Reliability," February 1979.

Washington Public Power Supply System, "Comparison of Condensation Oscillation and Chugging Loads for Assessment of WNP-2," report 602-81-552, December 1981.

date ---, "Final Safety Analysis Report, Nuclear Project No. 2,"

date ---, "Preliminary Safety Analysis Report, Nuclear Projects 1 and 4,"

Weston Geophysical Research, "Magnetic Modeling Columbia Plateau area," report prepared for the Washington Public Power Supply System, Richland, WA, 1978.

---, "Magnetic Modeling in the Vicinity of Snake River, Wallula Gap, Washington, and Warm Springs, Oregon," report prepared for the Washington Public Power Supply System, Richland, WA, 1980.

Woodward-Cycle Consultants, "Offshore Alaska Seismic Exposure Study," v. II, prepared for Alaska Subarctic Offshore Committee, 1978.

---, "Report of the Evaluation of Maximum Earthquake and Site Ground Motion Parameters Associated with the Offshore Zone of Deformation, San Onofre Nuclear Generating Station," report prepared for Southern California Edison Company, 1979.

---, "Seismological Review of the July 16, 1936 Milton-Freewater Earthquake Source Region," report submitted to Washington Public Power Supply System, Richland, WA, 1980a.

---, "Recent Seismicity of the Hanford Region," report submitted to Washington Public Power Supply System, Richland, WA, 1980b.

---, "Task D3, Quaternary Sediments Study of the Pasco Basin and Adjacent Area," report submitted to Washington Public Power Supply System, Richland, WA, 1981a.

---, Task D9, the July 16, 1936, Walla Walla Earthquake," report submitted to Washington Public Power Supply System, Richland, WA, 1981b.

---, "Logs of Trenches at Finley Quarry," submitted to Washington Public Power Supply System, Richland, WA, 1981c.

---, "Task 7b, Area Versus Magnitude Relationships," report submitted to Washington Public Power Supply System, Richland, WA 1982a.

---, "Task 7b, Maximum Average Rate of Strike-Slip Displacement on RAW," report submitted to Washington Public Power Supply System, Richland, WA, 1982~~b~~a.

---, "Review of the Magnitude of the July 16, 1936, Walla Walla Area Earthquake," report submitted to Washington Public Power Supply System, Richland, WA, 1982c.

Wyss, M., "Estimating Maximum Expectable Magnitude of Earthquakes from Fault Dimensions," Geology, v. 7, 1979.

all cap

APPENDIX F

Documentation of the Staff Rationale for Accepting the Plant-Unique Pool Dynamic Loads

Contents

Contents (Continued)

Contents (Continued)

Figures

Figures (Continued)

Page

Tables

F.1 EVALUATION OF WNP-2 PLANT-UNIQUE POOL DYNAMIC METHODOLOGIES

Introduction

This appendix documents the staff's evaluation of the WPPSS methodologies that were used for WNP-2 design assessment to accommodate hydrodynamic loads generated as a result of a LOCA or safety/relief valve (SRV) actuation.

Section F.1.1 contains the proposed plant-unique condensation oscillation load and the staff evaluation. Section F.1.2 summarizes the applicant's proposed, and the staff's evaluation of, the chugging load specification. Section F.1.3 presents the SRV methodology and the staff evaluation of the associated loads.

Brookhaven National Laboratory assisted the staff in evaluating the applicant's plant-unique pool dynamic loads.

F.1.1 Evaluation of the WNP-2 Condensation Oscillation Load Position

F.1.1.1 Background

(1) Generic Condensation Oscillation (CO) Load Definition

In late December 1981, a summary report was issued by the applicant for WNP-2 entitled "Comparison of Condensation Oscillation and Chugging Loads for Assessment of WPPSS Nuclear Project No. 2.[1] In order to evaluate this comparison, and the conclusions reached from it regarding assessment of WNP-2 for CO loads, it will be useful to recall the generic CO load specification described in detail in Reference 2 and evaluated in Reference 3. The specification was based on data from the TS5200 test series conducted by General Electric for the Mark II Owners in the 4T test facility[4]; this test series became known as the 4TCO tests. Both the interim and the almost identical final generic CO specification that were developed from these results contain many conservatisms.[3] Besides being based on data from tests with small pool-to-vent area ratios as well as conservative temperature ranges, the generic CO specification does not take credit for either multivent effects or fluid structure interaction (FSI) effects. The multivent effect is the most significant. The staff's review of the generic CO load specification has noted that pressure amplitudes during CO from the JAERI multivent facility were significantly below comparable 4TCO single vent tests at all frequencies.[3] These considerations have led the staff to conclude that the generic CO load specification is sufficiently conservative for design purposes.

(2) Data Bases

While condensation oscillation-like phenomena have been observed at all test facilities where steam blowdowns into a suppression pool were conducted, only two data bases are of direct applicability for the WNP-2. They are the single-vent 4TCO tests, which provided the entire data base for the generic CO specification, and the multivent JAERI tests. In addition, the analysis of the CO data from these multivent tests regarding vent phasing by the JAERI staff provided the justification used by the applicant for considering multivent effects in the application of CO loads to the applicant's Mark II containment.

(3) WNP-2 Plant Uniqueness

As is pointed out in the chugging load review, the WNP-2 plant differs from other domestic Mark II plants in two respects; the containment is a steel shell rather than reinforced concrete and the suppression pool has a sloping instead of a flat floor. Because of these differences, which can put some structural responses from WNP-2 outside the range of the other Mark IIs, the applicant developed a plant-unique chugging specification for WNP-2 which is more conservative than the generic specification. Based on this extra conservatism in the chugging specification and because the applicant feels the generic CO specification is unreasonably conservative for WNP-2, the applicant has presented arguments contending that a separate analysis for response to CO loads of the WNP-2 containment is not necessary.

F.1.1.2 WNP-2 Justification for Omitting Assessment for CO Loads

The justification for omitting the assessment for CO loading is in Reference 1. The report concludes that boundary pressures for a multivent Mark II containment during CO will be smaller than during chugging and, therefore, the CO load does not represent a governing load. This conclusion is based on three main findings made from an evaluation of CO and chugging test data:

(1) At an individual vent exit, the CO load varies randomly in amplitude and frequency content similar to the chugging load.

(2) In a multivent facility the CO loads recorded at different vent exits are desynchronized in a random manner similar to the chugging load.

(3) In the single vent 4TCO facility, the bounding wall pressure traces recorded during CO are enveloped by the bounding boundary pressure traces corresponding to the design chugging load for WNP-2 except for two pressure traces. For these two 4TCO pressure traces, there is poke through of the design chugging load at two spots below 7 Hz, but these traces are found not be controlling for the WNP-2 design.

The applicant, therefore, concludes that the above findings show CO loads are not governing and need not be considered when assessing the design adequacy of WNP-2 structures, piping, or equipment.

F.1.1.3 Staff Evaluation of the WNP-2 Justification for Omitting Assessment for CO Loads

To initiate the evaluation of the WNP-2 CO load position, the staff reviewed the merits of the applicant's findings listed in Section F.1.1.2. The following paragraphs give the results of this evaluation.

(1) The staff does not completely agree with the statement that, at an individual vent exit, the CO load variation is similar to chugging in its random variation of amplitude and frequency content. While there is variation in the amplitude of successive condensation oscillations, 4TCO data show that it is much smaller than the variation in successive chug amplitudes.

However, the staff does feel that the data show condensation oscillation is not far from chugging in nature. While CO amplitudes are generally lower than those of chugging, the gross time scales for both events are similar. Power spectral density (PSD) plots of many CO traces have a wide band of high frequency content similar to chugging traces.

(2) The staff feels that above 10 Hz desynchronization at different vent exits in a multivent facility is supported by the test data that the applicant cites. While the evidence for desynchronization is not completely clear below 10 Hz, the vents are undoubtedly desynchronized above this frequency. Condensation oscillation traces from the first eight blowdown tests conducted at JAERI in Japan, were statistically analyzed by the JAERI investigators.[5] PSDs of CO pressure oscillations at pairs of vent outlets with corresponding transfer function, coherence function, phase angle, and cross power spectral density (CPSD) are shown for most combinations of instrumented vents in Reference 5. No evidence of synchronization above 10 Hz between vents can be found in any of these results.

It should be noted that steam blowdowns were also conducted at the three vent full-scale (but not prototypical) GKSS test facility in Germany. Their staff likewise reported desynchronization among vents during condensation oscillation.

(3) Based on the analysis provided by the WNP-2 applicant in Reference 1, the bounding wall pressure traces measured during condensation oscillation in the 4TCO facility are, with the exception of two poke throughs, enveloped by the bounding wall pressure traces of the WNP-2 design chugging load when calculated for 4TCO. Also, the staff is satisfied with the applicant's calculational results showing that the CO event traces that caused the poke throughs are not governing for the WNP-2 design.

In addition to the above considerations, some observations of the chugging specifications are in order. The WNP-2 chugging specification (described in Section F.1.2 of this appendix) is more conservative than the generic one in terms of source strength at all frequencies. The extra margin of conservatism is substantial for most frequencies. Phasing (i.e., desynchronization) of the WNP-2 sources is also more conservative than the generic chugging desynchronization, because in the WNP-2 specification three vents in a radial row chug simultaneously and not individually. This means that the strength of a pool chug is spread over only 34 separate events instead of over the 102 individual vent chugs the generic specification would call for if applied to WNP-2. Because chugging and CO loading are similar as far as this overall event and application times as well as in frequency content, it is highly unlikely that condensation oscillation would excite different modes than chugging. The real difference in the generic specification between chugging and CO loads lies in the synchronous application of the latter and the dephasing of the former. However, data from multivent facilities such as JAERI have shown that in reality condensation oscillation is not in phase between vents and certainly not at the higher frequencies (i.e., above 10 Hz). In response to staff questions, the applicant has stated that application of the generic CO specification below 10 Hz presents no problem for the present WNP-2 plant design. It should be noted also that at the lower frequencies the chugging load specification is more in phase than at the higher frequencies; i.e., obviously the effect of desynchronization increases with frequency in the chug specification. All multivent test facility data show that this synchronism at higher frequencies is not present.

Because of the extra conservatism in the WNP-2 chugging load specification, the more conservative phasing of the WNP-2 chug sources, and the fictitious nature of CO synchronization at higher frequencies, the staff feels that the applicant does not need to assess the WNP-2 plant with a CO loading in addition to the chugging load specification. Of course, for all load combinations where CO loads were previously part of the total load, chugging loads must now be used in place of the CO contribution.

F.1.1.4 Summary of Evaluation

The staff agrees with the applicant that, in view of the very conservative nature of the WNP-2 chugging specification and the desynchronization of condensation oscillation especially at higher frequencies, CO loads need not be considered by the applicant when assessing the design adequacy of WNP-2 safety features. Assessment using the WNP-2 plant-unique chugging specification is sufficient to cover any load occurring during condensation oscillation. For load combinations, chugging loads must be used whenever condensation oscillation or chugging loads are specified.

F.1.1.5 References

(1) Ettouney, M. M., "Comparison of Condensation Oscillation and Chugging Loads for Assessment of WPPSS Nuclear Project No. 2," Summary Letter Report, Burns and Roe, Inc., December 23, 1981.

(2) General Electric Co., "Generic Condensation Oscillation Load Definition Report," GE Proprietary Report Nuclear Regulatory Commission, NEDE-24288-P, November 1980.

(3) "Mark II Containment Program Load Evaluation and Acceptance Criteria," NUREG-0802, August 1981.

(4) Bird, P. F., et al., "4T Condensation Oscillation Test Program Final Test Report," General Electric Proprietary Report NEDE-24288-P, November 1980.

(5) Statistical evaluation of steam condensation loads in pressure suppression pool - JAERI Report 9618-M, 1981 JAERI memo 9618.

F.1.2 WNP-2 Improved Chugging Load

F.1.2.1 Background

A general background on the chugging phenomena and load specification history can be found in Reference 1. The applicant initiated a plant-unique program to develop an improved chugging load specification early on. To obtain a reduction from the conservative lead plant chugging load specification,[2] the applicant developed a chugging specification that was submitted to the staff in 1979. This method was the first to provide sources at the vent exit from which containment boundary pressures would be computed. The staff reviewed this method and expressed concern regarding the averaging of the 4T data used to arrive at a source specification.

During 1979 and early 1980, the Mark II Owners Group, with the help of GE, conducted additional tests in a modified 4T facility, because some questions about condensation phenomena remained. These tests were conducted with prototypical vent lengths, as well as conservative mass flows. The new tests included chugging events with peak pressures significantly greater than those observed in the original 4T tests. The tests also showed that certain combinations of mass flow, air content and temperature occurring during a blowdown could produce higher chugging loads than other blowdown conditions. Therefore, a gross averaging of all chugging data from a whole blowdown would not be conservative. The applicant responded to the new data (referred to as 4TCO data) by selecting new sources corresponding to 4TCO observations and modifying the modelling of the chugging phenomena. The applicant's revised chugging specification is detailed in Reference 4. The staff's review of this document resulted in a list of concerns. These concerns were addressed by the applicant at a meeting in Richland, Washington on September 16 and 17, 1981.

F.1.2.2 Chugging-Load Description

(1) Design Source Description

The revised WNP-2 chugging load specification consists of seven design sources that were inferred from actual chugs occurring in the 4TCO tests. Details of how the final sources were selected from the 4TCO data are given in Reference 4. The design sources are defined as impulsive pressure gradients (i.e., fluid accelerations) applied over the steam/water interface at the vent exits. The waveform of the design source impulse consists of a 2-millisecond negative amplitude spike followed by a 98-millisecond positive triangular impulse. The exact waveform and the impulse and system parameters that vary from source to source are given in Table 4-2 of Reference 4. These parameters are the amplitude of the spike and triangle of the source, the water and steam acoustic velocities, and the water and steam damping.

(2) Design Source Application

The design source pressure gradients are inferred from a coupled linear model of the vent, pool, and structural portions of the 4TCO facility. This model can be used to infer the final sources by using trial sources to produce wall pressures that match those actually recorded in the 4TCO tests. The application of the sources inferred from 4TCO to the actual multivent WNP-2 containment also utilizes a coupled model of the plant containment, which accounts for such plant-specific parameters as downcomer length, 3D multivent suppression pool geometry including the sloped bottom, and the structural properties of the WNP-2 containment.

The seven design sources are applied separately to the plant and the response from all seven sources is used in plant evaluation.

(3) Chug Desynchronization

The generic chug desynchronization methodology[5] has been adopted by the applicant with one modification. The three vents in each of the 34 radial lines of downcomers are assumed to chug in phase. Therefore, the chug start time for each radial line of three vents, rather than for each individual vent, is assigned according to the generic methodology.[5] So, this set of 34 start times that has the minimum variance is selected from 1000 Monte Carlo trials within a 50-millisecond time window.

(4) Asymmetric-Load Case

Two load cases, an asymmetric and a nearly symmetric load case, are considered by the WNP-2 applicant. Similar to the Mark II generic specification, the variation of chug strength from vent to vent has been eliminated by the simplification of applying the same source strength at each vent. The asymmetric and symmetric cases are attempts to evaluate the effects of the most adversely extreme variation (or lack of variation) in source strengths.

The spatial distribution of the asymmetric specification is shown in Figure 4-11 of Reference 4. Basically, each source is applied with its strength increased by 14% at one row of 3 radial vents in the containment and decreased by 14% at the row 180 degrees away, (i.e., directly opposite). Variation between these extremes is linear so that the rows at 90 and 270, for instance, have their source strengths neither increased or decreased.

(5) Nearly Symmetric Case

In the nearly symmetric case, the sources are applied at all vents with the same strength (i.e., the one specified in Table 4-2 of Reference 4). This is done to maximize axisymmetric response. To account for a likely departure from axisymmetry, however, one row of three vents has a source strength applied that is 24% higher than that applied at all other vents--hence the term "nearly symmetric."

Both the asymmetric and nearly symmetric cases are applied with the vent sources desynchronized as explained above.

F.1.2.3 Chugging-Load Evaluation

(1) WNP-2 Plant Uniqueness

Before beginning an actual evaluation of the WNP-2 chugging load specification, it may be worthwhile to reflect on the need for a unique methodology different from that used by most of the other Mark II plants.

The WNP-2 plant differs from other domestic Mark II plants in two important respects:

- The containment is a steel shell rather than a reinforced concrete structure.
- The pool has a sloping rather than a flat floor.

The steel containment means that structural stiffness factors affecting the frequency content of the chugging load specification will be considerably outside the range of other plants with concrete containments. Although each Mark II plant will differ somewhat in construction and therefore stiffness, the WNP-2 steel containment will produce a larger difference than that among the other plants.

The sloping floor of WNP-2 also presents a problem for the generic method because the generic pool acoustic model presumes a flat-bottomed plant. So, the generic method would have to be modified considerably to apply it to WNP-2.

A plant-unique approach to the WNP-2 chugging loads appears justified and necessary.

(2) Data Base

The data base for the WNP-2 specification is the same as that for the generic methodology: the 4TCO data were used for the actual single-vent source specification, while the JAERI data was used to account for such multivent effects as vent desynchronization.

As stated in Reference 1, the staff finds these data provide an acceptable and appropriate basis for load assessment and load specification.

(3) Selection and Source of Chugging

The chugs selected by the applicant from the 4TCO data base for inferring sources are, for the most part, identical to those used in the Mark II generic chugging methodology. Of the 14 key and companion chugs used in the WNP-2 methodology, 10 are identical to the chugs used in the generic method. One key chug and three companion chugs occurring in three separate tests are different in the WNP-2 method.

The reasons cited by the staff[1] on why the chugs selected for the generic method represent a conservative subset of chugs from the 4TCO data are obviously applicable for the WNP-2 selections also because they overlap. Where the WNP-2 choices differ, their selection is as conservative, or more so, than the generic choices for the WNP-2 containment. As outlined in Reference 6, the chugs used by the applicant that differ from the generic are more critical in the higher frequencies than the generic choices, and it is in the higher frequencies that the WNP-2 plant is more sensitive than the other domestic Mark II plants.

The staff concludes that the 4TCO chugs selected by the WNP-2 applicant to infer the source specification are appropriate and conservative with respect to amplitudes, frequency content, and power. The staff finds the WNP-2 selection acceptable.

(4) Modeling of 4T and WNP-2 Plant To Infer and Apply Sources

As stated previously, the WNP-2 sources are inferred using a coupled model of the 4TCO facility representing the steam in the vent and the water in the suppression pool, as well as the tank structure and its supports. By fully coupling the steam in the vent to the rest of the system, the applicant had eliminated the need of adding sinusoidal terms representing the vent frequencies to the forcing function as was done in the generic method. A purely impulsive source, as described in Section F.1.2.2(1) above, can be inferred using this finite element model. The applicant states that all test facility characteristics have been accounted for, thus producing a source untainted by such facility specific properties as fluid structure interaction (FSI) magnitudes and frequencies. While not familiar with all the details of the model, the staff is convinced from the results presented by WNP-2 that the extraction of sources from the 4TCO data using the WNP-2 model is done in an appropriate manner. Similarly, the staff considers the modeling of the WNP-2 suppression pool for source application adequate to eliminate concerns about FSI. Boundary pressures are calculated in the pool from the application of a source in phase at three vents in a radial row. These boundary pressures are then applied to a structural model of the WNP-2 containment and the response obtained. By superposition, the total building response can be found by summing the responses from all the radial vent rows with appropriate amplitude and phasing factors for each row. The applicant has shown that the models are adequately detailed to transmit both the vent and pool frequency ranges of interest for structural assessment.

The staff also feels that the values of system parameters as listed in Table 4-2 of Reference 4 are appropriate and cover the range of interest of sonic speed and damping for both the vent steam and pool water.

(5) Desynchronization of Chug Start Times

As stated in Section F.1.2.2(3) above, the WNP-2 applicant has adopted the generic chug desynchronization methodology. Therefore, the staff comments[1] stating why this method is acceptable also are valid. The staff agrees with the WNP-2 applicant that having three vents of each radial row chug in phase is acceptable.

(6) Comparison with JAERI Data

The applicant compared the applicant's chugging load specifications with data obtained in the JAERI multivent facility. This comparison did not use a direct application of the specification. Instead, an averaging and enveloping approach similar to the generic chugging load comparison was conducted.[5] The staff's comments in Reference 1 regarding this comparison are valid for WNP-2. An additional comment is necessary, however. Unlike the generic comparison, the WNP-2 modeling of the JAERI facility was not done with only a minor change of the model used for plant application, because the latter requires an axisymmetric geometry. An entirely separate model for JAERI was constructed. Therefore, although the comparison with JAERI is reassuring with regard to source strengths, it does not provide additional verification of the WNP-2 plant application model.

(7) Plant Application

Downcomers with 28 in Diameters

One of the staff's concerns with the WNP-2 chugging load specification was the use of 28-in. diameter downcomers in the WNP-2 plant. Both the 4TCO and JAERI data were obtained using 24-in diameter vents. Although the majority of the 102 downcomers in WNP-2 are 24 in, there are 18 downcomers with 28-in. diameters.

The applicant analytically accounts for the bigger vents by increasing the 4TCO based chugging sources by 36% for the bigger vents. This percentage increase comes from a ratio of the cross sectional area of a 28-in. vent divided by that of a 24-in. vent. Further calculations by the WNP-2 applicant showed that the structural response of the containment would be increased by 10%. Therefore, the 28-in. diameter vents are allowed for in the structural response of WNP-2 by increasing the response calculated for an all-24-in.-diameter-vent case by a factor of 1.1.

The staff feels that this is an acceptable way to account for the effect of the 18 vents with 28-in. diameters in WNP-2. The increase of source strength proportional to vent diameter has been observed in foreign and domestic lateral load data for vents ranging from 12 to 24 in.[1] Extrapolation to 28 in. based on the area ratios is also appropriate one would expect source strength to be dependent on mass flux, which is directly proportional to cross-sectional area. Because the 28-in. vents are spaced fairly symmetrically around the containment, they should not be the cause of any significant imbalance.

Asymmetric Load

The asymmetric load specification should represent a conservative extreme of the possible imbalance in loading the containment can experience as a result of variation in chug strength among vents. The staff's remarks[1] concerning the conjectures involved in an asymmetric specification apply here also, because the WNP-2 specification follows the general outlines of the generic one. The WNP-2 asymmetric load specifies a linear variation in source strength from one side of the pool to the other, as noted in Section F.1.2.2(4). The generic specification calls for an entire half of the pool to be at the same source strength. However, as the WNP-2 applicant has shown,[6] because of the increased WNP-2 design load, the overturning moment is actually greater for the the applicant's case and, therefore is, acceptable to the staff. In general, the staff finds that the WNP-2 asymmetric chugging load specification is adequate in that it provides a reasonable measure of asymmetry.

Nearly Symmetric Load

A conservative measure of the net vertical force on the basemat and maximum net pressure acting on the containment walls during a pool chug is provided by the WNP-2 "nearly symmetric" load specification. The staff finds this specification acceptable and agrees with the applicant that for this load case the synchronization of vents in a radial row, as well as the increase of source strength by 24% in one row, represent added conservatisms.

F.1.2.4 Summary of Evaluation

The staff has already found the 4TCO and JAERI data as acceptable basis from which a load specification can be derived.[1] Based on its review of the WNP-2 reports (References 3, 5, and 6) and from discussions with the applicant, the staff concludes that the WNP-2 improved chugging specification as described in the above references is acceptable for application to WNP-2. F.1.2.5 References

(1) U. S. Nuclear Regulatory Commission, "Mark II Containment Program Load Evaluation and Acceptance Criteria," USNRC Report NUREG-0808, August 1981.

(2) ___, "Mark II Containment Lead Plant Program Load Evaluation and Acceptance Criteria," USNRC Report NUREG-0487, October 1978.

(3) Burns and Roe, Inc., "Chugging Loads - Improved Definition and Application Methodology to Mark II Containments," Technical Report for WPPSS Nuclear Project No. 2, June 1979.

(4) ___, "Chugging Loads - Revised Definition and Application Methodology for Mark II Containments (Based on 4TCO Test Results)," Technical Report for WPPSS Nuclear Project No. 2, July 1981.

(5) General Electric Co., "Generic Chugging Load Definition Report," GE Report NEDE-24302-P, Class III, April 1981.

(6) Handout provided at the Meeting with WPPSS in Richland, Washington, September 16 and 17, 1981.

F.1.3 SRV Discharge Methodology

F.1.3.1 Introduction

(1) SRV Discharge Load Phenomena

The WNP-2 plant is equipped with SRVs to control large primary system pressure transients. The SRVs are mounted on the main steamlines inside the drywell with discharge lines routed through the drywell floor into the suppression pool. When an SRV is actuated, the steam released from the primary system is discharged into the suppression pool and condensed.

Actuation of an SRV can be either automatic, at a preset pressure, or manual by means of an external signal. A preselected number of SRVs are used for the ADS which is designed to reduce the reactor pressure and permit operation of the low pressure emergency core cooling systems. The ADS performs this function by automatic actuation of the specified SRVs following receipt of specific signals from the reactor protection system.

Upon actuation of an SRV, the air column within the partially submerged discharge line is compressed by the high pressure steam and, in turn, accelerates the water leg into the suppression pool. The water jets thus formed create pressure and velocity transients that are manifested as drag or jet impingement loads on submerged structures.

Following water clearing, the compressed air is discharged into the suppression pool forming high pressure air bubbles. These bubbles execute a number of oscillatory expansions and contractions before rising to the suppression pool surface. The associated transients again create drag loads on submerged structures as well as pressure loads on the submerged boundaries. These loads are referred to as SRV air clearing loads.

Following the air clearing phase, essentially pure steam is injected into the pool. Experiments indicate that, for sufficiently high steam fluxes, the steam jet/water interface that exists at the discharge line exit is relatively stationary, so long as the local pool temperature is low. Thus, the condensation proceeds in a stable manner and no significant loads are experienced. Continued steam blowdown into the pool will increase the local pool temperature. The condensation rates at the turbulent steam/water interface are eventually reduced to levels below that needed to readily condense the discharged steam. At this "threshold" level, the condensation process becomes unstable; i.e., steam bubbles are formed and shed from the pipe exit, the bubbles oscillate and collapse giving rise to severe pressure oscillations that are imposed on the pool boundaries. To preclude unstable condensation, limits are established for the allowable suppression pool temperature and restricted to those values in the plant Technical Specifications. These restrictions are referred to as the pool temperature limits.

Following closure of the SRV, the pressure in the discharge line decreases rapidly due to the outflow of the remaining steam. At a sufficiently low pressure, pool water will re-enter the line (reflood) resulting in a further decrease in line pressure as the remaining steam is condensed by the inflowing water. The reduced pressures also actuate vacuum breakers that are installed in the discharge line allowing drywell air/steam to enter the line and equilibrate the pressure differential. Experiments indicate that these events occur in a very transitory fashion before a new equilibrium state is achieved. Specifically, the water column within the discharge line has been observed to overshoot the original water level followed by several oscillations about a new equilibrium level that is generally below the normal value. Pressure fluctuations and corresponding actuations of the vacuum breaker accompany these excursions in water column elevation. The experiments also indicate that if an SRV is actuated during this transient period, the pressure loads on the pool boundary can be substantially higher than those associated with normal or "first" actuations of the SRV. This type of SRV discharge is referred to as a "subsequent" actuation. The increase in loads can generally be attributed to a reduction in steam condensation rates on the (heated) discharge line walls and, if the timing of the valve actuation is right to the increase in water column length. Both of these effects enhance the potential for compressing the air in the discharge line leading to the introduction of higher than normal pressure bubbles into the suppression pool.

Concurrent with the events described above, the discharge line itself is subjected to dynamic pressure and thermal loadings. In addition, a variety of thrust loads can be generated at the end of the discharge line and, of course, transmitted to any support or tie-down arrangement as may exist.

(2) SRV Load Mitigation

Experiment and operating experience has shown that the magnitude of the SRV discharge-related loads is a strong function of the geometry and configuration of the discharge device utilized. Early experience with straight-pipe configurations indicated very high loads. Some mitigation of these high loads has been achieved in the past by the use of elbows and "ramshead" discharge devices. Current practice involves installation of so-called "quencher" devices, which consist of two or more lengths of perforated pipe sections. Such devices have been found to substantially reduce hydrodynamic discharge loads in comparison to those observed with the other configurations. In addition, the quenchers exhibit improved performance in terms of their ability to maintain stable steam condensation at elevated pool temperatures.

The quencher device used in the WNP-2 plant is the GE cross-quencher (or X-quencher), which consists of four perforated arms. It is a GE-modified version of the quencher device originally developed by KWU. X-quenchers similar to those utilized in WNP-2 are currently in use in two foreign Mark II plants that have performed inplant SRV tests (Caorso plant and Tokai-2 plant) and are in use in GE Mark III plants.

(3) SRV Air Clearing Load Methodologies

The present SRV load specification methodology for X-quenchers is described in the Mark II DFFR. The calculation procedure for predicting air clearing loads is based primarily on the results of an extensive series of reduced-scale and in plant tests. It consists of specification of peak boundary pressure, pressure time history, and pressure spatial distribution on the pool boundaries. The peak pressure amplitude is computed using an empirical formula that is established through statistical analysis of test results to account for plant parameters and data scattering.

The load calculation procedure based on the statistical model involves two elements: (1) calculation of mean values of peak positive loads using the empirical formula, and (2) calculation of a confidence margin. A confidence level of 90%-90% was selected in the calculation of the design loads. This calculation procedure and the 90%-90% confidence level for the design loads have been reviewed and found acceptable by the staff as described in NUREG-0487.[1]

Recent in-plant test results from Caorso and Tokai-2[1-3] showed that the design load calculated from the DFFR methodology may be overly conservative. In view of this, the applicant has proposed an alternate methodology based on Caorso test results. The staff's evaluation of this alternate methodology is presented in the following paragraphs.

F.1.3.2 Proposed Load Specification

The alternate load specification proposed by the applicant is described in Reference 4. It is a dynamic pressure loading to be applied directly to the submerged boundaries. As in the DFFR methodology, it consists of specifications on peak pressure amplitude, pressure time history and pressure spatial distribution on the pool boundaries.

(1) Selection of Data Base

The proposed load specification is based on results from Caorso inplant tests, which were performed in two phases. The 52 Phase I tests were conducted during July and August of 1978 and included only single-valve first and subsequent actuation tests at normal operating reactor pressures. The 53 Phase II tests were conducted during January and February of 1979 and included repeats of some of the Phase I tests as well as tests involving multiple valve actuations, low reactor pressures, and leaky valves. Results of these tests were presented in References 2 and 3 for Phase I and Phase II tests, respectively.

Test results that were selected as the data base to determine the WNP-2 load specification were 68 pressure traces measured at pressure transducer P19 from both first and subsequent actuation of Valve A.[2,3] Examination of the frequency spectra (or Fourier spectra) of these pressure traces showed two types of pressure wave forms. Most of the pressure traces were categorized by the applicant as having "multiple frequency wave form (MFP)," which is characterized by a few high frequency, high amplitude pressure spikes in the early part of the pressure time history, and by a rich frequency content in the frequency range above the dominant frequency (6-10 Hz). Only seven pressure traces, all from subsequent actuation tests, were identified as having "single frequency wave form (SFP)." This wave form exhibits primarily a single characteristic frequency of oscillation, from about 6 to 10 Hz, for the whole duration.

(2) Development of Design Loads from Data Base

Specifications of both pressure amplitude and pressure wave form (pressure time history) were obtained from statistical analyses of test data. The 90%-90% confidence values were computed from these analyses and were used as design values.

Design Pressure Amplitude

Statistical analyses of pressure amplitudes showed that the pressure amplitude is higher for SFP traces than for MFP traces. In MFP traces, the pressure amplitude from subsequent actuation tests was found to be higher than that from first actuation tests. The 90%-90% confidence limits for the various types of pressure traces are 9.37 psi for SFP traces, 7.62 psi for MFP traces from subsequent actuations, and 5.75 psi for MFP traces from first actuations. The 90%-90% confidence value for SFP traces, 9.37 psi, was selected as the design value for both the SFP and the MFP design wave forms by the applicant.

Design Pressure Wave Forms

The design wave forms were developed from statistical evaluation of the Fourier amplitude spectra of pressure traces. To avoid unnecessary conservatism in the load specification, two separate design wave forms were defined: one exhibiting the characteristics of MFP traces and the other having the characteristics of SFP traces. Fourier amplitude spectra of 90%-90% confidence level were first constructed for the two types of wave forms using using pressure traces from subsequent actuation tests only. Design wave forms were then established to bound the 90%-90% confidence spectra in the frequency domain. The MFP design wave form was obtained artificially by a trial and error approach, taking into consideration all major characteristics of the MFP traces. The SFP design wave form was selected from measured traces; measured trace from Test 2202 was considered as a typical SFP trace and was selected as the design wave form. The applicant has demonstrated that the spectrum from the design wave forms with a pressure amplitude of 9.37 psi can bound the 90%-90% confidence spectra of both types of traces (see Section 3.1).

(3) Modification of Design Pressure Amplitude from Caorso Test Conditions to WNP-2 Design Conditions

Maximum pressure loads on pool boundaries from SRV air clearing were found to depend on plant parameters whose values of WNP-2 design conditions are different from those of Caorso test conditions. Modification of the design pressure load is therefore required. The applicant used the empirical correlation presented in the DFFR methodology[5] to accomplish this modification.

Important parameters identified in the DFFR correlation and their values during Caorso tests and WNP-2 design are presented in Table F.1.1. The 90%-90% confidence design values were calculated, according to DFFR correlation, for single valve, subsequent actuation under both WNP-2 design conditions and Caorso test conditions. The ratio of these two calculated design values (1.20) was used by the applicant to modify the design value obtained from Caorso data (9.37 psi) to WNP-2 design conditions (11.2 psi).

(4) Frequency Sweeping of Pressures

The design pressure wave forms were modified to account for the variations in frequencies due to (1) variability in dominant frequencies exhibited in test data and (2) differences in plant conditions. The modification involves compressing and expanding the design pressure time histories to cover a frequency range (for characteristic dominant frequency) of 4.0 to 12.0 Hz.

(5) Circumferential Pressure Distribution

The applicant has investigated two approaches to calculate the circumferential pressure distributions around pool boundaries due to SRV actuation. They are:

- distribution obtained from a finite element analysis of the suppression pool

- DFFR attenuation law as presented in Reference 5.

The DFFR attentuation law was selected for WNP-2 design evaluation because it is more conservative.

(6) Vertical Pressure Distribution

The vertical pressure distribution on pool boundaries proposed by the applicant is a constant pressure between the bottom of the suppression pool and the quencher centerline. The pressure then decreases linearly to zero at pool surface. This distribution is based on applicant's evaluation of test results from Caorso and Tokai-2, as well as analytical results from finite element analysis with a pressure source at the quencher location.

(7) SRV Discharge Load Cases

The SRV discharge cases that are considered for WNP-2 design evaluation are:

- single-valve discharge case

- two-valve adjacent quenchers) discharge case

- ADS valve discharge case

- all-valve discharge cases

Two design conditions are associated with the all valve discharge case. They are the axisymmetric loading condition assuming simultaneous discharge, in-phase oscillation from all valves, and the nearly symmetric loading condition assuming some imbalance during actuation of all SRVs.

In all the discharge cases, the same pressure load specification (including pressure amplitude, wave forms, and frequency range) is used to calculate the dynamic responses of the WNP-2 reactor building. The only exception is the all-valve, nearly symmetric loading case where the peak pressure is assumed to be 12.5 psi at 0 and 5.6 psi at 180. The circumferential pressure distributions for other cases are obtained from DFFR attenuation law. However, the more conservative linear superposition assumption is used, instead of the SRSS (square root of the sum of squares) assumption recommended in DFFR, to calculate resultant pressure from several quenchers in multiple valve cases.[6]

F.1.3.3 Evaluation of Load Specification

The staff's evaluation of the proposed load specification consists of two major considerations: (1) the evaluation of the conservatism of the load specification with respect to the given data base (Caorso test results) from which it is derived, and (2) the evaluation of the adequacy of the Caorso data base in providing a conservative representation of the performance of the quencher device in WNP-2 plant under design conditions.

From evaluation of the material presented in Reference 4, the staff finds that the load specification derived from the Caorso data base is a conservative and acceptable specification for a plant under similar conditions as those in Caorso tests. However, from the review of Caorso test program and WNP-2 plant design conditions, the staff also finds that the modifications (to the load specification) proposed by the applicant to take into account the differences between Caorso test conditions and WNP-2 design conditions may not be adequate to cover all the limitations and uncertainties associated with the application of the data base to WNP-2 plant. The staff, therefore, felt that further modifications, or justifications, to the proposed load specification are required to ensure conservatism of the load specification for WNP-2 design. In response to the staff's concern, the applicant has provided further justification as well as additional modifications to the proposed load specification which the staff finds satisfactory. It is, therefore, the staff's judgment that the proposed load specification, as presented in Reference 4, with the modifications, as presented in Reference 7, constitutes an acceptable load specification for WNP-2 design. Details of the staff's evaluation of the proposed load specifications are presented in the following paragraphs.

(1) Derivation of Design Load from Data Base

The principal requirement in the derivation of design loads fr... a data base, set forth by the applicant is that they bound the 90%-90% confidence values of the pressure data base in both amplitude and frequency spectrum. The use of 90%-90% confidence level for design load determination is consistent with that proposed in the DFFR[5] which has been found acceptable by the staff, as discussed in NUREG-0487.[1]

The design load developed by the applicant includes two pressure wave forms, which exhibit major characteristics of the pressure traces in the data base, and a pressure amplitude of 9.37 psi to be used with both wave forms. The specification also requires that the pressure wave forms be expanded and compressed to increase the frequency range of the design wave forms to cover a frequency range of from 4 to 12 Hz.

It is, therefore, the staff's judgment that the design load derived by the applicant is an acceptable load specification for a plant under similar conditions as those from which the data base was obtained. This judgement is based on the applicant's requirements regarding the derivation of the load specification from a data base, as well as the fact that the frequency spectrum from the load specification can envelope the frequency spectrum of every pressure trace in the data base for the frequency range of interest.

(2) Application of Caorso Data to WNP-2 Plant Design

The adequacy of the Caorso data base in providing a conservative representation of the quencher performance for WNP-2 plant under design conditions is discussed in this section. From this evaluation, the staff finds that the data base is, in general, adequate and acceptable for the development of a design load specification. There are uncertainties, however, associated with the conservatism of the data base in terms of covering the worst conditions that may occur in a plant and with the modifications required to bring test data from test conditions to WNP-2 design conditions. Because of these uncertainties, the staff feels that modifications to the proposed load specification are required to ensure conservatism of the load specification.

Selection of Data Base From Caorso Data

Test results that were selected by the applicant for load specification are measurements at pressure transducer P19 from single-valve actuation tests involving Valve A, for which most of the Caorso single-valve tests were conducted. The staff's evaluation of the Caorso test program shows that tests involving single-valve actuations of Valve A have covered a broad range of valve actuation conditions and provide an acceptable basis for load evaluation purposes.

The selection of measurements at pressure transducer P19, which is located on the pool bottom about 4 ft from the quencher centerline, is also acceptable because of its location with respect to the quencher device when compared with other sensors and because of the fact that largest pressure amplitudes were recorded by this transducer and a nearby transducer (P13) for most of the tests.

Fluid Structure Interaction (FSI) Effect in Caorso Data

Pressure on pool boundaries measured from a particular facility will contain the effect of FSI, which is characteristic of that facility and must be removed from the measured (total) pressures before they are used for other facilities. The applicant has evaluated the FSI effect in Caorso test results and concluded that the effect is small and negligible. Pressure traces from Caorso tests were, therefore, used without any adjustment for FSI in the derivation of design load specification. The load specification is subsequently applied to the WNP-2 plant as rigid wall pressures in the structural analyses of WNP-2 plant.

The applicant's evaluation of FSI effect involves the estimate of the interaction pressure, which is the portion in the measured pressure attributed to FSI effect. The estimate is made by the use of a hydrodynamic added mass matrix obtained from analytical modelling of Caorso plant and of measured boundary accelerations from Caorso tests. The estimated interaction pressure is very small when compared with measured total pressures. This indicates that FSI effect is negligible and that test data can be used as rigid wall pressures without modification.

The staff finds the applicant's evaluation of FSI effect adequate and the conclusion resulting from the evaluation acceptable.

Effect of Vacuum Breaker Performances on Pressure Loads

The vacuum breakers installed on the SRV discharge line will allow drywell air to enter the discharge line when the pressure inside the line is lower than that in the drywell which occurs after closure of the SRV. The performance of vacuum breakers will, therefore, affect the initial conditions for subsequent valve actuations and consequently pressure loads from such actuations.

Most of the Caorso subsequent actuation tests were conducted with Valve A with one of the two vacuum breakers blocked. These data are used by the applicant to derive the design loads. There were only four subsequent actuation tests performed with Valve U which had both vacuum breakers operating.[2,3] The conservatism of the data base used by the applicant is questionable because the maximum peak boundary pressure obtained with two vacuum breakers (9.4 psi), which is prototypical for Mark II plants, is higher than that with only one vacuum breaker (8.7 psi). The mean value of peak boundary pressure is also higher for the former (7.3 psi) than the latter (5.7 psi).

For subsequent actuation tests, the only significant difference between Valve A and Valve U is the number of vacuum breakers utilized. Because of the small number of tests performed, it cannot be said with certainty that the higher pressure loads are caused by the operation of the additional vacuum breaker, which would admit more air into the discharge line prior to subsequent actuation. Nonetheless, it introduces large uncertainties about the conservatism of the data base used in the design and great concern over the effect of vacuum breaker performance on pool boundary loads. The vacuum breakers utilized in WNP-2 plant and the Caorso plant are different, although both are 10 in. vacuum breakers (See Table F.1.2). From the information received from the applicant, the staff cannot establish the equivalence of performance of these different vacuum breakers. This introduces further uncertainty in the use of data.

Because of the uncertainties discussed above, the applicant has agreed to increase the statistically derived design value of 9.37 psi by 1.84 psi, which represents the difference between the mean value for subsequent actuation tests with two vacuum breakers functioning and the mean value for subsequent actuation tests with only one vacuum breaker functioning (5.44 psi). The staff finds this modification to design load specification to account for vacuum breaker effect the best estimate available and acceptable.

Effect of Multiple Valve Actuations (MVA) on Pressure Loads

The design values for SRV air clearing loads in WNP-2 plant are based on single valve actuation data from Caorso tests. These values are then used in load cases involving multiple valve actuations without adjustment for multiple-valve effect. Comparison of pressures measured during Caorso tests shows that the peak pressure in multiple-valve tests is in general greater than that in single-valve tests under similar test conditions: the mean value of peak boundary pressure for the six four-valve actuation tests (5.97 psi, excluding Test 31 because of the large distance between sensors and operating quenchers) is greater than that for single valve tests under similar first actuation conditions (4.4 psi).

The design basis operational SRV actuation events investigated for WNP-2 are listed in Table F.1.3. It indicates that the most severe all-valve actuation occurs only under first actuation conditions. It is noted that the design pressure amplitude for WNP-2 is based on the seven SFP traces from subsequent actuations. These traces have a mean peak pressure of 6.95 psi, which is higher than the mean value from MVA tests. The use of subsequent actuation data as the basis for multiple valve first actuation case is, therefore, acceptable.

As shown in Table F.1.3, only the six lower set-point valves may discharge at subsequent actuation conditions. These valves correspond to quenchers located at the inner quencher circle, adjacent to the RPV pedestal. The distance between these quenchers and pool boundaries in WNP-2 is greater than that in Caorso tests. Because boundary pressure is basically inversely proportional to distance, the pressure expected in WNP-2 plant from actuations of these valves will therefore be smaller than that in Caorso if other conditions remain the same. Furthermore, although the pressure amplitude may be higher for six-valve actuation, the effect on the containment vessel structure may still be smaller than that from all-valve first-actuation case because of the number of valves, and, therefore, the total load on containment structure involved in these cases.

MVA tests in Caorso also resulted in slightly different frequency spectra when compared with results from single-valve tests under similar conditions: MVA tests usually have higher energy content in the range of 20 to 60 Hz. The applicant has shown that the design envelope frequency spectrum bounds the envelope of frequency spectra of all MVA tests. This is the case even in the high frequency end of the spectrum.

Based on the above discussions, the staff concludes that the proposed load specification, without further modification to account for MVA effect, is acceptable for multiple valve actuation cases.

<u>Effect of Leaky Valve Actuations on Pressure Loads</u>

Caorso test results showed that first actuations of a leaky valve (LV) resulted in lower peak pressures but quite different pressure time histories when compared with other tests. The predominant frequencies for LV tests are approximately from 20 to 30 Hz, which are higher than the 5 to 10 Hz normal range. Because LV is not an uncommon occurrence, the design load specification should be able to bound loads resulting from the actuation of leaky valves.

A comparison between the design envelope response spectra and the LV first actuation spectra indicates that the design curve completely envelopes the LV first-actuation envelope. It is, therefore, the staff's opinion that the proposed load specification is acceptable for LV actuation conditions.

Application of DFFR Correlation

To take into account the differences between WNP-2 design conditions and Caorso test conditions, a pressure amplitude multiplier, based on DFFR correlation, is used to obtain the WNP-2 design values. The pressure amplitude multiplier used by the applicant is the ratio of the predicted design pressure at WNP-2 and that at Caorso (test conditions) using DFFR correlation. The staff finds such application of the DFFR correlation unacceptable. The DFFR correlation is based on the mean pressure from large-scale tests and a term for each variable which adjusts that mean from large-scale conditions to plant conditions. Each term in the DFFR correlation represents the expected change in wall pressure due to departure from test condition of that variable. It is therefore the difference, not the ratio, between the two predicted design pressures that should be used to obtain the WNP-2 design values.

This issue was discussed with the applicant at a meeting held on September 1981. The applicant has agreed to use the pressure differential calculated with the DFFR correlation to account for differences between Caorso plant test conditions and WNP-2 design conditions.

Effect of Discharge Line Air Volume

Previous test results show that peak air clearing pressure increases with increasing air volume, reaches a maximum, and then decreases. To make conservative predictions, the DFFR correlation does not take credit for the decreasing trend of pressure with air volume and takes the pressure as constant when air volume exceeds 1.77 m^3 (VAAQ = 0.255). According to this correlation, adjustment of pressure amplitude from Caorso to WNP-2 is, therefore, not required because air volumes of both the discharge line tested in Caorso and the longest discharge line in WNP-2 are greater than 1.77 m^3. A closer examination of test results, from which the DFFR correlation is derived, reveals that this is not appropriate for the present case. The smallest air volume of WNP-2, which is 1.62 m^3 (VAAQ = 0.234) and associated with the lowest set valve, is less than the air volume tested at Caorso (1.88 m^3, VAAQ = 0.272 from Reference 2). Modification to design pressure values may be required to account for this air volume effect.

Examination of the discharge line air volumes in the WNP-2 plant shows that only four quenchers have discharge line air volumes less than that tested in Caorso (by about 1.4% to 13%), while the average air volume of all WNP-2 discharge lines, as well as the air volumes of all ADS lines, is greater than that of Caorso tests. The four quenchers that have smaller air volume are all located in the inner quencher circle near the RPV pedestal. For all the SRV discharge cases (see Section III.2.11) involving the actuations of an inner circle quencher, the peak design pressure is assigned on the pedestal from basemat to about quencher centerline elevation. Credit for the reduced load as a result of larger distance is not taken. According to the applicant,[6] the pressure attenuation as a result of the larger distance is 55%, more than that required to offset the possible increase in bubble pressure as a result of the smaller air volume. Consideration of the air volume effect will, therefore, have no impact on WNP-2 design assessment. The applicant then concluded that there is no need to modify the existing load specification to account for air volume differences between Caorso and WNP-2. The staff finds the applicant's conclusion acceptable. This acceptance is also based on the following considerations: (1) the average air volume of all valve case and the air volume of all discharge lines in the ADS case are greater than that tested in Caorso and (2) with the same peak boundary pressure, the governing single-valve case is from the actuation of an outer circle quencher whose air volume is greater than that tested in Caorso.

Effect of Other Plant Parameters

Other parameters that affect the peak boundary pressure as identified in DFFR are the steam flow rate, the pool temperature, the length of water column, and the valve opening time. The applicant uses the DFFR correlation to adjust the peak boundary pressure from Caorso to WNP-2 with respect to these parameters. The staff finds this acceptable.

From the limited number of low reactor pressure tests in Caorso, a rough estimate can be made of the trend of peak pressure with the steam flow rate parameter used in DFFR correlation (MNAQ). For the range of interest in the present case (MNAQ greater than 6.89), the slope of peak pressure (bar) with MNAQ from DFFR correlation is 0.01. This is smaller than that obtained from the Caorso tests (0.04, using results from Tests 37, and 38 and the mean value of other normal first actuation tests from Caorso). This indicates that the trend established in DFFR correlation may not be conservative for this parameter at values of interest here. However, the use of DFFR correlation for this parameter because of the small amount of extrapolation required is accepted for WNP-2. As given by the applicant in Reference 6, the value of MNAQ for WNP-2 is 0.766 and the value for Caorso test is 9.397.

The other parameter that can be checked using Caorso test results is pool temperature. With regard to this parameter, Caorso test results seem to confirm the trend established in DFFR correlation. It is noted that the design value of this parameter for WNP-2, as given in Reference 4, is 200°F and it represents the major contribution to the modification from Caorso test conditions to WNP-2 design conditions. The applicant later modified this design value to 110°F which is the Technical Specification limit on suppression pool temperature for WNP-2 plant. The use of Technical Specification limit as design pool temperature for SRV air clearing load is acceptable to the staff.

The design values of valve opening time and water column length for WNP-2 are very close to that of Caorso, and contributions to design load modification from these parameters are consequently small. The use of DFFR correlation to account for differences between Caorso test conditions and WNP-2 design conditions for these parameters is, therefore, acceptable.

Vertical Pressure Distribution

The proposed vertical pressure distribution used by the applicant is constant between the bottom of the suppression pool and the quencher centerline and then decreases linearly to zero at the pool surface. Figure F.1.1 shows the comparison between the proposed specification and Caorso test results. In the evaluation of the mean value and the range of test results presented in Figure F.1.1, only those Caorso phase II tests with peak positive pressure greater than 5 psi are used. Reference 2 does not report pressures measured by sensors P10 and P11 because of excessive zero drift.) Test results from Test 2313, although exhibiting a peak pressure greater than 5 psi, are not included in the evaluation because the distribution from these measurements is much worse than those from other tests and is believed to be not representative. It is noted that although the pressures measured by Sensors P10 and P11 for phase II tests are reported in Reference 3, they are also characterized as drifted more than 10% during the test program.

Figure F.1.1 shows that although the proposed distribution bounds the mean value of test results (with the exception of measurements from sensor P9), it cannot bound the worst distribution among the tests considered. Also showing in the figure is the distribution from the staff's generic acceptance criteria set forth in NUREG-0487, Supplement 2, Item II.B.4.d.[1] This generic distribution can bound the worst distribution from measurements of sensors P10, P11, and P14 with margin to cover the uncertainty from lack of bounding of measurements from Sensor P9.

Because actuations of multiple valves would have an averaging effect on boundary pressure distribution and because the exceedance of the worst recorded pressure distribution above the proposed distribution is not significant, it is the staff's opinion that the proposed vertical pressure distribution is acceptable for multiple-valve-actuation cases. This conclusion is further supported by the considerations of the conservatisms in the load specification of multiple-valve-actuation cases in (1) the assumption of inphase oscillation of pressures from different quenchers and (2) assignment of maximum (design) pressures to all the quenchers involved in the case without taking credit of the randomness in pressure amplitude from multiple quenchers. However, for single valve actuations, the staff's position is that the generic acceptance criteria from NUREG-0487, Supplement 2 should be used because the conservatisms for multiple-valve actuations discussed above do not exist.

The applicant accepted the staff's position on vertical pressure distribution in a manner compatible with presently implemented analyses by the applicant. The modification made by the applicant to accommodate the revised distribution is to increase the pressure load by 10.7% but maintain the original proposed pressure distribution. As shown in Figure F.1.2, this modification preserves the total load applied to the vertical boundaries and is, therefore, acceptable.

Circumferential Pressure Distribution

The circumferential pressure distributions are calculated by the applicant using DFFR methodologies with the following modifications (Reference 6):

- The straight line distance is used instead of the "line-of sight" distance recommended in DFFR.

- The SRSS assumption is replaced with the more conservative linear superposition assumption.

The applicant has shown that the circumferential pressure distribution calculated by the above methodology is conservative when compared with Caorso test results.[6]

The applicant also used an analytical model for the WNP-2 suppression pool to calculate the circumferential pressure distribution. Comparison of the distributions obtained by the modified DFFR method and that by the analytical calculation showed that the DFFR method is more conservative, particularly in areas farther away from the pressure source (quencher). The modified DFFR method is, therefore, used to calculate design loads for various SRV actuation cases. Because the proposed method overpredicts the pressures on the opposite side of the pool of the discharge quencher, there is a concern about whether this will give a conservative pressure distribution for the asymmetric case because this overprediction reduces the asymmetric conditions that may occur in this case. For the asymmetric case, the analytical model may be more appropriate in predicting pressure in locations farther away from the quencher where the pressure source can be viewed as a point source as employed in the analytical model. The applicant reported in Reference 7 that this has been considered in the evaluation of the asymmetric case.

Accordingly, it is the staff's judgment that the proposed method for calculating circumferential pressure distribution by the applicant is acceptable.

SRV Discharge Load Cases

Five SRV discharge load cases are considered in WNP-2 design evaluation. They are the single-valve discharge case, the two-valve discharge case, the ADS-valve discharge case, the all-valve discharge case with axisymmetric loading condition, and the all-valve discharge case with nearly symmetric loading condition. They are consistent with the generic requirement set forth in NUREG-0487. The all-valve sequential discharge case required in NUREG-0487 will be replaced in the WNP-2 evaluation by the all-valve case with nearly symmetric loading conditions, which assumes some imbalance in pressure loading around pool boundaries because of sequential discharging from all SRVs.

The nearly symmetric case assumes a maximum pressure amplitude of 12.5 psi at 0 and 5.6 psi at 180. This would give an average pressure on the whole boundary of 9.1 psi. This is more than 50% higher than the mean value of the peak pressures from the six Caorso four-valve tests. The difference between the maximum and the minimum value (the imbalanced part) in this case is 6.9 psi, which is about six times the standard deviation exhibited in the six four-valve tests. Although the design loads for WNP-2 are expected to be higher than the measured loads from Caorso tests, the margins discussed above should be able to cover this expected increase in pressure loads. The nearly symmetric all-valve load case is, therefore, an acceptable replacement for the all-valve sequential load case required in NUREG-0487.

Frequency Range of Load Specification

The forcing function used to evaluate the SRV discharge load cases described above has a frequency range of 4 to 12 Hz for the dominant frequency. This satisfies the requirement set forth in NUREG-0487 for the quencher device installed in the WNP-2 plant.

The dominant frequency for the pressure traces obtained from those Caorso tests which were performed under conditions applicable to WNP-2 is from about 5.3 Hz to 9.5 Hz. The frequency range for WNP-2 is expected to be wider than that from Caorso tests because of the greater variation in discharge line air volumes in WNP-2. The ratio of the air volume in WNP-2 to that tested in Caorso varies from 0.87 to 1.33. Because pressure oscillation frequency is generally inversely proportional to the cubic root of the air volume, the expected frequency range for WNP-2 is from 4.8 Hz to 10.0 Hz, which is bounded by the specification.

Another parameter that affects forcing function frequency is the wetwell pressure which, except for ADS case, is atmospheric for all other SRV discharge cases. The ADS valves are expected to actuate during a postulated small break (SB) loss-of-coolant accident (LOCA). The conditions prior to actuations of ADS valves are therefore a pressurized drywell and wetwell and a depressed discharge line water leg. The latter is due to the operation of SRV line vacuum breakers caused by a drywell-to-wetwell pressure differential occurring in an SB event. Theoretical calculations and past experimental results show that the two factors, increased wetwell pressure and increased discharge line air mass (through operation of vacuum breakers)--have compensating effects on forcing function frequency. The evaluation of ADS case presented in NUREG-0802 shows that the forcing function frequency for ADS case is comparable to that for other SRV discharge cases for typical Mark II plants.

As discussed above, the proposed frequency range provides additional margin when compared with that of test results after modification with respect to discharge line air volume for WNP-2. It is the staff's judgement that this margin is sufficient to cover the uncertainties associated with additional frequency modifications. The specification in the frequency range is, therefore, acceptable.

(3) Inplant Test

The WNP-2 design load specification for SRV air clearing is based primarily on Caorso test results that lack complete dynamic and geometric similarity with the WNP-2 plant. Although modifications to design pressure amplitude are made to account for some of the differences, as discussed in previous sections, confirmation of design load by other inplant test results is required because of additional differences between WNP-2 and Caorso plant, such as those in quencher device geometrics and suppression pool configurations.

In addition to Caorso test results, inplant test results for GE cross-quenchers are also available from two other foreign plants--Tokai-2 and Kuosheng. The quenchers used in these plants, as well as that installed in WNP-2, are very similar, but not identical, as shown in Table F.1.4 (details of Tokai-2 quencher are not available). The quenchers are identical in hole size and hole pattern but are different in hub design and arm orientation. Of these plants, Caorso and Kuosheng have concrete containments and WNP-2 and Tokai-2 have steel containments. With the exception of Kuosheng plant (Mark III), the others have Mark II containment design. The WNP-2 plant is unique among these plants because it has a slanted suppression pool bottom.

Toakai-2 test results were used by the applicant to confirm the WNP-2 load specification. The maximum pressure amplitude reported from Tokai-2 tests (11.2 psi) is greater than that from Caorso tests (9.4 psi). The applicant argued that this difference is caused by the differences in structure design between Tokai-2 and Caorso (steel containment versus concrete containment). The applicant estimated that a maximum of 1.45 psi in Tokai-2 measurements can be attributed to FSI effect as compared with negligible FSI effect in Caorso data. The estimate was based on a combination of analytical calculations (of added mass matrix of the Tokai-2 suppression pool) and test results (acceleration measurements of Tokai-2 pool boundaries). With this consideration, the applicant concluded that the pressure amplitudes from Caorso and Tokai-2 are similar and that the load specification is confirmed. The staff notes that test conditions and their effects on test results were not evaluated in the comparison and that the maximum pressure amplitude from Tokai-2 tests was obtained from a first actuation test. Despite these uncertainties, it is the staff's judgment that there is sufficient conservatism in the load specification, such as the simultaneous-discharge, inphase oscillation assumptions used in the all-valve case, to cover the uncertainties discussed above.

A preliminary review of the results from the recently completed Kuosheng inplant tests shows greater peak pressure amplitude than Caorso tests under corresponding test conditions. The exceedance is quite significant in all test categories (e.g., SVA, MVA, etc.). This raises additional uncertainties about the effects of the detailed quencher/pool geometrics on air clearing load. It is noted, however, that Kuosheng test results are still under evaluation-comparison of frequency spectra of the measured pressure time histories may show more favorable results.

Based on the information available to date, the staff finds that an inplant test at WNP-2 for the confirmation of pool boundary load during SRV air clearing is not required. However, the staff may require further justification/confirmation by the applicant or an inplant test at WNP-2 if final evaluation of Kuosheng test results shows significant differences from previous inplant test results.

(4) Evaluation Summary

The staff and its consultants have reviewed the SRV load specification proposed in Reference 4. As discussed in the previous sections, the staff finds that the load specification, with modifications discussed in this evaluation, is conservative and acceptable for use in the evaluation of WNP-2 plant.

F.1.3.4 References

(1) U.S. Nuclear Regulatory Commission, "Mark II Containment Lead Plant Program Load Evaluation and Acceptance Criteria," NUREG-0487, October 1978.

(2) General Electric Co., "Caorso SRV Discharge Tests Phase I Test Report," GE Report NEDE-25100-P, May 1979.

(3) ___, "Caorso SRV Discharge Tests Phase II Test Report," GE Report NEDE-24757-P, May 1980.

(4) Burns and Roe, Inc. "SRV Loads - Improved Definition and Application Methodology for Mark II Containments," Technical Report, July 1980.

(5) General Electric Co., "Mark II Containment Forcing Function Information Report," GE Report NEDO-21061, Revision 3, June 1978.

(6) Washington Public Power Supply System Responses to Questions - SRV Methodology, WPPSS Letters G02-81-183 and -196, Docket No. 50-397, July 1981.

(7) ___, Responses to NRC/CSB Issue 47, Acceptable SRV Design Load Specification, October 1981.

Figure F.1.1 Normalized vertical distribution of
pool boundary pressures

Figure F.1.2. Vertical distribution of
pool boundary pressure

Table F.1.1 Comparison of Caorso test conditions and WNP-2 design conditions

Plant parameter	Caorso test*	WNP-2 design
Pool temperature	76-97°F	200°F
Valve opening time	39-56 ms	20 ms
SRV mass flux	800,000 lbm/hr	906,200 lbm/hr
Reactor pressure	980 psi	1,250 psi
Pool surface area	3,997 ft	4,520 ft
Quencher submergence	17.7 ft	17.4 ft
SRV line air volume	66.5 ft	57.2-88.1 ft
Number of SRVs	16	18

*Actuations of Valve A during Phase I and II testing.

Table F.1.2 Comparison of vacuum breakers

	WNP-2	Caorso
Manufacturer	GPE controls	Atwood & Morrill Co.
Size	10 in.	10 in.
Type	Single wafer type with swinging disk	Single straight through with swinging disk
Number	18	16
Flow area	38.48 in.^{2}	78.54 in.^{2}
Design conditions:		
Flow	1966	14000 cfm
Pressure	-0.5 to 2 psig	0.0 psig
P	0.115 psid	7 psid
Set point	0.1 pdis	Not available
Opening time	0.21 sec 0.4 psid	Not available
A/K	0.278 ft^2 (40 in.^{2})	0.72 ft^2 (104 in.^{2})

*Acceptance point at 0.115 psid.

Table III.3 WNP-2 design basis operational SRV actuations

ITEM	FSAR Section	Event	No. of SRVs Actuated 1st Blowdown	No. of SRVs Actuated 2nd Blowdown
1	15.1.1	Feedwater controller failure	18	2
2	15.1.3	Pressure regulator failure-open	2	2
3	15.1.4	Inadvertent SRV opening	1	-
4	15.2.1	Pressure regulator failure-closed	18	2
5	15.2.2	Generator load rejection-bypass on	18	2
6	15.2.2	Generator load rejection-bypass off	18	2
7	15.2.3	Turbine trip-bypass on	18	2
8	15.2.3	Turbine trip-bypass off	18	2
9	15.2.4	MSIV closures	18	6
10	15.2.5	Loss of condenser vacuum	18	6
11	15.2.6	Loss of auxiliary power transformers	2	2
12	15.2.6	Loss of all grid connections	18	2
13	15.2.7	Loss of feedwater flow	2	2
14	15.3.1	Trip of both recirculation pumps (one main valve)	6	2
15	15.3.2	Recirculation flow control failure (both main valves)	2	2
16	15.3.2	Recirculation flow control failure	6	2

Table F.1.4 X-quencher comparison

	WNP-2	Caorso	Kuosheng
Reducer length, ft	2.66	1.97	1.67
Hub length, ft	2.61	2.3	3.23
Bottom cap length, ft	No Bottom Cap	1.0	1.0
Hub to end of arm, ft	4.94	4.88	4.88
Hub to first row of holes, ft	1.90	1.90	2.63
Length of hole pattern, ft	2.63	2.63	2.63
Hub diameter, in.	24	24	24 SCH 80
SRVDL diameter, in.	12 SCH 80	10 SCH 40	10 SCH 80
Arm diameter, in.	12 SCH 80	12 SCH 80	12 SCH 80
Hole diameter, in.	0.39	0.39	0.39
No. of holes (total)	1496	1496	1496
Reducer taper, degrees	10.0	13.5	17.1
Angle between arms, degrees	80-100-80-100	80-80-80-120	80-80-80-120

F.2 MARK II CHUGGING LOAD SPECIFICATION EFFECTS OF DESYNCHRONIZATION

F.2.1 Introduction

This appendix documents the work performed by Professor George Bienkowski Princeton University on the effects of desynchronization on the Mark II chugging load specifications. This work was performed as part of the technical assistance program at Brookhaven National Laboratory to support the NRC staff in reviewing the chugging load specifications. This appendix also documents the results of the additional studies performed by the WNP-2 applicant and the staff's evaluations and conclusions.

F.2.1.1 Background

Following receipt of Professor Bienkowski's report, the staff conducted a preliminary evaluation of its contents and concluded that a deficiency exists in the chugging methodology proposed by the Mark II Owners Group. The staff recommended that additional studies of this issue be conducted with input from the owners of Mark II plants. The staff also concluded that other conservatisms in the chugging loads are such that adequate safety margins are maintained to allow licensing activities to continue.

This appendix is the product of the review conducted by the applicant, the NRC staff, and Professor Bienkowski. The remainder of this section and section F.2.2 contain in its entirety. Professor Bienkowski's report. Section F.2.2 presents an executive summary of Professor Bienkowski's report, Section F.2.2 also presents the mathematical evaluation of the effect on desynchronization on chugging loads. Section F.2.3 contains the applicant's comments on our consultant's report and the results of additional analyses performed to confirm the conservatisms of the existing chugging load specifications. Section F.2.4 presents the staff's evaluation of the applicant's analyses and its conclusion regarding the chugging load specifications.

F.2.1.2 Executive Summary

While the data bases, source strengths, or calculational procedures may differ between the generic, Susquehanna Steam Electric Station (SSES) and WNP-2 chugging load specifications, the procedure for desynchronization of chug start times is identical. Both the symmetric and asymmetric specifications are based on the application of the minimum variance set of start times (at the N vents of the plant), from 1000 such sets based on uniform probability distribution within a 50 msec time window. The same set of start times is used for all of the sources in the specifications of both the symmetric and asymmetric loading.

The NRC staff review of the specifications concluded that the data bases, deduced design sources, and application are conservative for the symmetric load, and, while difficult to quantify for the asymmetric case, provide a reasonable measure of asymmetry. The justification of the selection of the minimum variance set of start times was based on an examination of the root-mean square (RMS) values of vertical force and overturning moment. The decrease of the rms value of vertical force with start time variance and the relative insensitivity of overturning moment RMS aplitude convinced the staff that the specification was "reasonable." No information was presented, by either GE or the individual plant owners, on the sensitivity of the frequency content of the loads to the specific selection of start times. Clearly the underestimation of even small amounts of energy at major natural frequencies of the overall plant configuration could lead to potential nonconservatism in individual loads or accelerations at various structural components.

Section F.2.2 (The Effects of Desynchronization on Chugging Loads) examines the potential impact of the specific selection of a single set of start times on the frequency content in the vertical force and overturning moment for three plant configurations and specifications (generic, SSES, and WNP-2). Figures F.2.11 through F.2.14 summarize the results. All four figures show that both the vertical force and overturning moment can have a reasonable chance of 1/1000 of exceeding the specification by as much as a factor of 10 at frequencies with significant energy in the source. Alternatively, one can interpret these results to conclude that there is a high exceedance probability (approaching one) that at some frequency in the 20-50 Hz range the true load on the structure will substantially exceed the specified load.

The consequences of the potential nonconservatism on the response spectrum level at specific nodes of the structure are difficult to assess without access to the full computer codes for the individual plants. The analysis and calculations of Section F.2.2 suggest, however, that a specific set of start times will always produce substantial cancellation of any measure of structural response at some frequencies above 20 Hz. Because these frequency "holes" are dependent on the specific selection and assignment of start times to individual vents, it is virtually impossible to guarantee a low exceedance probability at any frequency above 20 Hz on the basis of the specified desynchronization. Because the choice of the minimum variance set optimizes the synchronization to maximize the symmetric load at low frequencies, no generalization of this hypothesis can be justified either at higher frequencies or for other measures of structural response.

The possible high probability of exceedance of the specified chugging loads, of course, does not necessarily imply lack of safety margin of any individual component in the plant. Other loads could be bounding in the relevant frequency range or other design constraints may have resulted in safety margins well above those imposed by chugging. Individual assessment, component by component, is clearly a difficult procedure at best. If one retains the "physical" intuition that the symmetric and asymmetric loadings provide two "extreme" conditions that adequately describe the "major" structural excitations, one has a clear and attainable objective. The specification must provide loading conditions with low exceedance probability of both the vertical force and overturning moment, or frequency regions where the exceedance probability is high have to be bounded by other specifications. For instance, the generic condensation oscillation load provides adequate margin for the vertical force PSD in the range of 20-50 Hz because of the synchronous application of the loading. Unfortunately, the lack of any appreciable energy in that frequency range in the KWU CO specification fails to provide the same conservatism for the SSES plant. No other asymmmetric loading appears as an obvious candidate to bound the chugging induced overturning moment.

Relatively simple "fixes" to the present specification can define loading conditions that provide an exceedance probability of less than 1 in 1000 for the vertical force and overturning moment. For instance, the addition of a loading specification which applies the sources at about 20% amplitude but is synchronized in time will provide adequate bounds over the 20-50 Hz range for the generic, SSES, and WNP-2 symmetric load. The application of the asymmetric loading with an asymmetric factor increased slightly above the specification and full synchronization in time can ensure a low exceedance probability of the overturning moment over the entire frequency range. Whether these are the best--or the easiest--procedures to provide adequate conservatism is not obvious without a more detailed examination of the actual application of these loading conditions.

F.2.2 The Effects of Desynchronization on Chugging Loads

F.2.2.1 Introduction

A substantial body of experimental evidence exists to indicate that chugging has a random character. Although mean values and standard deviations exhibit dependence on both the properties of the fluid and the nature of the steam being condensed, any individual chug amplitude can be defined only on a probabilistic basis. Both subscale and fullscale multi-vent tests[1-4] also indicate that while on a gross time scale associated with the repetition rate, events at different vents are synchronized; on the time scale of the chug itself start times have a highly random character as well.

The proper assessment of a chugging design load (or response spectrum) on a Mark II containment must take full cognizance of the stochastic nature of the phenomena. An evaluation of the conservatism associated with any loading configuration or any local response can only be performed on the basis of an exceedance probability. This is true whether or not the probabilistic nature of the data base is used directly or indirectly in defining the loading condition. It is also true that different measures of a loading may yield different levels of exceedance probabilty for a given loading configuration. Conversely, a given exceedance probability will require different loading configurations if different global or local measures of the load are used.

For a combination of practical and historical reasons the load specification for Mark II plants consists of two loading configurations, the symmetric and the asymmetric cases. The measures chosen for evaluation of conservatism in the loads are total vertical force for the symmetric case and total overturning moment for the asymmetric loading configuration. Although the data base and detailed application are different, the fundamental definitions of the loading configurations are essentially the same in the generic and the plant-unique methodologies.

The symmetric loading configuration consists of the application of chugs of equal strength A at all vents (WNP-2 applies an increased amplitude at three vents). The start times, however, are chosen from that sequence of random numbers that produced a minimum variance in 1000 Monte Carlo trials from a uniform distribution within a 50 msec time window. In the WNP-2 methodology each group of three vents at given angle ϕ are taken to chug synchronously. The source strength and time history are different in the generic and the 5525 and WNP-2 methodologies. All procedures, however, are a source strength that is greater than the mean of the data on which it is based to account for the probability of an event significantly different from the "average" or "expectation value" event.

The asymmetric configuration is obtained by distributing the source strengths asymmetrically; $(A+B \cos\phi)$ distribution in SSES $(1+\alpha)A$ and $(1-\alpha)A$ on opposite sides of a containment diameter in the generic methodology, and $A(1+CR \cos\phi)$ in WNP-2. The values B, C and α, in each case, are chosen from some evaluation of the variance in amplitudes of the respective data bases for the methodologies. The start times, however, are chosen in exactly the same way as in the symmetric case.

Because each of the design loading configurations consists of a "single" distribution of source strengths and start times at the vent exits in the containment, the quantitative value of exceedance probability for any given load associated with that specific configuration is difficult to assess. The use of a "minimum variance" event in assigning start times appears intuitively conservative for the net force as a measure of symmetric load. The use of the minimum variance event is much more difficult to justify for the asymmetric case.

To provide a formalism within which the exceedance probabilities of the design load specifications can be assessed, a formal fully probabilistic analysis is presented below. These theoretical results are compared to theoretically predicted results using the SSES specification in Section F.2.2.3. Some results of Monte Carlo computations are presented in Section F.2.2.4, and a discussion of the implications on the symmetric and asymmetric load specifications is presented in Section F.2.2.5.

F.2.2.2 Stochastic Formulation

Because of the linear nature of both the fluid description (IWEGS/MARS)[5] and the structural analysis (ANSYS),[5] any measure of either global or local load can be represented as a sum over the responses due to each source applied independently at each vent exit. The specific measure of response due to any individual source can be represented in terms of linear operator L_υ (Green's function or

influence coefficient) acting upon that source $S_\upsilon(t)$. A generalized response R_υ due to a source of amplitude A_υ with a start time t_υ can be symbolically written as

$$R_\upsilon = L_\upsilon(A_\upsilon S(t-t_\upsilon)) = A_\upsilon L_\upsilon(S(t-t_\upsilon)) \qquad (1)$$

The total response to all of the sources in a Mark II containment can then be obtained by a straightforward summation,

$$R = \sum_{\upsilon=1}^{N} A_\upsilon L_\upsilon(S(t-t_\upsilon)) \qquad (2)$$

where N is the number of vents.

To facilitate the stochastic analysis and to provide better measures of the loading it is convenient to replace the time variable by the frequency variable through the Fourier transform $f(\omega) = \int_{-\infty}^{\infty} f(t)e^{i\omega t}dt$. The response measure R_υ can now be written as

$$\bar{R}_\upsilon(\omega) = A_\upsilon e^{i\omega t_\upsilon} H_\upsilon(\omega)\bar{S}(\omega) \tag{3}$$

where $H_\upsilon(\omega)$ is now the operator in Fourier space and $\bar{S}(\omega)$ is the Fourier transform of the normalized source with a start time at $t_\upsilon=0$. Note that $H_\upsilon(\omega)S(\omega)$ can be considered the unit response or just the contribution at frequency $f = \frac{\omega}{2\pi}$ to the response $\bar{R}(\omega)$ from a normalized source with a zero start time. The total response R at frequency f is then just the sum over the amplitude factors $A_\upsilon e^{i\omega t_\upsilon}$ times the unit responses. Since $A_\upsilon e^{i\omega t_\upsilon}$ is a complex number there will clearly be both an in-phase contribution $Re(A_\upsilon e^{i\omega t_\upsilon}) = A_\upsilon \cos \omega t_\upsilon$ and an out-of-phase contribution $Im(A_\upsilon e^{i\omega t_\upsilon}) = A_\upsilon \sin \omega t_\upsilon$.

Because both A_υ and t_υ are random variables, each with an associated probability distribution, the specific response $R(\omega)$ will clearly be random in character with some resultant probability distribution $P(R)$.

For N sufficiently large, the central limit theorem[6] states that $P(\bar{R})$ will approach the normal distribution with a mean $\mu = \sum_{\upsilon=1}^{N} \mu_\upsilon$ and a variance $\sigma^2 = \sum_{\upsilon=1}^{N} \sigma_\upsilon^2$ under some relatively weak condition on boundedness of the random variables $\bar{R}_\upsilon$. Experience shows, that unless the probability distribution of $\bar{R}_\upsilon$ is very peculiar, the number N need not be very large for the normal distribution to become a very good approximation for $\bar{R} = \sum_{\upsilon=1}^{N} \bar{R}_\upsilon$.

therefore probabilities of any measure of loading $R(\omega)$ exceeding some preselected value will be examined on the assumption that N of the order of 100 in a Mark II containment is sufficient for the central limit to hold.

The mean value μ_υ and the variance $\sigma_\upsilon{}^2$ can be obtained on the basis of the prescribed probability density $f_a(A)$ for the amplitudes A_υ and the probability density $f_t(t_\upsilon)$ for the start times t_υ. If it is assumed that probability densities are independent of each other and further take

$$f_t(t_\upsilon) = 1 \qquad \frac{\tau}{2} \leq t_\upsilon \leq \frac{\tau}{2}$$

$$= 0 \qquad t_\upsilon > \frac{\tau}{2} \tag{4}$$

the resultant mean values become

$$\mu_\upsilon = \mu_a \frac{\sin(\omega\tau/2)}{(\omega\tau/2)} H_\upsilon(\omega)\bar{S}(\omega) \qquad \text{inphase}$$

$$= 0 \qquad \text{out of phase} \tag{5}$$

where μ_a is the mean value of the chug amplitudes.

$$\mu_a = \int_0^\infty f_a(x)\ x\ dx \tag{II.6}$$

The associated variances become

$$\sigma_{\upsilon_1}{}^2 = \left(\frac{1 + (\frac{\sigma a}{\mu_a})^2}{2} \left(1 + \frac{\sin\omega\tau}{\omega\tau} \right) - \left(\frac{\sin(\omega\tau/2)}{\omega\tau/2} \right)^2 \right) \mu_a^2\ H_\upsilon^2(\omega)\bar{S}^2(\omega)$$

in phase

and (7)

$$\sigma_{\upsilon_2}^{\ 2} = \left(\frac{1 + (\frac{\sigma a}{\mu_a})^2}{2} \left(1 - \frac{\sin \omega\tau}{\tau\omega} \right) \right) \mu_a^{\ 2} H_\upsilon^2(\omega) \overline{S}^2(\omega)$$

out of phase

where $\sigma_a^{\ 2}$ is the variance of the amplitude probability distribution

$$\sigma_a^{\ 2} = \int_0^\infty fa(x)(x - \mu_a)^2 dx \tag{8}$$

The normalized mean $\overline{\mu}_\upsilon$ and the associated normalized standard devisions $\overline{\sigma}_{\upsilon_1}$ and σ_{υ_2} (normalization is performed by dividing by the response due to the average chug $\mu_a H_\upsilon(\omega)\overline{S}(\omega)$ is shown as a function of $\omega\tau$ in Figure F.2.1(a), (b), and (c)). The corresponding frequencies $f = \omega/2\pi$ are also indicated on the abscissa for τ = 50 msec. The standard deviations are plotted for several normalized variances of the amplitude distribution $\overline{\sigma}_a^2 = (\frac{\sigma_a}{\mu_a})^2 = 0.1$, 0.3, 0.5 and 1.0. Note that for low values of $\omega\tau$ (near synchronization) the inphase standard deviation from the mean is primarily determined by the variance of the chug amplitudes but at higher values of $\omega\tau$ both the inphase and out-of-phase standard deviations arise primarily from the dephasing of start times and are only weakly affected by the variance of amplitudes.

The specific response amplitude (a global load, local deflection, or response spectrum) for any given exceedance probability p_e can be simply determined from the normal probability distribution as

$$\overline{R}_1(\omega,p_e) = \sum_{\upsilon=1}^{N} \mu_\upsilon(\omega) + z(p_e) \sqrt{\sum_{\upsilon=1}^{N} \sigma_{\upsilon 1}^{\ 2}} \qquad \text{inphase}$$

(9)

$$\overline{R}_2(\omega,p_e) = z(p_e)\sqrt{\sum_{\upsilon=1}^{N} \sigma_{\upsilon 2}^2} \qquad \text{out of phase}$$

where $z(p_e)$ is a factor obtained from the normal distribution. For $p_e = 10^{-3}$, $z_e \approx 3.09$ and for $p_e = 10^{-5}$, $z_e \approx 4.28$. If the total amplitude $R(\omega) = \sqrt{\bar{R}_1^2(\omega)+\bar{R}_2^2(\omega)}$ is to be determined, or some combination such as $\sqrt{\bar{R}_x^2+\bar{R}_y^2}$ where $\bar{R}_x$ and $\bar{R}_y$ are two loads along mutually orthogenal axes the results can be determined from different integrals of the multi-dimensional normal distribution. While in general the results may be very complicated, for the low levels of $p_e \leq 10^{-3}$ the effect is primarily to change the function $z(p_e)$ to some new function $z(p_e; \mu, \sigma_1, \sigma_2)$. For instance if R_x and R_y represent moments about two perpendicular axes, the results for a symmetric containment show that if one picks an axis and asks for the exceedance of a fixed moment about that axis for $p_e = 10^{-5}$, $z_e = 4.28$, while if one asks for the exceedance of the magnitude of the load in any direction at the same p_e, $z(p_e; o, \sigma, \sigma) = 4.80$ implying only a 12% higher amplitude. Alternatively, the magnitude of the moment about a fixed axis for an exceedance probability of 10^{-5} corresponds to the magnitude independent of direction at an exceedance level of about 10^{-4}. Therefore, rather than getting involved with the complexities associated with any loads or Fourier coefficients that must be summed as the square root of the sum of the squares, the net inphase vertical force and the net inphase overturning moment about a fixed but arbitrary axis as measures of the symmetric and asymmetric loads will be examined. In the following section these loads are computed based on the analysis above and compared to the SSES specification.

F.2.2.3 Stochastic Analysis of Vertical Force and Overturning Moment

(1) Symmetric Load

If one uses the total vertical force as a measure of the symmetric load as done in the SSES Design Assessment Report (DAR), each source's contribution to the force $H_\upsilon(\omega)\bar{S}(\omega)$ corresponds to the Fourier transform of the integral of the pressure from the vent υ over the entire basemat. Because the major contribution comes from near the vent, except for fringe effects near the pedestal and outer wall, each of the contributions can be considered identical and interpreted as the basemat pressure times some effective area $(\bar{P}(\omega)A)$. Using this interpretation the value of $(\sigma_a/\mu_a)^2 \sim 0.11$ can be reduced as being consistent with the DAR evaluation of the low frequency filtered amplitudes and with the RMS values in both GKM and JAERI. The results of Figure F.2.1 can be applied together with

equation 10 to plot the effective symmetric amplitude factor $A_s(\omega)$ versus

frequency for any desired exceedance probability. The inphase component of the vertical force are shown as the solid lines in Figure F.2.1 for

$p_e = 10^{-3}$ and 10^{-5}. The DAR load specification is represented by dashed lines,

with both the expectation value μ for totally random selection of start times and the 3σ deviation from that value shown. Since the specification uses the most synchronized set out of 1000 sets of starting times and the symmetric load increases with increasing synchronization, the $\mu+3\sigma$ is considered to be more representative of the specification. The inphase vertical force, therefore, is expected to be represented generally conservatively over the entire relevant frequency range, with the greatest conservatism near the lower frequencies where most of the energy is concentrated.

The out-of-phase component can also be analyzed by the present technique and compared to the specification. As can be seen from Figure F.2-1 the major contribution will come at higher frequencies. If the start time set is assumed to be the most conservative out of 1000 trials for the out-of-phase component, the load resulting from the specification corresponds to an exceedance probability of 10^{-3}. Because the contribution of the out-of-phase component to the total amplitude of the vertical force at low exceedance probability is small, the proper matching of that component is not very important. For the present analysis at $p_e = 10^{-5}$ the total amplitude is never more than 12% higher than

the in-phase component; thus even if the specification start times were to produce no out-of-phase component, the comparison would not significantly change from that shown in Figure F.2.2(a).

(2) Asymmetric Load

If one uses total overturning moment as a measure of asymmetric loading as done in the SSES DAR, each source's contribution to the moment ($H_U(\omega)\bar{S}(\omega)$) corresponds to the Fourier transform of the integral over the basemat of the pressure multiplied by a moment arm from the selected axis. As in the symmetric case, the fact that the major contribution comes from beneath the vent allows one to approximate $H_U(\omega)\bar{S}(\omega)$ by $L_U\bar{P}(\omega)A$, where L_U is the perpendicular distance from the selected axis to the vent location. Using this interpretation plus the value of $(\sigma a/\mu a)^2 = 0.11$ deduced from the amplitude variance, and the data presented in the DAR the effective asymmetric amplitude factor $\bar{A}_a(\omega)$ for any exceedance probability p_e can be generated based on the present fully stochastic analysis.

Figure F.2.2(b) shows a comparison of the inphase component of $\bar{A}_a(\omega)$ from the present analysis for exceedance probabilities of 10^{-3} and 10^{-5} (shown as solid lines) to the possible results from the application of the DAR load specifications. The fact that the asymmetric load depends not only on the specific selection of start times but also on the distribution of those start times around the containment makes it difficult to precisely define the loading arising from the specification. For the asymmetric specification both the expectation value and the $\pm 3\sigma$ values are shown, roughly covering the range of possibilities within 1000 trials. Because the minimum variance in start times does not necessarily lead to highest loads as in the symmetric case, it cannot be assumed that the specification will produce the $(\mu+3\sigma)$ values. For frequencies below about 10 Hertz for τ = 50 msec, the specification is clearly conservative, with even the worst result $(\mu-3\sigma)$ always bounding the 10^{-3} exceedance level.

For higher frequencies the asymmetric specification is clearly not conservative. However, the symmetric specification with nonsynchronized events leads also to a moment and can thus in principle cover the high frequency asymmetric amplitude factor. Shown on Figure F.2.2(b) are the plots for the resulting amplitude for σ, 2σ, and 3σ values. While a very fortuitous choice of distribution of start times around the containment could approach the 3σ values and thus correspond to 10^{-5} exceedance probability even at high frequencies, this is clearly unlikely. The more probable result around 1σ leads to an exceedance probability of about 10^{-1} for frequencies above about 15 Hertz (see below).

The results of Figure F.2.2 show clearly that the use of amplitude factors in the SSES DAR specification, coupled with random selection of start times leads to loads with statistical properties that are generally more conservative than the random selection of both amplitudes and start times that could be considered the more "realistic" representation of multi-vent chugging. The more disturbing feature is the behavior of the actual application of the specification (a single application of minimum variance start times) at frequencies above 15 Hz. Because of the possible cancellation of contributions from different vents, a single selection of start times can indeed does lead to "holes" in frequency at which, regardless of the source, no net effect on vertical force or moment may be transmitted. This appears particularly pronounced for the asymmetric load. To investigate this effect of desynchronization more fully, many Monte Carlo calculations have been performed. The results are presented in the following section.

F.2.2.4 Monte Carlo Computations Compared to Symmetric and Asymmetric Load Specifications

To more fully evaluate the potential lack of conservatism resulting from a single application of a specific set of minimum variance start times, a number of Monte Carlo calculations were performed for the SSES, generic, and WNP-2 configurations and specifications. For each of these the net vertical force and overturning moment were computed on the same basis as the theoretical evaluations in Section F.2.2.3, i.e., equal contribution from each vent to the force and a moment contribution proportional to the moment arm of each vent about a preselected axis.

For each of the plant configurations considered, 1000 Monte Carlo trials were performed. Start times were selected randomly from a uniform distribution within a 50 msec time window. For the variable amplitude cases, source amplitudes were selected from a normalized distribution using a JAERI-established variance of $\bar{\sigma}_{\alpha}$ = 0.11. The symmetric and asymmetric amplitude factors and spatial distributions were selected for each configuration on the basis of the relevant specification. A number of statistical measures were calculated and compared to the theoretical results from Section-II.3 where appropriate. The inphase and out-of-phase expectation values and standard deviations, determined "experimentally" from the 1000 trials, agree so well with the "theoretical" values that on a figure such as F.2-1 or F.2-2 they are indistinguishable.

A summary of the results is presented in Figures F.2-3 through A.6.2-8. For each plant configuration and corresponding specification the vertical force results are presented as the square of the force amplitude normalized by N times the contribution from a single vent versus the frequency. (N is the number of vents in the configuration.) The overturning moment is presented as the amplitude squared normalized by the results from synchronized sources distributed geometrically as shown on the figure label. Both results can be interpreted as the <u>PSD</u> one would obtain with random phasing, normalized by the PSD for synchronized sources and specifed spatial distribution. These results are therefore independent of the frequency content of the source. The figures show: (1) the effect desynchronization has on the transmission of the frequency content in the source to overall measures of structural response such as force and moment and (2) the comparison of true bounds in 1000 trials to the results of the direct application of the appropriate specification.

Figure F.2.3 shows the PSD for the vertical force for the SSES plant normalized by the PSD one would obtain for synchronized application of average chugs. The "true" bound of 1000 trials of variable amplitude chugs applied at random start times to the SSES plant configuration of 87 vents is shown as a solid line. The use of the symmetric specification amplitude factor, defined in the DAR with random start times, leads to a bound in 1000 trials that is conservative over the entire frequency range (designated as -·-). However, the use of the amplitude factor together with the application of the specific set of start times with minimum variance is only conservative at frequencies below 20 Hz. Because minimum variance does not uniquely determine the start times, two results from two different sets of 100 trials are shown (dashed lines ---).

Note that the specific frequency "hole," where the PSD will be virtually zero regardless of the energy content within the source, does depend on the particular minimum variance set. Regardless of the specific set chosen, the DAR specification can lead to high exceedance probability over some significant (5-10 Hz) frequency range at some frequency above 20 Hz.

Figure F.2.4 shows similar results for the PSD of the overturning moment for the SSES configuration normalized by the PSD one would obtain from a fully synchronized application of the chugs with a (1 + cos ϕ) distribution of amplitudes. Note that again the use of the asymmetric load factor of 0.4, combined with desynchronized start times, leads to a generally conservative bound within a 1000 trials. Four possible applications of the specification using a minimum variance set of start times lead to a very pronounced lack of conservatism above about 10 Hz. Clearly if the overturning moment is a reasonable measure or a loading configuration significant to the structure, the DAR specification may totally miss energy input at quite moderate frequencies of 10-50 Hz.

The generic specification does not explicitly use any statistical information on the distribution of amplitudes. To compare the results of the "more realistic" variable amplitude chugging to the generic specification, the effective amplitude factor for each of the generic sources has to be estimated. Table F.2-1 gives the results computed on the basis of the RMS pressure in the generic chugging Report.[7] The amplitude factor is based on the ratio of the specified source RMS pressure to the "local" mean RMS pressure of the chugs within a ± 20% mass flow variation around the "key" chug used for that particular source specification. For all of the sources except No. 807 the amplitude factor is > 1.29, which is quite comparable to the SSES specification. Source 807 comes from run 20 in 4TCO near a region of nearly constant chug amplitude resulting in an effective amplitude factor of 1.13. Because the PSD of Source 807 is bounded by other sources at frequencies above about 10 Hz, an amplitude factor of 1.29 was used in the comparisons of the Monte Carlo trials to the generic specification.

Figures F.2-5 and F.2-6 show analogous information to that shown in Figures F.2-3 and F.2-4 but using the generic specifications[7] for comparison and the same 87 vent configuration. The conclusions are not very different. The vertical force spcification can be appreciably below the bound of 1000 trials above 20 Hz, and the overturning moment specification can be orders of magnitude below the "true" bound for virtually any frequency above about 5 Hz.

The WPPSS specification, while using very different calculational procedures,[8] relies on the minimum variance set of start times as done in the generic and SSES specifications. The start times, however, are selected for groups of three vents going synchronously rather than being selected for all 102 vents independently. Figures F.2-7 and F.2-8 show the results of the specification compared to the "true" bound based on 1000 trials of randomly selected amplitudes and start times for all 102 vents. Note that the greater synchronization produced by grouping of three vent sets is a conservative procedure. The vertical force specification therefore is generally near the "true" bound over

Table F.2-1 Generic chugging amplitude factor

Source	Run	No. of Chugs*	RMS Statistics Peak	Mean	GE Avg	Spec	A = Spec/Mean
801	26	4	5.46	4.30	4.96	5.54	1.29
802	19	4	4.21	2.16	3.05	3.22	1.49
803	1	5	4.42	2.33	3.28	3.45	1.48
804	25	4	5.16	3.51	4.53	5.13	1.46
805	15	4	5.19	3.05	4.31	4.38	1.43
806	15	4	3.42	2.41	3.13	3.34	1.39
807	20	5	4.26	3.14	3.63	3.55	1.13
808	1	5	4.42	2.33	4.42	5.06	2.17
809	25	4	5.16	3.51	5.16	6.90	1.97
810	15	4	5.19	3.05	5.19	5.37	1.76

* (± 20% mass flow) used as criterion

almost the entire relevant frequency range. The overturning moment, while showing the characteristic sensitivity to the specific "minimum variance" set chosen, does come closer to the "true" bound than either the generic or SSES specification. Note, however, that an "unlucky" choice of the minimum variance set could still lead to a PSD "hole" at virtually any frequency above 5 Hz.

Two general conclusions from Figures F.2-3 to F.2-8 can be drawn:

- The amplitude factors for the symmetric load and the spatial distributions for the asymmetric load lead to representations of the loading conditions with statistical properties that produce a higher load at the same exceedance probability than that resulting from statistically distributed chug amplitudes.

- The specification of a single set of start times (no matter how determined) does not give a result which corresponds to, even approximately, the same exceedance probability at all frequencies. Indeed frequency "holes," where virtually no energy is transmitted from the source to the resultant measure such as force or moment, will in general rise for any single set of start times. This conclusion is relevant to any other response of the structure whether local or global, although the importance of this effect may be significantly reduced for local measures of structural response.

The conservatism of the loading on a Mark II containment depends both on the conservatism in the source strengths and on the methodology of application. Reference 7 shows an application of the generic sources to the JAERI facility compared to the JAERI data. To match statistics of the application to the quantity of data available, the theoretical computation used the bounds of eight "Monte Carlo" trials averaged over 20 such sets of 8 trials each. The information presented in Figure 6.3 of Reference 7 suggests a conservatism in the source strength of the order of three or higher over most frequencies up to 50 Hz. To test whether this conservatism could be consumed by the demonstrated nonconservatism in the asynchronization specification, Monte Carlo trials analogous to those presented in Figures F.2-3 to F.2-8 were performed for the JAERI configuration.

Figure F.2-9 shows a comparison for the normalized PSD of the vertical force (the moment is not meaningful for this configuration) as computed for Figure 6.3, in Reference 7 to the results based on variable amplitudes and synchronization based on the specification. The same potential nonconservatism exists for this facility as for the full-scale plant configurations, although the specific minimum variance results may actually be more conservative than the (bound of 8 average over 20) GE result at frequencies below about 25 Hz. If one applies the ratio of the "minimum variance" result to the GE result to Figure 6.3 of Reference 7, one can compare the actual application of the generic specification to the measurements in the JAERI facility. Figure F.2-10 shows such a comparison. Note that above 25 Hz the specification does not provide any conservatism over the data, and may indeed miss a small, although significant, amount of energy above 40 Hz. While the source strengths in the JAERI facility may indeed be conservatively bounded by the specified sources based on 4TCO data, the application of the specified desynchronization could lead to either no margin or even some nonconservatism for the seven-vent configuration in JAERI. While no information on asymmetric loading can be deduced from JAERI, a comparison of Figure F.2-2 to F.2-5 shows that a lack of margin in the symmetric load suggests a very high potential for exceedance in the asymmetric load because of the greater sensitivity to the specific selection of start times. The comparison to JAERI results cannot, therefore, be used to show overall conservatism in the specification of chugging loads.

F.2.2.5 Discussion and Conclusions

To examine the effect of desynchronization on some specific sources the PSDs of the vertical force and overturning moment were computed for both SSES and the generic specifications. The results of section F.2.25 were applied directly to the bottom center pressures computed on the basis of the appropriate design sources.

For the SSES comparison, PTH No. 6 based on Source 306 was used as an example. This source was selected because it exhibits the highest energy content in the 25-50 Hz range. Figures F.2-11 and F.2-12 show the symmetric and asymmetric results respectively. Note that the PSD of the vertical force shows a potential nonconservatism at a significant peak around 29 Hz. While the energy content potentially missed by the specification is a small fraction of the total energy in the vertical force, it may have important consequences if a natural frequency of the structure exists in the underestimated frequency range. The potential nonconservatism of the specification of the overturning moment is even more evident in Figure F.2-12. The energy content may clearly be underestimated at virtually all frequencies above 10 Hz.

Similar results for the generic specification are presented in Figures F.2-13 and F.2-14 based on the bottom center pressure PSD bound of all the generic chugging sources (Figure 4-27 of Reference 7). The potential underestimation of energy content in the vertical force above 20 Hz and in the overturning moment above 10 Hz is clearly evident. For the specific choice of start times used, it is quite clear that any possible excitation of an asymmetric mode of the structure with a natural frequency above 10 Hz could be totally missed by the specification.

The consequences of the potential nonconservatism on the response spectrum level at specific nodes of the structure are difficult to assess without access to the full computer codes for the individual plants. The theoretical results of Section F.2.2.3, together with the Monte Carlo trials of Section F.2.2.4, suggest, however, that a specific set of start times will always produce almost total cancellation of any measure of structural response at some frequencies above the frequency ($f_o = 1/\tau$) associated with the time window τ. Because these frequency "holes" are dependent on the specific selection and assignment of start times to individual vents, it is virtually impossible to guarantee a low exceedance probability at any frequency above f_o on the basis of the specified desynchronization. While the choice of the minimum variance set optimizes the synchronization to maximize the symmetric load at frequencies below f_o, no generalization of this hypothesis can be justified either at higher frequencies or for other measures of structural response.

The possible high probability of exceedance of the specified chugging loads, of course, does not necessarily imply lack of safety margin on any individual component in the plant. Other loads could be bounding in the relevant frequency range or other design constraints may have resulted in safety margins well above those imposed by chugging. Individual assessment, component by component, is clearly a difficult procedure at best. If one retains the "physical" intuition that the symmetric and asymmetric loadings provide two "extreme" conditions that adequately describe the "major" structural excitations, one has a clear and attainable objective. The specification must provide loading conditions with low exceedance probability of both the vertical force and overturning moment, or frequency regions where the exceedance probability is high have to be bounded by other specifications. For instance, the generic condensation oscillation load (Reference 9, Figure 2-1) provides adequate margin for the vertical force PSD in the range of 20-50 Hz because of the synchronous application of the loading. Unfortunately, the lack of any appreciable energy in that frequency range in the KWU CO specification fails to provide the same conservatism for the SSES plant. No other asymmetric loading appears as an obvious candidate to bound the chugging induced overturning moment.

Relatively simple "fixes" to the present specification can define loading conditions that will provide an exceedance probability of less than 1 in 1000 for the vertical force and overturning moment. For instance, the addition of a loading specification that applies the sources at about 20% amplitude but synchronized in time will provide adequate bounds over the 20-50 Hz range for the generic, SSES, and WNP-2 symmetric load. The application of the asymmetric loading with an asymmetric factor increased slightly above the specification and full synchronization in time can ensure a low exceedance probability of the overturning moment over the entire frequency range. Whether these are the best--or the easiest--procedures to provide adequate conservatism is not obvious without a more detailed examination of the actual application of these loading conditions.

F.2.3 WNP-2 Approach to Resolving Vent Phasing Concern

The WNP-2 response to the vent phasing concerns raised by Professor Bienkowski's report is essentially contained in two letter reports.[10,11] The basic points of the applicant's argument for the adequacy of the applicant's existing chugging specification are the following: While the specification is divided into a nearly symmetric and asymmetric part, mainly for historical reasons, it can be shown that containment response to the asymmetric specification is not significantly different from response to the nearly symmetric specification. Therefore, it will suffice if the symmetric specification can be shown to be adequately conservative with regard to the frequency "holes" mentioned in Professor Bienkowski's report (Section F.2.2). The symmetric specification can be shown to be conservative from comparison with "required design" curves from the Bienkowski report, as well as from comparison with data measured in the JAERI multivent facility.

In answer to a request by the staff, the applicant provided in Reference 11 the reactor building structural model responses to chugging loads for both the nearly symmetric and the asymmetric loading conditions, at various containment locations. Specifically, acceleration responses from 0 to 150 Hz at seven containment locations at crucial points in the drywell, wetwell and secondary containment were presented for the horizontal and vertical directions. At all locations shown, the response to the asymmetric loading was within 20% of the response to the nearly symmetric loading over most of the frequency range. The applicant stated that this similarity in response was typical of all locations compared and that there were no locations where the asymmetric response was significantly larger than the response to the nearly symmetric load. For each of the locations compared in Reference 11, the applicant also provided the acceleration response to the safe shutdown earthquake (SSE) loading for which WNP-2 is analyzed. Except at the drywell floor and in the wetwell at vent exit level, the acceleration response to SSE exceeded that of the chugging response over the entire frequency range and by an order of magnitude. The SSE comparison show that many containment locations are designed to withstand "G" levels from other loads that are much higher than those as a result of chugging, whether nearly symmetric or asymmetric.

The applicant concluded that the asymmetric load specification does not excite any modes that are not also excited by the nearly symmetric mode. In other words, the containment does not respond with any rocking or overturning motion to the asymmetric specification that was not also excited by the nearly symmetric load. Furthermore, loads resulting from the SSE elicit a much greater response from many points on the containment than do either of the chugging loads.

F.2.4 Staff Evaluation of WNP-2 Approach

The staff's view on these conclusions are the following: The acceleration response spectra contained in Reference 11 do indeed indicate that the structural response of the containment does not distinguish between the nearly symmetric and asymmetric loading to any great degree. This is not particularly surprising if one looks at the actual load specifications. The designations of "nearly symmetric" and "asymmetric" refer only to the spatial distribution of the load amplitudes and were coined at a time in the development of the load specification when all vents were designated to chug simultaneously. Since then a more realistic desynchronized specification has evolved in which all the vents are assumed to chug independently within a 50 insec time window for both the nearly symmetric and asymmetric portions of the specification. This desynchronization in time then means that at any particular instant there will be an asymmetric spatial loading on the containment when either portion of the chugging load specification is applied. As a matter of fact, at all but the lowest frequencies, the asymmetry as a result of the time desynchronization is greater than the asymmetry as a result of the variation in amplitudes of the asymmetric specification. These amplitudes vary only about + 14% from the nearly symmetric source strength when going from one side of the containment to the other. At the lowest frequencies the acceleration response spectra in Reference 11 show that the containment does not respond with any fundamental rocking mode to the chug loads. In the staff's judgement, the applicant's conclusion regarding the similarity in structural response to the nearly symmetric and asymmetric portions of the load specification is valid. The staff also feels that comparison of response from chugging with that from SSE loading adds perspective to the relative load contributions the chugging loads impose on different portions of the containment.

In Reference 10, the applicant provided two comparisons to prove that the applicant's nearly symmetric specification is adequately conservative, even in light of the concern raised by Professor Bienkowski. The first is a comparison of the WNP-2 design loads with the so-called "required design values" referred to in the Bienkowski report. This is a frequency-by-frequency comparison of the ratio PSD for desynchronized application divided by PSD for synchronized application as shown in Figures F.2-16 through F.2-18. Each figure compares three curves. The curve shows that the required design values or bound of 1000 Monte Carlo trials consisting of the envelope of all the minimum variances give the highest ratio value at each frequency as estimated in the Bienkowski report. Another curve shows a possible design outcome if a particular minimum variance is chosen for a set of start times. The third curve shows this possible design outcome after it has been adjusted for the conservatisms in the WNP-2 single-vent design source load definition. This adjustment is made by using the two curves in Figure A.2-15 that which represent the envelope of the 4TCO bottom center pressure obtained from applying the WNP-2 design sources "design spectrum" and the envelope obtained when the mean chugs "required average spectrum" from the 4TCO data time windows as defined in Reference 7 is applied. The ratio of these two curves at each frequency is used to multiply the possible design outcome in Figures F.2-16 through F.2-18 and thereby obtain the adjusted outcome also shown on the figures. Figures F.2-18 through F.2-18 show three possible choices of design outcomes and their adjusted values. Similar curves are given in Reference 10 for the 6-foot and 12-ft wall elevations in 4TCO, and they show similar margins between the adjusted design values and the required design values. As can be seen from these figures, the adjusted possible design outcome values of the WNP-2 specification envelope by a good margin the required design values. It is also noted in Reference 10 that the comparisons of Figures F.2-16 through F.2-18 are estimates because the actual analytical procedures implemented on WNP-2 we-e not available for the Bienkowski comparison; their use would make the comparison even more favorable.

As further evidence of the conservatism of the WNP-2 chugging load specification, a PSD comparison is made in Reference 10 between the rigid wall pressures calculated on the walls of the JAERI facility if the WNP-2 load specification is applied and the data measured on the rigid walls of that facility. An envelope of the data obtained by a method similar to that described in Reference 7 is compared with an envelope calculated with the WNP-2 sources. The data comes from the eight largest chugs in Test 0002, which contains some of the largest chugs recorded in the JAERI facility. The values calculated using the WNP-2 chugging load specification bound the data envelope by a significant margin over the entire frequency range of (0 to 50 Hz.)

The staff concurs with the arguments presented in Reference 10 regarding the adequacy of the nearly symmetric specification, even in light of Professor Bienkowski's phasing concern. The additional conservatism in the WNP-2 single-vent design source, as well as the simultaneous chugging of each radial row of vents, has made the dephasing issue less of a concern for WNP-2 than for some other Mark II plants. The staff feels that the adjustment made in Reference 10 of the possible design outcomes is a valid one and that the evidence shown in Figures F.2-16 through F.2-18, does prove the adequacy of the WNP-2 nearly symmetric chugging load specification. The comparison with the JAERI data further confirms the adequacy of the WNP-2 chugging load specification, because it was applied in the desynchronized way defined in the specification.

The staff feels that the applicant's approach for resolving the vent phasing concern is sound. The evidence presented in References 10 and 11 shows that the nearly symmetric WNP-2 chugging load specification is still conservative when compared to the required design values of the Bienkowski report, as well as when compared to the JAERI data. Also, the material presented shows that structural response to the asymmetric specification is very similar to that obtained from application of the nearly symmetric specification and no critical mode is excited by one that is not excited by the other. Therefore, the staff concludes that the WNP-2 chugging load specification discussed in Appendix F.1 is adequate as it stands.

It should be noted that since the issuing of References 10 and 11 by the applicant, additional evidence on the similarity of response to symmetric and asymmetric chug specifications has been presented by other Mark II plants. The symmetric generic specification has been shown to adequately bound JAERI data in pressure response comparisons. Because the WNP-2 chugging load specification is even more conservative than the generic specification, this is additional proof of the adequacy of the chugging load specification for WNP-2.

F.2.5 References

(1) "Japan Atomic Energy Research Institute," Data Report on Reliability Proving Tests of Containment Pressure Suppression System." JAERI Test No 0002, Feb. 1979.

(2) "NRC Meeting With PP&L to Discuss Susquehanna Steam Electric Station Plan Unique Containment Program," March 7, 1980.

(3) "Chugging Parametric Test Report - Small Scale," GE, NEDE-21851-P, June 1978.

(4) "Comparison of Single and Multivent Chugging - Phase 2," GE Repor , NEDE-25289-P, August 1980.

(5) ___, "Mark II Improved Chugging Methodology," GE Report, NEDE-24822-P, May 1980.

(6) Feller, W., An Introduction to Probability Theory and Its Applications, Volume I (2nd Edition), John Wiley & Sons, Inc., New York (1957), pp. 238-241.

(7) "Generic Chugging Load Definition Report," GE Report, NEDE-24302-P, April 1981.

(8) Burns and Roc "Chugging Loads - Revised Definition and Application Methodology for Mark II Containments (Based on 4TCO Test Results," Burns and Roe, Inc., July 1981.

(9) "Generic Condensation Oscillation Load Definition Report," GE Report, NEDE-24288-P, November 1980.

(10) Burns & Roe, Inc., transmitted by J. Verderber of Burns & Roe, Inc., to B. A. Holmberg of WPPSS, entitled: "Review of Prof. Bienkowski's Concern

Regarding Effects of Desynchronization on the Chugging Load Specification Used for WPPSS-Nuclear Project No. 2," March 2, 1982.

(11) ---, letter report transmitted by J. J. Verderber of Burns & Roe, Inc., to B. A. Holmberg of WPPSS, untitled, March 30, 1982.

Figure F.2-1 Probability parameters

Figure F.2-2 Comparison of present analysis to PP&L specification

Figure F.2-3 PP&L symmetric load vertical force

Figure F.2-4 PP&L asymmetric load overturning moment $\alpha = 0.4$

Figure F.2-5 Generic 87-vents symmetric load vertical force

Figure F.2-6 Generic 87-vents asymmetric load overturning moment
$A(1 + \alpha)$ with $A = 1.29$, $\alpha = 0.155$

Figure F.2-7 WPPSS symmetric load vertical force A = 1.29

Figure F.2-8 Asymmetric load overturning moment
$\alpha = 0.14$, $A = 1.29$, $A(1 + \alpha L_x)$

Figure F.2-9 JAERT symmetric load vertical force generic

Figure F.2-10 Comparison of generic specification to JAERI data (1800 mm location)

Figure F.2-11 SSES-87 vents symmetric load PTH No. 6 - source 306

Figure F.2-12 SSES-87 vents asymmetric load PTH No. 6 - source 306

Figure F.2-13 Generic-87 vents symmetric load based on bounding envelope of sources 801-810

Figure F.2-14 Generic-87 vents asymmetric load envelope of sources 801-810

Figure F.2-15 Design spectrum and required average spectrum - 4TCO bottom center (channel 28)

Figure F.2-16 WNP-2 vertical force comparison: design required vs possible design outcome 1st trial

Figure F.2-17 WNP-2 vertical force comparison: design required vs possible design outcome 2nd trial

Final Review
Geology
M. H. Hait
D. D. Dickey
Seismology
S. T. Algermissen
D. M. Perkins
P. C. Thenhaus
E. P. Arnold
S. R. Brockman
June 29, 1982

Washington Public Power Supply System
Nuclear Project No. 2
Hanford, Washington
Docket No. 50-397

Introduction

The Hanford facility has a long history (since 1943) as a site that has accomodated plutonium production reactors, fuel fabrication plants and spent fuel reprocessing plants. Recently the facility has been the proposed site for a number of public power reactors. Work done since 1975 and reviewed by the USGS for Project No. 2 includes the Final Safety Analysis Report (FSAR) Chapter 2.5, Amendment No. 18, and Questions and Responses on this document. Also consulted were the Skagit/Hanford Nuclear Project PSAR Appendixes 2N, 2O, and 2R, as well as other selected references. USGS personnel attended meetings and field inspections (shown by (F)) with personnel representing the applicant and the Nuclear Regulatory Commission (NRC) on the dates 12/5/80, 1/26-27/81, 3/23/81 (F), 3/31/81, 4/28-29/81 (F), 6/25-26/81, 8/4-5/81 (F), 10/16-17/81 (F), 11/17-18/81, 12/8-9/81 (F), 1/21-22/82, 2/9-10/82, 4/12-14/82 (F), and 5/18/82.

Geology

The geologic analysis by the applicant is based on the published literature and independent geological and geophysical studies done by them and their consultants specifically for the WNP 1, 2, and 4 sites.

The Site

The WNP 2 site is located in the Pasco Basin, a physiographic subdivision of the Columbia River Basalt Plateau Province. The site, about 1 mi west of the WNP Nos. 1 and 4 sites, is situated on a broad terrace of the Columbia River at about a 440-ft elevation. In the site area a thin blanket of eolian sand overlies a sequence of glaciofluvial sands about 40 ft thick; and of moderately indurated sands approximately 480 ft thick, silts, clays, and gravels of the Ringold Formation, and late Tertiary Columbia River Basalt at least 5,000 ft thick. Above the basalt, strata range from unconsolidated to semiconsolidated, and are essentially horizontal in the site area.

The site is situated in the Pasco Basin, an area that appears to have been subsiding since the first extrusions of the Columbia River Basalt in Miocene time. Topics related to the geologic safety of the plant site that were of major concern during this review are discussed below.

Anticlinal Ridges

Beginning in late Miocene(?) or in Pliocene time the basalt was slowly folded into a series of long, predominantly asymmetrical, anticlinal ridges that trend generally east-southeast from the foothills of the Cascades to the vicinity of the Pasco Basin. Locally, near the basin, these folds display northward overturning of the folded basalt, minor associated thrust faulting, and normal faulting which parallels the folds.

The principal development of the ridges and associated faults appears to have preceded the Ringold deposition (Rockwell Hanford Operations, 1979; Bentley and others, 1980; Goff and Myers, 1978; Hays and Schuster, in preparation). Rockwell Hanford Operations (1979, p. IV-17, 20, 21) concludes that most deformation in the Pasco Basin area occurred between 10.5 and 5 million years ago. Uplift of the Yakima Ridge was complete prior to 1 million years ago when the Tieton Andesite was emplaced in an erosional reentrant across the truncated northern flank of the anticline.

Bentley and others (1980, p. 60) state that much of the deformation in the Simcoe volcanic field area was complete before these eruptions (5 to 1 million years ago).

Bentley (1977, p. 354) concluded that most of the deformation along Manastash Ridge occurred prior to development of the 1-million-year-old Thrall pediment surface on its north flank.

Southeast Anticline

The southeast "anticline" is a buried ridge of basalt extending southeastward from Gable Mountain to within about 5 km of the site. A thrust fault dipping about 35^{0} southwest superposed basalt of the Elephant Mountain Member of the Saddle Mountain Basalt over itself to form a ridge about 100 ft high. Ten drill holes on a line perpendicular to the ridge were cored and logged geophysically to define the geologic relations (Golder Associates, 1982). Interpretation of these data permit displacement on the fault of no more than 20 or 30 cm (about 1 ft) in the last several million years. We concur with the applicant's conclusion that the fault is not capable.

Cle Elum-Wallula Alinement (CLEW)

A 200-km-long northwest-trending structural zone within the Columbia Plateau, passes southwest of the site, forming a line between Cle Elum and Wallula Gap. This has been interpreted as a diffuse zone of dextral strain with accompanying northwest-trending folds and faults that appear to have formed synchronously with the predominantly more west-trending folds. Surface expression of the elements of this structure takes many forms--folds, faults, airphoto lineations etc. These were investigated by field mapping, trenching, drilling and seismic, gravity and magnetic surveys. No single through-going surface structure is present along this alinement. Gravity maps indicate no change in basement rocks across this structure, and strike-slip movement, if present, is of limited extent (PSAR illustration 2.5-9). Because of young faulting (exact age undetermined) in the Wallula fault zone, discussed in sections on young faulting, CLEW may be capable (FSAR amendment number 18, page 2.5-128).

Recent Work

Considerable geologic and geophysical work, much of it by the applicant, has been done over the past few years. This work was aimed toward developing comprehensive structural models and dating the structures.

Three trenches across lineaments on the north side of Rattlesnake Mountain revealed that the lineaments did not result from faults (field inspection 4-12-82). Trenches across the Wallula fault zone east of Wallula Gap and at Yellepit, west of Wallula Gap, showed unfaulted latest Pleistocene sediments resting on faulted Miocene basalt (WPPSS 1977, FSAR p. 2.5-96). Trenching of the south fault on Gable Mountain exposed no faulting of the glaciofluvial deposits (Golder Associates 1981, FSAR p. 2.5-86).

Young Faulting

However, since 1977, Quaternary faulting has been identified in five areas. (1) Toppenish Ridge, approximately 85 km west of the WNP 2 site (Campbell and Bentley, 1980; Woodward-Clyde Consultants, 1981a); (2) Wallula fault zone about 45 km southeast of the site, from the vicinity of Wallula Gap on the Columbia River southeastward to the Walla Walla/Milton-Freewater area (Shannon and Wilson, Inc., 1980); (3) on the eastern end of Gable Mountain approximately 18 km north of the site (Golder Assoicate, 1981); (4) on the northern flank of Ahtanum Ridge at Union Gap approximately 93 km west of the site; (Campbell, in Rigby and Othberg 1979) and (5) Wenas Valley fault, approximately 100 km west of the site (Glass, 1977).

Toppenish Ridge is a west-trending anticlinal structure on the Yakima Indian Reservation. Geologic work in the area is reported in Rigby and Othberg (1979), Bentley and others (1980), and Campbell and Bentley (1981). Unpublished work was done for the applicant by C. E. Glass (1979, 1981), W. Kiel and G. Davis (1980), and G. Davis (1981). The age of the youngest faults is established as Holocene but the mode of origin is in doubt. They may be either tectonic or gravity-induced (landslide). Thus they are not proven to be nontectonic and for safety reasons are assumed to be capable faults.

The Wallula fault zone from The Butte just west of Wallula Gap and southeastward shows evidence of Quaternary faulting. At Finley Quarry in trenches at the northwest end of The Butte, Woodward-Clyde Consultants (1981b) mapped faults which cut sediments of probable Pleistocene age. Near Warm Springs, pre-Touchet colluvium is displaced (Shannon and Wilson, Inc., 1979a; Woodward-Clyde Consultants, 1981c). South of Umapine, Oreg., faults of tectonic or slump origin displace Touchet beds a maximum of 1.5 ft (Shannon and Wilson, Inc., 1979b). The Buroker thrust fault east of Walla Walla offsets the base of the Pleistocene Palouse Formation about 3 ft; overlying loess deposits appear to be unfaulted (Shannon and Wilson, Inc., 1980). Near Little Dry Creek, south of Milton-Freewater, Palouse soil is downdropped 1.5 ft.

At Gable Mountain the 3km long Central fault displaces glaciofluvial deposits and clastic dikes derived from them (Golder Associates, 1981). The displacements are 0.2-0.3 ft over a linear distance of 1,100 ft.) in sediments dated from ash as being between 13,000 and 19,000 years old.

Faulting in late Cenozoic sediments on Ahtanum Ridge was mapped by Campbell (in Rigby and Othberg, 1979). He observed faulting of Ellensberg sediments and cemented basalt gravels, but found no evidence of faulting in recent loess or stream alluvium overlying the surface of the ridge.

The Wenas Valley fault is expressed as a 9-km-long scarp in Quaternary sediments. Landslides on the downhill side of the fault offer the possibility that the origin may be the result of gravitational sliding rather than tectonic.

Of the discussed fault the Central fault was considered capable of generating the largest ground motion and was used for design purposes (FSAR amendment 18, page 2.5-136).

The capable faulting would be a matter of concern only if the noted elements could be related to a large structure which would be capable of rupturing over a distance longer than any yet recognized. The Cle Elum-Wallula lineament appeared to be the longest possible structure in the Pasco

Basin but the results of intensive investigation makes it seem highly unlikely that fault rupture of great distance or large throw will occur along it.

Seismotectonic provinces

The applicant used physiographic provinces to define areas of similar seismicity (p. 2.5-125 and figures 2.5-1 and 2.5-39). The following discussion of seismotectonic provinces includes concepts developed by R. Tabor and K. F. Fox, Jr., of the U. S. Geological Survey. The authors of this report are responsible for the overall conclusions of the geology review.

Interpretation of seismotectonic provinces and significance of the 1872 earthquake

By seismotectonic province we mean a part of the Earth's crust that is homogeneous with respect to earthquake generation in response to the present-day stress. This means that a seismotectonic province is homogeneous with respect to the maximum-sized earthquake possible. Major problems include how to recognize such provinces and how to define their boundaries, which are probably transitional. For example, a province may be recognized by homogeneity of its rocks at a specified scale, style and fabric of deformation, history of deformation in the recent geologic past, crustal thickness, and earthquake history.

The tectonic provinces delineated by the applicant as the Northern Cascades, Middle Cascade Mountains, and Columbia Basin tectonic provinces (FSAR, p. 2.5-125; fig. 2.5-39), are mostly geologic provinces, defined on the basis of differences in stratigraphy and geologic history. For instance, the applicant's western boundary for their Columbia Basin tectonic province is simply a stratigraphic boundary, drawn along the generalized western contact of the Miocene Columbia River Basalt Group.

It is suggested that at least some of the Yakima fold belt (FSAR, fig. 2.5-4) within the applicant's Columbia Basin tectonic province may be in fact part of a single seismotectonic province which includes not only the applicant's Northern Cascades tectonic province but the northern part of their Middle

Cascade Mountains province as well. Where within a broad zone the boundaries actually lie cannot be determined with certainty.

In Washington State along and east of the Quaternary volcanoes, the current stress regime may be caused in part by, or at least associated with, the slowly subducting Juan de Fuca plate. However, earthquake focal mechanism solutions for the region east of the Olympic Peninsula indicate roughly north-south horizontal compression in crustal rocks throughout western and central Washington, indicating that the orientation of stress trajectories is markedly influenced by the wrenching couple between the Pacific and North American plates (Fox and Engebretson, 1981). This general orientation of compressive stress is common to the several seismotectonic provinces considered here.

The elongate Northern Cascades seismotectonic province may change in tectonic character from north to south; however, the change is gradual. As far south as about 46°30' the strong northwest grain, so prominent in the exposed older rocks to the north, is reflected as northwest-oriented folds in the younger volcanic rocks.

East of the Cascade crest the strongly deformed early Tertiary and older rocks exposed in the Northern Cascades continue under the edge of the Columbia River Basalt Group to the southeast. Many of the major, long active structures in the older Tertiary rocks have expression in the structures of the Miocene basalt. Two major ridges that show stratigraphic evidence of being highs in Eocene and Oligocene time are continuous with ridges and major broad folds in the Yakima Basalt Subgroup. For instance, the northwestern end of Manastash Ridge, underlain by upfaulted pre-Miocene rocks, splits to become Manastash Ridge and Umtanum Ridge in folds in the basalt (FSAR, fig. 2.5-4). At least parts of the Wenatchee Mountains have been high since early Eocene time and they continue into uparched Miocene basalt to the south. The Chiwaukum graben, an active tectonic depression in middle and upper Eocene time, is expressed in a major downwarp in the Miocene basalt (see Tabor and others, in press/a, Tabor and others, in press/b). The cluster of folds, mostly ridges and basins making up the Yakima fold belt, south of the aforementioned structures may be superimposed also on older folds, grabens, or horsts of similar trend in the underlying rocks.

A clue to the southeastern extent of the Northern Cascades seismotectonic province may be found in the change in trend of the Yakima folds from northwest to east-west (FSAR, fig. 2.5-4). This could represent a place where the older rocks no longer influence the fold trend in the present-day north-south stress regime because the older rocks are more deeply buried. How far east the seismotectonic character of the Northern Cascades seismotectonic province influences the Columbia Plateau physiographic province with regards to earthquake activity cannot be determined with great certainty. It would seem reasonable to conclude that any influence on earthquake activity would not extend farther east than any possible structural influence which might be inferred.

Both from a geologic and an earthquake standpoint, the eastern part of the applicant's Columbia Basin tectonic province, including the Hanford site, appears to be a seismotectonic province distinct from the Northern Cascades seismotectonic province. We will continue to refer to this restricted province as the Columbia Basin seismotectonic province.

Based on the historic difference in seismic activity alone (fig. 1) the central part of the Columbia Plateau area appears to be less active than the Northern Cascades seismotectonic province as defined here. Perkins and others (1980, pl. 1) show a difference, and more recent work confirms the higher historic seismicity of much of the Northern Cascades (Perkins, oral commun., 1982).

The applicant does not consider the 1872 Washington earthquake as important with regard to the site, apparently on the basis that its epicenter could have been no farther south than the Chelan area, and that it probably lay near the Canadian border in the Northern Cascades tectonic province. (see FSAR, fig. 2.5-39 and section 2.5.2.1.1.1). A panel convened to review the available data on the 1872 earthquake (PSAR, subappendix 2RA) concluded that the hypocenter of the 1872 earthquake was more than 10 km deep and somewhere between Chelan and the Canadian border, clearly in the Northern Cascades seismotectonic province and probably much closer to the site than implied in the FSAR. Although some workers have suggested that the 1872 earthquake might have occurred along the Straight Creek fault, no offsets attributable to the quake have been found, and it remains a crustal earthquake without a known generating structure.

Based on structural geologic history from early Tertiary through the Miocene and on the present stress regime, the Northern Cascades seismotectonic province should encompass at least the area shown on figure 1. The boundary between the Northern Cascades and the Columbia Basin is indefinite, but the thickening of the basalt and the change in fold trends from northwest to east-west suggest a fundamental change, about in the middle of the boundary zone shown on figure 1.

Under present NRC rules, the applicant would have to consider the effects of a deep-seated 1872 intensity earthquake at the edge of the Northern Cascades seismotectonic province as here redefined. However, the transition zone from one to the other probably could be viewed as transitional in seismic properties; such a transitional zone is not homogeneous nor is it exactly like the provinces to either side.

We conclude that the 1872 earthquake was a deep-seated event in crustal rocks of the Northern Cascades seismotectonic province. The Northern Cascades seismotectonic province, a region of the Earth's crust that can be expected to respond homogeneously with respect to earthquake frequency and maximum magnitude in today's stress regime, cannot be excluded with confidence from the western portion of the Yakima fold belt and northern part of the Middle Cascade Mountains tectonic province as defined by the applicant. The boundaries of the seismotectonic provinces are indefinite and gradational probably encompassing a zone tens of kilometers wide. The transitional boundary between the Northern Cascades and the Middle Cascade Mountains seismotectonic provinces appears to lie south of Snoqualmie Pass, and the transitional boundary between the Northern Cascades and Columbia Basin seismotectonic provinces appears to lie somewhere west of the site within the Yakima fold belt.

If the 1872 earthquake were moved into the transition zone it still would not become the controlling source mechansim for design purposes for the SSE (see section of this report on seismicity).

Volcanic hazard

The only apparent significant volcanic hazard at the site is possible ashfall.

1. **Potential source volcanoes**.--The applicant (FSAR, p. 2.5-103) cites Mount Ranier (ca. 193 km, 120 mi) and Mount Adams (ca. 164 km, 102 mi) as the potential source volcanoes for an ashfall that would reach the site. Although these volcanoes are the closest to the site, they are potentially less explosive than the historic record of Mount St. Helens (ca. 224 km, 139 mi) and perhaps Mount Hood (ca. 222 km, 138 mi), the two other potential sources. St. Helens and Hood are essentially equidistant from the site and can be modeled as the same source. St. Helens is the most likely source because of its history of explosive dacitic eruptions. For more conservative thickness calculations, Adams is the closest; for potential explosivity, St. Helens is the closest.

2. **Compacted ash thickness**.--The Mount St. Helens Yn ashfall is a reasonable, probably conservative, design ashfall. The WPPS applicant defines 7.4 cm (3 in) of compacted ash at the site. Other estimates come from plotting the Yn ashfall data of Mullineaux (1976) and Crandell and Mullineaux (1978) on FSAR figure 2.5-24. These data are as follows:

   20 cm (8 in) at 100 km (62 mi)
   6 cm (2.4 in) at 200 km (125 mi)
   5 cm (2.0 in) at 280 km (174 mi)

   Thus, at the distance of Mt. Adams (164 km, 102 mi), the scaled-off compacted thickness is about 8.4 cm (3.3 in), and at the distance of Mount St. Helens, about 5.8 cm (2.2 in). The applicant's 7.4 cm (3 in) estimate appears to be reasonable between a nearer, but less likely eruption from Mount Adams, and a farther, but more likely eruption from Mount St. Helens.

3. **Uncompacted ash thickness**.--Fluff-up factors to estimate the initial thickness of uncompacted ash are based on estimates of the amount of compaction. Initial thickness is empirically based on direct observations of the May 18, 1980, Mount St. Helens ashfall near Ritzville, Washington. There, about 50 percent compaction took place in roughly two days after the end of ashfall, and about 50 percent more by summer 1981--a total of about 75 percent (A. M. Sarna-Wojcicki, oral commun., June 1982). These observations suggest that initial thickness is difficult to estimate confidently and may be meaningless because the ash probably compacts partly under its own weight while it accumulates.

   Compaction estimates given by the WPPS applicant are 20-40 percent (FSAR, p. 2.5-103). Compaction measurements range from 20 percent (Griggs,1922) for Katmai ash sometime within 10 years after the 1912 Katmai eruption, through about 40-45 percent (Minakami, 1942; Thorarinsson, 1967). The validity of 75 percent compaction for design ashfall has not been determined, but it suggests that a more conservative compaction factor be applied to the WNP-2 site. Applying a 50-60 percent compaction factor to the ash (7.4 cm, 3 in) would result in 14.8-18.5 cm (5.8-7.4 in) of loose ash at the site distance of 224 km (139 mi).

   A consideration that cannot be evaluated at this time in terms of design ashfall is the "distal ash maximum." Ashfall from the May 18, 1980, eruption of Mount St. Helens was greater at Ritzville, Washington, than at some sites closer to the source. Such a distal thickness maximum is not known from the Mount St. Helens Yn ash or other ashfall data. Until more is known about the complex of factors that result in a distal thickness maximum, and how to apply that understanding to design ashfalls, we feel it is appropriate to use the other ash data.

4. **Grain size**.--The estimated grain-size distribution for the WNP-2 site is given by the applicant as 50 percent greater than .075 mm (75

microns) and 50 percent less than .075 mm (FSAR, p. 2.5-103). comparing the applicant's figures with size data from the Mount St. Helens ashfall of May 18, 1980 (Sarna-Wojcicki and others, 1981, fig. 342), the applicant's figures overestimate the amount of ash smaller than .075 mm which would fall at the site, and are therefore conservative.

5. **Ashfall rate**.--The applicant (FSAR, p. 2.5-103) estimates average rate of ashfall as .37 cm/hr (.15 in/hr), which, over a 20-hour ashfall duration, results only in the compacted-ash thickness (7.4 cm, 3 in). A higher ashfall rate must be estimated to result in a conservative thickness of loose ash. Using the uncompacted ash thickness (14.8-18.5 cm) calculated in section 3 above, a 20-hour ashfall duration requires .74-.92 cm/hr (ca .3-.36 in/hr). Allowing for the possibility of slightly higher ashfall rates for a few hours, the Katmai rate of 1.1 cm/hr (.44 in/hr) adds some conservatism.

Safe Shutdown Earthquake

The design safe shutdown earthquake is based on an earthquake assigned to the Rattlesnake-Wallula alinement (the southeast end of CLEW). The assigned intensity VIII (MM) earthquake seems conservative in light of the rarity and lack of continuity of young displacements along this structure. The applicant states that intensity VIII is larger than any known earthquake on the Columbia Plateau and our assessment of the geology gives us no reason to dispute this statement.

Response to Questions

Review of responses to questions 360.20-.25 submitted to the applicant on April 7, 1982, indicate that they have considered the pertinent geological data available and incorporated it into their summary and illustrations satisfactorily. The updated geologic model of the Columbia Plateau presented is a collation of work done by many workers and is reasonable. Figures 361.20-2a, 361.21-1, 361.21-2, and 361.24-1 provide an adequate summary of the geology. The preponderance of seismic events portrayed are at shallow depths and therefore presumably related to identifiable structures. This gives credence to the applicant's approach which attempts to identify and determine age of shallow structure. Some seismicity originates at depths below known structure. Significance of this seismicity must be evaluated mostly from geophysical evidence (see section on seismicity).

In response to question 361.23, the applicant states that a continuous detachment or decollement beneath the entire folded portion of the Columbia Plateau is unlikely. Several logical reasons are given in support of this statement. However, they are not compelling and the paucity of information at depth leaves doubt as to whether a detachment is likely or not. The absence of a seismicity pattern defining its position argues against its capability if it is present.

Conclusion

The applicant has provided through the geologic data gathered and evaluated by their consultants and combined with related existing literature an adequate analysis of the geologic factors relating to the seismic design of the WNP-2 facility.

Seismology

Introduction

The applicant proposes the following vibratory ground motion for the WPPSS Nuclear Project No. 2 site: "A 0.25g vibration level at ground surface in the site area is assigned as the design basis for the Safe Shutdown Earthquake (SSE). This value is consistent with the conservatism previously adopted for design criteria at the Hanford Reservation (AEC, 1972)[1,2,3] and is consistent with the vibratory accelerations associated with an intensity VIII (MM) earthquake (Figure 2.5-60), which is larger than any known earthquake east of the Cascades in Washington or Oregon. This earthquake is assigned to the Rattlesnake-Wallula alignment, the closest tectonic structure of significance to the site. Since no attenuation is taken in the selection of the SSE, this is a conservative approach." For the Operating Basis Earthquake: "An

Operating Basis Earthquake (OBE) equivalent to 0.125g, or one-half of the Safe Shutdown Earthquake (SSE), is used in the design of all Seismic Category I structures. The chosen value for the OBE is based on the largest level of vibratory ground motion expected at the site, as discussed in 2.5.2.4. The design response spectra for the OBE are shown on Figures 3.7-3 and 3.7-4."

The SSE and OBE ground accelerations proposed for the WPPSS Nuclear Project No. 2 are essentially those reported in U.S. Atomic Energy Commission (1972), for the Fast Flux Test Facility.

Our review of the WPPS No. 2 FSAR has concentrated on the pertinent data and interpretations of those data that have become available since the 1972 review. Specifically, we have concentrated on:

1. Seismicity in the site region.

2. Reanalysis of seismicity data and new seismological research on historical earthquakes that might affect evaluation of vibratory ground motion estimated for the site.

3. Determination of vibratory ground motion at the site using both deterministic and probabilistic approaches.

4. Evaluation of reflection and refraction data.

Data and interpretations submitted by the applicant and listed in the references together with technical papers in the geophysical literature deemed significant to the evaluation of the site have been reviewed.

Seismicity

The site is located in an area of moderate historical seismicity to distances of about 90 miles from the site; a radius of 200 miles around the site encompasses most of the seismicity of the Puget Sound region where earthquakes with maximum Modified Mercalli (MM) intensities of up to MM VIII have occurred and are well documented in numerous reports (see, for example, Hopper and others, 1975). Most of the larger shocks of the Puget Sound region are believed to have occurred at depths of about 40-60 km and do not produce significant ground motion at the site nor are they related to the tectonics of the site area.

The degree of completeness of the historical seismic record is a difficult parameter to assess, particularly in a lightly populated area such as Washington State east of the Cascades. The FSAR states on page 2.5-106 that: "Seismicity data within a 200-mile radius of the site are thought to be complete from 1833 to the present for intensity VII (MM) and larger earthquakes. The completeness of the data for intensity VI (MM) and smaller earthquakes improved steadily with population growth from 1833 to 1906." We believe that the applicant's assessment of the completeness of the seismological record particularly within 100 miles of the site is overly optimistic for the following reasons: (1) the region is lightly populated; (2) the instrumental seismograph network was extremely poor prior to the installation of the World-Wide Standardized Seismograph Network (WWSSN) in the early 1960's; and (3) the realization, only over the past 10-12 years, that the December 14, 1872 Washington earthquake was considerably larger than previously estimated. Significant new data on the 1872 earthquake were only uncovered during the past 10-12 years, and these data have been the subject of several intensive studies during that time period. Other significant earthquakes may have been overlooked, particularly during the last century. While the completeness of the historical seismicity catalog in a 200 mile radius of the site cannot be determined with absolute certainty, we believe that the estimates of completeness given in Woodward-Clyde Consultants (1980b), (Table 4) previously submitted by a consultant to the applicant represents a more realistic and certainly more conservative appraisal of the completeness of the historical record.

We believe that the earthquakes of most importance in an evaluation of the vibratory ground motion at the WPPSS Nuclear Project No. 2 site are: (1) the seismicity in the vicinity of the site using data from the several seismograph networks operated near the site from 1969 through 1980; (2) the July 16, 1936 Milton-Freewater, Oregon earthquake (M_s = 5.75; Woodward-Clyde Consultants, 1982); and, (3) the December 14, 1872 Washington earthquake. These topics will be discussed separately.

1. **Seismicity in the vicinity of the site:**

The FSAR contains, in Table 2.5-5, ". . . a listing of all reported earthquakes of intensity III (MM) or greater and for instrumental earthquakes greater than magnitude 3 known to have occurred within 200 miles of the site in Washington through January 1976 and in Oregon through April 1976". Table 2.5-5 of the FSAR was compiled from a number of earthquake catalogs as listed in sect'on 2.5.2.1 of the FSAR. A discussion of the seismicity from 1969-1980 in the vicinity of the site is contained in Woodward-Clyde Consultants (1981a). This reference also contains a discussion of the magnitude detection threshold in the vicintiy of the site (100-150 km), various frequency magnitude relationships, and an estimate of the maximum possible earthquake (not related to a specific structure). The earthquakes located near the site during the time period 1969-1980 are shallow, the deepest shocks having depths of less than about 25 km.

The earthquake monitoring in the vicinity of the site during the period 1969 to 1980 shows a pattern of seismicity common in areas of moderate seismicity with some spatial and time clustering of small events. No definitive alignments of epicenters appear to emerge from the earthquake locations. The rate of occurrence of magnitude (M_c) 3 to 4 events is about the normally expected level of activity for a broad area in Washington State east of the Cascades. The applicant's consultant has estimated the maximum M_c of these earthquakes at 4.0. We believe that on the basis of the historical seismicity in this area, it would be more realistic and conservative to assume the maximum M_c of this "background" seismicity as about 5.0. We further believe that an earthquake of this magnitude will not produce significant ground motion at the site.

2. **The July 16, 1936, Milton-Freewater, Oregon, earthquake**

The July 16, 1936, Milton-Freewater earthquake (M_s = 5 3/4, Woodward-Clyde Consultants, 1982) (called the State line earthquake

Figure F.2-17 WNP-2 vertical force comparison: design required vs possible design outcome 2nd trial

Figure F.2-18 WNP-2 vertical force comparison: design required vs possible design outcome 3rd trial by Neumann, (1938) and Brown, (1937)) poses some special problems relevant to the estimation of vibratory ground motion at the WPPSS Nuclear Project No. 2 site. In the 1972 evaluation of vibratory ground motion for the fast flux reactor on the Hanford Reservation (U.S. Atomic Energy Commmission, 1972), the 1936 earthquake was assigned to the Rattlesnake-Wallula alignment primarily on the basis of the isoseismal map developed for the earthquake (Neumann, 1938).

In a 1980 consultants report to the applicant (Woodward-Clyde Consultants, 1980a) the magnitude of the 1936 earthquake was determined using instrumental data from selected seismograph stations. An M_L magnitude of 6.1 was computed. The report, Woodward-Clyde Consultants, 1982, submitted by the applicant indicates that a M_S = 5 3/4 magnitude was determined for the earthquake by Gutenberg and Richter (1965). Reevaluation of Gutenburg's original data using station corrections that were subsequently developed yielded a magnitude of $M_S = 5.7 \pm 0.3$ (Woodward-Clyde Consultants, 1982). We consider the M_S = 5 3/4 as a more reliable measure of the magnitude of the 1936 earthquake than the M_L magnitude. The M_L magnitude was determined using stations at greater distances than originally intended for the M_L scale and for crustal and mantle structure not specified for the original M_L scale. The relationship of the M_L calculated for the 1936 earthquake to the original M_L scale is open to question.

It is the applicant's position that the 1936 earthquake occurred at a shallow depth on a trace of the Hite fault system. The epicenter given in Woodward-Clyde Consultants (1980a) is 46°12.5'N, 118°14.0'W, about 13 km west of a segment of the Hite fault. The semi-major axis of the 90% confidence ellipse is oriented N89°E and has a length of 16 km; the semi-minor axis of the 90% confidence ellipse is oriented N179°E (actually S01°E) and has a length of 11 km. Because of the size and orientation of the 90% confidence ellipse, there is a question as to whether the earthquake occurred on the Hite fault or on another unknown, more or less north south striking fault closer to the site. The fact that the proposed location is not one for which a fault is known to exist suggests the possibility that unknown faults may be buried near the site beneath the Columbia Plateau basalts and that an earthquake of 1936 type might occur on such a fault. The accuracy of the epicenter of the 1936 earthquake is therefore of considerable importance.

There are several problems with the earthquake relocation as presented in Woodward-Clyde Consultants (1980a). Seismograms for as many North American stations as possible were collected for those stations which reported a first arrival to the International Seismological Summary (ISS) for this event (International Seismological Summary, 1947). It is unfortunate that seismograms were not collected from stations in North America which reported a shear-wave first arrival. A re-examination of such seismograms may very well have allowed the reading of a true first arrival and, even if not, the use of S-waves in locating an earthquake is not only possible but in this particular case it would seem to be desirable.

A second difficulty is that no attempt was made at collecting seismograms for the stations which reported this earthquake from outside North America. The observations as they were reported in the ISS were uncritically used. Apparently, no attempt was made to consult the station bulletins for these stations. If this had been done it would have been noted that the observation for Pulkovo, although specifically tied to this earthquake, was regarded by the seismogram reader as highly suspect. (The parentheses around the arrival time was not copied into the ISS from the station bulletin). The same is true for the S-reading as well. This situation is hardly surprising since the Pulkovo station had a gain of only 1000 in 1936; at a distance of almost 8000 kilometers the signal must have been exceedingly small indeed. The same argument applies to the station Sverdlovsk. The point of this discussion is that with so few P readings both PUL and SVE have very high weights in any hypocentral solution. Very preliminary experimentation by us indicates that if the two Russian observations are dismissed (along with that for Dakar) the epicenter moves south and somewhat east of the location given by the consultants to a position just within the maximum isoseismal as given by Neumann (1937). It also moves the epicenter closer to the Hite fault.

It was not noted in the report that even though 3 Russian observations of this earthquake were reported, there were no European observations at all even though they are in the same distance range. In 1936 it is surprising that none of the large number of high quality stations of relatively high gain in Europe would not report the earthquake. Only a few European stations reported surface waves for this event. Improved locations might have been determined had the consultant obtained either original or high quality microfilms of both Soviet and European stations before including their readings in a location. The Soviet Union has a very high seismicity of its own and these observations may very well be readings from smaller Soviet events that just happened to coincide with the expected readings from this event. It is a fact that this situation occurs far more often than is commonly realized.

Another suspicious characteristic of this data set is that the three Russian stations for which there are observations all knew of this event and were obviously looking for it. (At the present time one does not know whether this applied to Dakar or not, but it should be easy to find out by consulting ORSTOM* in Paris). On this basis, a re-examination of seismograms from many areas including the eastern United States, central and northern South America, and the Far East may very well turn up more readings which might lend accuracy to this epicentral determination.

---

* Office de la Recherche Scientifique et Technique Outre-Mer.

We also note the Jesuit Seismological Association (Hughes, 1982) reported an epicentral position for this earthquake of 46.0^{o}N by 118.1^{o}W which is almost precisely where our own preliminary relocation places it, that is, on the state line near the Hite fault. It should be pointed out that a solution near this position would relieve the applicant of the necessity for long and complex arguments for the instrumental epicenter being far removed from the macroseismic one.

A more complete study of the original seismograms or high quality copies and station bulletins may have resolved this location uncertainty.

The program MEVENT the applicant's consultants used to make the hypocentral determination is a good one that makes use of the method of uniform reduction (Jeffreys, 1961), but some vital information concerning the constants used for weighting each station are not given in Woodward-Clyde Consultants (1980a). The two parameters required are the standard deviation of one observation from a particular station for a particular phase and the ratio of the frequency at the mode and at the flanks of the relationship between frequency of occurrence and residuals of a particular magnitude. Typical magnitudes for these two parameters are about one second for the standard error and about .05 for the second parameter. Unexpectedly enough, these parameters have not changed significantly over the history of instrumental seismology. While it is not entirely clear in Woodward-Clyde Consultants (1980a), it is possible that the standard deviation was determined solely from the estimated timing accuracy of individual stations. If this be true, it is an incorrect application of the theory behind the method of uniform reduction. The method of uniform reduction can, however, be used within the confines of the program MEVENT to successfully deal with a mixture of arrivals from various phases by varying these parameters alluded to above. In essence, later arrivals, typically but not exclusively S, have standard deviations and second parameters larger than those for first arrivals. Consequently, they have lesser but non-zero weights in the normal equations which are formed from them. The effects of the additional arrivals, even with the lesser weights, is that an event observed with multiple phases at only a few stations can be located with considerably more accuracy than with first arrivals alone. No focal depth is given for the 1936 shock in Woodward-Clyde Consultants (1980a), but a subsequent report (Woodward-Clyde Consultants, 1981b) places the depth at about 5 km.

It is not clear that reanalysis of the April 8, 1979 earthquake contributed greatly to our understanding of the seismicity. It was so small that it was recorded on a totally different set of stations thus precluding its use as a master event. The focal parameters given as a solution to this earthquake are also subject to some doubt, most particularly the focal depth. The table of residuals given in the report are typical of a focus which is placed too deep, especially if one considers the two closest observations to be phases different from the first arrivals predicted by the velocity model considered. The velocity model used appears reasonable and it has the advantage of being based on an extensive analysis of actual observations. The 1.75 kilometer depth given in the original solution for the earthquake appears to be reasonable. If the earthquake is as shallow as calculated, the possibility of surface fault rupture cannot be excluded.

The only possible revelance of the 1979 earthquake to the discussion of the 1936 one is the similarity of their focal mechanism solutions, the reason being, of course, that they might very likely lie on the same geological structure. The focal mechanism solution in Woodward-Clyde Consultants (1980a) for the 1936 shock is poorly constrained because of only one observation of a dilatation in the data set. Woodward-Clyde Consultants (1981b) provides a focal mechanism based on surface waves that supports the mechanism given in Woodward-Clyde Consultants (1980a). Again, however, a re-examination of the seismograms not already read could very well be of some use especially if S-motions and S-polarization angles could be observed.

In summary, the association of the 1936 earthquake with a specific structure such as the Hite fault or the Wallula alignment is sufficiently uncertain that the possibility must be considered that a 1936 type earthquake could occur in the vicinity of the site. If this earthquake can be reasonably located on the Hite Fault or the Wallula alignment it will lend support to the thesis that any earthquake of this size must occur on a sizeable fault whose existence is already known. As already outlined, it is possible that additional work on the location of the 1936 event might serve to resolve the problem.

3. <u>The December 14, 1872, Washington earthquake</u>

This earthquake has been extensively studied (for example, Bechtel, 1976; Coombs and others, 1976; Scott, 1976; Woodward-Clyde Consultants, 1976; Weston Geophysical Research, 1976; Algermissen and others, 1977) since it became evident about ten to twelve years ago that the earthquake was larger than previously realized. For example, in <u>Earthquake History of the United States</u>, it was assigned a maximum MM intensity of VI (Coffman and von Hake, 1973).

We have recently reviewed all of the reevaluations of the 1872 earthquake and have also attempted to analyse the available intensity data ourselves (Hopper and others, 1982). In general, our results are in agreement with an earlier report prepared by a U.S. Geological Survey-National Oceanic and Atmospheric Administration Ad Hoc Working Group on Intensities of Historic Earthquakes (Algermissen and others, 1977). This report concludes that: "Based on the reports and documents provided to us by the Washington Public Power Supply System and on independent analyses of Algermissen, Brazee, and Stover, the USGS/NOAA Ad Hoc Working Group on Intensities of Historic Earthquakes has concluded that the intensity of the Washington earthquake of December 14, 1872, was greater than VIII and that it conceivably could be as high as X. We assign intensity IX as the maximum for this earthquake. We have further concluded that the location of the earthquake has not been accurately determined." A point not made clear in this report is that the estimation of a maximum intensity of IX for this earthquake does not depend on the assignment of intensity IX to ground effects. The assignment of high intensity to ground effects was heavily discounted by the committee. The assignment of a probable maximum intensity of IX to the 1872 earthquake was based principally on the areas shaken at each intensity level and the comparison of the areas shaken with areas shaken in other earthquakes for which the maximum intensities and magnitudes were known. In addition, our recent work leads us to the following conclusions:

a. Consideration of all of the interpretations of the intensity data listed above as references together with our own review of the data lead us to believe that the epicenter of the 1872 main shock is located in the vicinity of Lake Chelan. For all of the isoseismal maps considered, the intensity VI isoseismal seems best constrained by the data; the centers of the intensity VI contours for all of the maps considered lie within a radius of 60 km of the point 47.9N^o lat. and 120.3^{o}W long. This circle wholly contains Lake Chelan, the town of Wenatchee and approaches the town of Okanagan.

b. The magnitude of the 1872 earthquake is approximately 7 (M_s) based on the areas shaken at the various intensity levels.

c. There is a strong possibility that the contemporary seismicity in the vicinity of Lake Chelan represents aftershocks of the 1872 event.

These conclusions require that consideration be given to the relationship of this probable magnitude 7 earthquake and its location with regard to the WPPSS Nuclear Project No. 2 site. The question is whether or not an earthquake of magnitude 7 similiar to the 1872 event could occur near or at the site. While it is not possible to prove conclusively that such an earthquake could not occur at the site, we are in general agreement with the rationale presented in the FSAR and other supporting documents that the occurrence of such an earthquake very near the site is unlikely.

We believe that the 1872 event was in the Northern Cascades province, and that there is a natural (but broad) division between a Northern Cascades province and a Middle Cascades province. The boundaries between the Cascades provinces and Columbia Plateau province, though not necessarily coincident with the basalt flows boundary (where the applicant places it) is in most cases close to it. The closest approach of either of the Cascades provinces to the site is about 90 km.

Probabilistic Estimates of Ground Motion at the Site

Two reports have been prepared that estimate the probability of exceedance of the design ground motion at the WPPSS Nuclear Project No. 2 site (Woodward-Clyde Consultants, 1980b; Powers and others, 1981). The earlier of the two reports which was completed in 1980 is a regional type of probabilistic study with earthquake sources modeled to distances of more than 320 km from the site. No background seismicity in the vicinity of the site was modeled and no earthquake sources were considered for distances closer than about 45 km from the site. For an acceleration of 0.25 at the site the annual probability of occurrence estimated in this study is about 3×10^{-5}.

A later probabilistic study completed in 1981 modeled the seismicity as faults, considering structures only within 50 km of the site that contributed significant ground motion at the site. A probability distribution for maximum magnitudes was developed for each fault using a variety of techniques. The annual probability of occurrence of .25g at the site estimated in this study is about 1×10^{-4} (Powers and others, 1981). This ground motion estimate is in general agreement with our regional probabilistic ground motion mapping in this area for rock sites (Algermissen and Perkins, 1976; Perkins and others, 1980).

Maximum Magnitude

Estimation of the maximum magnitude presents a difficulty when only one earthquake with significant damage potential has occurred within 100 km of the site in historic time (the M_s = 5.75, 1936 Milton-Freewater shock). In response to question 360.014 from the Geoscience Branch of NRC, the applicant has estimated total fault length, rupture length and maximum magnitudes for the Wallula fault, the Rattlesnake Mountain fault and the Rattlesnake-Wallula alignment. Using the closest distance of each fault to the site, and the magnitudes associated with the rupture segments, the applicant's consultants attenuated the ground motion from each fault to the site using attenuation curves developed by the consultants. We find the applicant's fault lengths, s egments, and maximum magnitudes reasonable. Using recently published attenuation curves (Campbell, 1981) and the applicant's maximum magnitudes and fault to site distances we found the applicant's estimation of accelerations at the site to be conservative. With regard to the question of maximum magnitude, consultants to the applicant have estimated the moment of the 1936 Milton-Freewater earthquake at 3.6×10^{24} ergs (Joyner and Boore, 1981). We calculate the moment magnitudes of the 1936 earthquake at M = 5.67. Placing the 1936 earthquake on the Rattlesnake Mountain fault at the closest distance of the fault to the site and using the acceleration attenuation curve of Joyner and Boore (1981), we obtain a median peak acceleration of .11g at the site and the 84th percentile acceleration of .20g at the site.

Using the hypothesis that an earthquake of the 1936 Milton-Freewater size (M_s greater than or equal to 5.75) cannot be associated with any known fault system and then moving this earthquake to the vicinity of the site, we estimate as a rough approximation that the probability of exceedence of an earthquake of this size within a radius of 15 km of the site is about 2×10^{-5} per year. This is based on the assumption that the earthquakes in seismic source zones 4 and 5 of Perkins and others (1980) could occur anywhere in these zones. The probability of exceedence is then the area in a 15 km radius around the site divided by the combined area of seismic source zones 4 and 5 in Perkins and others (1980) multiplied by the calculated historical rate of occurrence of earthquakes M_s greater than or equal to 5.75 in the two zones.

In view of the fact that no Holocene or younger faulting has been found in the vicinity of the site (radius of 15 km) and the low estimated probability of occurrence of an earthquake with M_S = 5.75, we find the choice of a M_S = 5.75 earthquake within 15 km of the site to be a conservative estimate of the maximum magnitude earthquake that might affect the site. The applicant was requested by NRC to drill the Southeast anticline structure near the site. We are satisfied that the southeast anticline is not capable at this point based on their new data. However, in refraction and reflection surveys made for the waste disposal program, there are indications that other faults in the basalt may displace sediments at least into the lower Ringold formation. Because these surveys were not designed to investigate near-surface structures in the sediments, the question of capability cannct be resolved without further investigations, such as reprocessing, high-frequency surveys, drilling, etc. If capable faulting is found, re-evaluation of the estimated maximum magnitude earthquake at the site would be required.

Ground Motion at the Site

In response to question 361.17 from the Geosciences Branch of NRC, the applicant has supplied a site dependent response spectrum for a magnitude M_L = 6.1 earthquake occurring near the site by averaging the response spectra computed from accelerograms recorded during earthquakes of magnitude M_L = 6.1 $\pm$ 0.3 within an approximate distance range of 0 to 25 km. The SSE design spectrum envelopes the statistical site-specific response spectra except in the period range of 0.13 to 0.22 seconds. The SSE design spectra provides a slightly improved envelope for the statistical site specific response spectra when the spectra used are weighted such that their contribution to the composite statistical spectra is equal to the probability of a random event occurring at the distance from the site that the spectra were recorded. Placing a magnitude M_L = 6.1 earthquake at a distance of 15 km from the site and using the attenuation curves in Campbell (1981), we calculate a 84 percentile value of acceleration at 0.18g. As a further conservative measure, we assumed that a M_L = 6.1 earthquake might occur not at a distance of 15 km from the site but might occur anywhere within a 15 km radius of the site. We then weighted the accelerations with regard to probability of the M_L = 6.1 earthquake occurring at various distances from the site out to a radius of 15 km from the site. We found the average 84 percentile acceleration to be .28g (using the acceleration attenuation curves of Campbell (1981)). Using an acceleration of .28g as a high frequency anchor for the SSE design spectrum allows the SSE spectrum to completely envelope all of the spectra used by the applicant in the development of a site specific spectrum. However, a spectrum enveloping all of a number of 84 percentile spectra is itself more conservative than an 84 percentile estimate.

<u>Conclusions</u>

On the basis of our review of the documents submitted by the applicant we have concluded that:

1. An estimate of an M_L = 6.1 earthquake within 15 km of the site is a conservative estimate of a maximum magnitude earthquake that might affect the site.

2. The selection of acceleration of 0.25g for the SSE and 0.125 for the OBE are conservative estimates of ground acceleration at the site.

3. The design spectra submitted by the applicant for the SSE and OBE adequately envelops the spectra for earthquakes in the M_L = 6.1 $\pm$ .3 range as submitted by the applicant.

Geology References cited

Bentley, R. D., 1977, Stratigraphy of the Yakima basalts and structural evolution of the Yakima ridges in the western Columbia Plateau, in Brown E. H., ed., Geological excursions in the Pacific Northwest: Geological Society of America, Annual Meeting, Seattle, 1977, p. 339-389.

Bentley, R. D., Anderson, J. L., Campbell, N. P., and Swanson, D. A., 1980, Stratigraphy and structure of the Yakima Indian Reservation, with emphasis on the Columbia River Basalt Group: U.S. Geological Survey Open-File Report 80-200, 83 p.

Campbell, N. P., and and Bentley, R. D., 1980, Late Quaternary faulting, Toppenish Ridge--southcentral Washington: Geological Society of America, Abstracts with Programs, v. 12, no. 3, p. 101.

______ 1981, Late Quaternary deformation of the Toppenish Uplift--a Yakima fold in southeastern Washington: Unpublished manuscript submitted to Geology.

Crandell, D. R., and Mullineaux, D. R., 1978, Potential hazards from future eruptions of Mount St. Helens volcano, Washington: U.S. Geological Survey Bulletin 1383-C, 26 p.

Fox, K. F., Jr., Engebretson, D. C., 1981, Horizontal tectonic stress during the late Cenozoic in the Northwestern United States: U.S. Geological Survey Open-File Report 81-362.

Frizzell, V. A., Jr., and Tabor, R. W., 1977, Stratigraphy of Tertiary arkoses and their included monolithologic fanglomerates and breccias in the Leavenworth fault zone, Central Cascades, Washington: Geological Society of America Abstracts with Programs, v. 9, no. 4, p. 421.

Glass, C. E., 1977, Remote sensing analysis of the Columbia Plateau: Washington Public Power Supply System WNP-1/4, Preliminary Safety Analysis Report, Amendment 23, 19p., Appendix 2RK.

Goff, F. E., and Myers, C. W., 1978, Structural evolution of east Umtanum and Yakima ridges, south-central Washington: Geological Society of America Abstracts with Programs, v. 10, no. 7,p. 408.

Golder Associates, 1981, Geologic structure of Umtanum Ridge--Priest Rapids Dam to Sourdough Canyon: Northwest Energy Services Company, 54 p.

______1982, The southeast anticline fault--Evaluation of attitude and displacement: Washington Public Power Supply System.

Griggs, R. F., 1922, The valley of Ten Thousand Smokes: Washington, D. C., National Geographic Society, 340 p.

Minakami, Takeshi, 1942, The distribution of Mt. Asama pumice in 1783, Part 2 of On distribution of volcanic ejecta: Tokyo University Earthquake Research Institute Bulletin, v. 20, p. 93-105.

Mullineaux, D. R., 1976, Volcanic hazards--Extent and severity of potential tephra hazard interpreted from layer Yn from Mount St. Helens, Washington: Geological Society of America Abstracts with Programs, v. 9, no. 4, p. 472.

Perkins, D. M., Thenhaus, P. C., Hanson, S. L., Ziony, J. J., and Algermissen, S. T., 1980, Probabilistic estimates of maximum seismic horizontal ground motion on rock in the Pacific Northwest and the adjacent outer continental shelf: U.S. Geological Survey Open-File Report 80-471.

Rigby, J. G., and Othberg, K., 1979, Reconnaissance surficial geologic mapping of the Late Cenozoic sediments of the Columbia Basin, Washington: Washington Department of Natural Resources Open-File Report 79-3.

Rockwell Hanford Operations, 1979, Geologic studies of the Columbia Plateau, a status report: Richland, Washington, Report RHO-BWI-ST-4.

Sarna-Wojcicki, A. M., Shipley, Susan, Waitt, R. B., Jr., Dzurisin, Daniel, and Wood, S. H., 1981, Areal distribution, thickness, mass, volume, and grain-size of air-fall ash from the six major eruptions of 1980 in Lipman, P. W., and Mullineaux, D. R., eds., The 1980 Eruptions of Mount St. Helens, Washington: U.S. Geological Survey Professional Paper 1250, p. 577-600.

Shannon and Wilson, Inc., 1979a, Evaluation of faulting in the Warm Springs Canyon area, southeast Washington: Washington Public Power Supply System, 18 p.

______1979b, Geologic reconnaissance of the Wallula Gap, Washington--Blue Mountains--LaGrande, Oregon, region: Washington Public Power Supply System, 63 p.

______1980, Geologic evaluation of selected faults and lineaments, Pasco and Walla Walla Basins, Washington: Washington Public Power Supply System, 25 p.

Tabor, R. W., Waitt, R. B., Jr., Frizzell, V. A., Jr., Swanson, D. A., and Byerly, G. P., in press/a 198_a , Geological map of the Wenatchee 1:100,000 quadrangle, Washington: U.S. Geological Survey Miscellaneous Investigations Map I-1311.

Tabor, R. W., Frizzell, V. A., Jr., Vance, J. A., and Naeser, C. W., in press/b 198_b , Ages and stratigraphy of lower and Middle Tertiary sedimentary and volcanic rocks of the Central Cascades, Washington--Application to the tectonic history of the Straight Creek Fault: Intended formal publication.

Thorarinsson, Sigurdur, 1967, The eruptions of Hekla in historical times, a tephrochronological study, v. 1 of Series on the eruption of Hekla, 1947-48: Reykjavik, Societas Scientiarum, 170 p.

Washington Public Power System, 1977, Preliminary safety analysis report: Nuclear Projects No. 1 and 4, Amendment 23.

______1981, Final safety analysis report: Nuclear Project No. 2, Amendment 18."

Woodward-Clyde Consultants, 1981a, Toppenish Ridge study: Washington Public Power Supply System, 33 p.

______1981b, Logs of trenches at Finley Quarry--Field logs: Washington Public Power Supply System.

______ 1981c, Wallula fault trenching and mapping: Washington Public Power Supply System (draft in preparation).

Seismology References Cited

Algermissen, S. T., and Perkins, D. M., 1976, A probabilistic estimate of maximum acceleration in rock in the contiguous United States: U.S. Geological Survey Open-File Report 76-416, 45 p.

Algermissen, S. T., Brazee, R. J., Stover, C. W., and Pakiser, L. C., 1977, Maximum intensity of the Washington earthquake of December 14, 1872: USGS/NOAA Ad Hoc Working Group on Intensities of Historic Earthquakes, 20 p.

Bechtel, Inc., 1976, December 14, 1872 earthquake: Report prepared for Puget Sound Power & Light, October, 1976.

Brown, B. H., 1937, The state line earthquake at Milton and Walla Walla, Seismological Society of America Bulletin, vol. 27, no. 3.

Campbell, K. W., 1981, Near-source attenuation of peak horizontal acceleration, Bulletin Seismological Society of America, vol. 71, no. 6.

Woodward-Clyde Consultants, 1981a, Analyses of the Instrumental Seismicity of the Columbia Plateau WNP-2 Amendment 18, Appendix 2.5J, Report prepared for Washington Public Power Supply System.

Woodward-Clyde Consultants, 1981b, The July 16, 1936, Walla Walla earthquake, Report prepared for the Washington Public Power Supply System, Contract No. H.O.52028, interim report for task D9.

Woodward-Clyde Consultants, 1982, Review of the magnitude of the July 16, 1936 Walla Walla area earthquake, report prepared for the Washington Public Power Supply System, February, 1982.

DAVID B. SLEMMONS
CONSULTING GEOLOGIST
2995 GOLDEN VALLEY ROAD · RENO, NEVADA 89506 · (702) 972-8877

June 18, 1982

Dr. Robert E. Jackson, Chief
Geosciences Branch
Division of Engineering
U.S. Nuclear Regulatory Commission
Washington, D. C. 20555

Dear Dr. Jackson:

This letter responds to your request of November 6, 1981 that I prepare an independent assessment of geologic and seismologic data to determine fault capability and earthquake parameters for the Washington Public Power Supply System Nuclear Project No. 2. My review includes study of reports, responses to questions, and other types of geological, geophysical, seismological and tectonic data on the regional relationships and seismic design at the site.

Appended to this letter is the report entitled "Fault Capability and Earthquake Parameters for the Washington Public Power Supply System Nuclear Power Project No. 2."

Sincerely yours,

David B. Slemmons

D. Burton Slemmons
Consulting Geologist

CONTENTS

TABLES

FIGURES

1.0 INTRODUCTION

1.1 Purpose of Study

This study was initiated on November 6, 1981 at the request of Dr. Robert E. Jackson, Chief, Geosciences Branch, Division of Engineering, U. S. Nuclear Regulatory Commission. The study provides an independent assessment of maximum credible earthquakes for capable faults near the Washington Public Power Supply System Nuclear Project No. 2, at Hanford, Washington. The report reviews and evaluates geological, seismological, and tectonic data and factors that may be used to estimate maximum credible earthquakes and recurrence intervals affecting the site.

1.2 Scope of Work

My report is based on the information summarized in the applicant's PSAR and FSAR for Nuclear Projects Nos. 1, 2 and 4, and review of publications on the regional and local geological, seismological, and tectonic setting. My previous work in the area included regional remote sensing analysis of the region and aerial reconnaissance of many of the major faults and folds of the area.

The remote sensing and aerial reconnaissance work led to a summary report for the U.S. Corps of Engineers (Slemmons and O'Malley, 1979, revised in 1980), which is entitled "Faults and Earthquake Hazard Evaluation of Five U.S. Corps of Engineers Dams in Southeastern Washington". The Corps of Engineers study included an extensive review of published reports, evaluation of local and regional imagery, and aerial reconnaissance of major faults, folds, and lineaments of the region.

The work for this report included study of reports, responses to questions, other types of geological, geophysical, seismological and tectonic data on the regional relationships and seismic design at the site.

1.3 Terminology and Abbreviations

For clarity and brevity of expression, the following terms are herein defined:

<u>Active fault</u> is a fault that has ruptured during the present seismotectonic regime and is likely to have renewed displacement in the future.

<u>Capable fault</u> is a fault which has exhibited one or more of the following characteristics (U.S. Nuclear Regulatory Commission, 1975):

"(1) Movement at or near the ground surface at least once within the past 35,000 years or movement of a recurring nature within the past 500,000 years.

(2) Macro-seismicity instrumentally determined with records of sufficient precision to demonstrate a direct relationship with the fault.

(3) A structural relationship to a capable fault according to characteristics (1) and (2) of this paragraph such that movement on one could be reasonably expected to be accompanied by movement on the other."

Noncapable fault is an inactive fault that does not exhibit any of the characteristics of the U.S. Nuclear Regulatory Commission (1975) definition for a capable fault.

Maximum earthquake or maximum credible earthquake are defined for this report as the strongest earthquake that is believed to be possible for an active or capable fault, or, alternatively, for a site. These two terms are used synonymously in this report.

CLEW, or the Cle Elum-Wallula Lineament, is the moderately well expressed topographic, and, at least partly, structural feature that extends between Cle Elum on the north, and the southern termination of the Wallula fault, with a total length of about 240 km.

RAW, or Rattlesnake-Wallula Alignment is the southern part of CLEW, and extends from Rattlesnake Hills-Umtanum Ridge to the southern termination of the Wallula fault, with a total length of between 115 and 140 km (fig. 1).

WCC is an abbreviation for Woodward-Clyde Consultants.

WPPSS is an abbreviation for Washington Public Power Supply System.

2.0 SEISMOLOGIC SETTING

2.1 General Statement

The Columbia Plateau and adjoining provinces are within a region of low seismic energy release (Ryall and others, 1965) and scattered, low magnitude earthquakes (Smith, 1978). There is no pattern or correlation between the geologic structures, faults and folds, and the earthquake epicentral locations or swarm distributions. Both CLEW and RAW have a lack of historic seismicity. The regional seismographic coverage is better in the Columbia Plateau than for most other parts of western United States, and detection levels in recent years have been expanded down to about magnitude 1 or 2.

2.2 Seismicity

The lack of correlation between zones or patterns of seismicity and regional geologic structures is suggested in recent seismicity maps (WPPSS, PSAR, Amendment No. 23, Figure 2.5J-8, 1977). The strongest earthquake within the Columbia Plateau was the July 15, 1936 earthquake near Milton-Freewater, Oregon, with a MS = 5.75 (Gutenberg and Richter, 1954). This earthquake appears to be the only moderate size historic earthquake that may be associated with major faults in or near the Columbia Plateau. This earthquake was near the south end of the RAW zone and the complex pattern of faults of the Hite fault system. The available data do not resolve assignment of this earthquake to the RAW alignment (southern portion of CLEW), the system of faults in the western portion of the Hite fault zone (Glass, 1977) or an undefined structure.

Most of the recorded earthquakes in the Columbia Plateau have shallow focal depths (up to 30 km) and some pattern of seasonal seismicity that may be controlled by precipitation or irrigation in mid-summer and winter seasons. Some of these small earthquakes are not in areas of heavy irrigation, or occur during other seasons. The focal mechanisms for earthquakes of this region are known for only a few events and support a general north-south compression axis (WPPSS, FSAR, Appendix 2.5J, 1981a).

3.0 TECTONIC SETTING

3.1 Structural Setting

This region has been the focus of many geological, geophysical, seismological, and tectonic studies for a variety of public and private organizations. These include extensive studies by WPPSS, Puget Sound Power and Light Company, the U.S. Geological Survey, Rockwell International, several universities and many consulting firms.

These various studies suggest the deformation may include extensive, thin-skinned type of folding, with various combinations of faulting, including strike-slip and reverse-slip mechanisms. The tectonics of these structures have not been resolved, as has been summarized by WCC (in WPPSS, FSAR, Appendix 2.5K, 1981a). The main zone of deformation, CLEW and/or RAW, can be explained by either a right-lateral, strike-slip model (Laubscher, in WPPSS, FSAR, Appendix 1.5-0, 1981 , and Davis in WPPSS, Appendix 2.5N, 1981) or by a fold model with north-south crustal shortening required without a through-going strike-slip fault system (Price, 1981; Rockwell Hanford Operations, 1979). Both of these models are considered by the author to be viable alternatives explaining the tectonic process of this region.

The region appears to have no active fault connections to the north. There does appear to be possible connections southward into the Basin and Range Province of Oregon, but such connections appear to be at least partly diffuse. The known major structures, such as the graben at Grande Ronde Valley, have very low rates of activity and appear to be in a waning stage of tectonic deformation.

3.2 Timing and Rate of Deformation

The applicant has established several lines of evidence that suggest the main regional deformation occurred during the Miocene and Pliocene. The more intense deformation occurred after Elephant Mountain deposition (10.5 mybp) with the most intense deformation about 8 mybp to 3.5 mybp. The evidence for continued late Quaternary faulting is based on features that are generally suggestive or non-definitive. This evidence includes the possible assignment of earthquake epicenters to the southern portion of RAW, geomorphic evidence for recent fault activity southeast of Wallula Gap, and permissive evidence for Pleistocene fault activity near Finley Quarry, Yellepit, and Warm Springs

(Slemmons and O'Malley, 1980). Geodetic data indicate that deformation in the area has either stopped or is continuing at a low rate (Savage and others, 1981). My observations include the weakly-active Grande Ronde Valley, with only one short fault segment with evidence for late Quaternary offset of a calcium carbonate bearing soil, of probably pre-Wisconsin age (pre-70,000 bp, Slemmons and O'Malley, 1980).

3.3 Assessment of Structural Setting

My assessment is similar to that of the applicant and consultants to the applicant. The evidence indicates that CLEW is either an older Tertiary structure or is a deeper structure that currently has no shallow activity or capability as a shallow fault zone. RAW is assessed as an active structure in the Wallula fault zone and the structure should be assumed to be capable along the northern part of RAW. The applicant and consultants to the applicant differ in opinion as to whether RAW is a right-slip fault zone (WPPSS, FSAR, Appendices, 2.5, 2.5N, and 2.5-O, 1981a) or is a reverse-oblique-slip or reverse-slip fault zone (WPPSS, FSAR, Appendix 2.5K, 1981a). I consider both as viable theories, but favor a right-oblique-slip fault zone for RAW, with a very low rate of activity during the late Quaternary.

This report uses three models for RAW:

(1) The strike-slip model and a 7.5 to 20 km tectonic rooting of the fault into the basement with a low to moderate seismogenic character.

(2) The reverse-slip or right-oblique-slip model and a 7.5 to 20 km tectonic rooting of the fault into the basement with a low to moderate seismogenic character, and

(3) The detachment faulting model for the brachydomes with a non-seismogenic, or weakly seismogenic character.

4.0 DETERMINATION OF MAXIMUM CREDIBLE EARTHQUAKE MAGNITUDE

4.1 General Statement

The following five methods may be used to estimate maximum earthquakes for capable faults and fault zones:

(1) Maximum historic eqrthquake method
(2) Paleoseismicity method
(3) Fractional fault rupture length method
(4) Total fault length method
(5) Fault slip rate method

Methods (1), (2) and (3) have been used for assessing all types of faults: strike-slip, reverse-slip, normal-slip, and combination-slip (Slemmons 1982, 1983; Slemmons and Chung, 1982; Slemmons and others, 1982). These methods use the relations of earthquake magnitude to fault parameters shown in Tables

1 to 4 and Figures 2 to 7. Methods (4) and (5) have only been used for strike-slip faults (Slemmons, 1982, 1983) and use the relationships shown in Table 5 and Figs. 8 and 9. Their applicability to reverse, and reverse-oblique faults is uncertain. The data base for use with these methods will be presented in this section with indications of limitations in applicability for various slip type, slip-rate and structural settings.

4.2 Maximum Historic Earthquake Method

The maximum historic earthquake method assumes that the largest historical earthquake on a fault, along a fault segment, or in a seismic zone or region, is the maximum credible earthquake for the structure or area. This method provides reasonable values for those structures with a high magnitude historical event, for faults with very high slip or strain rates, for regions with very long historical and seismological records, and for a few fortuitous cases where the observational record includes the characteristic or representative earthquake of an earthquake cycle. Many earthquakes that have magnitudes of more than 6.5 and associated surface faulting may either be maximum events or approach the maximum earthquake magnitudes, but many, perhaps most, do not. This method would be ideal for structures with very long observational periods, exceeding the recurrence interval for the fault (which may exceed 100,000 years for faults with low slip rates). This is generally not the case, so the method has limited applications in most regions of active faulting, and is inappropriate for the low slip-rate faults in the Columbia Plateau.

4.3 Paleoseismicity Method

This method was developed by Wallace (1978) for normal-slip faults of the central Nevada region of the Basin and Range Province. By photogeological and field methods, fault scarps are mapped, and the rupture length and maximum displacement from prehistoric earthquakes are determined. Using seismic moment and the empirical regressions for earthquake magnitude, maximum surface displacement, and associated surface faulting rupture length, the magnitude of the paleoseismic events is estimated. The advantage of this method is when the recurrence interval is greater than the historic record. This method has been applied to all fault slip-types and is applicable in areas where fault scarps are preserved, or where abundant soil-stratigraphic and stratigraphic data are available, but is inappropriate for the Columbia Plateau, where data is lacking, except Gable Mountain.

4.4 Fractional Fault Rupture Length Method

This method was proposed by Albee and Smith (1966) for faults of the southern California region. They noted that surface faulting from larger earthquakes in the area ruptured between one-fifth and one-half of the known mapped length of the faults affected. This method has been widely accepted and used with various fractional rupture lengths, depending on the degree of conservatism required. This method applies to all fault slip types, although the original application was for a region of mainly strike-slip faulting.

Slemmons (1982), Slemmons and Chung (1982), and Slemmons and others (1982) refined the method for strike-slip faults by tabulating and regressing the relations for 9 strike-slip faults that were sources for earthquakes of above 6 magnitude. These data are revised and shown in Table 5 and Figure 8. This method is appropriate for models of strike-slip faulting in the Columbia Plateau. The applicability to reverse-slip or reverse-oblique-slip models, based on the original work of Albee and Smith (1966), is less secure, but may be appropriate.

4.5 Total Fault Length Method

The data of Slemmons (1982, 1983), Slemmons and Chung (1982), and Slemmons and others (1982) for the 9 strike-slip faults with earthquakes of above 6 magnitude, as revised in Table 5 and Figure 9, suggest a relationship between earthquake magnitude and the total fault length of strike-slip faults. The data are for faults with slip rates that are generally measured at more than 1 mm/yr, and with total lengths greater than 280 km. The application to other fault-types, to faults with total lengths less than about 100 to 200 km, or to lower slip rates should be used with caution, but may be applicable in the Columbia Plateau.

4.6 Fault Slip Rate Method

This method originally was proposed by Woodward-Clyde Consultants for the San Onofre docket in 1979 and was refined by the WCC (1980a) response to question 361.38 (fig. 10). No data are used for slip rates less than 0.1 mm/yr and only two data points are available for slip rates less than 1 mm/yr, but the method may be applicable to the low-slip rate structures in the Columbia Plateau. The data may be checked by use of Table 1 and Figure 11.

5.0 FAULT SEGMENTATION

The probability that faults are segmented is shown by the basic assumptions and methods of WCC (1982b) report for WPPSS NRP No. 2.

The theory that potential surface fault ruptures occur along specific segments or sections of faults is not well developed. There is a tendency for many historical surface ruptures to terminate at the intersection with cross-cutting faults, at the junction of two branching faults, at irregularities of surface pattern, at points of en echelon step overs, and at geophysical, geometrical or thermal anomalies in pattern. Termination may be related to asperities on a fault plane, although many large earthquakes are multiple earthquakes that are thought to occur when rupturing breaks through an asperity, perhaps with a pause or change in the character or rate of the rupturing process.

The use of changes in fold relations for segmentation, such as en echelon or chain of folds, may be unwarranted. These features are likely to be secondary to the primary rupture process as shown in the limited amount of possible faulting from the 1933 Long Beach earthquake (Guptill and Heath, 1981), and the apparent lack of correlation of the 30 km of aftershocks with the known distribution of wrench fault anticlines (Woodward-Clyde Consultants, 1979).

The seismological and geological aspects of the surface faulting associated with strike-slip faults are limited in present applications. The best set of definitions and discussion is by Woodward Clyde Consultants (1982c). The present weak data are provided by the above reference, Segall and Pollard (1980), Bakun and others (1980), Reasenberg and Ellsworth (in press) and other workers.

The question of the use of the full segment length, or a fractional segment length when determining magnitude values has not been resolved. The use of full segment lengths in formulations of Table 5 and Figure 9 is more conservative, but there is no known rationale for the assignment of a potential full segment rupture length, a half segment length, or some smaller fractional length. The use of one-half length is customary for analyses, but there is no presently available justification for this use. More than a full segment length appears to have been involved during the 1857 right-slip event on the San Andreas, with inconsistent amounts of displacement noted on several sections of the San Andreas and the possible inducing of the earthquake by prior movement near Parkfield and/or Cholame by a lower magnitude earthquake and movement on a different segment. This makes the use of segments a difficult process for the San Andreas fault.

The data of Table 5 and Figure 8 suggest that major, strike-slip movement involves an average segmentation of less than 20 percent of the entire fault length for strike-slip faults of less than 300 km length, to almost 40 percent of the total fault length for faults of about 1300 km length. This agrees well with an earlier data compilation (Slemmons, 1980). Less is known for faults of minor character, for lengths of less than 300 km, and for faults of normal-slip, reverse-slip or combination-slip character. The application of these segmentation methods is uncertain for the RAW structure of about 120 km length.

The following comments should be made for faults of different character than the strike-slip faults that are summarized in Table 5 and Figures 8 and 9.

(1) The normal-slip to normal-oblique-slip faults of 1954 faulting in Nevada affect several faults across the grain of several horsts and grabens with uncertain segmentation. Apparently several segments were involved in the rupture process.

(2) Segmentation of the reverse-slip fault responsible for the 1952 California event is uncertain, although it appears that about one-third of the total fault length was affected by the earthquake of about Ms = 7.6.

(3) The segmentation of the 1971 reverse-slip and reverse-oblique-slip faulting in the Transverse ranges of California was over about 15 km of a zone that is between 120 and 210 km long. This is less than 12.5 percent fractional rupture length for the entire fault zone.

6.0 SEISMIC POTENTIAL AND FAULT RUPTURE PARAMETERS OF CAPABLE AND INFERRED CAPABLE FAULTS

6.1 General Statement

This report describes evidence for, or suggestive of, capability for each of the major fault zones that could affect WPPSS Nuclear Power Project No. 2 and recommends maximum credible deterministic magnitudes for the site. Use of any single method of estimation has important uncertainties but the overall evaluation provides values that are believed to be conservatively obtained and reasonable. The determination of the maximum credible magnitude is considered to be accurate within one or two tenths of a magnitude and be conservatively established.

6.2 CLEW, the Cle Elum-Wallula Lineament

The CLEW lineament appeared to be capable for the 115 to 120 km segment along the southern part (RAW) and was poorly defined and considered noncapable in the northern 120 km from Cle Elum to the north end of RAW. The evidence for capability, or inferred capability, of all parts of this zone includes the following:

(1) The original evaluation of OWL, the Olympic Wallula Lineament, of E. Raisz (1945), indicates that a topographic lineament between the Olympic Mountains on the northeast and along the Blue Mountains to the southeast may be a continuous feature.

(2) The Wenas Valley features are shown as faults on the maps of Glass (1977) and have possible Holocene fault scarps from normal faulting along the northwest-trending structures that are coincident with CLEW.

(3) The northern termination of the eastern Moxee Valley fault appears to be a left-slip fault that terminates against CLEW and is parallel to the capable-appearing structures of the northwestern zone of fissuring.

(4) CLEW is parallel to, and coincident with, offsets of the Hite fault and youthful, small-scale faults such as the features at Buroker, offsets of the Ringold Formation gravels (Foundation Sciences, Inc., 1980; Keinle and others, 1977) at various locations between Finley Quarry and the Hite fault system.

(5) The capability of the Hite fault system is uncertain. The seismicity report of WCC (1980b) suggests that the 1936 earthquake was on a fault of the Hite fault system. The work of Foundation Sciences Associates (1980) suggest that this fault zone may be dead or noncapable and that the RAW zone may be younger.

(6) There is uncertainty regarding location of the 1936 earthquake and its aftershocks with the main shock being either on RAW or possibly on or near faults of the Hite fault system.

The original evidence against the first three factors includes the following:

(1) Topographic features of the Oregon-Washington Lineament (OWL) structure are not shown as conspicuous features on the recent 1:24,000 scale maps and do not show evidence for capability (Glass and Slemmons, 1978; Slemmons, 1977). Aerial examination and reconnaissance was conducted with fixed wing aircraft and helicopter along the general trend of OWL near Cle Elum, to the northwest in the Cascade range, on the projection of OWL within the Blue Mountains, and to the southeast on the OWL trend. This aerial reconnaissance showed no evidence for activity and geomorphic expression southeast of the Hite fault system.

(2) The Wenas Valley faults shown on the maps of Glass (1977) were interpreted by him to be northwest-trending faults of 25 km length that appeared to have normal-slip scarps of late Quaternary to Holocene age. Scarps up to 1½ to 2 m in height developed in late Pleistocene to Holocene materials or surfaces, with the most conspicuous development opposite the gravity slides. The extension direction suggested by the scarps is not compatible with the apparent compression of most of the fault plane solutions, by the geodetic data, and the orientation of folds in the area. The general location of the scarps, the results of the photo interpretation, and the field study of scarps is described by Woodward-Clyde Consultants (field guide of April 13, 1982). Based on both field and aerial photograph interpretation, their conclusions are that (a) the scarps are probably the result of landsliding of the Ellensburg Formation, and (b) anomalous, or changed tectonic activity is not precluded for the less than 10 km length of the zone.

(3) The Moxee feature is interpreted by Glass (1977) as a possible Holocene scarp, based on photogeological interpretation and aerial reconnaissance, with a western branch of possible gravitational-spreading origin, about 20 km in length, and an eastern left-slip branch of about 25 km length. This fault was evaluated by Woodward-Clyde Consultants (field trip guide, April 13, 1982) by both field and photogeological methods. Their interpretation is that the western zone is formed mainly by conjugate joint sets with no evidence for Holocene or Pleistocene activity. They further conclude that the eastern branch of Moxee Valley fault is about 10 km in length and represents a fault of minor right-slip faulting of mainly Miocene age. They observed no definitive or suggestive evidence for Holocene or Pleistocene activity. Their interpretation is for up to 60 m of vertical separation and about 300 m of right-lateral separation of Miocene or earlier age.

I spent one day in the field and studied three sets of aerial photographs of the site (including synoptic U-2 black and white area photographs of the entire region, detailed ektachrome aerial photographs of most of the area at a moderate scale, and excellent low-sun angle black and white aerial photographs at a scale of about 1:18,000). I conclude that the scarp is controlled by gravitational effects. The following evidence leads me to these conclusions: (1) the most conspicuous development of scarps is within the moderately to steeply dipping beds, (2) the scarps are only developed opposite the landslide area, and (3) there is an anomalous relation between the earthquake magnitude based on the maximum displacement, $Ms = 6.67 + 0.75 \log 2 = 6.90$, and that based on rupture length of paleoseismic events, $Ms = 0.85 + 1.33 \log 9{,}000 = 6.11$, or an average $Ms = 6.5$. This is assigned a low probability of being a paleoseismic event and is not believed by me to define CLEW.

My conclusions are as follows:

(1) The lineaments of the western branch of Moxee Valley are joint- and fault-controlled and there is no evidence for capability.

(2) The lineaments of the eastern branch of the Moxee Valley fault system are controlled by basement faults with mainly strike-slip offset, and there is no evidence for capability.

(3) No evidence for paleoseismic events is inferred on either branch of the Moxee Valley zones by Woodward-Clyde Consultants (WCC, 1982a) and there is no evidence for activity established by my photogeological work.

(4) The evidence of Davis (1977 and 1981) shows that if the northern CLEW exists it is a deep structure with no apparent activity. The lack of shallow activity is indicated by the lack of seismicity, the lack of geological continuity, the orientation of folds across the inferred lineament, and the lack of geophysical continuity of the structure (based on gravity and aeromagnetic data).

(5) The gravity residuals and their derivative values are not offset horizontally by the CLEW feature.

6.3 RAW, the Rattlesnake-Wallula Alignment

6.3.1 General Statement

The RAW alignment is the NW - SE trending structural zone that extends from the area near the northeastern bend of Rattlesnake Hills, a series of brachydomes of the Wallula fault zone (or CLEW zone, Slemmons and O'Malley, 1980), to near the southeast end of Wallula fault zone near truncating faults of the Hite fault system in the Milton-Freewater area.

The escarpments near the 900 ft elevation on the northeast slope of Rattlesnake Hills appeared to be active or capable fault scarps of post-Touchet age (figs. 12 and 13). These lineaments were observed from the air during December, 1981 and during a field trip of April 12, 1982. However, inspection of their features and the trench logs of WCC (April 12, 1982) showed that there is no tectonic deformation of the Touchet sediments.

The seismicity of RAW is low and ill-defined. Because of the low seismic rate of activity there is disagreement regarding the continuity, fault slip rate, recurrence interval, fault slip type, segmentation, total surface length of the seismogenic structure, and the maximum credible earthquake for the zone. Following is a review of these parameters with comments and recommendations regarding the required deterministic analyses for this structure.

6.3.2 Fault Continuity

The RAW structure is divided into sections (or segments) according to interpretations of its relationships to adjoining features. There is little definitive evidence provided by the seismological studies, since there is little seismic activity associated with the zone, poor definition of the zone, and no consistent pattern of focal mechanisms. A 1936 earthquake of between Ms = 5.75 (Gutenberg and Richter, 1945) and M_L = 6.1 (Woodward-Clyde Consultants, 1977, 1982b) has its epicenter near or on RAW, but the exact location of the epicenter has been assigned to various locations between Milton-Freewater, Oregon, the area of the junction of RAW and the nearest faults of the northeasterly Hite fault system, and the Hite fault system near Waitsburg, Washington.

Gravity data show little definition of the structure, except for a weak depression of the Pasco Basin (Weston Geophysical Research, Inc., October, 1977, in Appendix 2R E of the FSAR, 1981). There is no noticeable strike-slip offset of gravity defined features along RAW. The aeromagnetic definition of the structure is also ambiguous, with anomalies generally resulting from topographic features, paleomagnetic reversals in the basaltic stratigraphy, and the distribution of local faults and dikes. The pattern changes from northwest of Wallula Gap, with well-defined brachydomes, to the southeast with possible dikes and en echelon faults of the Milton-Freewater area and the Hite fault system. The definition of a structure and its continuity along a narrow zone from the northern end of Rattlesnake Hills to Milton-Freewater is a judgemental assessment, but the geologic implications and the possible segmentation of this structure are debatable at this time.

The length of this feature is from the northeast corner of Rattlesnake Hills to a point south of Milton-Freewater. 115 km is used by the applicant (Woodward-Clyde Consultants, 1981b) and 120 km by the U.S. Nuclear Regulatory Commission. The latter length will be used for this computation, although the results from either value are very similar. The only similar deterministic analogs are calculated for the Offshore Zone of Deformation and other faults near the San Onofre Nuclear Reactor Site and the Calaveras and Hayward fault zones (Slemmons 1982, 1983) and are for major active faults at major active plate boundaries with slip rates that are above 0.5 mm/yr. Accordingly, the results of this evaluation of maximum credible earthquake for lengths of 115 and 120 km are considered to be very conservative based on the shorter length and the lower slip rate of RAW and the internal tectonic nature of this zone. Based on the data for Table 3, the following linear regression is obtained for the total fault length method, which assumes activity along the entire zone of 115 to 120 km length and assumes the method will apply to faults of less than 280 km length: for the maximum credible earthquake:

Ms = 6.618 + 0.0012 x L (in km) = 6.78 for both lengths (115 km and 120 km).

The results of this evaluation lead to the following:

(1) The length used for the RAW zone may be excessive at 115 to 120 km.

(2) The structure may not be seismogenic. The lineaments of the 900 ft elevation of Rattlesnake Hills are not of tectonic origin (figs. 12 and 13).

(3) The relations may be difficult to apply due to reverse-oblique rather than mainly strike-slip character.

(4) The faults of the RAW zone are intraplate in character, rather than at or near a major earth plate boundary.

(5) The apparent rate of slip of RAW is less than 0.2 mm/yr and the equation is developed from faults of above 0.5 mm/yr slip rate.

(6) The equation is developed from the 9 faults in the world that had highest magnitudes.

(7) The minimum value for a fault of 0 length, a "floating" or earthquake of random location, is 6.62, a value that appears to be too high.

The above results are regarded by me to be overly conservative and lead to a magnitude value which may be too high.

For a fractional segmentation using the methods of Slemmons and Chung (1982), the data for strike-slip faults leads to the following estimate of rupture:

Pr (Percentage of fault rupture) = 15.76 + 0.012 x L (in km) = 17.2% of total length for the 120 km length estimate of RAW, or about 20 km rupture length.

This appears to be similar to the result of about 15 km segments obtained by Tom Rockwell (written communication, 1982) for the 120 km (length of the Sierra Madre-Cucamonga fault zone of California, a zone of similar compressive tectonic activity. For 15 km segments the fault zone provides the following estimates of magnitude, using linear regression relationships of Slemmons and others (1982).

$M_s = 1.404 + 1.169 \log L$ (in m) = 6.29 for 15 km rupture length (strike-slip faults).

$M_s = 1.199 + 1.271 \log L$ (in m) = 6.51 for 15 km rupture length (reverse-oblique-slip faults).

For 20 km segments of the fault zone, the following are the estimates of magnitude:

$M_s = 1.404 + 1.169 \log L$ (in m) = 6.43 (for strike-slip faults).

$M_s = 1.199 + 1.271 \log L$ (in m) = 6.68 (for reverse-oblique-slip faults).

6.3.3 Fault Slip Rate

The data for RAW have been summarized by the applicant (WPPSS, 1977; 1981) assuming a N-S compression based on the models of Bentley and others (1980) and Laubscher (1981). The lack of strike-slip offsets of the gravity lines, with less than 3 km of offset being discernable, provides an upper bound value for probable estimates of the strike-slip offset. Woodward-Clyde Consultants (1982d) have estimated an upper bound value of 0.2 mm/yr for RAW. This value appears greater than that of Slemmons and O'Malley (1980) assuming an age of 128,000 years and a dip of 60°W for the fault in La Grande graben, although the continuity for a connection between the La Grande graben and RAW is not established. The value from the La Grande graben gives about 0.014 mm/yr slip rate. With strike-slip models for RAW, and using the fault slip rate data of Woodward-Clyde Consultants (1979 and 1980a) the best fit of the data for a fault slip rate on strike-slip faults of 0.1 mm/yr is Ms = 5.3 from the line bounding the maximum observed historical earthquakes (HEL) or about Ms = 6.1 for the synthetic earthquake limit (SEL) and about Ms = 5.8 and 6.4, respectively, for a slip rate of 0.2 mm/yr. Similar relationships have not been established for reverse-oblique or reverse-slip faults.

6.3.4 Recurrence Interval

The recurrence interval, or time between small to moderate earthquakes is very long. There is sparse evidence for Holocene surface offsets in any part of the RAW alignment. The evidence from Finley Quarry and the Warm Springs trenches of the Wallula fault suggests that there has been no significant displacement for a period from 70,000 to 200,000 years. The writer made an estimate of the activity based on the assumption of earthquakes along RAW with a recurrence interval of slightly greater than 13,000 years, and one-fifth surface rupture length, which suggests an average recurrence interval of at least 50,000 years. This is based on the relationships of Figure 11 that a magnitude 6.5 earthquake with an average slip rate of less than 0.01 (0.014) mm/yr, which is very low and similar to that of the La Grande graben. This suggests that the average recurrence interval is at least between 10,000 and 100,000 years for Ms = 6.5 events. This corresponds to an 0.8 m surface offset and surface rupture length of 20 km. Accordingly, the value of the maximum credible earthquake of Ms = 6.5 appears to be conservative.

6.3.5 Fault Slip Type

The fault-slip type of RAW is not clearly established, but the definition of slip-type has evolved from purely strike-slip (right-slip) fault mechanisms proposed in most of the earlier discussions of tectonics or mechanisms (Davis, 1977; Laubscher, 1977, 1981) to increased emphasis on right-oblique or reverse-slip mechanisms in recent publications (Davis, 1981, Woodward-Clyde Consultants, 1981b). The seismological data are erratic, although there is a tendency for a general north-south compression axis, particularly over the plateau region. The orientation of the CLEW-RAW structure is about N 60°E, which suggests that the main fault zone may include right-oblique-slip components, although as noted, there is less than 3 km right-slip separation at the northeast end of Rattlesnake Mountains as indicated by the gravity gradients. The amount of monoclinal separation is small, as evidenced in the area to the northwest of Richland, at the Yakima crossing of the Cold Creek lineament, but increases to the southeast along the Wallula fault zone, where a low monocline forms the northern boundary along the northern edge of Horse Heaven Hills. This relationship is shown by the weak development of the Pasco Basin as is indicated by the gravity map and by cross sections (Rockwell Hanford Operations, 1979). The Warm Springs and Finley Quarry trenches (Woodward-Clyde Consultants, 1981a) have many fault striations that include horizontal or oblique-slip orientations, which may indicate combinations of strike-slip, oblique-slip, and either normal- or reverse-slip components. This issue has not been resolved and both right-slip and right-reverse-oblique-slip models are considered for the RAW structure.

6.3.6 Segmentation

The problem of segmentation of RAW, particularly northwest of Wallula Gap, is present in the record. If either earthquake magnitude or moment magnitude is used to estimate the size of potential earthquakes for RAW, the most important element of analysis is the segmentation that should be used for RAW. Experience with wrench fault tectonics (summarized in Woodward-Clyde Consultants, 1979 and 1980 for the Newport-Inglewood zone of earthquakes in 1933). The present record does not indicate that the surficial or secondary anticlines have much effect on the primary faulting and aftershock activity. For wrench fault tectonics, and a purely strike-slip model, it would appear that the distribution of brachydomes would have little effect on the analysis of earthquake segmentation along RAW. Conversely, if reverse-oblique, or reverse mechanisms apply to RAW, then the distribution of the nearly parallel orientation of axes of brachydomes may have a primary control that could affect the segmentation of the zone. With the latter case, the general assumptions of the applicant's case and the Woodward-Clyde Consultants (1981b) analysis is a reasonable interpretation and the results of the WCC exposure analysis are generally valid. This type of analysis is difficult to apply to RAW and the present data do not clearly resolve the size of strike-slip components at the structure. This creates difficulty in verifying the amount of segmentation proposed by the applicant and in using all aspects of the seismic exposure study. However, the empirical data from plate boundary faults of strike-slip zones suggest that some type of segmentation applies and it is likely that the segmentation of structures of 120 km length should have segments of about 20 km in length. With the present data, I believe that there is no segmentation process that can be used directly or quantitatively using either moment magnitudes or earthquake magnitudes.

6.4 Wallula Fault

The Wallula fault is in the southern section of RAW and is considered to be capable by evidence described in Section 6.3. This fault zone has geomorphic evidence for a fault origin and for capability. The maximum earthquake was estimated by Slemmons and O'Malley (1980) at Ms = 6.3 to 6.8. This estimate was based on aerial reconnaissance of the en echelon branches of the Wallula fault, the scarps along Warm Springs Canyon, lineaments in Vansycle Canyon, faceted spurs near Wallula Gap, and the permissive evidence for activity during the late Pleistocene at Yellepit. The evidence obtained during December 1981, reconfirmed my earlier impression, by showing suggestive evidence for capability at VanSycle Canyon (fig. 13), near Warm Springs Valley (figs. 14 and 15), and at the escarpment 3 miles south of Umapine, Oregon (fig. 16), although the evidence is not definitive (WCC, 1981 and WPPSS, 1981). This magnitude value is based on a fault half-length of 40 km in a segment between the area south of Umapine to Yellepit.

The maximum credible earthquakes for this paper are estimated from the total fault length, for a fault slip estimated at 0.1 mm/yr, and for a fractional fault percentage. The estimates of maximum credible earthquakes for the Wallula fault are as follows:

> Ms = 6.618 + 0.0012 x L = 6.76 based on fault length of 120 km, which may be overly conservative,
>
> Ms = 5.3 for the HEL or 6.1 for the SEL of WCC (1980),
>
> Ms = 1.404 + 1.169 log L (in m) = 6.35 for a strike-slip mechanism,
>
> Ms = 1.199 + 1.271 log L (in m) = 6.69 for reverse-oblique-slip mechanism.

The fault is capable between Wallula Gap and near Milton-Freewater, and the maximum credible earthquake is Ms = 6. to 6.5. For conversatism, this earthquake value is assumed to be representative of all of the RAW alignment, including the northern part of RAW as well as the suggested activity shown in Figures 14, 15, and 16.

6.5 Cold Creek and Kennewick Lineaments

The Cold Creek and Kennewick lineaments were studied by the author from aerial reconnaissance flights, field study, diamond drill cores, and evaluation of reports for WPPSS. Aerial reconnaissance indicated that the Cold Creek and Kennewick lineaments appeared to be separate and the latter is more active in appearance. Field study of the two features indicates that the Cold Creek lineament showed no offset of basaltic units along the Yakima River and from the drill cores at the bridge across the Columbia River northeast of Richland. The field relations and the report of WPPSS in the FSAR, Appendix 18 (1981) indicate that the feature may be controlled by deposition and erosion during the Missoula floods.

The geologic studies by WCC of the Kennewick lineament (WPPSS, FSAR, Appendix 18, 1981) show that there is less than 100 feet of offset across the Kennewick lineament. Deposits on the south of the lineament are old with extensive caliche and underlie pre-Missoula deposits. They show no sign of tectonic deformation at the lineament. Although this feature is geomorphically sharp, controls the distribution of springs, and is parallel to RAW, it is considered to be an erosional feature of the Missoula flood. I conclude that the Cold Creek and Kennwick lineaments are depositional - erosional effects of the Missoula flood. These features are of non-tectonic origin and are not assigned a maximum credible earthquake value.

6.6 Central Fault of Gable Mountain

The Central Fault of Gable Mountain was examined in the field. Evidence for capability includes a 340 m near surface rupture length with a maximum offset of about 0.06 m in deposits of the Missoula flood. The estimated age of these Pleistocene deposits is 13,000 to 19,000 years before present. There are clastic intrusions in dikes within the flood deposits as well as along the fault plane in surficial deposits and into the bedrock. It is possible that the fault is a nonseismogenic feature that occurred at the time of the flood by relief of residual stress. The faulting may be a surficial expression of flexural slip and may be a nonseismogenic type related to folding and flexural-slip (Yeates and others, 1981). The relief of slowly accumulating tectonic stress cannot be precluded, however, and the structure is assigned a capable classification. The structure is assigned a length that is related to the width of the Gable Mountain anticline. There is no direct evidence for the depth of the structure, but the primary structure appears to be detachment from the basement and plastic deformation of the upper crust. Since there is no evidence for activity on the faults of the southern side of the anticline and the depth to the basement rocks is considered to be several kilometers, the small earthquakes listed in Table 6 are considered to be appropriate for the evaluation of the fault zone. The results of the analysis are only partly appropriate by means of the estimation of magnitudes and a proper analysis should use seismic moment magnitude values. The average strain rate appears to have a maximum value that is near 0.06 meters for over 13,000 years. Accordingly, the maximum strain rate is about 0.005 mm/yr. The maximum credible earthquake is low and falls near or below the cutoff magnitude of Ms = 5.5 at the data for the lower limit of Tables 1 to 4 and Figures 2, 3, 6, 7 and 11. The seismic moment magnitude value would be similar to the surface magnitude value.

6.7 Southeast Anticline Fault

The fault near the southeast side of the Southeast Anticline is explored only by drill holes. I have examined the drill core from all but one drill hole and examined the drill logs from a series of diamond and rotary drill holes of the fault zone. Inspection of the drill cores and of the technical reports on the area indicate that the fault shows little or no escarpment in about 10,000,000 old basalts, and the fault does not appear to enter sediments of the lower Ringold Formation, approximately 3.5 to 10 million years old. Since there is no apparent offset of younger, but paleomagnetically reversed deposits (at least 700,000 years old) the fault is provisionally classified as noncapable and no maximum credible earthquake is assigned to this fault.

6.8 Toppenish Ridge Structure

The descriptions of Campbell and Bentley (1981) and WPPSS, FSAR, Appendix 18 (1981)and the inspection of the zone during an aerial reconnaissance flight, suggest that the Toppenish Ridge structure may be a capable complex zone of reverse faults. The available evidence is suggestive, but not conclusive, of capability and there is field evidence for reverse-slip faulting in a zone 32 km in length with possible displacements of over 4 m. If the entire zone ruptured in a single event the earthquake magnitude can be estimated from the relations:

$$Ms = 2.021 + 1.142 \log L = 2.021 + 1.142 \log 32,000 = 7.2$$

$$Ms = 6.793 + 1.306 \log D = 6.793 + 1.036 \log 4 = 7.60$$

The displacement estimate is strongly dependent on the possibility of multiplicity of movements. For example, if the offset result from two events of 2 m each, the magnitude estimate is decreased from Ms = 7.6 to 7.0.

This fold is the longest anticline in the region west of CLEW-RAW and extends west to the Cascade Range where it appears to be truncated by many north-south trending faults (Glass, oral communication, February 1982). Whether or not this structure is unique and seismogenic is not well established. There is a possibility that this faulting is caused by flexural slip and is not seismogenic (Yeats and others, 1981). The available data lead to the conclusion that it could provisionally be considered a capable fault with a potential for a maximum earthquake of Ms = 7.4 with a standard error of estimate of about 0.3. Detailed field studies could affect the capable classification, reduce the maximum credible assessment of the magnitude, or lead to the assignment of a non-tectonic origin.

6.9 Seismic Exposure Analysis

The seismic exposure analyses are a systematic part of the WCC (1981b) analysis and are included as WPPSS FSAR, Appendix 2.5K (1981). The WCC (1981b) report lists three parameters that are essential for the analysis of a specific site:

(1) Location and geometry of earthquake sources relative to the site,

(2) recurrence of various earthquake magnitudes up to the maximum for each source, and

(3) attenuation from the source to the site.

These estimates included possible faulting by primary tectonic to secondary detached control, by various options for segmentation, by varying widths for various dips of the assumed fault plane at depth, and by various source models that varied from deeply rooted to surficial models. The possibility of high magnitudes for all structures was considered but assigned a lower weighting. Although the detailed assumptions differ in the numbers assigned for a given weighting, the seismic exposure analysis provides a basically sound and conservative model for the likelihood of earthquakes for each structure and a probabilistic analysis for the site.

7.0 CONCLUSIONS

7.1 Fault Capability

The following are my conclusions regarding fault capability for faults and features of the Hanford region, Washington:

(1) The CLEW Lineament, extending from Cle Elum to Rattlesnake Hills is regarded as a noncapable feature, and is not assigned a maximum credible earthquake.

(2) The RAW Alignment includes the Wallula fault and is regarded to be a structural feature extending from Rattlesnake Hills to the Hite fault system near Milton-Freewater, Oregon. Although the evidence for its capability is not conclusive, there is sufficient suggestive data at or near the Wallula fault and of continuity and linearity with the northern part of RAW to provide a provisional and conservative classification of capable.

(3) The Kennewick and Cold Creek Lineaments show little or no offset of the uppermost basalts and have surficial features that may be related to erosional features associated with the Missoula and earlier floods. These lineaments are concluded to be nontectonic and noncapable geomorphic features.

(4) The Central Fault of Gable Mountain has a mapped length of 340 m and offsets Missoula flood deposits of 13,000 to 19,000 years age. There is abundant evidence for clastic dike intrusion and the structure offsets youthful deposits of late Pleistocene age. It appears that the structure was activated at about the time of flooding and clastic dike intrusion. For conservatism it should be classified as a capable structure with a length that is secondary to the Gable Mountain fold. The width of the fold at depth is the maximum size for the feature. Since it may originate by a detachment mechanism within the deposits of the Columbia Plateau volcanic rocks sequence, and shows no apparent activity along the sides of the fold, it appears to be a minor feature to the main structure of the region, the RAW Alignment.

(5) The Southeast Anticline faults were examined and appear to be of pre-early Ringold Formation age. There is little or no scarp above the basalts and there is no evidence noted for faulting within the Ringold Formation, which is about 3.5 to 10 million years old. Current data are incomplete for this structure, so a final decision must be withheld until all evidence is collected; current data support classification of the fault as provisionally noncapable.

(6) Features northeast of Rattlesnake Hills are of uncertain origin, but are of nontectonic character. Field inspection included examination of the three trenches and the pit.

There is no evidence for any tectonic deformation of the Holocene deposits of the region and they are noncapable lineaments that only affect the surface of the Touchet sediments of the area.

7.2 Fault Slip Rate

The following are my conclusions regarding the fault slip rate for the major features of the Hanford region, Washington:

(1) There is no evidence for youthful deformation of the CLEW Lineament near the Hanford site. There is strong evidence that the gravity features are not displaced by the weak CLEW Lineament, and the net right-lateral offset is no more than 3 km and may be nil. In view of the noncapability, it is assigned zero offset both for the horizontal and the vertical deformation along CLEW.

(2) For the strike-slip model, the evidence for capability appears to be mainly on the southern part of the RAW Alignment. The strike-slip separation is no greater than 0.1 to 0.2 mm/yr as determined from the deformation models of Bentley and others (1980), Davis (1981), or Laubscher (1981). These are greater rates than were observed for the La Grande graben faults, where the rate appears to be about 0.01 mm/yr. For the second model, of reverse-slip separation, the evaluation of the rates leads to the assessment that these are conservative rates, based on the best interpretation of the geometry of deformation. Accordingly, the value of 0.2 mm/yr is regarded as the worst case type of deformation, and the value of 0.1 mm/yr is a conservatively selected best fit case for the RAW Alignment.

(3) The Kennewick and Cold Creek Lineaments are considered to be depositional and nontectonic features; accordingly, they are assigned a zero fault slip rate.

(4) The Central Fault of Gable Mountain has the highest displacement for the shortest time, a rate of 60 mm/12,000 years, or 0.005 mm/yr. This appears to be a conservative value for the deformation at the Central Fault since the tectonic activity is assumed and not established, the slip rate is determined from the maximum offset along the fault, and the rate is assumed to occur at the surface and uses a very young 12,000 year age for the deformation.

(5) The Southeast Anticline appears to be a Miocene feature; accordingly, it is assigned a zero current rate of fault slip.

(6) The Features northeast of Rattlesnake Hills, near the 900 ft elevation are considered to be nontectonic; accordingly, they are assigned a zero fault slip rate.

7.3 Recurrence Intervals

The following recurrence intervals are assigned to the major features of the Hanford region, Washington:

(1) There is no evidence for capability or fault slip along or across the CLEW Lineament. No recurrence interval is assigned to this feature.

(2) There is suggestive evidence on RAW for an earthquake recurrence of greater than 50,000 years for earthquakes of Ms = 6.5 for the strike-slip model and longer for reverse-slip models.

(3) There is no evidence for capability or fault slip along the Kennewick or Cold Creek Lineaments. No recurrence interval is assigned to these features.

(4) The recurrence interval for the Central Fault of Gable Mountain is at least 13,000 to 19,000 years, even for low magnitude events and for the assumed low fault slip rate. This interval results from an assumed rather than a definitive capability and an assumed low fault slip rate. This is considered to be a conservative value rather than a best fit model for the recurrence interval.

(5) The Southeast Anticline is provisionally designated noncapable and is not assigned a recurrence interval.

(6) The Features northeast of Rattlesnake Hills are considered to be nontectonic in origin and the features are not assigned a recurrence interval.

7.4 Maximum Credible Earthquakes

The following structures are the assigned maximum credible earthquakes for major structures of the Hanford area:

(1) The RAW structure is assumed for conservatism to have a capability, to have very low fault slip rates, and to have very long recurrence intervals for earthquakes with Ms = 6.5. Accordingly, as discussed under Section 6, it is assumed to have a capability of having an earthquake magnitude of about Ms = 6.5. The capability for having earthquakes of this or larger magnitude is considered to be very low.

(2) The Central Fault of Gable Mountain is assigned maximum credible earthquake of about Ms = 5 to 5.5, based on the low average fault slip rate and its relationship as a cross fault to the Gable Mountain anticline.

7.5 Seismic Exposure Analysis

The seismic exposure analysis was prepared by WCC as part of the applicant's study (WPPSS, FSAR, Appendix 2.5K, 1981). Although the values given each weighting factor will vary with the individual investigator, my personal values are similar to those used by the applicant. I believe that the analysis is conservative and reasonable and provides a useful probabilistic evaluation of the likelihood of earthquakes for sources along each major structure.

8.0 ACKNOWLEDGEMENTS

The writer is grateful for the sabbatical leave program of the University of Nevada for time to conduct research on the general relationships between earthquake magnitude and surface rupture parameters.

9.0 REFERENCES

Albee, A.L., and Smith, J.L., 1966, Earthquake characteristics and fault activity in Southern California: Engineering Geology in Southern California, Special Publication, Association of Engineering Geologist, p. 9-33.

Bakun, W.H., Stewart, R.M., Bufe, C.G., and Marks, S.M., 1980, Implication of seismicity for failure of a section of the San Andreas fault: Bull. SSA, v. 70, no. 1, pp. 185-201.

Bentley, R.D., Anderson, J.L., Campbell, N.P., and Swanson, D.A., 1980, Stratigraphy and structure of the Yakima Indian Reservation, with emphasis on the Columbia River Basalt Group: U.S. Geological Survey, Open-File Report 80-200, 83 p.

Campbell, N.P., and Bentley, R.D., 1981, Late Quaternary deformation of the Toppenish Ridge uplifes in south-central Washington: Geology, v. 9, pp. 519-524.

Davis, G.A., 1977, Tectonic evaluation of the Pacific Northwest, Precambrian to Recent: in Washington Public Power Supply System, Inc., Preliminary Safety Analysis Report, Amendment 23, p. 46.

Davis, G.A., 1981, Late Cenozoic tectonics of the Pacific Northwest with special reference to the Columbia Plateau: Appendix 2.5N of Washington Public Power Supply System FSAR for WNP-2.

Foundation Sciences, Inc., 1980, Geologic reconnaissance of parts of the Walla Walla and Pullman, Washington and Pendleton, Oregon $1^{\circ} \times 2^{\circ}$ AMS quadrangles: Report submitted to U.S. Army Corps of Engineers, Seattle District under Contract No. DACW67-80-C-0125.

Glass, C.E., 1977, Remote sensing of the Columbia Plateau, Washington Public Power Supply System PSAR WNP-1/4, Amendment 23, Subappendix 2R K.

Glass, C.E., and Slemmons, D.B., 1978, Imagery in earthquake analysis: in State-of-the-Art for Assessing Earthquake Hazards in the United States, U.S. Army Engineer Waterways Experiment Station, Vicksburg, Mississippi, Miscellaneous Paper S-73-1, Report 11, 234 p.

Guptill, P.D., and Heath, E.G., 1981, Surface faulting along the Newport-Inglewood Zone of Deformation, Calif. Geol., v. 34, no. 7, pp. 142-148.

Gutenberg, B., and Richter, C.G., 1954, Seismicity of the earth and associated phenomena: Hafner Publishing Company, New York and London, reprinted 1965, 310 p.

Kienle, C.F., Jr., Bentley, R.D., and Anderson, J.L., 1977, Geologic reconnaissance of the Cle Elum-Wallula Lineament and related structures: Washington Public Power Supply System, Inc., Preliminary Safety Analysis Report, Amendment 23, Volume 2A, Subappendix 2R D.

Laubscher, H.P., 1977, Structural analysis of post-Yakima deformation, Columbia Plateau, Washington: Draft report prepared for Washington Public Power Supply System.

Laubscher, H.P., 1981, Models for development of Yakima deformation: Appendix 2.5-O in Washington Public Power Supply System FSAR for WNP-2.

Price, E.H., 1981, Structural geometry, strain distribution and tectonic evolution of Umtanum Ridge at Priest Rapids and a comparison with other selected localities within Yakima fold structures, south-central Washington: Ph.D. dissertation, Washington State University, 195 p.

Raisz, E., 1945, The Olympic-Wallowa Lineament: American Journal of Science, v. 243-A, p. 479-485.

Reasenberg, P., and Ellsworth, W.L., (in press), Aftershocks of the Coyote Lake, California, earthquake of August 6, 1979: A detailed study.

Rockwell Hanford Operations, 1979, Geologic studies of the Columbia Plateau - a status report: Report No. RHO-BWI-ST-4.

Ryall, A., Slemmons, D.B. and Gedney, L., 1966, Seismicity, tectonism, and surface faulting in the western United States during historic time. Seis. Soc. of Amer. Bull., v. 56, no. 5, p. 1105-1135.

Savage, J.C., Lisowski, M., and Prescott, W.H., 1981, Geodetic strain measurements in Washington: Journ. Geophysical Res., v. 86, no. B6, p. 4929-4940.

Segall, P., and Pollard, D.D., 1980, Mechanics of discontinuous faults: Jour. Geophysical Res. v. 85, no. B8, p. 4337-4350.

Slemmons, D.B., 1977, Faults and earthquake magnitude: in State-of-the-Art Assessing of the Earthquake Hazards in the United States, U.S. Army Engineer Waterways Experiment Station, Vicksburg, Mississippi, Miscellaneous Paper S-73-1, Report 6, 169 p.

Slemmons, D.B., 1980, Letter to R.E. Jackson, NRC, dated November 5, 1980, and errata dated December 4, 1980: Appendix E of SRE (Geology and Seismology) related to the operation of SONGS, unit 2 and 3, Docket Nos. 50-361 and 50-362, submitted by Southern California Edison, and others, pp. E.1 - E.28.

Slemmons, D.B., 1982, Determination of design earthquake magnitudes for microzonation: in Proceedings of the Third International Earthquake Microzonation Conference.

Slemmons, D.B., 1983 (in press), Fault assessment; review of State-of-the-Art Methods: Assoc. Eng. Geologists Bull.

Slemmons, D.B. and Chung, D.H., 1982, Maximum credible and probable earthquakes for the Calaveras and Hayward fault zones: Conference on Earthquake Hazards in the eastern San Francisco Bay Area, Calif. Div. Mines and Geology.

Slemmons, D.B. and O'Malley, P., 1980, Fault and earthquake hazard evaluation of five U.S. Army Corps of Engineers dams in southeastern Washington: Prepared for Seattle District U.S. Army Corps of Engineers.

Slemmons, D.B., O'Malley, P., Whitney, R., Chung, D.H., and Berneuter, V., 1982, Assessment of active faults for maximum credible earthquakes in the southern California - northern Baja California region: Lawrence Livermore National Laboratory publication.

Smith, R.B., 1978, Seismicity, crustal structure, and intraplate tectonics of the interior of the western Cordillera: in Cenozoic Tectonics and Regional Geophysics of the Western Cordillera, Geol. Soc. Amer. Mem. 152, p. 111-114.

U.S. Nuclear Regulatory Commission, 1975, Reactor site criteria, seismic and geologic siting criteria(amendments): Federal Register, v. 38, no. 318, 2 p.

Wallace, R.E., 1978, Geometry and rates of change of fault-generated range fronts, north-central Nevada: J. Res., U.S. Geol. Survey, v. 6, no. 5, pp. 637-650.

Washington Public Power Supply Systems, 1977, Preliminary Safety Analysis Report, WNP-1 & 4, Amendment 23.

Washington Public Power Supply System, 1981a, Final Safety Analysis Report, WNP-2, Amendment 18.

Washington Public Power Supply System 1981b, Answer to Question's 360.16 and 360.18.

Weston Geophysical Research, 1977, Geophysical and seismological studies in the 1872 earthquake epicentral region: in Washington Public Power Supply System Inc., Preliminary Safety Analysis Report, Amendment 23, Appendix 2R E.

Weston Geophysical Research, Inc., 1981, Compilation and interpretation of gravity in Washington, Oregon, and adjacent parts of British Columbia and Idano: Report prepared for Washington Public Power Supply System, FSAR for WNP-2, Appendix 2.5-L, 28 p.

Woodward-Clyde Consultants, 1980a, Response to NRC Question 361.38, submitted by Southern California Edison.

Woodward-Clyde Consultants, 1980b, Seismological review of the July 16, 1936 Milton-Freewater earthquake source region: Report prepared for the Washington Public Power Supply System, Richland, WA, 44 p.

Woodward-Clyde Consultants, 1981a, Logs of trenches at Finley Quarry: Trench logs prepared for Washington Public Power Supply System, Richland, WA.

Woodward-Clyde Consultants, 1981b, Seismic exposure analyses for WNP-2 and WNP 1/4, Washington Public Power Supply System FSAR for WNP-2, Amendment 18.

Woodward-Clyde Consultants, 1981c, Wallula fault trending and mapping: Draft report prepared for Washington Public Power Supply System, Richland, WA.

Woodward-Clyde Consultants, 1982a, Field guide: Moxee Valley and Wenas Valley faults, Day 2: April 13, 1982.

Woodward-Clyde Consultants, 1982b, Review of the magnitude of the July 16, 1936 Walla Walla area earthquake: Report prepared for Washington Public Power Supply System, Richland, WA.

Woodward-Clyde Consultants, 1982c, Segmentation: Report prepared for Washington Public Power Supply System, Richland, WA.

Woodward-Clyde Consultants, 1982d, Letter report of June 17, 1982 on "Maximum Average Rate of Strike-Slip Displacement on RAW." To Mr. Bill Kiel, Washington Public Power Supply System.

Yeats, R.S., Clark, M.M., Keller, E.A., and Rockwell, T.K., 1981, Active fault hazard in southern California: ground rupture vs. seismic shaking: Geological Soc. Amer. Bull., v. 92, no. 4, p. 189-196.

Table 1. Data for earthquake magnitude and faulting parameters; fault types with A = normal-slip, B = reverse-slip, C = normal-oblique-slip, D = reverse-oblique-slip, and D = strike-slip; length of fault ruptures (in meters); maximum fault displacements (in meters); dates of main earthquakes; locations; name of activated surface faults; and references.

FAULT TYPE, NO.	DATE OF EVENT	MAG. (M_s)	LENGTH (meters)	MAX. SURF. DISPLACEMENT (meters)	NAME OF FAULT(S)	LOCATION * = N. AMERICA	REFERENCE
A1	05-03-1887	7.40	.7600E+05	.5100E+01	Pitaycachi	Sonora, Mexico*	Herd and McMasters, 1982 Natali and Sbar, 1982
A2	09-31-1896	7.20	.3600E+05	.4250E+01	Senya	Riku-U, Japan	Usami, 1979 Matsuda et al, 1980
A3	10-02-1915	7.75	.6050E+05	.5800E+01	Pleasant Valley	Pleasant, Valley, NV*	R.E. Wallace (personal comm.) Coffman and Von Hake, 1973
A4	01-06-1928	7.10	.3200E+05	.3350E+01		Subukia, Kenya	Richter, 1958
A5	04-14-1928	6.80	.4700E+05	.5000E+00		Chirpan, Bulgaria	Karnik, 1969 Richter, 1958
A6	04-18-1928	7.00	.4000E+05	.3500E+01		Popvitsa, Bulgaria	Karnik, 1969 Richter, 1958
A7	03-12-1934	6.60	.1150E+05	.5200E+00	Kosmo	Hansel Valley, Utah*	Neumann, 1936 Eppley, 1965
A8	12-14-1950	5.60	.8900E+04	.6000E+00		Ft. Sage Mnts., CA*	Gianella, 1957
A9	07-06-1954	6.60	.1800E+05	.3100E+00	Rainbow Mt.	Fallon-Stillwater, NV*	Richter, 1958 Tocher, 1956
A10	08-23-1954	6.80	.3060E+05	.7600E+00	Rainbow Mt.	Fallon-Stillwater, NV*	Richter, 1958 Tocher, 1956
A11	12-16-1954	6.80	.6120E+05	.3250E+01	Several	Dixie Valley-Fairview Peak, NV*	Romney, 1957 Slemmons, 1957
A12	08-17-1959	7.10	.2910E+05	.6100E+01	Several	Hebgen Lake, Montana*	Witkind, 1964
A13	06-02-1961	6.40	.4000E+05	.1900E+01		Ethiopia	Rothe, 1969 Sykes and Landisman, 1964
A14	03-28-1970	6.90	.4500E+05	.2200E+01	Several	Gediz, Turkey	Dewey, 1976 Ambraseys and Tchalenko, 1972
A15	06-20-1978	6.40	.1300E+05	.3800E+00	Several	Thessaloniki, Greece	Papazachos, et al, 1979 Barker and Langston, 1981
B1	07-11-1952	7.60	.1160E+06	.4000E+01	Chi Lieu Shau	Yumen Changma, China	Lee, et al, 1978 Bonilla and Allen, 1975
B2	01-13-1945	7.10	.2200E+05	.2000E+01	Fukozu and Yokosuka	Mikawa, Japan	Tsuya, 1946 Usami, 1979 The Research Group for Active Faults, 1980
B3	07-21-1952	7.70	.5600E+05	.1200E+01	White Wolf	Kern County, CA*	Buwalda and St. Amand, 1955 Geller, 1976
B4	09-09-1954	6.70	.9000E+04	.1000E+01		El Asnam, Algeria	Rothé, et al, 1977
B5	10-14-1968	6.90	.3700E+05	.3100E+01	Several	Meckering, Australia	Gordon, 1971 Denham, et al, 1980
B6	03-10-1970	5.90	.3500E+04	.3400E+00		Calingiri, Australia	Denham, et al, 1980
B7	09-16-1978	7.70	.8500E+05	.3000E+01		Tabas-E-Golshan, Iran	Berberian, et al, 1979 Berberian, 1979
B8	10-10-1980	7.30	.3200E+05	.3000E+01		El Asnam, Algeria	Burford, et al, 1981
C1	03-26-1872	7.80	.1100E+06	.6440E+01	Owens Valley	Owens Valley, CA*	Slemmons, 1977 Hanks, and Kanamoori, 1973
C2	12-16-1954	7.10	.5800E+05	.5620E+01	Several	Fairview Peak, CA*	Romney, 1957 Slemmons, 1957
C3	02-19-1956	6.80	.1930E+05	.9800E+00	San Miguel	Baja, Mexico*	Shor and Roberts, 1958

Table 1 . (Cont'd)

FAULT TYPE, NO.	DATE OF EVENT	MAG. (M_s)	LENGTH (meters)	MAX. SURF. DISPLACEMENT (meters)	NAME OF FAULT(S)	LOCATION * = N. AMERICA	REFERENCE
C4	11-14-1979	6.60	.2000E+05	.1400E+01		Ghaenat, Iran	Haghipour and Amidi, 1980 Niazi and Kanamoori, 1981
D1	10-28-1891	8.00	.8000E+05	.8000E+01	Several	Hino-Owari (Nobi), Japan	Matsuda, 1974 T. Matsuda (personal comm.) Usami, 1979
D2	11-25-1930	7.00	.3200E+05	.3600E+01	Several	North Izu, Japan	T. Matsuda (personal comm.) Usami, 1979 The Research Group for Active Faults, 1980
D3	04-21-1935	7.10	.5000E+05	.3000E+01	Tunzuchio & Chihhu	Taiwan	Bonilla, 1975; 1977
D4	11-25-1951	7.30	.4000E+05	.2100E+01	Yuli	Taiwan	Bonilla, 1975; 1977 Hsu, 1962
D5	12-04-1957	8.00	.2700E+06	.9000E+01	Bogdu	Gobi-Altai, Mongolia	Okal, 1976 Florensov and Solonenko, 1965
D6	09-01-1962	7.25	.1030E+06	.7600E+00	Ipah	Buyin-Zara, Iran	Ambraseys, 1963 Nowroozi, 1976
D7	10-01-1969	6.20	.1600E+05	.1400E+01	Huaytapallana	Pariahuanca, Peru	Deza, 1971 Philip and Megard, 1977
D8	02-09-1971	6.60	.1460E+05	.2500E+01	Several	San Fernando, CA*	Geller, 1976 Sharp, 1981
D9	11-27-1979	7.10	.6000E+05	.4700E+01	Dasht-E-Bayaz	Ghaenat, Iran	Haghipour and Amidi, 1980 Niazi and Kanamoori, 1981
E1	10-16-1848	7.10	.1000E+06	.6100E+01	Awatere	NE Marborough, N.Z.	Eiby, 1973 Lensen, 1968; 1970 Scholz, 1977
E2	01-09-1857	8.25	.3600E+06	.9500E+01	San Andreas	Ft. Tejon, CA*	Sieh, 1978 Hanks and Kanamoori, 1979
E3	10-21-1868	6.80	.4800E+05	.9000E+00	Hayward	Hayward, CA*	Toppozoda, et al, 1980 Radbruch, 1967 Lawson, et al. 1908
E4	09-01-1888	7.0	.8000E+.05	.2600E+01	Hope	Amuri, N.Z.	Freund, 1971 Berryman, 1980
E5	04-18-1906	8.25	.4350E+06	.6100E+01	San Andreas	San Francisco, CA*	Kanamoori, 1977 Lawson, et al, 1908
E6	12-27-1939	8.00	.3500E+06	.3800E+01	N. Anatolian	Turkey	Dewey, 1976 Ambraseys and Zatopek, 1969
E7	05-18-1940	7.10	.6440E+05	.5800E+01	Imperial	Imperial Valley, CA*	Ulrich, 1941 Richter, 1958
E8	12-20-1942	7.00	.5000E+05	.2020E+01	N. Anatolian	Turkey	Ambraseys and Zatopek, 1969 Dewey, 1976 Ambraseys, 1970
E9	11-26-1943	7.30	.2700E+06	.1800E+01	N. Anatolian	Turkey	Ambraseys and Zatopek, 1969 Dewey, 1976 Ambraseys, 1970
E10	02-01-1944	7.30	.1900E+06	.3600E+01	N. Anatolian	Turkey	Ambraseys and Zatopek, 1969 Dewey, 1976 Ambraseys, 1970
E11	03-18-1953	7.30	.5800E+05	.4300E+01	N. Anatolian	Yenice-Gonen, Turkey	Rothe, 1969 Ambraseys, 1970 Ambraseys and Zatopek, 1969

Table 1. (Cont'd)

FAULT TYPE, NO.	DATE OF EVENT	MAG. (M_s)	LENGTH (meters)	MAX. SURF. DISPLACEMENT (meters)	NAME OF FAULT(S)	LOCATION * = N. AMERICA	REFERENCE
E12	07-10-1958	7.90	.3500E+06	.6580E+01	Fairweather	Alaska*	Kanamoori, 1977 Plafker, et al, 1978 Sykes, 1971
E13	06-27-1966	6.40	.2500E+05	.1800E+00	San Andreas	Parkfield-Cholame, CA*	Lindh and Boore, 1981 Wu, 1968 Brown and Vedder, 1967
E14	08-19-1966	6.80	.3000E+05	.3000E+00	N. Anatolian	Varto, Turkey	Wallace, 1968 Dewey, 1976 Ambraseys and Zatopek, 1969
E15	07-22-1967	6.90	.8000E+05	.1900E+01	N. Anatolian	Mudurnu Valley, Turkey	Dewey, 1976 Ambraseys and Zatopek, 1969
E16	04-09-1968	6.70	.3300E+05	.3800E+00	Coyote Creek	Borrego Mt., CA*	Geller, 1976 Allen, et al, 1968
E17	08-31-1968	7.30	.8000E+05	.4800E+01	Dasht-E-Bayaz	Iran	Niazi, 1969 Ambraseys and Tchalenko, 1969
E18	02-04-1976	7.50	.2300E+06	.3400E+01	Motagua	Guatemala	Plafker, et al, 1976 Kanamoori and Stewart, 1978
E19	10-15-1979	6.80	.3000E+05	.8000E+00	Imperial	Imperial Valley, CA*	Archuleta and Sharp, 1980 McNally, et al, 1979
E20	01-24-1980	5.80	.6500E+04	.3000E-01	Greenville	Livermore, CA*	Schwartz, et al, 1980 Bonilla, et al, 1980

Table 1. Data for regressions of earthquake magnitude, reported surface rupture length (in meters), and maximum displacement (in meters). Fault slip types are coded as follows: A = normal-slip, B = reverse-slip, C = normal-oblique-slip, D = reverse-oblique-slip, and E = strike-slip faults. Bibliography for references is in Slemmons and others (1982).

FAULT TYPE, NO.	DATE OF EVENT	MAG. (M_s)	LENGTH (meters)	MAX. SURF. DISPLACEMENT (meters)	NAME OF FAULT(S)	LOCATION * = N. AMERICA	REFERENCE
A1	05-03-1887	7.40	.7600E+05	.5100E+01	Pitaycachi	Sonora, Mexico*	Herd and McMasters, 1982 Natali and Sbar, 1982
A2	09-31-1896	7.20	.3600E+05	.4250E+01	Senya	Riku-U, Japan	Usami, 1979 Matsuda et al, 1980
A3	10-02-1915	7.75	.6050E+05	.5800E+01	Pleasant Valley	Pleasant, Valley, NV*	R.E. Wallace (personal comm.) Coffman and Von Hake, 1973
A4	01-06-1928	7.10	.3200E+05	.3350E+01		Subukia, Kenya	Richter, 1958
A5	04-14-1928	6.80	.4700E+05	.5000E+00		Chirpan, Bulgaria	Karnik, 1969 Richter, 1958
A6	04-18-1928	7.00	.4000E+05	.3500E+01		Popvitsa, Bulgaria	Karnik, 1969 Richter, 1958
A7	03-12-1934	6.60	.1150E+05	.5200E+00	Kosmo	Hansel Valley, Utah*	Neumann, 1936 Eppley, 1965
A8	12-14-1950	5.60	.6900E+04	.6000E+00		Ft. Sage Mnts., CA*	Gianella, 1957
A9	07-06-1954	6.60	.1900E+05	.3100E+00	Rainbow Mt.	Fallon-Stillwater, NV*	Richter, 1958 Tocher, 1956
A10	08-23-1954	6.80	.3060E+05	.7600E+00	Rainbow Mt.	Fallon-Stillwater, NV*	Richter, 1958 Tocher, 1956
A11	12-16-1954	6.80	.6120E+05	.3250E+01	Several	Dixie Valley-Fairview Peak, NV*	Romney, 1957 Slemmons, 1957
A12	08-17-1959	7.10	.2910E+05	.6100E+01	Several	Hebgen Lake, Montana*	Witkind, 1964
A13	06-02-1961	6.40	.4000E+05	.1900E+01		Ethiopia	Rothé, 1969 Sykes and Landisman, 1964
A14	03-28-1970	6.90	.4500E+05	.2200E+01	Several	Gediz, Turkey	Dewey, 1976 Ambraseys and Tchalenko, 1972
A15	06-20-1978	6.40	.1300E+05	.3800E+00	Several	Thessaloniki, Greece	Papazachos, et al, 1979 Barker and Langston, 1981
B1	07-21-1952	7.60	.1160E+06	.4000E+01	Chi Lieu Shau	Yumen Changma, China	Lee, et al, 1978 Bonilla and Allen, 1975
B2	01-13-1945	7.10	.2200E+05	.2000E+01	Fukozu and Yokosuka	Mikawa, Japan	Tsuya, 1946 Usami, 1979 The Research Group for Active Faults, 1980
B3	07-21-1952	7.70	.5600E+05	.1200E+01	White Wolf	Kern County, CA*	Buwalda and St. Amand, 1955 Geller, 1976
B4	09-09-1954	6.70	.9000E+04	.1000E+01		El Asnam, Algeria	Rothé, et al, 1977
B5	10-14-1968	6.90	.3700E+05	.3100E+01	Several	Meckering, Australia	Gordon, 1971 Denham, et al, 1980

Table 1. (Continued)

FAULT TYPE, NO.	DATE OF EVENT	MAG. (M_s)	LENGTH (meters)	MAX. SURF. DISPLACEMENT (meters)	NAME OF FAULT(S)	LOCATION * = N. AMERICA	REFERENCE
B6	03-10-1970	5.90	.3500E+04	.3400E+00		Calingiri, Australia	Denham, et al, 1980
B7	09-16-1978	7.70	.8500E+05	.3000E+01		Tabas-E-Golshan, Iran	Berberian, et al, 1979 Berberian, 1979
B8	10-10-1980	7.30	.3200E+05	.3000E+01		El Asnam, Algeria	Burford, et al, 1981
C1	03-26-1872	7.80	.1100E+06	.6440E+01	Owens Valley	Owens Valley, CA*	Slemmons, 1977 Hanks and Kanamori, 1979
C2	12-16-1954	7.10	.5800E+05	.5620E+01	Several	Fairview Peak, CA*	Romney, 1957 Slemmons, 1957
C3	02-19-1956	6.80	.1930E+05	.9800E+00	San Miguel	Baja, Mexico*	Shor and Roberts, 1958
C4	11-14-1979	6.60	.2000E+05	.1400E+01		Ghaenat, Iran	Haghipour and Amidi, 1980 Niazi and Kanamori, 1981
D1	10-28-1891	8.00	.8000E+05	.8000E+01	Several	Mino-Owari (Nobi), Japan	Matsuda, 1974 T. Matsuda (personal comm.) Usami, 1979
D2	11-25-1930	7.00	.3200E+05	.3600E+01	Several	North Izu, Japan	T. Matsuda (personal comm.) Usami, 1979 The Research Group for Active Faults, 1980
D3	04-21-1935	7.10	.5000E+05	.3000E+01	Tunzuchio & Chihhu	Taiwan	Bonilla, 1975; 1977
D4	11-25-1951	7.30	.4000E+05	.2100E+01	Yuli	Taiwan	Bonilla, 1975; 1977 Hsu, 1962
D5	12-04-1957	8.00	.2700E+06	.9000E+01	Bogdu	Gobi-Altai, Mongolia	Okal, 1977 Florensov and Solonenko, 1965
D6	09-19-1962	7.25	.1030E+06	.7600E+00	Ipah	Buyin-Zara, Iran	Ambraseys, 1963 Nowroozi, 1976
D7	10-01-1969	6.20	.1600E+05	.1400E+01	Huaytapallana	Pariahuanca, Peru	Deza, 1971 Philip and Megard, 1977
D8	02-09-1971	6.60	.1460E+05	.2500E+01	Several	San Fernando, CA*	Geller, 1976 Sharp, 1981
D9	11-27-1979	7.10	.6000E+05	.4700E+01	Dasht-E-Bayaz	Ghaenat, Iran	Haghipour and Amidi, 1980 Niazi and Kanamori, 1981
E1	10-16-1848	7.10	.1000E+06	.6100E+01	Awatere	NE Marborough, N.Z.	Eiby, 1973 Lensen, 1968; 1970 Scholz, 1977
E2	01-09-1857	8.25	.3600E+06	.9500E+01	San Andreas	Ft. Tejon, CA*	Sieh, 1978 Hanks and Kanamori, 1979
E3	10-21-1868	6.80	.4800E+05	.9000E+00	Hayward	Hayward, CA*	Toppozoda, et al, 1980 Radbruch, 1967 Lawson, et al. 1908
E4	09-01-1888	7.0	.8000E+.05	.2600E+01	Hope	Amuri, N.Z.	Freund, 1971 Berryman, 1980

Table I. (Continued)

FAULT TYPE, NO.	DATE OF EVENT	MAG. (M_s)	LENGTH (meters)	MAX. SURF. DISPLACEMENT (meters)	NAME OF FAULT(S)	LOCATION * = N. AMERICA	REFERENCE
E5	04-18-1906	8.25	.4350E+06	.6100E+01	San Andreas	San Francisco, CA*	Kanamori, 1977 Lawson, et al, 1908
E6	12-27-1939	8.00	.3500E+06	.3800E+01	N. Anatolian	Turkey	Dewey, 1976 Ambraseys and Zatopek, 1969
E7	05-18-1940	7.10	.6440E+05	.5800E+01	Imperial	Imperial Valley, CA*	Ulrich, 1941 Richter, 1958
E8	12-20-1942	7.00	.5000E+05	.2020E+01	N. Anatolian	Turkey	Ambraseys and Zatopek, 1969 Dewey, 1976 Ambraseys, 1970
E9	11-26-1943	7.30	.2700E+06	.1800E+01	N. Anatolian	Turkey	Ambraseys and Zatopek, 1969 Dewey, 1976 Ambraseys, 1970
E10	02-01-1944	7.30	.1900E+06	.3600E+01	N. Anatolian	Turkey	Ambraseys and Zatopek, 1969 Dewey, 1976 Ambraseys, 1970
E11	03-18-1953	7.30	.5800E+05	.4300E+01	N. Anatolian	Yenice-Gonen, Turkey	Rothé, 1969 Ambraseys, 1970 Ambraseys and Zatopek, 1969
E12	07-10-1958	7.90	.3500E+06	.6580E+01	Fairweather	Alaska*	Kanamori, 1977 Plafker, et al, 1978 Sykes, 1971
E13	06-27-1966	6.40	.2500E+05	.1800E+00	San Andreas	Parkfield-Cholame, CA*	Lindh and Boore, 1981 Wu, 1968 Brown and Vedder, 1967
E14	08-19-1966	6.80	.3000E+05	.3000E+00	N. Anatolian	Varto, Turkey	Wallace, 1968 Dewey, 1976 Ambraseys and Zatopek, 1969
E15	07-22-1967	6.90	.8000E+05	.1900E+01	N. Anatolian	Mudurnu Valley, Turkey	Dewey, 1976 Ambraseys and Zatopek, 1969
E16	04-09-1968	6.70	.3300E+05	.3800E+00	Coyote Creek	Borrego Mt., CA*	Geller, 1976 Allen, et al, 1968
E17	08-31-1968	7.30	.8000E+05	.4800E+01	Dasht-E-Bayaz	Iran	Niazi, 1969 Ambraseys and Tchalenko, 1969
E18	02-04-1976	7.50	.2300E+06	.3400E+0[illegible]	Motagua	Guatemala	Plafker, et al, 1976 Kanamori and Stewart, 1978
E19	10-15-1979	6.80	.3000E+05	.8000E+00	Imperial	Imperial Valley, CA*	Archuleta and Sharp, 1980 McNally, et al, 1979
E20	01-24-1980	5.80	.6500E+04	.3000E-01	Greenville	Livermore, CA*	Schwartz, et al, 1980 Bonilla, et al, 1980

Table 2. Relations of earthquake magnitude (M_S) regressed on log surface rupture length L (in m) from Slemmons (1983, in press).

MAGNITUDE VS. LOG LENGTH: Ms = A + B (LOG LENGTH)

	NUMBER	A	B	s	r	r^2	STU-T
NORTH AMERICA (NA)	23	1.267	1.238	.290	.904	.817	10.177
REST OF WORLD	33	2.855	.899	.286	.794	.630	8.153
WORLDWIDE (WW)	56	2.062	1.068	.297	.850	.722	12.859
A, normal-slip	15	.809	1.341	.318	.750	.563	4.722
B, reverse-slip	8	2.021	1.142	.197	.939	.882	6.921
C, normal-oblique-slip	4	.875	1.348	.143	.949	.900	4.367
D, reverse-oblique-slip	9	1.199	1.271	.273	.867	.752	4.953
E, strike-slip	20	1.404	1.169	.205	.938	.879	11.824
AC	19	.720	1.365	.293	.799	.636	6.105
BD	17	1.992	1.124	.266	.881	7.683	
CDE	33	1.793	1.112	.259	.889	.790	11.460
CD	13	1.147	1.284	.241	.887	.787	6.774
BE	28	2.435	.984	.287	.872	.761	9.746
ACE	39	1.817	1.103	.272	.875	.765	11.743
BDE	37	2.309	1.016	.292	.863	.745	10.878

Table 3. Relations of earthquake magnitude (M_S) regressed on maximum surface displacement (D, in m) for worldwide (WW) and North America (NA) data from Slemmons (1983, in press).

MAGNITUDE VS. LOG DISP: Ms = A + B (LOG D)

	NUMBER	A	B	s	r	r^2	STU-T
NORTH AMERICA (NA)	23	6.887	.847	.423	.780	.609	6.472
REST OF WORLD	33	6.768	.888	.337	.696	.485	6.471
WORLDWIDE (WW)	56	6.821	.847	.378	.742	.551	9.450
A, normal-slip	15	7.668	.750	.340	.707	.500	4.289
B, reverse-slip	8	6.793	1.306	.374	.759	.577	3.281
C, normal-oblique slip	4	6.635	1.307	.259	.821	.675	2.247
D, reverse-oblique-slip	9	6.657	1.076	.423	.637	.406	2.740
E, strike-slip	20	6.974	.804	.315	.846	.715	7.315
AC	19	6.673	.805	.330	.735	.541	5.218
BD	17	6.745	1.083	.415	.674	.454	4.302
CDE	33	6.892	.809	.361	.770	.593	7.659
CD	13	6.650	1.066	.380	.687	.471	3.780
BE	28	6.944	.856	.345	.809	.655	7.811
ACE	39	6.828	.802	.355	.774	.600	8.460
BDE	37	6.902	.849	.375	.761	.579	7.949

Table 4. Multiple linear regression of earthquake magnitude (Ms) on log maximum surface displacement (D, in m) plus log surface rupture length (L in m): Ms = A + B x log D (m) + C x log L, from Slemmons (1983, in press).

MAGNITUDE VS. LOG DISP PLUS LOG LENGTH: Ms = A + B log D + C log L

	NUMBER	A	B	C	r	r^2
NORTH AMERICA (NA)	23	2.367	0.263	0.991	0.910	0.843
REST OF WORLD	33	3.793	0.454	0.666	0.845	0.714
WORLDWIDE (WW)	56	3.204	0.365	0.802	0.883	0.780
A, normal-slip	15	2.735	0.378	0.894	0.792	0.627
B, reverse-slip	8	1.303	-0.292	1.219	0.943	0.890
C, normal-oblique-slip	4	-5.510	-1.407	2.867	1.000	0.999
D, reverse-oblique-slip	9	1.897	0.547	1.067	0.915	0.830
E, strike-slip	20	2.484	0.212	0.940	0.946	0.895
AC	19	2.447	0.343	0.963	0.824	0.673
BD	17	2.440	0.211	1.009	0.886	0.785
CDE	33	2.967	0.335	0.845	0.920	0.847
CD	13	1.970	0.394	1.069	0.911	0.830
BE	28	3.791	0.384	0.682	0.906	0.821
ACE	39	3.054	0.326	0.824	0.903	0.815

Table 5. Total fault length (L) and percent total fault ruptured (Pr) during earthquakes of about Ms = 6, or higher (from Slemmons, in press)

FAULT, DATE	Ms	TOTAL LENGTH (L) (km)	RUPTURE LENGTH (km)	PERCENT OF LENGTH (Pr)
San Andreas		1160		
1857	8.25		400	34.5
1906	8.25		435	37.5
North Anatolian		1300		
1939	8.0		350	26.9
1942	7.0		70	5.4
1943	7.3		270	20.8
1944	7.3		190	14.6
1957	7.0		40	3.1
1967	6.9		80	6.2
Fairweather-Queen Charlotte		1130		
1949	8.1		380	33.6
1958	7.9		350	31.0
1972	7.1		170	15.0
Motagua		1100		
1976	7.5		230	20.9
Awatere-Wellington		547		
1848	7.1		100	18.3
Clarence-West Wairarapa		600		
1855	7.6		160	26.7
Hope-East Wairarapa		410		
1888	7.0		80	19.5
San Jacinto-Cerro Prieto		290		
1934	7.1		?	?
1940	7.1		64.4	22.2
1968	6.7		33	11.4
Hayward-Rodgers Creek-Healdsburg-Maacama		280		
1868	6.8		48	17.1

Table 6. Fault parameters for earthquakes of between Ms = 3.5 and 6.4

No.	Fault Type	Mag. (Ms)	Calc. Ms from Multiple Regression	Length (km)	Max. Displ. (m)	Location
1	E	3.6	5.4	10	0.0023	Imperial, CA
2	E	6.4	6.5	37?	0.1830	Parkfield-Cholame, CA
3	E	5.2	5.6	7	0.015	Galway Creek, CA
4	A	5.7	5.2	10	0.055	Oroville, CA
5	E	6.2	6.7	7	0.30	Matsushiro, Japan
6	E	5.1	6.3	6	1.	Jebel Dumbeir, Sudan
7	E	5.2	6.0	6	0.1	Turkey
8	D	6.2	6.6	16	1.4	Pariahuanca, Peru
9	A	5.6	6.3	9	0.6	Ft. Sage Mountain, CA
10	B	5.9	6.0	3.5	0.3	Australia
11	E	5.8	5.7	6.5	.03	Livermore, CA
12	E	5.2	5.7	3.25	0.1	Homestead, CA

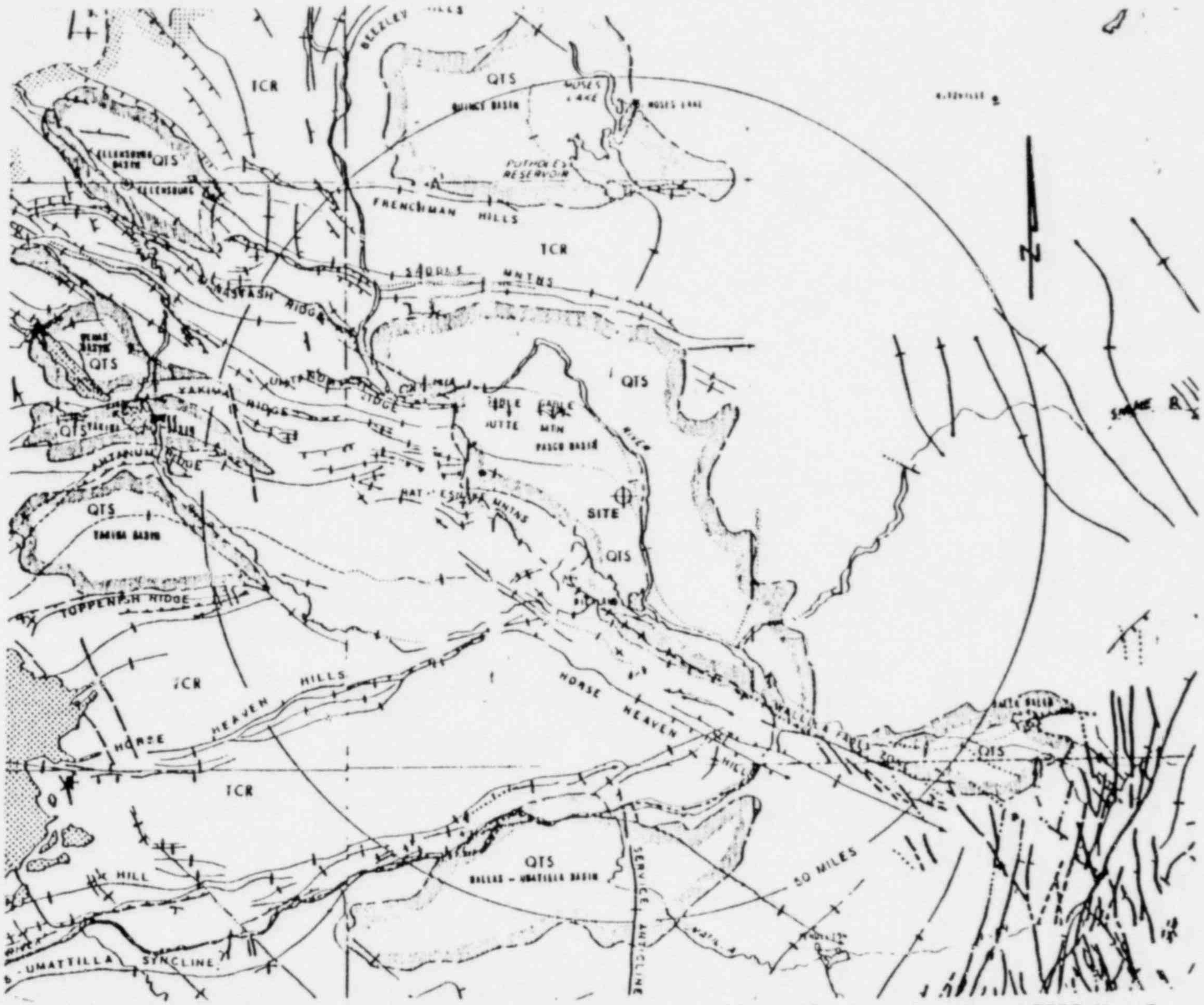

Figure 1. Regional geologic and tectonic elements map with a 50 mi radius from WPPSS No. 2.

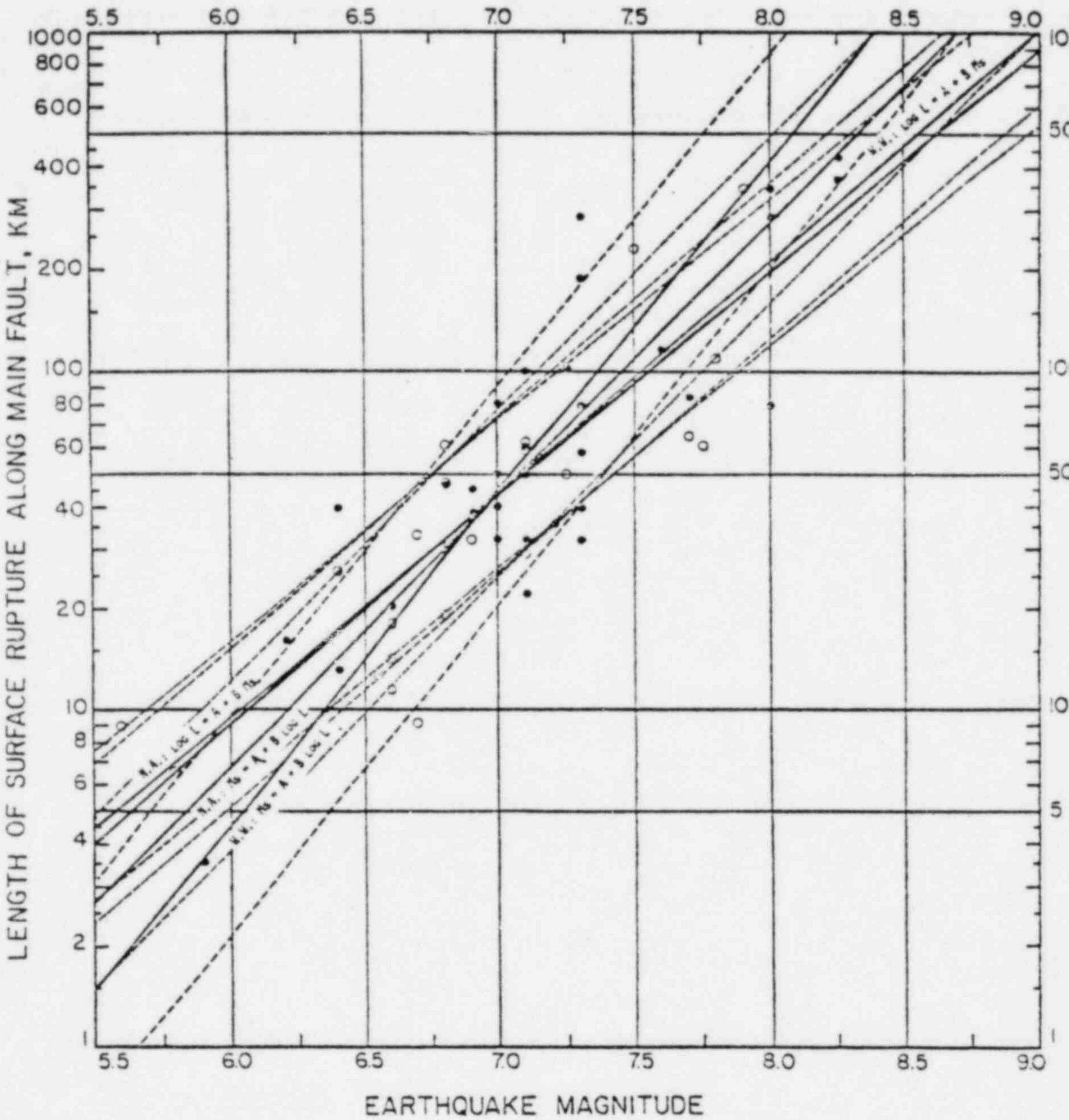

Figure 2. Relation of earthquake magnitude (Ms) to surface rupture length (L, in km) for worldwide (WW) and North America (NA) data (from Slemmons, in press).

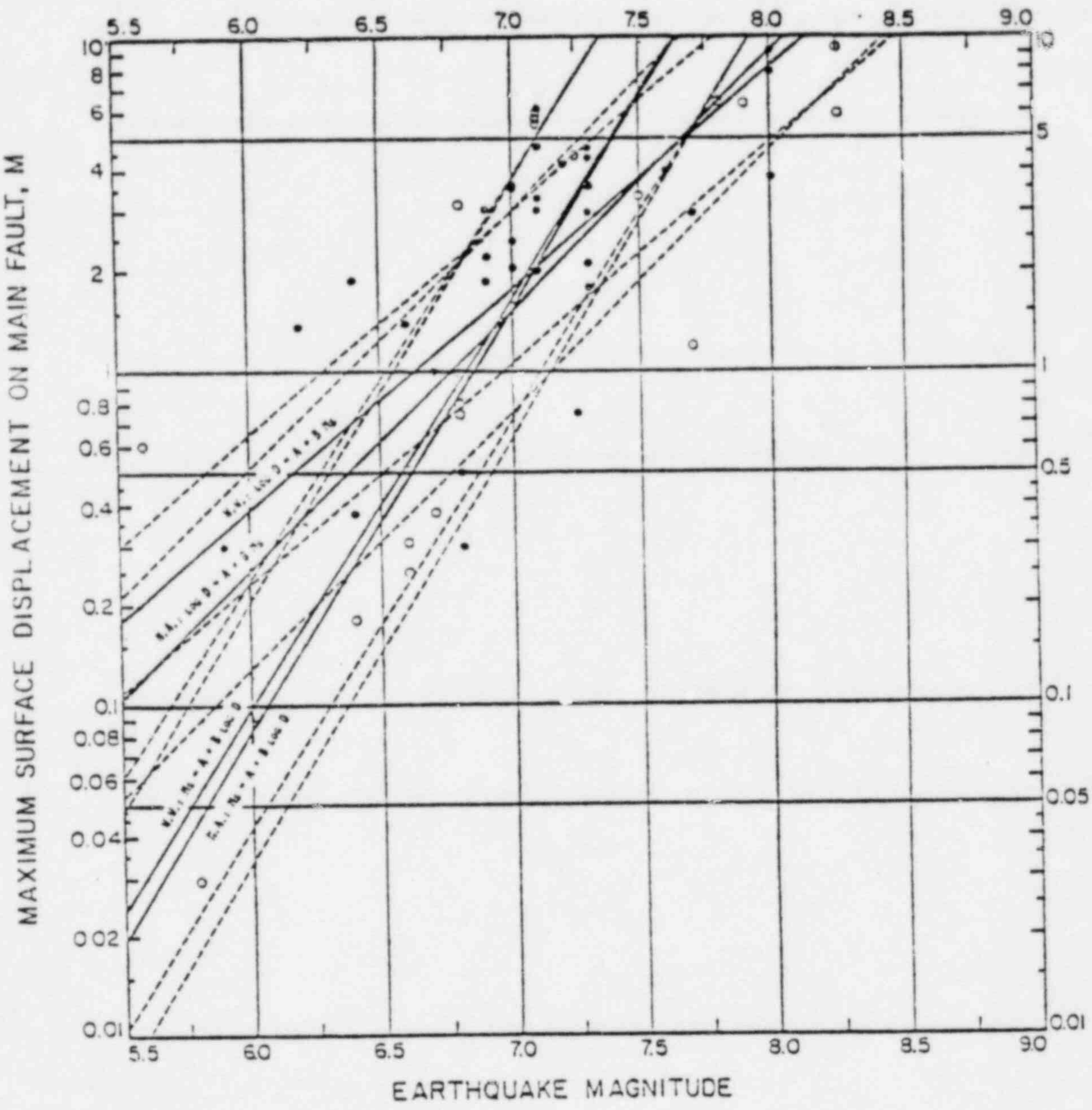

Figure 3. Relation of earthquake magnitude (Ms) to maximum surface displacement (D, in m) for worldwide (WW) and North America (NA) data (from Slemmons, in press).

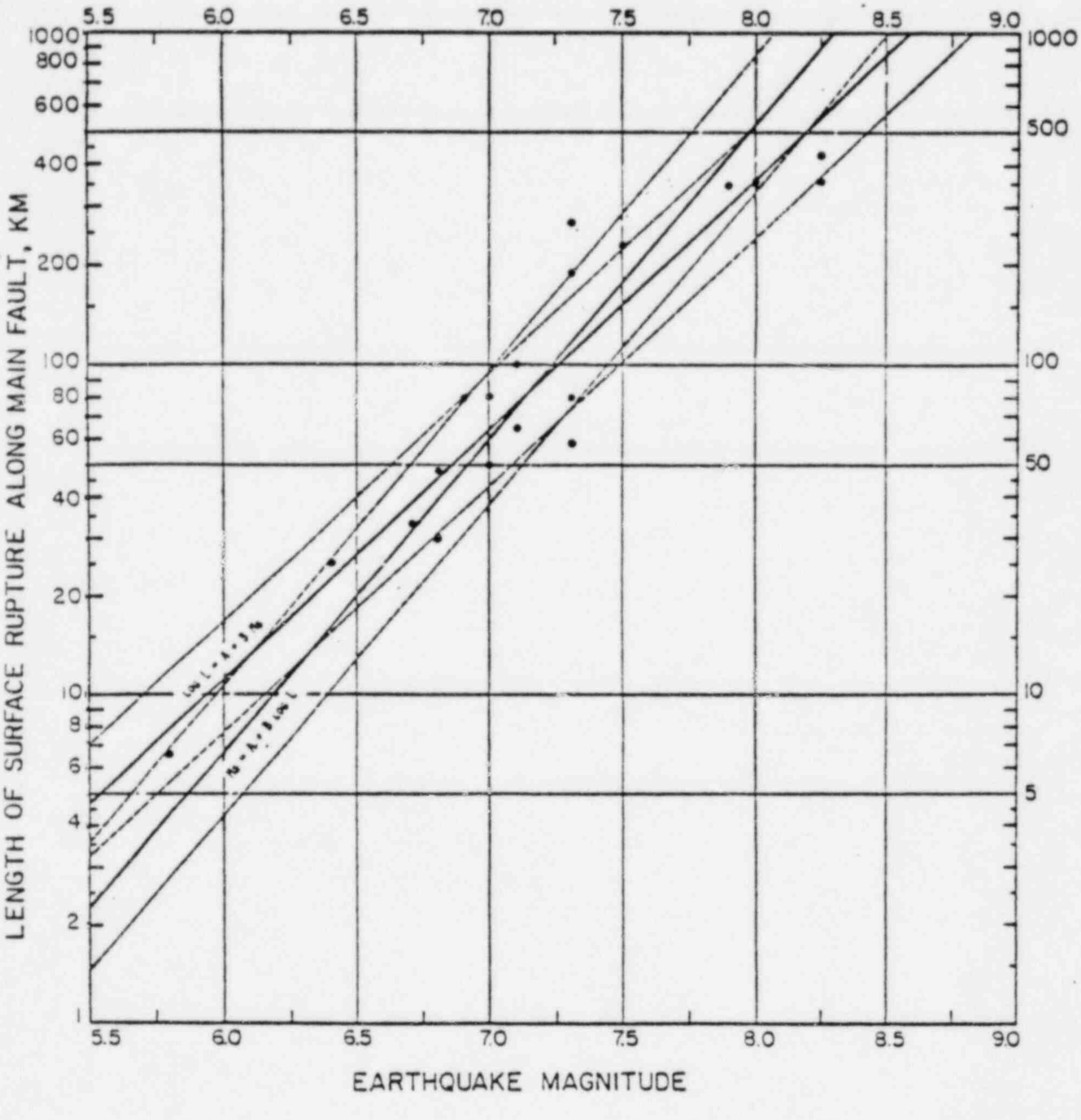

Figure 4. Relation of earthquake magnitude (Ms) to surface rupture length (L, in km) for strike-slip faults (from Slemmons, in press).

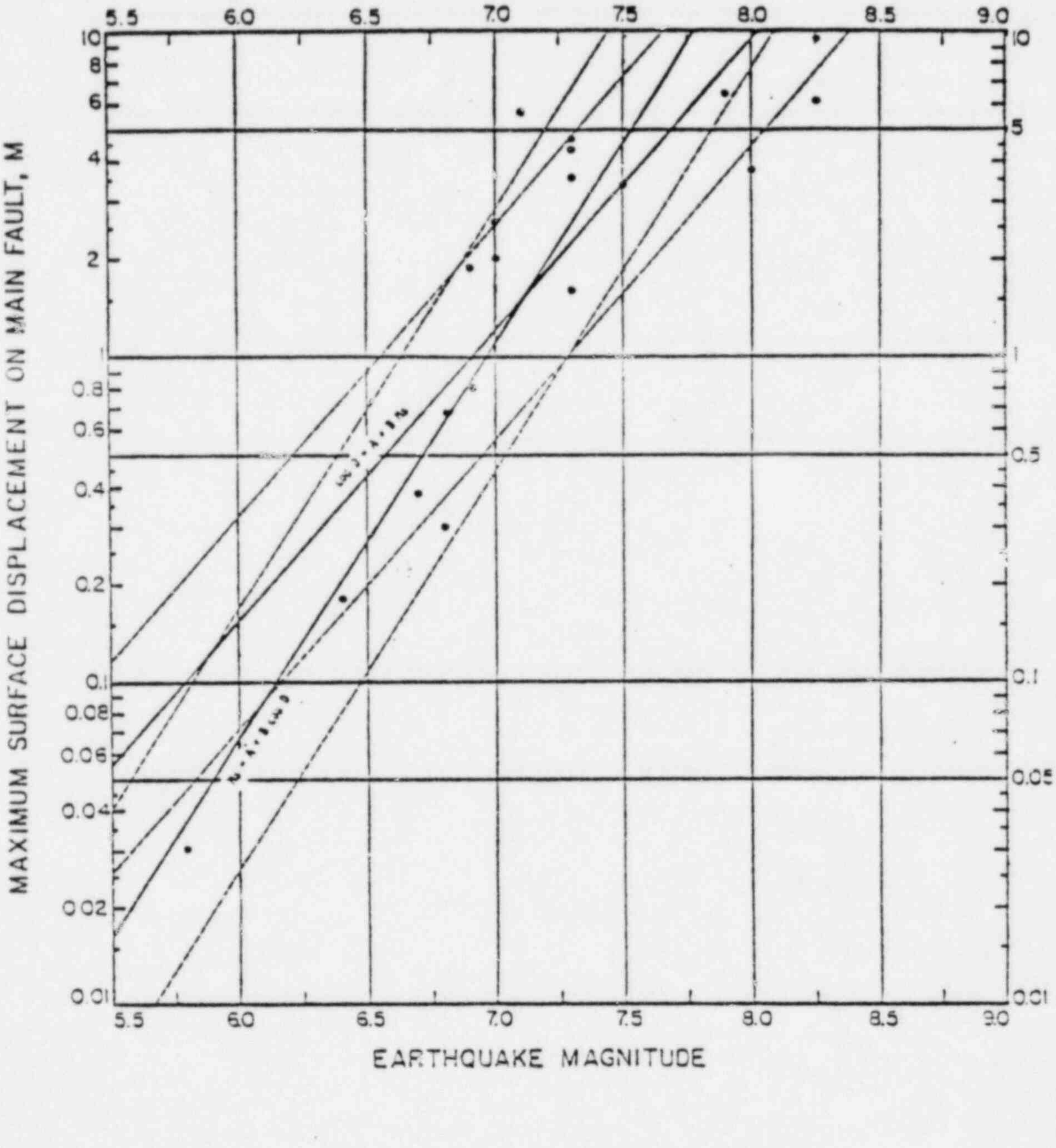

Figure 5. Relation of earthquake magnitude (Ms) to maximum surface displacement (D, in m) for strike-slip faults (from Slemmons, in press).

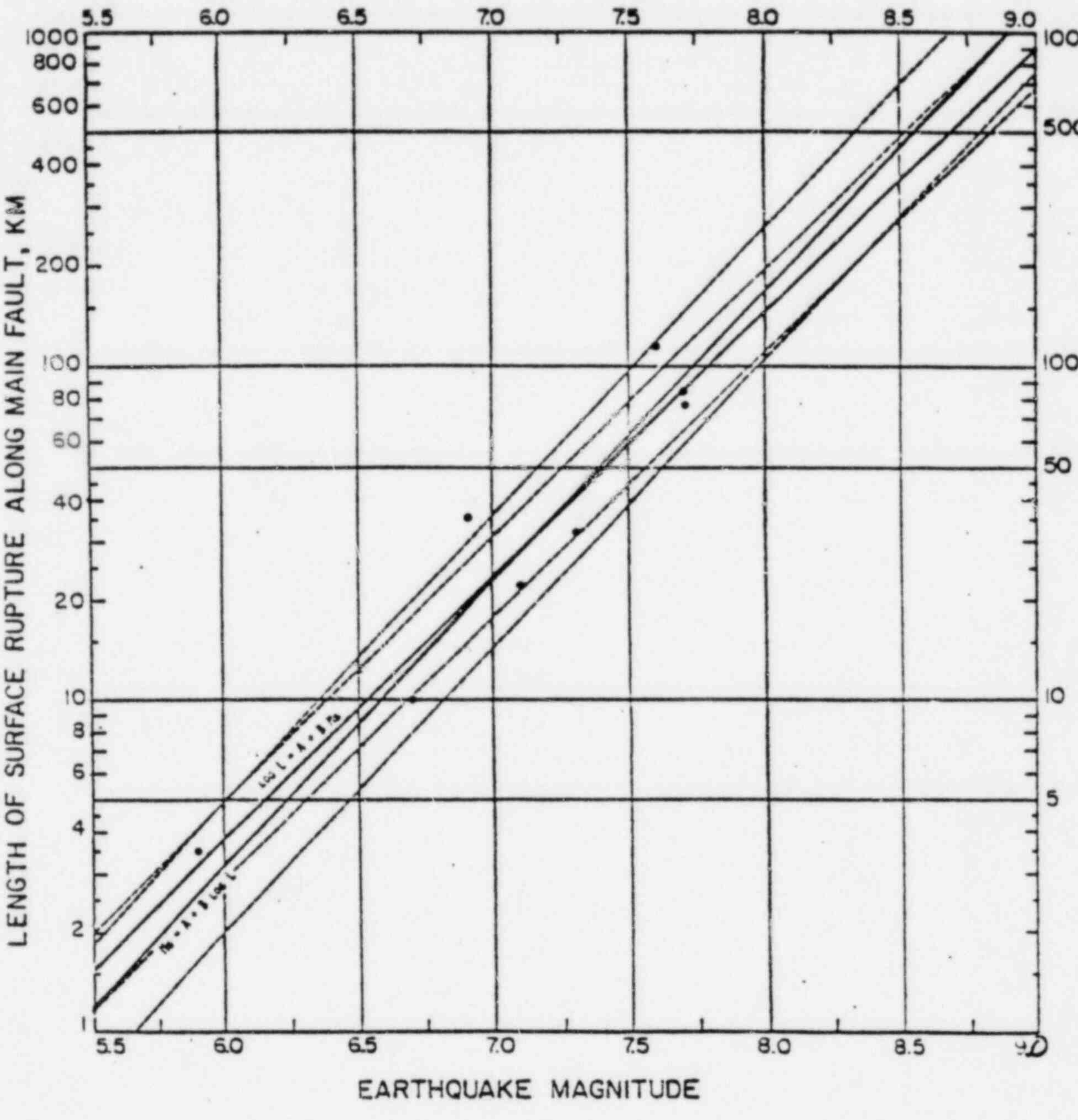

Figure 6. Relation of earthquake magnitude (Ms) to surface rupture length (L, in km) for reverse-slip faults (from Slemmons, in press).

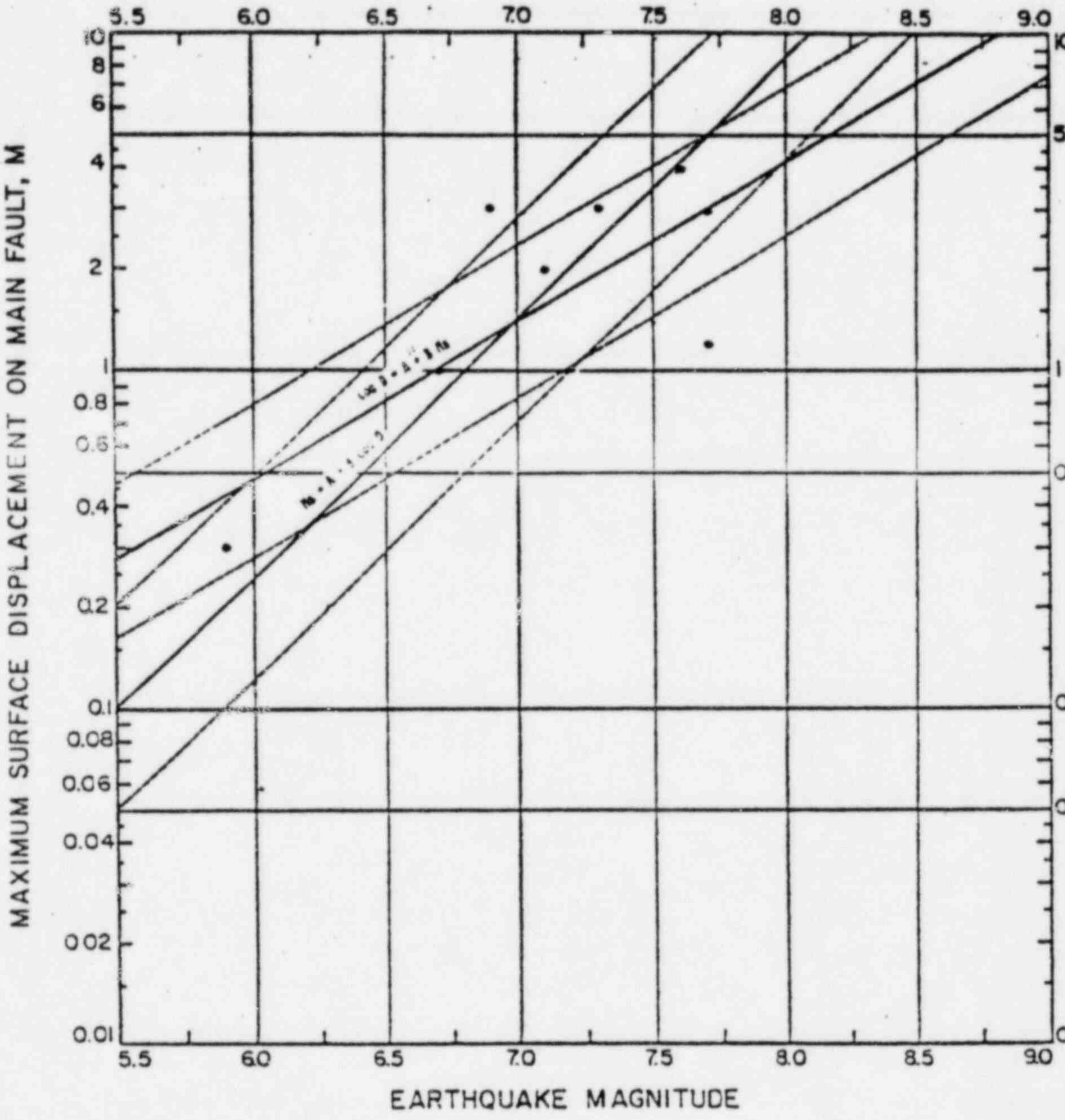

Figure 7. Relation of earthquake magnitude (Ms) to maximum surface displacement (D, in m) for reverse-slip faults (from Slemmons, in press).

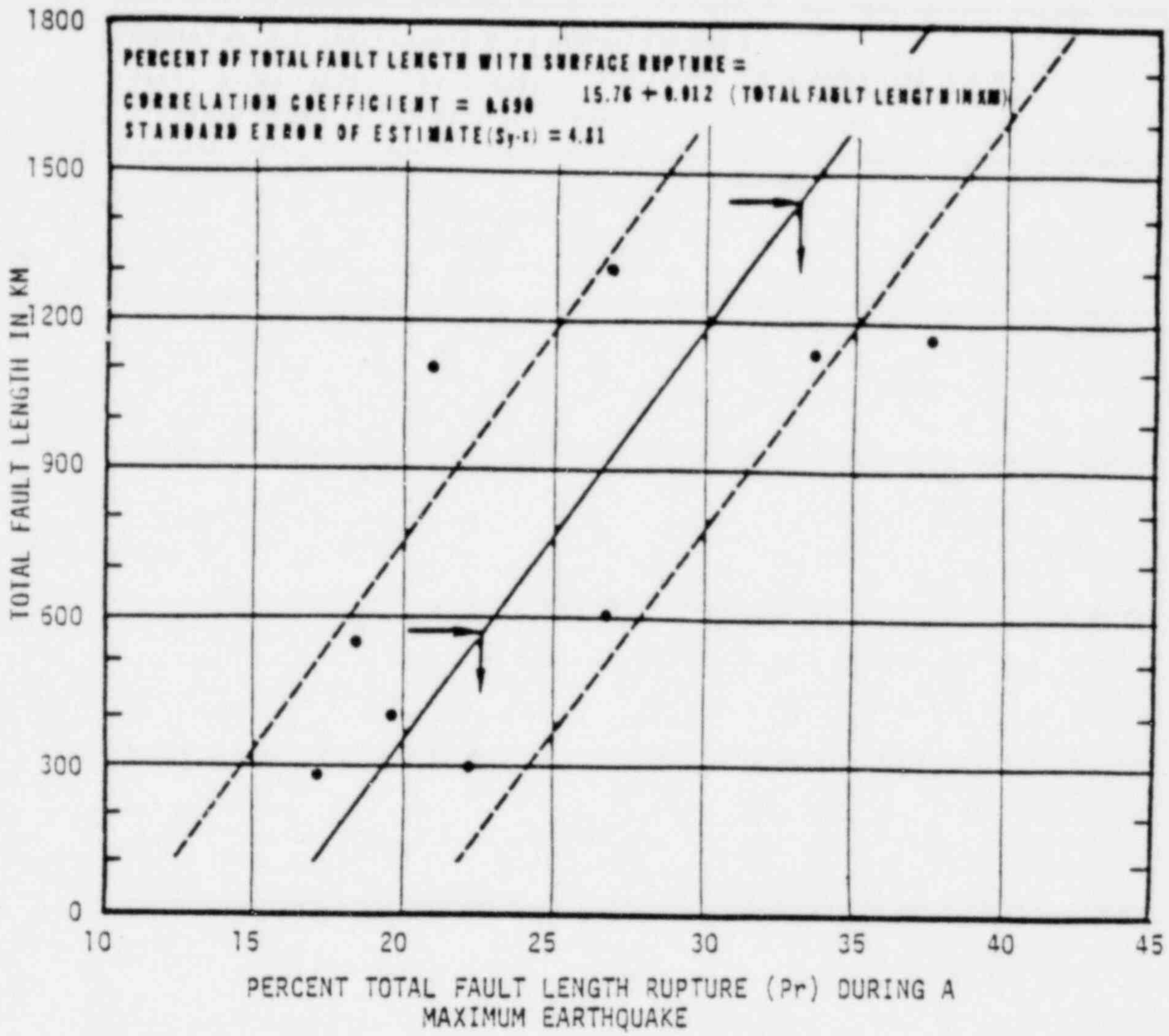

Figure 8. Relation of percent of total fault length ruptured (Pr) to total fault length (L) for strike-slip faults for 9 data points from worldwide data: Pr = 15.76 + 0.012 x L (in km), from Slemmons (1983, in press).

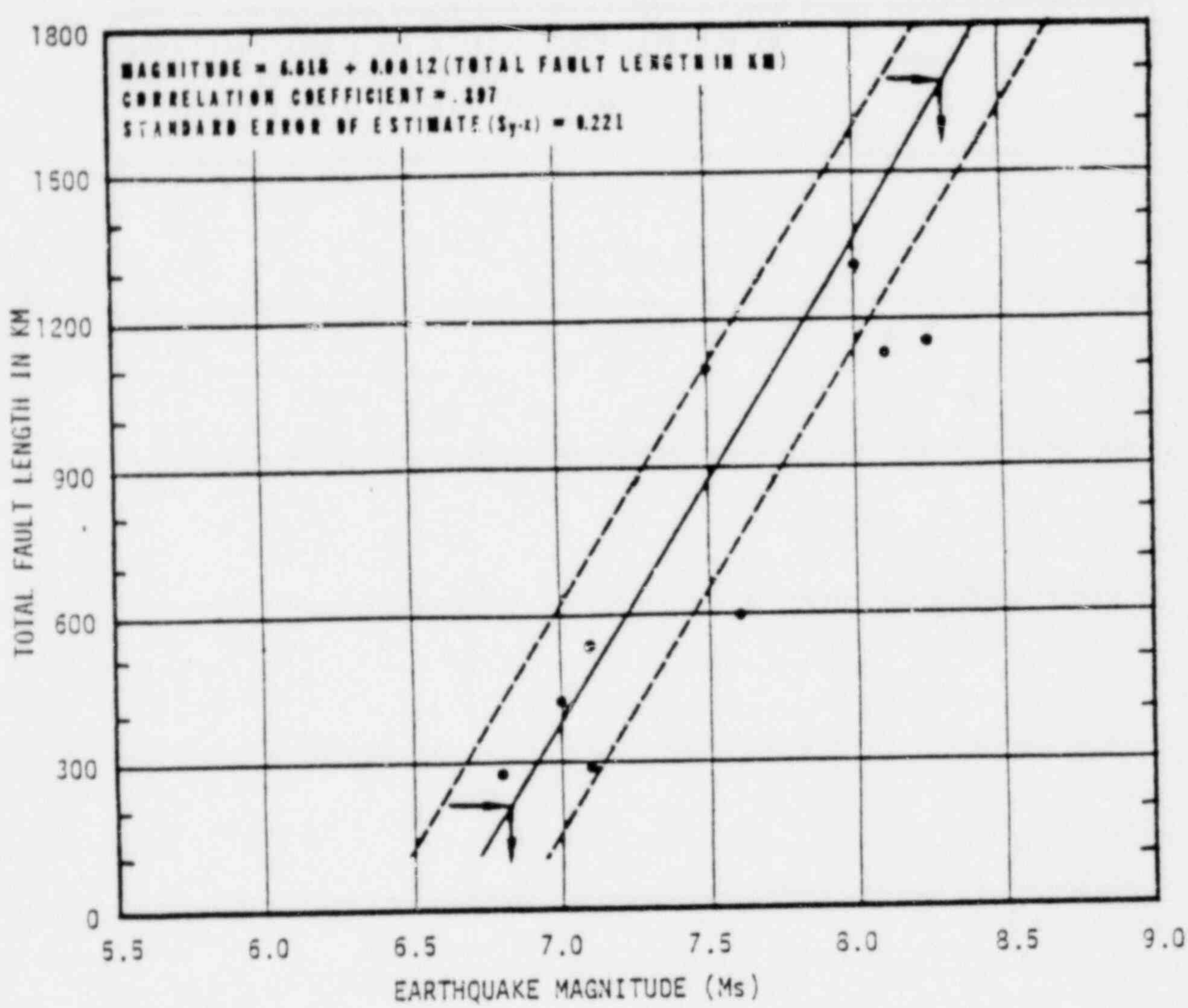

Figure 9. Relation of earthquake magnitude (Ms) to total fault length L (in km) for strike-slip faults. Regression for 9 data points: Ms = 6.618 + 0.0012 x L (in km) from Slemmons (1983, in press).

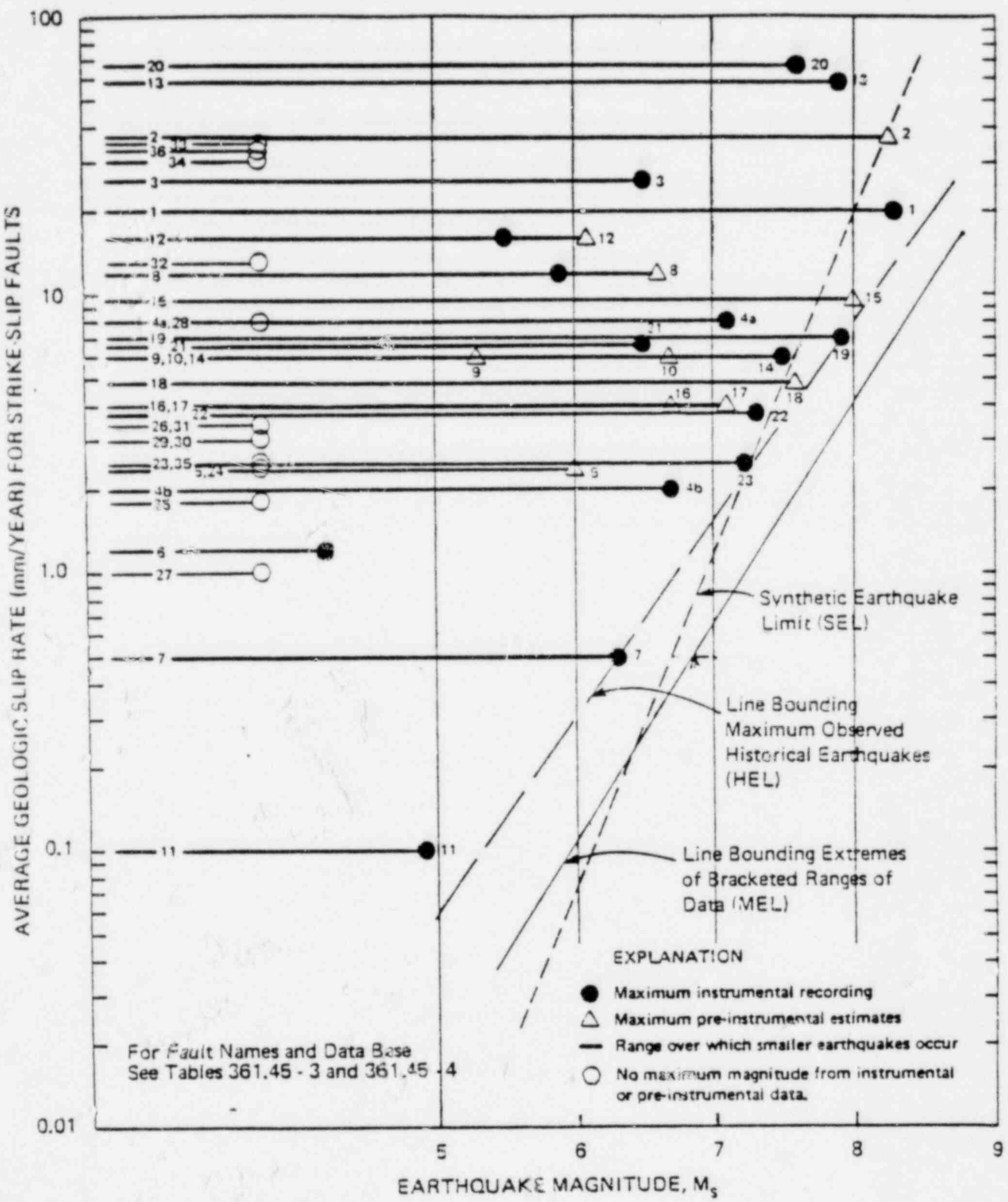

Figure 10. Relation of average geologic slip rate to earthquake magnitude (Ms) for strike-slip faults with a comparison of SEL, MEL, and HEL lines (after Woodward-Clyde Consultants, 1980).

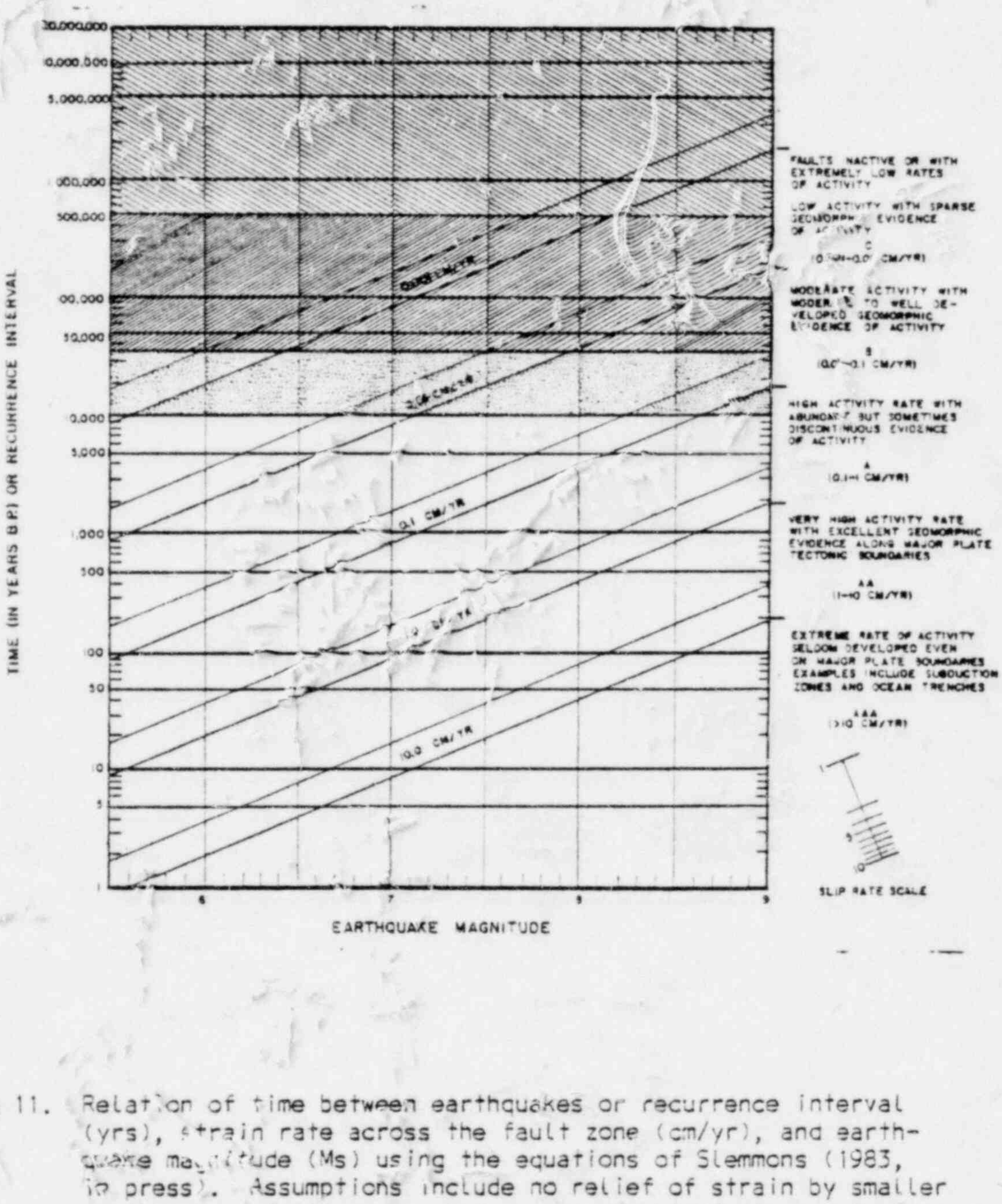

Figure 11. Relation of time between earthquakes or recurrence interval (yrs), strain rate across the fault zone (cm/yr), and earthquake magnitude (Ms) using the equations of Slemmons (1983, in press). Assumptions include no relief of strain by smaller earthquakes, fault creep, and average fault displacement of one-half the maximum displacement. The model also assumes that there is no plastic deformation by drag, folding, warping, or other processes. The estimates obtained from this chart are generally minimal; actual recurrence intervals may be much greater (Slemmons 1983, in press).

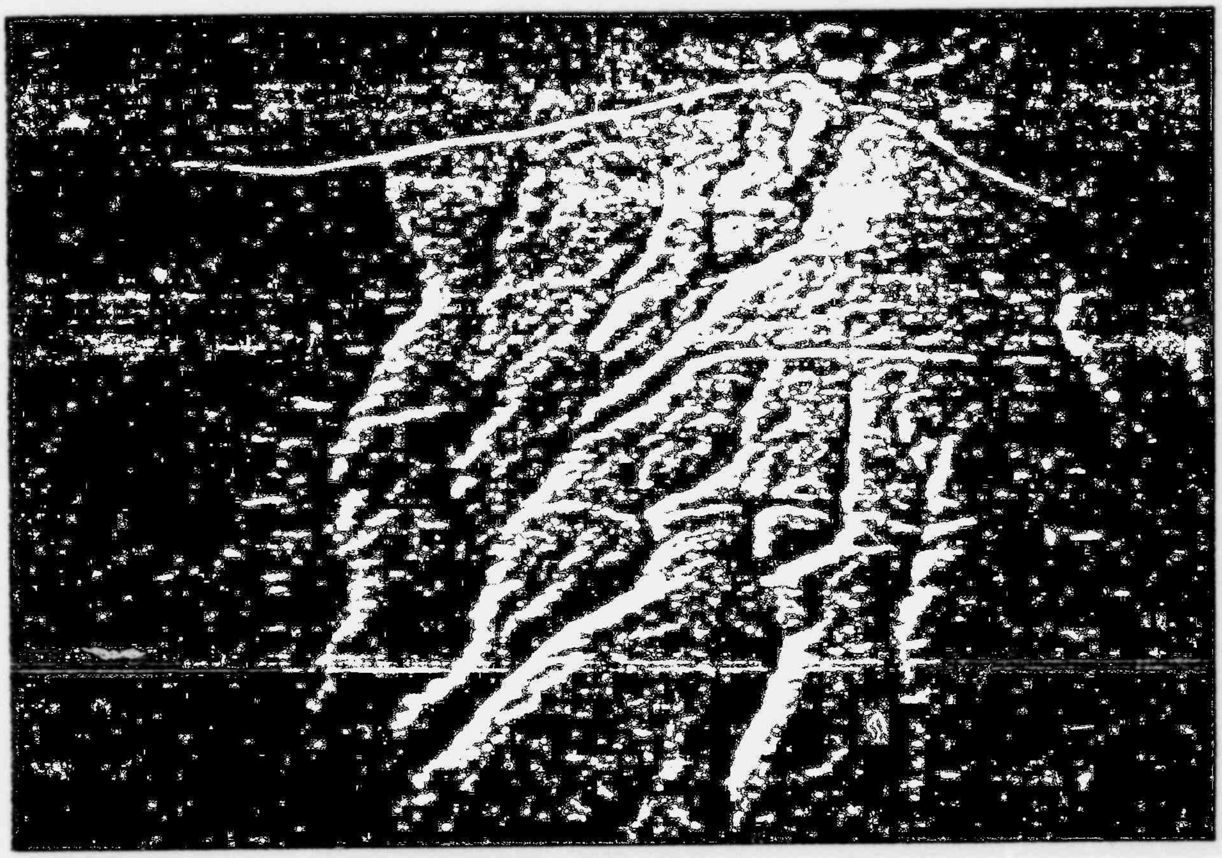

Figure 12. Linear features on the pediment-like surface on Touchet sediments, near 900 feet elevation, northeast of Rattlesnake Hills. Some of the features cross at least eight interfluves (Photograph by D.B. Slemmons in December, 1981).

Figure 13. Linear features on Touchet sediments, near the 900 feet elevation on the northeast slope of Rattlesnake Hills (Photography by D.B. Slemmons in December, 1981).

Figure 14. Linear features in Vansycle Canyon, with scarps in Warm Springs Valley in foreground (Photograph by D.B. Slemmons in December, 1981).

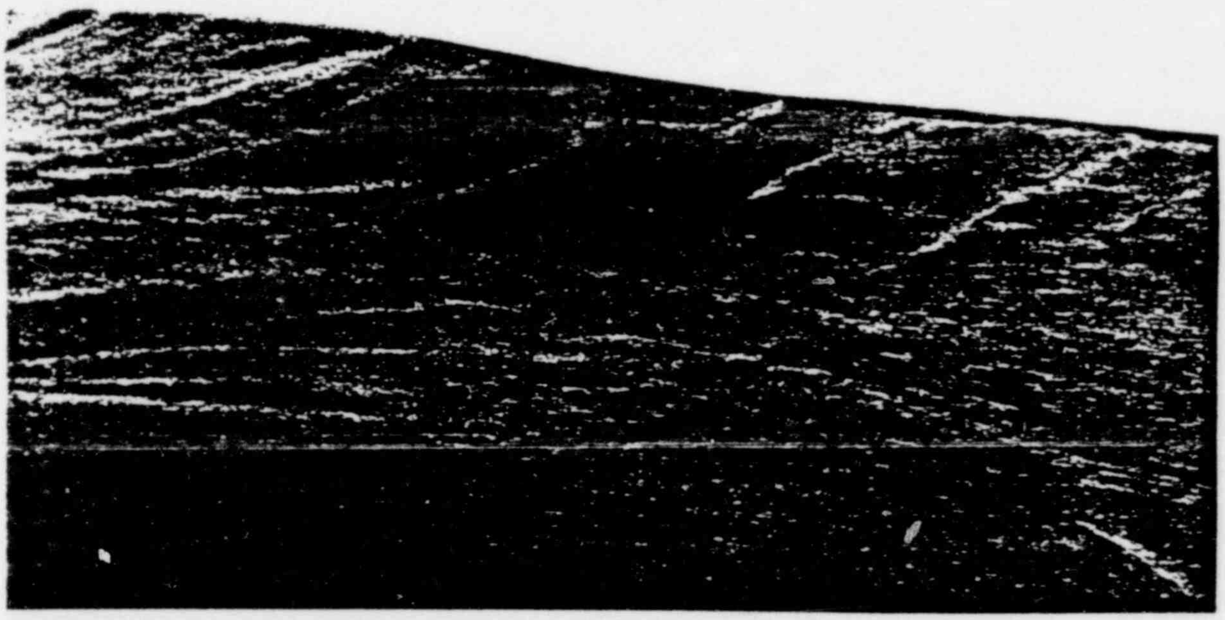

Figure 15. Scarps (close-up) on west side of Warm Springs Valley (Photograph by S. Brocoum in December, 1981).

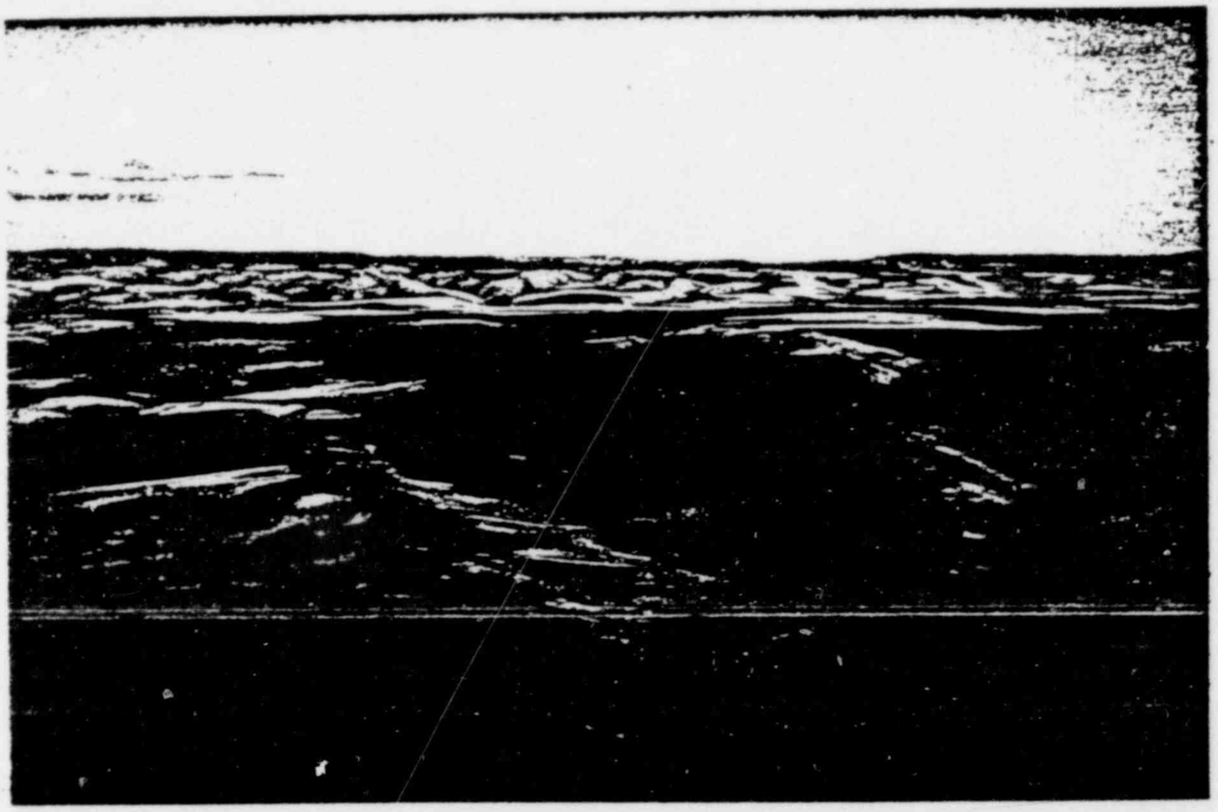

Figure 16. Scarps near the Rattlesnake-Wallula Alignment on the north slope of a hill about 3 miles south of Umpaine, Oregon (Photograph by R. Whitney in September, 1979).

APPENDIX I

ERRATA TO WNP-2 SAFETY EVALUATION REPORT

Page	Line	Change
1-11	14	For Open Item (1), Change "(2.6)" to "(2.5)."
1-11	23	For Open Item (9), Change "6.3.3" to "6.3.6."
1-11	28	For Open Item (13), Change "7.5.2.3" to 7.7.2.3."
1-12	4	For Open Item (19), Change "(13.1)" to "(13.2.2.5)."
1-12	5	For Open Item (20), Change "(13.1)" to "(13.5.1.4)."
1-12	10	For Open Item (25), Change "5" to "51."
1-12	13	For Open Item (27), Change "(6.3.5)" to "(6.3.6)."
1-13	2	For Confirmatory Item (9), Change "(4.2.1.2(h)), (4.2.3.2.(h))" to (4.2.1.2(8)), (4.2.3.2(8))."
1-13	3	For Confirmatory Item (10), Change "(4.2.1.3(d)), (4.2.3.3(d))" to "(4.2.1.3(4)), (4.2.3.3(4))."
1-13	5	For Confirmatory Item (11), Change "(4.2.3.1(e))" to "(4.2.3.1(5))."
1-13	6	For Confirmatory Item (12), Change "(4.2.3.2(d))" to "(4.2.3.2(4))."

Page	Line	Change
13-21	40	Delete the work "Acting."
13-24	28	Change "12 consectutive" to "16 consecutive."
E-2	27	Change "Maughey" to Haughey."